

University of Warwick institutional repository: <http://go.warwick.ac.uk/wrap>

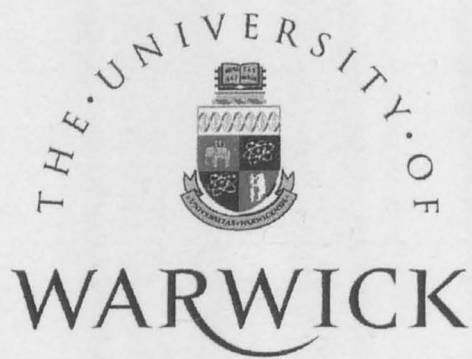
A Thesis Submitted for the Degree of PhD at the University of Warwick

<http://go.warwick.ac.uk/wrap/57744>

This thesis is made available online and is protected by original copyright.

Please scroll down to view the document itself.

Please refer to the repository record for this item for information to help you to cite it. Our policy information is available from the repository home page.



**LUBRICATION IN METAL CUTTING
UNDER BUILT-UP EDGE CONDITIONS**

A Thesis submitted to the University of Warwick for the Degree of

DOCTOR OF PHILOSOPHY

by

MARCIO BACCI DA SILVA

Department of Engineering

University of Warwick

OCTOBER 1998

To my wife Heloisa and my daughter Ana Luisa.

To the memory of my aunt Terezinha.

Summary

The effect of a mineral oil lubricant and sulphur (an EP additive) on machining of medium carbon steel has been investigated. The lubricant was applied with several different concentrations of an additive containing sulphur. The concentrations were 0%, 1%, 2%, 3%, 4% and 5% of the additive. The results were compared with dry conditions. The effect of cutting speed and feed rate was also investigated. During the tests cutting force, transient surface temperature and surface finish were measured. Cutting force and surface finish were measured using traditional equipment. To measure the temperature of the workpiece a new method was developed. The temperature of the transient surface was measured at three different positions below the cutting edge during the cut using an infrared sensor. The results were then extrapolated to obtain the temperature of the transient surface close to the cutting edge (the maximum temperature of the surface). The temperature results can be used to calculate the cooling rate of the surface. Quick stop tests were also used to obtain chip samples and information about BUE size and shape. The lubricant had no effect on forces, temperature or BUE size, but improved surface finish. This work suggests that the enhanced surface finish obtained when lubricant is applied is not due to lubrication on the rake face (preventing a BUE), but action on the machined surface after it has been formed. The BUE is squeezed parallel to the cutting edge and touches the workpiece altering the surface finish, by a rubbing action and also because periodically part of the BUE bonds to the surface. The lubricant works on this rubbing action and can avoid bonding of the squeezed BUE and also of debris particles that are inevitably formed during the operation. It has been shown that a very low volume of lubricant is enough to improve the surface finish because the area that requires lubrication is small.

Acknowledgements

I would like to thank

- Dr J. Wallbank for the supervision of this work, without whose ideas, enthusiasm, dedication and professionalism this work would not have been possible.
- Dr A.R. Machado for selecting me to try and continue the fine tradition that he has established.
- The technical staff of the Engineering Department. In particular Mr M.A. Robinson, Mr S. Fox, Mr B. Bryden and Ms V. Kading, for their extraordinary friendship and help.
- Dr T.H. Chu, for his assistance and contributions throughout the development of this work.
- Dr J.D. Bressan for his valuable suggestions and comments.
- Conselho Nacional de Desenvolvimento Científico e Tecnológico – CNPq and Universidade Federal de Uberlândia both in Brazil, for their financial support.
- Castrol Limited in the name of Mr G. Hornsby for providing the mineral oil and the additive.
- My mother Matilde, my aunt Ecléia and my brothers Marcelo, Hélio and Élcio.

Declaration

I declare that, except where specifically acknowledged, the material contained in this thesis is my own work and has neither been previously published nor submitted elsewhere for the purpose of obtaining an academic degree.

Marcio Bacci da Silva

TABLE OF CONTENTS

1 INTRODUCTION	1
2 LITERATURE SURVEY	5
2.1 Machining Process	6
2.2 Chip Formation	10
2.3 Cutting Forces	13
2.4 Chip Tool Interface	16
2.4.1 Built-Up Edge	19
2.4.2 Effect on Tool Wear	24
2.5 Stress Distribution on the Rake Face	25
2.6 Surface Conditions in Machining	27
2.7 Metal Cutting Temperature	38
2.7.1 Heat Generation in Metal Cutting	39
2.7.2 Temperature Measurement in Metal Cutting	44
2.7.3 Analytical and Numerical Models of Temperature Distributions	47
2.7.4 Temperature and Cutting Conditions	49
2.8 Cutting Fluids	53
2.8.1 Functions of Cutting Fluids	56
2.8.2 Action of Cutting Fluids	57
3 EXPERIMENTAL TECHNIQUES	63
3.1 Material and Conditions	64
3.2 Measurements	68

3.2.1 Forces	68
3.2.2 Surface Finish	69
3.2.3 Chip Thickness	69
3.3 Temperature Measurements	70
3.3.1 Experimental Apparatus	73
3.3.2 Measuring Temperature when Cutting Fluid is Present	75
3.3.3 Calibration of the Infrared Sensor	77
4 RESULTS	80
4.1 Cutting Forces	80
4.2 Temperature	88
4.3 Chip Thickness	98
4.4 Surface Finish	105
4.5 Quick Stop Samples	113
4.6 Machined Surface Samples	132
5 DISCUSSION	143
5.1 Temperature Measurement Technique	143
5.1.1 Errors	144
5.1.2 Effect of the Air	147
5.2 Effect of Lubrication on BUE Size	148
5.3 Cutting Forces	153
5.3.1 Effect of Lubrication on Absolute Value of Cutting Forces	153
5.3.2 Cooling Aspects on Forces	155
5.3.3 Effect of Lubrication on Force Oscillation	157
5.4 Workpiece Temperature	162

5.5 Surface Finish	166
5.5.1 Effect of Lubricant on Ra	166
5.5.2 Machined Surface Geometry	168
5.6 Optimised Cutting Fluid System	181
6 FUTURE WORK	186
7 CONCLUSIONS	189
REFERENCES	191
APPENDIX A: Contact on Tool Flank Face	213
APPENDIX B: Heat Generation and Workpiece Temperature	229

List of Figures

2.1-Manufacturing process according to the form of energy.	5
2.2-A turning operation using a single point tool.	7
2.3-Orthogonal cutting.	9
2.4-Forces acting on the primary and secondary shear planes [22].	14
2.5-Cutting forces in orthogonal cutting represented by the Merchant circle [22].	14
2.6-Stress distribution on tool rake face [25].	18
2.7-Built-up edge.	19
2.8-Different shapes of the BUE [29].	23
2.9-Rake face stress distribution [40].	26
2.10-Feed marks left on the surface of the workpiece.	30
2.11-Schematic diagram showing crack formation [43].	35
2.12-Heat generation zones in an orthogonal cutting.	41
2.13-Effect of cutting speed, feed and cutting fluid on temperature [112].	50
2.14-Distribution of temperature on the rake face of a tool [5].	51
2.15-Distribution of temperature on the rake face of tool when cutting high conductivity copper [5].	52
2.16-Temperature for different contact length and feed rates [114].	53
3.1-Microstructure of AISI 1040 steel used in the tests. a) diameter 100mm, b) diameter 190mm, 150x.	66
3.2-Microstructure of the tool material used in the tests, 1500x.	67
3.3-Positions where the temperatures are measured.	70
3.4-Scheme of the infrared sensor installed.	74
3.5-Sensor with compressed air to be used when cutting fluid is applied.	76
3.6-Infrared sensor in position to measure temperature on transient surface.	77
3.7-Calibration curve for the infrared sensor. a) dry, b) lubricated condition.	79

4.1-Variation of cutting force F_c during cutting, 40m/min, 0.1mm/rev, dry.	80
4.2-Variation of cutting force F_c during cutting, 40m/min, 0.1mm/rev, 0%.	80
4.3-Variation of cutting force F_c during cutting, 40m/min, 0.1mm/rev, 1%.	81
4.4-Variation of cutting force F_c during cutting, 40m/min, 0.1mm/rev, 5%.	81
4.5-Variation of cutting force F_c with cutting speed, 0.15mm/rev, dry condition.	83
4.6-Effect of cutting speed and feed rate on cutting force, dry.	84
4.7-Effect of cutting speed and feed rate on cutting force, 0%.	84
4.8-Effect of cutting speed and feed rate on cutting force, 1%.	85
4.9-Effect of cutting speed and feed rate on cutting force, 2%.	85
4.10-Effect of cutting speed and feed rate on cutting force, 3%.	86
4.11-Effect of cutting speed and feed rate on cutting force, 4%.	86
4.12-Effect of cutting speed and feed rate on cutting force, 5%.	87
4.13-Variation of temperature at 3mm below cutting edge after start of cutting. 30m/min, 0.1mm/rev, dry.	90
4.14-Variation of temperature at 3mm below cutting edge after start of cutting. 30m/min, 0.1mm/rev, 0%.	90
4.15-Variation of temperature at 3mm below cutting edge after start of cutting. 30m/min, 0.1mm/rev, 1%.	91
4.16-Extrapolation of temperature in the transient surface, 30m/min, dry.	91
4.17-Extrapolation of temperature in the transient surface, 30m/min, 0%.	92
4.18-Extrapolation of temperature in the transient surface, 30m/min, 1%.	92
4.19-Effect of cutting speed and feed rate on variation of temperature, dry.	93
4.20-Effect of cutting speed and feed rate on variation of temperature, 0%.	94
4.21-Effect of cutting speed and feed rate on variation of temperature, 1%.	94
4.22-Effect of cutting speed and feed rate on variation of temperature, 2%.	95
4.23-Effect of cutting speed and feed rate on variation of temperature, 3%.	95

4.24-Effect of cutting speed and feed rate on variation of temperature, 4%.	96
4.25-Effect of cutting speed and feed rate on variation of temperature, 5%.	96
4.26-Rise of temperature with cutting speed, 0.05mm/rev.	97
4.27-Rise of temperature with cutting speed, 0.1mm/rev.	97
4.28- Rise of temperature with cutting speed, 0.15mm/rev.	97
4.29-Variation of chip thickness with cutting speed, 0.05mm/rev.	100
4.30-Variation of chip thickness with cutting speed, 0.1mm/rev.	100
4.31-Variation of chip thickness with cutting speed, 0.15mm/rev.	100
4.32-Quick stop sample for 40m/min and 0.15mm/rev, dry condition. (a)14.1x, (b)150x.	102
4.33-Variation of primary shear plane angle with cutting speed, 0.05mm/rev.	104
4.34-Variation of primary shear plane angle with cutting speed, 0.1mm/rev.	104
4.35-Variation of primary shear plane angle with cutting speed, 0.15mm/rev.	104
4.36-Effect of cutting speed and feed rate on surface finish, dry.	108
4.37-Effect of cutting speed and feed rate on surface finish, 0%.	108
4.38-Effect of cutting speed and feed rate on surface finish, 1%.	109
4.39-Effect of cutting speed and feed rate on surface finish, 2%.	109
4.40-Effect of cutting speed and feed rate on surface finish, 3%.	110
4.41-Effect of cutting speed and feed rate on surface finish, 4%.	110
4.42-Effect of cutting speed and feed rate on surface finish, 5%.	111
4.43-Variation of surface finish with cutting speed, 0.05mm/rev.	111
4.44-Variation of surface finish with cutting speed, 0.1mm/rev.	112
4.45-Variation of surface finish with cutting speed, 0.15mm/rev.	112
4.46-Optical microstructure view of section through quick stop sample for 22m/min and 0.05mm/rev, dry, 300x.	113
4.47-Optical microstructure view of section through quick stop sample for 22m/min and 0.05mm/rev, 0%, 300x.	114

4.48-Optical microstructure view of section through quick stop sample for 22m/min and 0.05mm/rev, 1%, 300x.	114
4.49-Optical microstructure view of section through quick stop sample for 22m/min and 0.1mm/rev, dry, 300x.	115
4.50-Optical microstructure view of section through quick stop sample for 22m/min and 0.1mm/rev, 0%, 300x.	115
4.51-Optical microstructure view of section through quick stop sample for 22m/min and 0.1mm/rev, 1%, 300x.	116
4.52-Optical microstructure view of section through quick stop sample for 22m/min and 0.15mm/rev, dry, 150x.	116
4.53-Optical microstructure view of section through quick stop sample for 22m/min and 0.15mm/rev, 0%, 150x.	117
4.54-Optical microstructure view of section through quick stop sample for 22m/min and 0.15mm/rev, 1%, 150x.	117
4.55-Optical microstructure view of section through quick stop sample for 30m/min and 0.05mm/rev, dry, 300x.	118
4.56-Optical microstructure view of section through quick stop sample for 30m/min and 0.05mm/rev, 0%, 300x.	118
4.57-Optical microstructure view of section through quick stop sample for 30m/min and 0.05mm/rev, 1%, 300x.	119
4.58-Optical microstructure view of section through quick stop sample for 30m/min and 0.1mm/rev, dry, 300x.	119
4.59-Optical microstructure view of section through quick stop sample for 30m/min and 0.1mm/rev, 0%, 300x.	120
4.60-Optical microstructure view of section through quick stop sample for 30m/min and 0.1mm/rev, 1%, 300x.	120
4.61-Optical microstructure view of section through quick stop sample for 30m/min and 0.15mm/rev, dry, 300x.	121
4.62-Optical microstructure view of section through quick stop sample for 30m/min and 0.15mm/rev, 0%, 100x.	121
4.63-Optical microstructure view of section through quick stop sample for 30m/min and 0.15mm/rev, 1%, 300x.	122
4.64-Optical microstructure view of section through quick stop sample for 40m/min and 0.05mm/rev, dry, 300x.	122

4.65-Optical microstructure view of section through quick stop sample for 40m/min and 0.05mm/rev, 0%, 300x.	123
4.66-Optical microstructure view of section through quick stop sample for 40m/min and 0.05mm/rev, 1%, 300x.	123
4.67-Optical microstructure view of section through quick stop sample for 40m/min and 0.1mm/rev, dry, 150x.	124
4.68-Optical microstructure view of section through quick stop sample for 40m/min and 0.1mm/rev, 0%, 300x.	124
4.69-Optical microstructure view of section through quick stop sample for 40m/min and 0.1mm/rev, 1%, 300x.	125
4.70-Optical microstructure view of section through quick stop sample for 40m/min and 0.15mm/rev, dry, 300x.	125
4.71-Optical microstructure view of section through quick stop sample for 40m/min and 0.15mm/rev, 0%, 150x.	126
4.72-Optical microstructure view of section through quick stop sample for 40m/min and 0.15mm/rev, 1%, 300x.	126
4.73-Quick stop sample for dry condition at 30m/min and 0.1mm/rev, 18.6x.	127
4.74-Quick stop sample for dry condition at 40m/min and 0.05mm/rev, 22.9x.	128
4.75-Detail of the BUE of the sample of figure 4.74, 164x.	128
4.76-Quick stop sample for lubricated (0%) condition at 22m/min and 0.15mm/rev, 23.9x.	129
4.77-Quick stop sample for lubricated (0%) condition at 40m/min and 0.05mm/rev, 26.2x.	129
4.78-Detail of the BUE of the sample of figure 4.77, 213x.	130
4.79-Quick stop sample for lubricated (5%) condition at 40m/min and 0.05mm/rev, 20.3x.	130
4.80-Detail of the BUE for lubricated (5%) condition at 22m/min and 0.1mm/rev, 168x.	131
4.81-View of machined surface on the electron microscope, 22m/min, 0.05mm/rev, dry, 200x.	133
4.82-View of machined surface on the electron microscope, 22m/min, 0.05mm/rev, 5%, 200x.	133

4.83-View of machined surface on the electron microscope, 22m/min, 0.1mm/rev, dry, 197x.	134
4.84-View of machined surface on the electron microscope, 22m/min, 0.1mm/rev, 5%, 197x.	134
4.85-View of machined surface on the electron microscope, 22m/min, 0.15mm/rev, dry, 202x.	135
4.86-View of machined surface on the electron microscope, 22m/min, 0.15mm/rev, 5%, 228x.	135
4.87-View of machined surface on the electron microscope, 30m/min, 0.05mm/rev, dry, 100x.	136
4.88-View of machined surface on the electron microscope, 30m/min, 0.05mm/rev, 5%, 202x.	136
4.89-View of machined surface on the electron microscope, 30m/min, 0.1mm/rev, dry, 99.4x.	137
4.90-View of machined surface on the electron microscope, 30m/min, 0.1mm/rev, 5%, 202x.	137
4.91-View of machined surface on the electron microscope, 30m/min, 0.15mm/rev, dry, 202x.	138
4.92-View of machined surface on the electron microscope, 30m/min, 0.15mm/rev, 5%, 225x.	138
4.93-View of machined surface on the electron microscope, 40m/min, 0.05mm/rev, dry, 205x.	139
4.94-View of machined surface on the electron microscope, 40m/min, 0.05mm/rev, 5%, 200x.	139
4.95-View of machined surface on the electron microscope, 40m/min, 0.1mm/rev, dry, 196x.	140
4.96-View of machined surface on the electron microscope, 40m/min, 0.1mm/rev, 5%, 202x.	140
4.97-View of machined surface on the electron microscope, 40m/min, 0.15mm/rev, dry, 197x.	141
4.98-View of machined surface on the electron microscope, 40m/min, 0.15mm/rev, 5%, 200x.	141
5.1-Extrapolation of the results of temperature measured for dry cut at 40m/min and 0.15mm/rev.	145

5.2-Machining chart for WC+6%Co tool cutting 0.4% steel with hardness 200HV [5].	149
5.3-Electron microscope view of a quick stop sample for lubricated (0%) condition, 30m/min, 0.15mm/rev, 26.8x.	150
5.4-Electron microscope view of a quick stop sample when oil without sulphur is applied, 30m/min, 0.05mm/rev, 447x.	151
5.5-Electron microscope view of a quick stop sample for dry condition 40m/min, 0.1mm/rev, 21.3x.	152
5.6-Orthogonal cutting operation with BUE.	160
5.7-The cooling capacity of pure water [156].	165
5.8-Machined surface for dry cutting, 40m/min, 0.15mm/rev, 143x.	170
5.9-Same as figure 5.8, 469x.	170
5.10-Same as figure 5.8, 1020x.	171
5.11-View of the point where the cutting edge loses contact with the workpiece, 40m/min, 0.15mm/rev, dry, 296x.	173
5.12-View of the point where the cutting edge loses contact with the workpiece, 40m/min, 0.15mm/rev, 5%, 296x.	174
5.13-Machined surface of the workpiece of figure 5.12, 99x.	174
5.14-Electron microscope view of a machined surface, 40m/min, 0.05mm/rev, dry condition, 102x.	175
5.15-Same as figure 5.14, 201x.	176
5.16-Split workpiece.	177
5.17-Electron microscope view of a sample of machined surface of the workpiece of figure 5.16, 35m/min, 0.14mm/rev, dry condition, 348x.	177
5.18-Alteration of the machined surface by squeezed BUE and the action of cutting fluid.	178
6.1-Optimised tool geometry to improve surface finish.	186
A.1-Initiation of cut: a-tool touches the workpiece; b-elastic deformation; c-plastic deformation; d-about to start to cut.	215
A.2-Modes of deformation observed in the sliding of a hard spherical	217

A.3-The contact of a cylinder and a plane	218
A.4-Residual cutting forces. a)cutting force F_c , b)feed force F_f .	220
A.5-Shapes left on the material by a pyramidal indenter.	224
A.6-Cutting force against time, 22m/min, 0.001mm/rev.	225
B.1-Variation of workpiece temperature against power on shear plane.	231
B.2-Relationship between the coefficient of partition and temperature of the workpiece.	233
B.3-Variation of β with cutting speed when there is no BUE (after [3]).	234

List of Tables

3.1-Mechanical and physical properties of AISI 1040 steel [146].	65
4.1-Cutting forces and standard deviation.	82
4.2-Measured forces (F_c) used in an analysis of variance, 30m/min, 0.15mm/rev.	87
4.3-Temperature rise on transient surface.	89
4.4-Chip thickness for all the cutting conditions.	99
4.5-Primary shear plane angle for all cutting conditions.	103
4.6-Surface finish for all cutting conditions.	106
B.1-Work expended on the process.	230

Nomenclature

BUE	=	built-up edge
c	=	specific heat
d	=	width of cut
F	=	tangential force
F _c	=	cutting force
F _f	=	feed force
F _n	=	normal force on the rake face
F _{nz}	=	normal force on the primary shear plane
F _t	=	shear force on the rake face
F _u	=	resultant of force acting on the rake face
F _u	=	resultant of force acting on the primary shear plane
F _z	=	shear force on the primary shear plane
f	=	feed rate
N	=	normal force
N _c	=	cutting power
N _f	=	feed power
R _a	=	average roughness
r	=	nose radius
T	=	temperature
T _b	=	temperature of the bar
T _s	=	temperature of surface
t	=	time
t ₁	=	undeformed chip thickness
t ₂	=	chip thickness

s_c	=	standard deviation of cutting force
s_f	=	standard deviation of feed force
V_s	=	shear speed
V_c	=	cutting speed
V_{chip}	=	chip speed
v	=	volume
w	=	depth of cut
ℓ	=	contact length between chip and tool after BUE
α	=	clearance angle
β	=	proportion of heat that goes into the workpiece
χ	=	approach angle
ϕ	=	primary shear plane angle
γ	=	rake angle
μ	=	friction coefficient
ν	=	Poisson's ratio
ρ	=	density

1 INTRODUCTION

Machining is the most widely used process of manufacturing, and metals and alloys are the bulk of materials used in this process. Therefore the subject of metal cutting has been the focus of many researches and has produced several publications. Since man started to machine these materials many problems have developed and many solutions and ideas have been proposed. Great progress was achieved in increasing the metal removal rate and reducing the costs.

Increasing the metal removal rate means that more material can be cut in a shorter time and this has been achieved by increasing the cutting speed, feed rate and depth of cut. To do this in an economical way depends on many areas related to metal cutting: the machine tool, the cutting tool, cutting fluid and materials.

In respect of machine tools, it is necessary to increase power and accuracy. At the same time they are developed in such way as to facilitate their operation, change of cutting conditions, change of cutting tool and workpiece. Some cutting tool materials that are brittle like ceramics need to be used on rigid machines.

The increase in power to remove more material in a shorter time increases the heat generation near the cutting edge of the tool, as the power consumed in metal cutting is largely converted into heat [1,2]. This heat is dissipated by the four systems processing the material: the cutting tool, the workpiece, the chip formed and the cutting fluid.

This means that the cutting tool needs to support higher temperatures at acceptable wear rates. Normally the temperature achieved by the cutting tool is the factor that limits the rate of machining. This forced the developments of new materials for the cutting tools that can resist high temperatures. Moreover in some

operations which have an interrupted cut, like milling, the tool has to resist a thermal cycle, mechanical shock and needs to have good toughness to support high cutting speeds.

The effects of cutting temperature on surface integrity of the workpiece may be more important than the tool life [3,4].

As temperature is of fundamental importance in a metal cutting operations many attempts have been made to predict it and many methods have been developed to measure the temperature.

The cutting fluids used with some cutting operations play a very important role and many operations cannot be efficiently carried out without a fluid. Among their functions, they are used to cool the tool, workpiece and machine tool. They may act as a lubricant at the interface of tool-chip [5], depending on the conditions. At high cutting speeds it is unlikely that the fluid reaches this interface and some different forms of application have been experimented with [6], as well as the use of other ways of lubrication, using gases for example. If the fluid acts as a coolant it will remove heat from the cutting zone, and can help to increase tool life and prevent excessive dilatation of workpiece. If the fluid acts as a lubricant it will decrease the work done and so the heat generation. Both ways of acting should reduce the temperature. Lubrication can be effective at low cutting speeds where the aim is to increase tool life and improve surface finish. The better surface finish obtained at low cutting speeds when cutting fluid is applied is attributed to the lubrication of the rake face and consequently elimination of the built-up edge (BUE).

Surface finish of a workpiece is usually the most important parameter to be controlled in industrial application of the machining process. It will be dependent on the material, tool, process and cutting parameters like tool geometry, speed and feed

rate. A finishing operation is performed at high cutting speeds and low feed rates whenever it is possible to avoid the formation of BUE, which gives poor surface finish. During the operation tool wear and vibration of the tool and machine tool can also affect surface finish and so they need to be controlled.

The developments of new materials and alloys forced the developments of new cutting tool materials. Moreover, in respect to the work material much has been done to decrease the wear rate of tools through alloying. These additions behave like a solid lubricant at the interface between the tool and chip decreasing the stress and heat generation and decreasing the cutting force and so the work done [7]. Sulphur and lead are the main elements used in steel and they also promote other advantages, eg more easily handled chips.

This work studies the effect of a mineral oil lubricant and sulphur (an E.P. additive) on machining of AISI 1040 steel at low cutting speed. The effect is measured through cutting forces, surface roughness, chip thickness and workpiece temperature measured during the cut. Conventional equipment is used to measure forces, roughness and chip thickness but to measure workpiece temperature a new method was developed. An infrared sensor is used to measure temperature on the transient surface of the workpiece. Also samples of the machined surface are analysed in the scanning electron microscope to compare the effects of the lubricant on surface geometry. Chip samples obtained with the use of a mechanism of rapid stopping of the tool action (quick stop) are examined to detect the conditions where there is a BUE formation and to help to explain the lubrication action.

Chapter 2 gives a literature review on the machining process with special attention paid to research on BUE formation, surface integrity and heat generation. Chapter 3 describes the methodology used in the experimental tests and gives details

of the method used to measure temperature using an infrared sensor. The results are presented in chapter 4 followed by a discussion of the results in chapter 5, where the main objective is the discussion about the effect of lubrication on BUE size and how lubrication can improve surface finish. Some suggestions for future work that could continue the investigation into this subject are given in chapter 6 and finally the conclusions are presented in chapter 7.

2 LITERATURE SURVEY

The manufacturing processes can be classified in general according to the form of energy used to transform the material. They can be divided into two main classes: the processes that use stress and those that use heat as the main form of energy. Each class can be further separated in two sub-classes. The processes that use stress can be grouped into those when the stress is less than the rupture strength of the material being processed and those when the stress is higher. The ones that utilise thermal energy can be divided into the processes where the temperature is less than the melting point of the processed material and those that melt the material to manufacture. Figure 2.1 illustrates these divisions with some examples for each class. A more complete definition and specific characteristic for each process can be found in the literature [8,9,10,11].

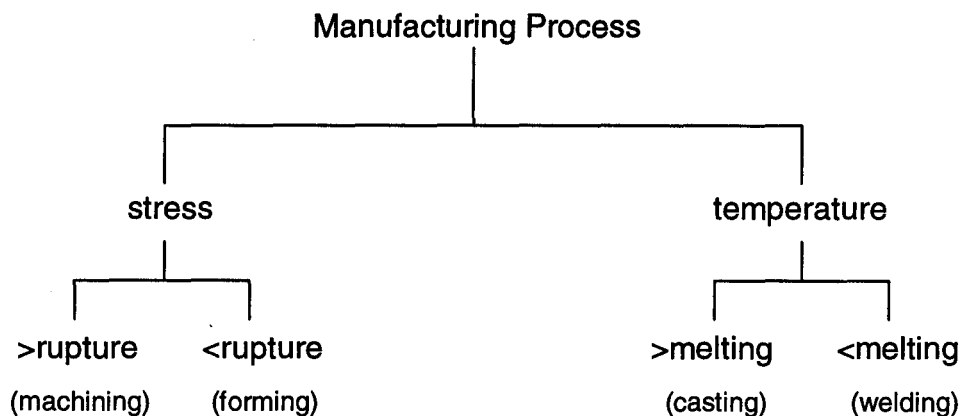


Figure 2.1 Manufacturing process according to the form of energy.

Machining is a process that utilises stress as the main form of energy to manufacture parts, and the applied stress is higher than the rupture limit of the material. It is the most used process of manufacturing and can be performed with almost all materials: metal, plastic, ceramic or composites. However metals are the

most used material and the term Metal Cutting is employed for machining operations using metal for the material of the workpiece [5].

To apply this stress it is necessary to have a tool that is harder than the material being processed and a machine tool to give the necessary relative movement between tool and workpiece. Material is then removed by a process of extensive plastic deformation and controlled fracture.

Machining is a generic nomenclature that covers a variety of different processes. According to the relative movement and the geometry of the tool it can be separated into different operations. Turning, milling and drilling are some examples of the most widely used machining operations. Each one of these has in turn a different form, different tool geometry and relative movements. Nevertheless some features are common to all the operations and conclusions from a research using one process can be extended to another. For example the action of the tool that results in the formation of a new surface and the chip and the effect of parameters like cutting speed, feed rate and depth of cut.

To understand the process better some definitions and nomenclatures are necessary as a first step. The next sections give some definitions and concepts used in this work and review some relevant work that has been done in the area of metal cutting.

2.1 Machining Process

Perhaps the most simple and complete definition of the cutting process that can be used for every machining operation is: the action of a tool, harder than the workpiece material, to remove material (in form of swarf) and give the final dimension and shape to the workpiece. The form of this action can vary depending on

the machining process. A turning operation is the most simple of them and is used to define some common terms and is the operation used in most of the research done due to its simplicity, mainly because of the cutting tool geometry and movements.

A turning operation using a single point tool can be used to define some parameters involved in the process. These parameters are the relative speeds and their direction, the geometry of the tool and the parameters that give the amount of material removed. A simple turning process is illustrated in figure 2.2 which shows some terminology and the most important parameters for this operation: cutting speed, feed, depth of cut, rake angle, clearance angle and approach angle.

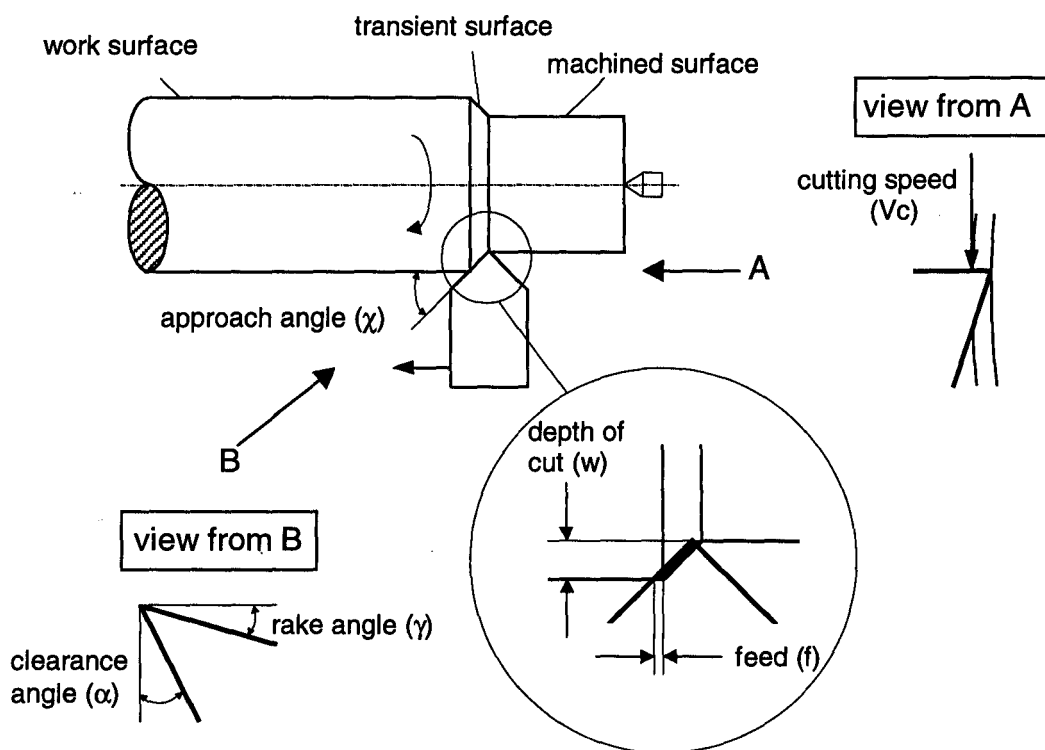


Figure 2.2 A turning operation using a single point tool.

The cutting speed, V_c , is given by the speed of the rotation of the workpiece and is normally measured considering the tool as stationary. It is the speed of the outside diameter of the workpiece, frequently measured in m/min. This is one of the

differences between turning and milling for example. While for the first one the cutting speed is given by the workpiece, in the last one the tool is moving and the workpiece is stationary.

While the workpiece is rotating the tool is moving in a direction parallel to the axis of the workpiece. This movement is the feed speed, normally it is measured by the increment at each revolution of the workpiece and it is called feed rate, f , and measured in mm/rev. The depth of cut, w , is the penetration of the tool into the workpiece to remove material, measured in a radial direction.

These three parameters, cutting speed, feed rate and depth of cut give the volume of material that is removed in the operation. The rate of metal removal is the product of cutting speed, feed and depth of cut ($V_c \cdot f \cdot w$). Thus, these parameters have a very important effect on machining.

For this simple operation illustrated in figure 2.2, the geometry of the tool is made very simple as well. However the main geometric parameters can be defined as rake angle (γ), approach angle (χ), rake face, cutting edge, clearance face (or flank face), clearance angle (α) and nose radius (r). The rake face is the surface where the chip flows after being formed. The rake angle is the angle of the tool rake face with the direction of feed and measured in a plane perpendicular to the cutting edge. A positive rake angle means that the rake face dips below the direction of feed. The approach angle is the angle of the cutting edge with the direction of the feed movement, measured in a plane perpendicular to the cutting speed.

More complete definitions are necessary for others processes, like milling for example, which can use more than one cutting edge at the same time and the cutting action is not continuous. This discontinuity has great effect on forces and temperatures. Complex and complete definitions of the terms, movements and

geometry can be found in standards and handbooks [12,13].

In respect of the tool, complex geometry is used in turning operations as well to improve the process. For this tool a simple definition using rake angle and approach angle could be very vague. Examples of such tools are those that have some grooves or obstructions on the rake face to control the shape or size of the chip formed or act as chip brakes.

Because the machining process is complex to study, some simplifications are made to facilitate analytical treatments. This is done in the orthogonal cutting. In the orthogonal cut the cutting edge is straight, perpendicular to cutting speed and to the feed direction. For this simplification the chip formation can be considered in two dimensions only, which takes place in a plane perpendicular to the cutting edge. A good approximation to such a process is the turning of a tube where the length of the cutting edge is bigger than the wall thickness.

Further simplifications are made in orthogonal cutting to simplify or allow analytical treatment. The chips formed are continuous, there is no BUE (see section 2.2) and the chip simply slides against the rake face of the tool. There is no spread of material due to the compression of the tool, and there is no contact of the machined surface with the tool flank face. Figure 2.3 illustrates the orthogonal process.

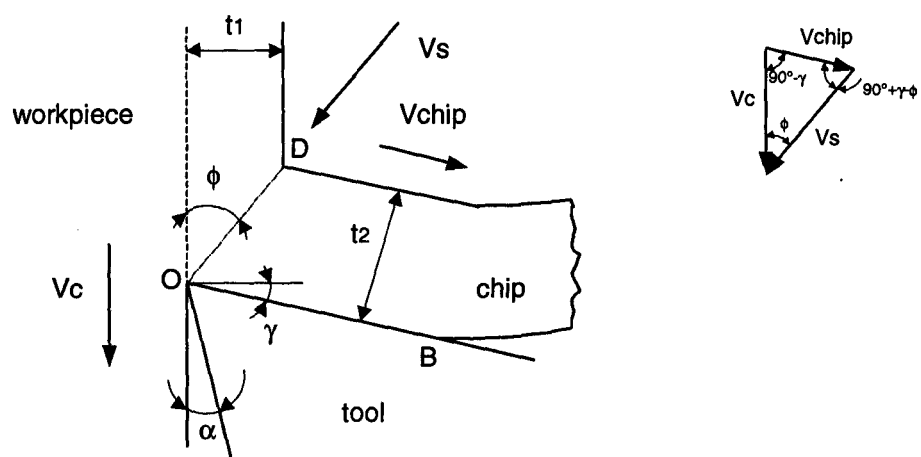


Figure 2.3 Orthogonal cutting.

2.2 Chip Formation

Using the orthogonal cut illustrated in figure 2.3, the action of the tool to form the chip can be simplified. The portion of the workpiece inside the undeformed thickness (t_1) approaching the tool will be under compression. This causes upsetting in the material until the shear strain limit of the material is reached. After that point the chip and the new machined surface are formed by shearing along the plane OD in figure 2.3. This plane is called the primary shear plane and its inclination relative to the direction of the cutting speed will be determined among others things by the material strength, cutting speed and rake angle. This inclination is measured by the primary shear plane angle, ϕ . It can be calculated using the values of the chip thickness (t_2), rake angle, and the undeformed thickness as:

$$\cot \phi = \frac{(t_2 / t_1) - \sin \gamma}{\cos \gamma} \quad (2.1)$$

It can be determined experimentally by direct observations of the cut to give an indication of the amount of deformation.

Some attempts to determine it as a function of some geometric parameters, friction on the rake face and properties of the workpiece material can be found in the literature [14,15,16]. The pioneer works of [14,15] consider that this angle will be such a value that the cutting force is minimum.

As the material is upsetting the chip is thicker than the undeformed thickness. Therefore, to allow continuity of movement the speed at which the chip moves along the tool rake face (V_{chip}) has to be lower than the cutting speed. Another velocity can be identified in the process, the velocity of shear on the primary shear plane, V_s . The ratios of V_{chip} and V_s to V_c according to the triangle of velocities in figure 2.3 are:

$$\frac{V_{chip}}{V_c} = \frac{t_1}{t_2} = \frac{\sin \phi}{\cos(\phi - \gamma)} \quad (2.2)$$

$$\frac{V_s}{V_c} = \frac{\cos \gamma}{\cos(\phi - \gamma)} \quad (2.3)$$

The orthogonal cut assumes a continuous chip being formed, but that is not always the case. The material is under a shearing action on the primary shear plane and when the compressive stress acting can prevent the propagation of any crack that could form there avoiding rupture the result is a continuous chip. This is the case in ductile materials like most of the steels (except at very low cutting speeds). In other cases the stress field on that plane can cause the rupture of the chip and a discontinuous one is formed. Grey cast iron is an example of material that produces a discontinuous chip. Depending on the cutting conditions an intermediary class of chip can be formed, the segmented chip [17]. This is the chip formed when machining alloys with poor thermal conductivity, like titanium alloys. Basically the form of the chip is determined by the material properties. Therefore a ductile material will form a continuous and long chip and a brittle material will form small discontinuous chips.

Chips can have different shapes and a classification of them can be found in [18]. Long chips are a problem in machining and some special tool geometry can be used to overcome the problem. Chip breakers are used to break the chip or change its shape to one that can be easily handled [19]. Control of chips is important when machining some ductile materials at high cutting speeds because the long chip formed can cause many problems for the operation. Long chips are difficult to handle, can affect the surface of the workpiece and mean high disposal volume. Chip breakers can be some obstacles on the tool to force the chip to change its direction of movement or even to force them to break. There are other ways to break the chip during cutting the

application of a cutting fluid at high pressure is one of them [6].

The shape and class of the chip formed is very dependent on the contact against the tool rake face.

The chip is formed and moves over the rake face of the tool, with a contact length OB in figure 2.3. This is not a simple sliding movement of two surfaces. The area of contact between chip and tool is very small and so the pressure is very high. This high pressure is enough to seize the chip avoiding movement at the interface. A strong bond is formed in that region and the movement of the chip is by shearing in its body, being the weaker material of the pair. Assuming that the deformation is restricted to a thin region, this interface is called secondary shear zone and will be described in more detail in section 2.4.

The force necessary to move the chip over the rake face affects the primary shear angle. The shear plane angle decreases as this force increases (chip thickness t_2 increases, equation 2.1), and the movement of the chip is more difficult. This interface between chip and tool is the target of lubrication. It is believed that a lubricant can act on that area and avoid seizure, or at least decrease the contact decreasing forces and tool wear.

It is assumed that the machined surface after being formed does not slide against the tool flank face if the tool is sharp. Contact between these two surfaces happens only if there is flank wear. This is unlikely to happen in a real cutting operation. Contact will exist there as on the rake face, and seizure conditions can exist [20]. For most ductile material there is some elastic deformation during cutting [21]. This elastic deformation suggests that a contact with the tool flank face is expected. In an orthogonal cutting it means that the tool needs to penetrate a specific distance into the material before starting to cut.

This makes the interface another deformation zone, and in some cases more important than the secondary shear zone, as it will directly affect the workpiece. If there is conditions of seizure, the deformation to allow the continuity of the movement takes place into the workpiece material leaving a deformed layer. This is another region where lubrication could have an effect.

2.3 Cutting Forces

Force measurements in machining are important for many reasons. From the point of view of the machine tool, the forces are an important parameter to be considered in the design and power of the machinery. Forces can limit the rate of removal of material because of deformation of the tool. Depending on the size of the workpiece it can affect the final dimensions or it can deform the workpiece. It is one of the most important considerations regardless of process limitation and design aspects [11].

An ideal cutting operation will require a force to shear the material on the primary shear plane to form the chip and the machined surface and the force to move the chip over the tool rake face on the secondary shear plane. Considering the resultant of these forces acting on the tool, there will be a force, F_u , acting in a specific direction upon the secondary shear plane. As a reaction there will be another force acting on the workpiece on the primary shear plane, F'_u . Resolving these forces on the respective plane result in two sets of forces: a normal force and shear force for each plane (F_n and F_t for the tool, and F_{nz} and F_z for the workpiece). These forces are represented for an orthogonal cut in figure 2.4.

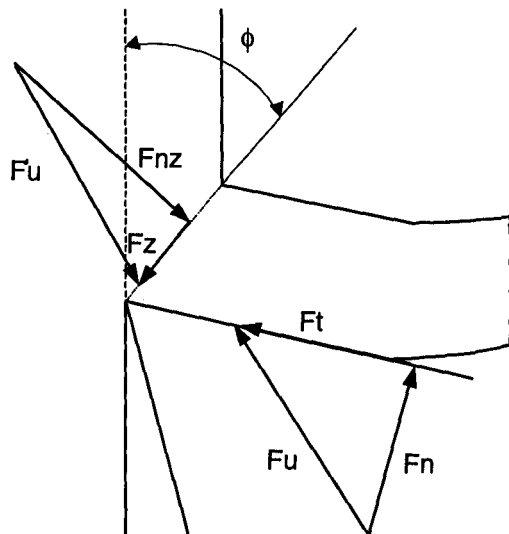


Figure 2.4 Forces acting on the primary and secondary shear planes [22].

The forces can be also resolved in the direction of the cutting speed and the feed resulting in the cutting force F_c and feed force F_f respectively. Considering the resultant force (F_u or F_u) acting on the cutting edge instead of the tool rake face or shear plane, it is possible to draw a convenient diagram shown in figure 2.5. The resultant force is the diameter of the reference circle. According to geometric properties of a right-angled triangle, the resultant force can be resolved into orthogonal components in any direction. The reference circle is called Merchant's circle.

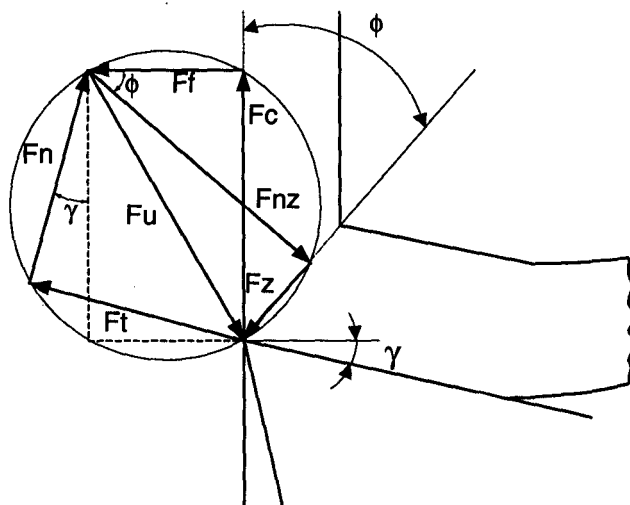


Figure 2.5 Cutting forces in orthogonal cutting represented by the Merchant circle [22].

In a single cutting operation as in figure 2.2, there is another force called thrust force F_t in the direction perpendicular to the cutting speed and feed. This force tends to push the tool away from the workpiece in a radial direction. Therefore in a cutting operation three forces are measured: cutting force F_c , feed force F_f , and thrust force F_t . The cutting force is the most important and is normally the highest, responsible for most of the work done during the process.

The power expended is the product of the forces and the respective speed components. Therefore the cutting power, N_c , is the product of the cutting force F_c by the cutting speed V_c . The feed power, N_f , is the product of feed force F_f (resolved in the rake face) by the speed of the chip, V_{chip} . According to this, the power necessary to shear the material on the primary shear plane for an orthogonal cutting operation (where the total power is equal to the cutting power) is:

$$N_s = N_c - N_f \quad (2.4)$$

Regarding the chip formation process, these forces will be dependent on two main factors:

- the length of contact between chip and tool;
- the shear strength of the workpiece material.

Any affect on these two factors has an effect on cutting forces. This includes materials (workpiece and tool) properties, tool geometry, tool wear, lubrication, cooling, and cutting conditions (cutting speed, feed rate and depth of cut). Forces increase with decrease of rake angle or increase in ductility of the workpiece material for example. Normally forces decrease with cutting speed because the temperature affects the material properties. An understanding of the conditions at the chip tool interface is fundamental to understanding the causes of variation of cutting forces.

Measuring forces in machining can give a good indication of the effects of these parameters.

2.4 Chip Tool Interface

In early attempts to formulate a theory for chip formation and the simplification in orthogonal cutting, the contact between tool and chip is considered as simple sliding. A coefficient of friction can then be calculated measuring the normal and tangential force and applying Coulombs law. As was stated in the last section this region is referred to as a secondary shear zone. This is because there is adherence between the two different materials (chip and tool) and sliding is not possible. This adherence is caused by the high compressive stress, which can be 3.5 GPa for some steels [19].

The Coulomb law can be applied in movements where the contact between surfaces is supported only by the asperities of both. When two surfaces are placed in contact, the tips of the asperities, which will support the load, form the first areas of contact. As this load increases, the area of contact increases. The increase in the area is due to the plastic deformation of the asperities that are in contact and new contact being formed by new asperities. The friction force is then a measure of the force necessary to brake these contacts to enable movement over the surfaces. For this case an increase in the normal load increases the friction force and a friction coefficient, which is proportional to the load, can be calculated.

This theory applies only when the real area of contact is smaller than the apparent. This is not the case in machining where the pressure is high enough for the surfaces to be in contact only at their asperities. Both surfaces will be in intimate

contact and the real area will be practically equal to the apparent. For this situation, the friction force is not proportional to the load any more, and will depend on the area of contact. There is adhesion between the surfaces instead of simple sliding movement and the high pressure that acts on the contact makes shearing between the two surfaces impossible and so shear will occur within the weaker material of the pair, in this case the chip. This forms another shear zone, the secondary shear zone [5].

Adhesion between metal surfaces depends on their cleanness [23]. If the surfaces are clean, free from oxide and other surface films and from adsorbed phases, then adhesion is observed between metals. A simple contamination by fingerprints is enough to change the contact and depending on the materials, oxide can eliminate adhesion or decrease the real area of contact. This effect of lubrication is verified in experiments with very clean metallic surfaces in high vacuum. The surface of the chip is a new and fresh surface and is free from any contamination. When it moves over the tool rake face it will clean it, creating conditions for adherence between them.

Through analyses of chip samples, obtained using a quick stop device [24], evidence for the conditions of seizure (or sticking) that exist at the tool work interface has been found. Actually due to the conditions of contact at the rake face the contact will vary from simple sliding to seizure and this depends on the stress distribution.

A model for the stress distribution on the tool rake face was proposed by [25]. Figure 2.6 shows this model, where the contact length is divided into two distinct regions: the sticking zone and the sliding zone. According to this model, the compressive stress is maximum at the cutting edge and decreases exponentially to zero in the point where the chip leaves the tool. The shear stress is constant through the sticking zone and then decreases exponentially, in the sliding zone, until zero at

the point where the chip leaves the tool.

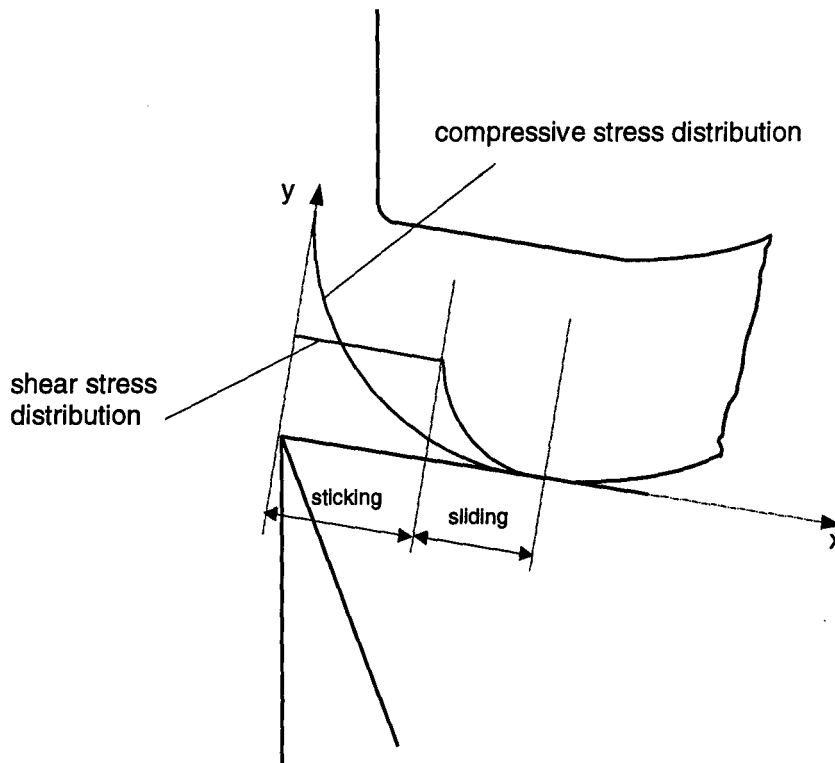


Fig.2.6 Stress distribution on tool rake face [25].

As the compressive stress decreases there is a possibility for the occurrence of sliding. Sliding can be observed at the periphery of the contact [26], where there is no flow zone.

In the sticking zone, the movement of the chip occurring through shearing within it, there is a gradient of speed in a thin region of the chip close to the interface. The material in this region is extremely highly deformed at extremely high strain rates, about 10^4 s^{-1} [5]. At high cutting speed, where the heat generation, and so the temperature, are high, the material deformation is like a viscous fluid movement and this zone is often referred to as a flow zone. The thickness of the flow zone varies normally between 0.01 and 0.08mm [27].

This deformation generates heat that is dissipated by the chip and tool. This heat affects the material deformation behaviour under stress. Therefore the conditions

in that region are dependent on the rate of strain and temperature [28].

Under strain the material will workharden, but this effect can be combined with the softening effect of temperature (recrystallisation), if there is enough time. Workhardening and recrystallisation will then be very dependent on the cutting speed, and so will the conditions at the chip tool interface.

2.4.1 Built-Up Edge

For some materials and certain cutting speeds instead of a flow zone at the chip tool interface, there is a built-up edge (BUE). When low cutting speeds are unavoidable (e.g. the use of small diameter drills) a phenomenon called built-up edge, is formed by material that adheres to the rake face of the tool. It is present during the cutting operation instead of the flow zone described in the last section. Figure 2.7 shows a schematic illustration of a BUE for orthogonal cutting with a continuous chip.

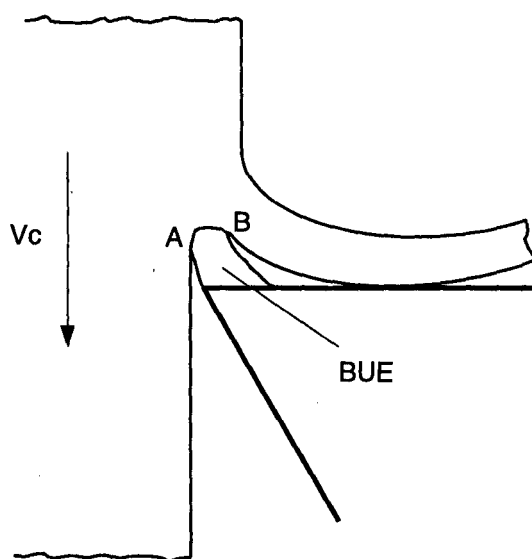


Figure 2.7 Built-up edge.

Before the tool starts to cut its surfaces are contaminated by grease and oxides, and these lubricate the contact with the chip. When the very first chip slides over the tool there is no adherence, but eventually by cleaning the surface of the tool it creates conditions of adherence for the next portion of material [29]. Once the first material or layer of material adheres to the tool, the movement of the chip is by shearing action inside the chip and there is no slip on the rake face. The adhered layer will suffer very high strains at very high strain rates and inevitably it strainhardens. A second layer of material can deposit and adhere to the first one and this occurs successively until BUE forms. As a consequence, instead of a thin flow zone there will be a considerable amount of material deposited on the rake face and the secondary shear zone is at some distance from the tool, with the BUE acting as an extension of the tool.

It is possible that once the BUE begins to nucleate, or the first layer adheres to the tool, adhesion between the work material (already on the tool face) and the chip follows (adhesion occurring between the same material) [30]. The adhesive shearing force between identical metals is generally much larger when compared to that of different materials.

In the orthogonal cut illustrated in figure 2.3, the under surface of the chip and the machined surface are formed by shearing action on the primary shear zone. Both surfaces form near the tool cutting edge. When there is a BUE these surfaces are formed at different regions. The machined surface is formed by fracture at position A, and the chip is formed at B, figure 2.7.

Once a BUE is formed it can be a stable structure or it can disappear and form again periodically. If it is an unstable structure it will lose some parts that are carried away with the under side surface of the chip or with the machined surface. They can be loose parts, which can damage the surface or they can still be attached to the

surface of the material. In both ways they will contribute to poor surface finish. BUE is not uniform along the rake face and neither is the machined surface generated in such conditions.

One important conclusion from the past research on the BUE is the fact that it does not form for every material. There is no BUE when machining pure metals for example. In this case the material is still adhering to the tool surfaces, workhardening, but instead of BUE there is just what is called a built-up layer of material on the rake face. It is suggested that a second phase in the material is required, and a difference in ductility between the second phase and the matrix in order to form a BUE. In experimental work machining various materials (single phase alloys, two phase alloys and free machining alloys) [31], it was observed that single phase materials have a smaller chip-tool contact length than two phase and only the last one forms a BUE. The presence of the second phase will limit the ductility resulting in fracture of the material along the tool rake face to form the BUE. Reduction in ductility, by non-metallic inclusions for example, may lead to the elimination of a big BUE. That is the principle in the free-machining alloys. [32] describes the effect of soft additives (Pb, Bi) on the BUE formation and the effect of BUE on several aspects of machinability and observed that they can reduce the size of BUE because they increase the formation and propagation of microfractures. [33] studied the effect of carbon content, inclusion type and metallurgical conditions on formation of BUE and suggested that the relative plasticity of the inclusions or phases in the material associated with a triaxial stress system controls the formation of the BUE. Apart from the second phase in the material to form the BUE, the plasticity of the phases needs to be different. The size of the BUE depends on this difference.

The cutting speed seems to be the most important parameter affecting BUE

formation. For very low cutting speeds there is no BUE, and the chip seems to simply slide against the rake face of the tool. As the cutting speed increases BUE starts to form, and will increase in size with cutting speed. The size of BUE reaches a maximum and then starts to decrease until it disappears. This behaviour is noticed in a graph of cutting force against cutting speed where critical cutting speeds can be defined. These speeds are the cutting speed when BUE starts to form, when its size is maximum and when it disappears. When the BUE increases in size the cutting force decreases, because of the effects of a greater apparent rake angle. As the BUE starts to decrease the force increases again until a maximum. After the BUE disappears the increasing temperature in the cutting zone decreases the force necessary to cut the material.

One effect of cutting speed is to change the temperature in the cutting zone, affecting the cutting conditions. The temperature increases with cutting speed and it affects the adhesion forces and the material properties.

The results of the experiment [30] show that the adhesive shearing force will be independent of the contact pressure after a specific value. This value decreases with increasing temperature. When the contact pressure is kept constant and temperature is variable the adhesive shearing force normally increases with temperature until a certain value (about 600°C for the material used by this author) and then decreases. They then associated temperature with cutting speed to compare with a cutting test to show the range of BUE formation.

Cutting temperature has been shown to affect the shape and size of the BUE [29] after observations of samples obtained using a mechanism of rapidly stopping the tool. The BUE shape was classified or divided into four different categories, namely positive wedge, rectangular, negative wedge and layer. These shapes are illustrated in

figure 2.8. The change from one class to another was explained by the effect of temperature and temperature distribution.

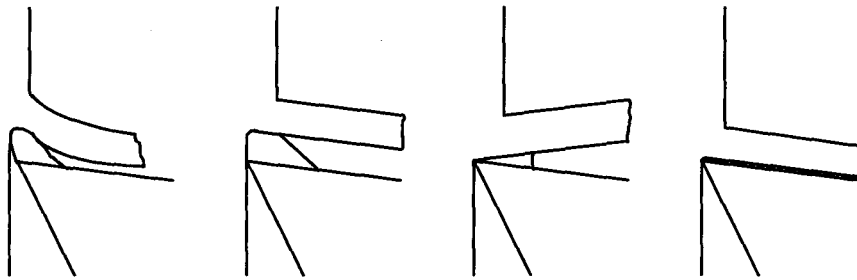


Figure 2.8 Different shapes of the BUE [29].

According to [34] the increased temperature and consequently increased plasticity of the work materials results in a reduction in thickness of the zone under secondary flow and a more or less rectangular shape results. The negative wedge is a result of the falling temperature gradient and consequently decreasing plasticity of the layers along the tool-chip contact length.

[33] also detected the same shapes of BUE. The transition between them is a phenomenon resulting from a combination of the amount of deformation necessary to cause microcracking and the temperature generated by the transformation of the work expended during deformation.

Feed rate increases the size of the BUE and depth of cut has no effect. The geometry of the tool affects the formation of BUE, the rake angle being the main parameter. As the rake angle increases the BUE disappears and the critical cutting speeds change.

The BUE forms because of adhesion between the material of the workpiece and the material of the tool, therefore the friction of the chip on the tool rake face has a great affect on its formation. A lubricant that could penetrate the interface between chip and tool may prevent adherence and so BUE formation. This fact is used to

explain why a lubricant improves surface finish. Because temperature affects adherence and the properties of the material and BUE size, a coolant can have an effect if it can cool the cutting zone very quickly.

2.4.2 Effect on Tool Wear

Tool wear is also affected by BUE. It acts like a tool cutting the material and can even protect the tool surface from contact with the chip and machined surface. However if the bond with the tool is so strong that parts of the cutting tool go with the broken part of the BUE this can be quite damaging to the tool. This is one of the wear mechanisms that are acting in the process of metal cutting and is termed attrition [5]. Abrasion is another wear mechanism. [35] studied BUE formation and its effect on tool wear for a mild steel (0.2%C) using a 5%Co HSS tool and observed abrasion of the tool and attributed it to the hardness of the BUE formed, 585 HV.

Abrasion wear occurs by ploughing of hard particles on the underside of the chip to remove material from the tool face by mechanical action. The hard particles are strain hardened fragments of an unstable BUE.

It may be possible that there is a stable BUE, if this is the case it will protect the rake face of the tool. The secondary shear zone and heat generation will be away from the chip tool interface, thus having less effect on tool material properties. Another effect of a stable BUE is that it will avoid the contact between machined workpiece and tool flank face.

If there is a flow zone the tool wear rate will depend on the main wear mechanisms that are acting on the interfaces. The literature presents different classifications for the wear mechanisms, however, most of the work in this area

considers six different mechanisms: superficial plastic deformation by shear at high temperature; plastic deformation under compressive stress; diffusion wear; attrition wear; abrasion wear; and wear under sliding conditions.

The high temperatures can affect the thermally activated wear mechanism, but other factors have to be considered. In diffusion for example, if the flow zone is saturated and stable it can act like a barrier decreasing tool wear. Otherwise if it is an unstable structure it will increase the wear by diffusion and other mechanisms, like attrition, can be present. Another wear mechanism is plastic deformation of the tool when machining materials of high strength and if the interface temperature is high enough to affect the tool material properties and reduce its strength. In this case the high cutting forces can damage the tool.

In the sliding zone, where the temperatures are likely to be relatively low, the thermally dependent wear mechanisms are less active. However it does not mean that tool wear is less in this region. Sometimes it can be even more intense than in the zone of adherence. That is the case for attrition and abrasion. The presence of oxides can affect the wear in this region, because this region is exposed to influence of the environment.

2.5 Stress Distribution on the Rake Face

The mean normal stress acting on the rake face zone can be determined by dividing the cutting force F_c by the contact area. However, although this mean stress is occasionally used for machinability analysis, the maximum stress is the one to be considered as the critical that must be supported by the tool. The mean stress is also not accurate because of difficulties in determining the real area of contact. It is

essential thus to know the normal stress distribution on the rake face and principally important to know the maximum value of this stress.

According to [25] the compressive stress has a parabolic distribution, figure 2.6, and therefore could not be represented by a mean stress. The same is true for the shear stress.

Experimental analyses of stress distribution have mainly used the photo-elastic technique [36,37,38,39] or split-tool dynamometers [40,41]. The results suggest that the maximum stress, indeed, occur at the cutting edge.

[40] determined the rake face stress distribution using a split-tool dynamometer for an steel (0.45% C, hardness HV=245). The results shown that the stress distribution depends on the cutting speed and feed rate. At 0.16mm/rev for example the distributions shown in figure 2.9 were obtained for various cutting speeds. In this graph x means a distance along the rake face from the cutting edge and l_c is the chip-tool contact length.

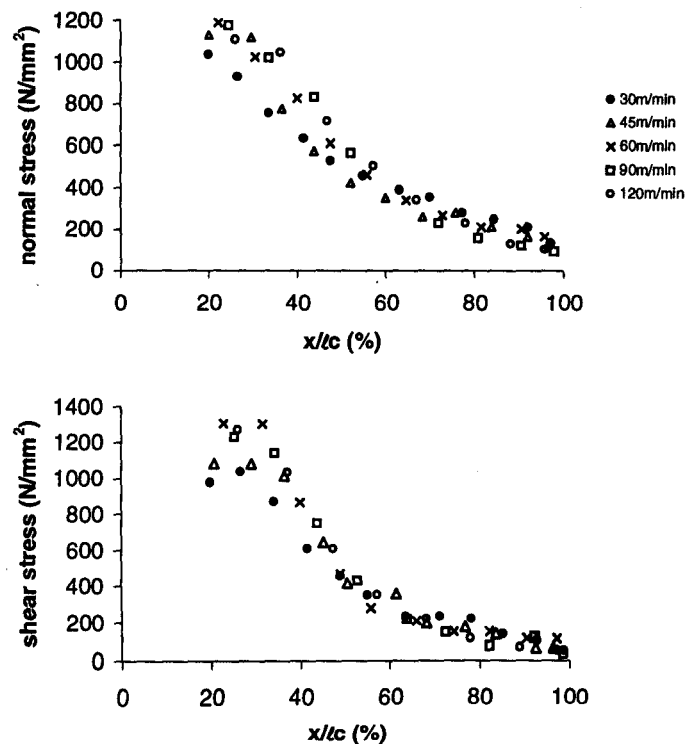


Figure 2.9 Rake face stress distribution [40].

According to the graphs both stresses (normal and tangential) are around the value of 1Gpa in the region close to the cutting edge. These results also indicate that the normal and tangential stresses on the rake face are distributed according to the distribution proposed by [25]. The normal stress decreases exponentially to zero at the point where the chip loses contact with the tool. The tangential stress remain constant until a certain distance from the cutting edge, after which they decrease exponentially to zero at the point where the chip loses contact with the tool. Another important conclusions from the results of [40] is that the maximum value of the normal stress increases with increasing cutting speed and feed but the maximum value of the shear stress increases with decreasing cutting speed and feed.

2.6 Surface Conditions in Machining

The term Surface Integrity is used to describe the quality of a surface, the conditions of a machined surface. The condition of a new surface in a process of machining involves plastic deformation, rupture, elastic recovery, heat generation, vibration, residual stress and sometimes chemical reactions. All these factors can have different effects on the new surface and the term surface integrity can embrace a great number of changes in the surface. Most of them are never measured in a normal production environment.

These changes or defects of the surface can be classified according to the parameter used to measure them, geometry for example. The most obvious defects are surface roughness and plastic deformation.

[42] listed the following surface alterations as the ones that can happen in a conventional metal removal process:

- plastic deformation as a result of hot or cold work
- tears, laps, and crevice-like defects associated with the BUE
- recrystallization
- change in hardness
- phase transformations
- intergranular attack and preferential solution of micro constituents
- microcracking and macrocracking
- residual stress distribution in the surface layer

In general these defects are caused by mechanical, thermal or chemical actions and can be classified into geometric elements and metallurgical elements and examples of each are [43]:

1.geometric: surface roughness, waviness, lay, distortion, surface texture, microcracks, macrocracks, laps, pits, tears voids and wear debris;

2.metallurgical: composition changes, plastic deformation, dislocation density and distribution changes, recovery, recrystallization, grain growth, residual stress, inclusions, vacancies, interstitial, Frenkel defects, solute atoms, twins, stacking faults, antiphase boundaries, domain walls, intergranular corrosion, hardness variation, thermodynamic property changes.

Normally a machined part is examined in terms of dimensions and surface roughness. It is inspected after an operation, or during the operation [44], according to

the dimensional tolerances and surface texture specified in the project. The dimensional errors are easy to measure and to control and rely mainly on the process and machine tool stiffness used. The surface texture includes, among others [45] surface roughness which itself has many parameters used to measure it. To represent a measurement of a surface, average roughness R_a and maximum peak to valley height on the surface are two examples.

In many cases surface roughness is used to control the process of manufacture. In fact surface roughness is controlled by various parameters: machine tool; material properties; tool material and manufacturing process. Statistical methods applied to the results of surface roughness can identify the contributions of these parameters [46]. For example in grinding it can reveal the efficiency of the process or the proportion of grains that are blunt. In turning it can identify tool wear, changes of the surface profile, and machine tool deterioration which can cause chatter affecting the surface. It is possible to measure the profile of the surface during cutting to monitor the process [47].

The profile of a surface can be obtained in three dimensions, but many aspects and features of a surface are not revealed when measuring the surface roughness. The electron microscope is the best way to analyse the geometric defects left on the machined surface by the process [48].

In a hypothetical machining operation where the tool is sharp, there is no friction between the surface in contact, and there is no vibration, or BUE, the surface finish will be the marks left on the workpiece by the tool due to the incremental feed each revolution of the bar. These feed marks are illustrated in figure 2.10 for external cylindrical turning using a single point tool with nose radius r .

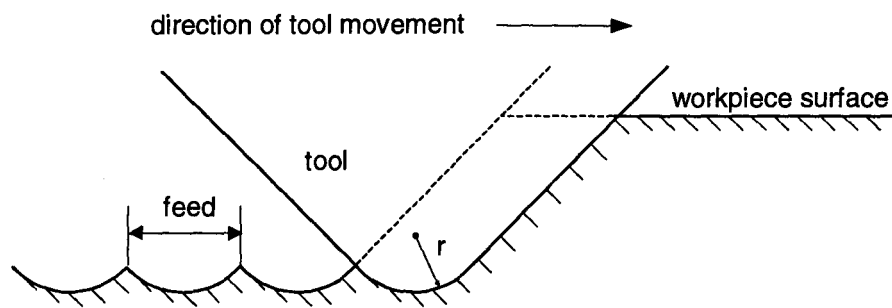


Figure 2.10 Feed marks left on the surface of the workpiece.

Surface finish for this case can be calculated as a function of the geometry of the process: tool nose radius/geometry and feed rate [2] according to:

$$Ra = \frac{f^2}{18\sqrt{3}r} \quad (2.5)$$

where:

Ra - average roughness (μm)

f - feed rate (mm/rev)

r - tool nose radius (mm)

There is some attempt in the literature to include in the calculations other parameters like cutting speed and depth of cut [49].

A real surface will differ considerably from the ideal case and this difference depends on the cutting conditions, mainly upon the cutting speed. Many factors will be responsible for the variation of surface roughness from the ideal value, amongst them BUE, wear of the tool, vibration, elastic recovery of workpiece material and flow of material perpendicular to the direction of cutting (side flow). The effect of each of these factors will depend on the cutting conditions but, BUE seems to be the

most important factor. [50] divided the effects of different parameters on surface roughness and concluded that 20-25% of the surface roughness is due to the BUE and 10 to 15% to groove wear and the rest to other factors like side flow, elastic recovery and tearing. Under such conditions several features on the surface formed can be identified like: chatter marks perpendicular to the direction of relative work-tool motion, long straight grooves parallel to the direction of relative work-tool motion, and intense surface damage in certain areas [51].

The cutting conditions have great effect on surface roughness. At low speed for example, where there is formation of a BUE the result is a rougher finish. An increase in feed rate at low speed results in an even worse surface. This normally is attributed to an increase in size of the BUE [52]. The effect of BUE on surface finish is thought to be due to the fact that parts of it are lost during the process and stay attached to the workpiece surface. Therefore the surface finish improves when the cutting speed increases because the BUE disappears.

When the BUE is a periodical phenomenon it can cause large variations in the cutting forces with time. These variations in size can affect surface finish because they can change the effective nose radius, as the BUE becomes the tool. Also cracks can start in the BUE structure and associated flow zones, which lead to portions of the BUE on the workpiece surface. Depending on the size of the BUE it can even affect the depth of cut.

With steels the conditions between chip and tool will change with cutting conditions and temperatures. Increasing cutting speeds increases heat generation and the BUE disappears. Instead of the BUE there will be a flow zone and under these conditions the surface roughness remains unchanged for higher speeds and any difference in it when compared to the theoretical one could be caused by [53]:

- a swelling of the work material along the front of the cutting edge;
- side flow;
- tool vibration;
- tool wear.

[54] compared the surfaces produced by a ceramic and a carbide tool and found some difference which was explained by the effect of temperature on BUE. The thermal conductivity of the ceramic is lower than that for carbide and so the temperature is higher for ceramic and the BUE formed is smaller, which resulted in a better surface.

There are different forms of tool wear and they will affect the surface finish in different ways. Groove wear on the clearance face of the tool is the main form of wear affecting the surface. There are quite a number of reasons which together cause groove formation [55]. One of the most important of these causes could be a work-hardened layer in the surface of the workpiece, left behind by the tool in the previous revolutions, this is a metallurgical alteration caused by the cutting action. It suggests that the alterations of the surface and subsurface are not isolated effects.

Another cause of groove wear could be the elastic recovery of material on the secondary cutting edge. It could be possible that in machining there is a minimum depth of cut that will remove material. This depth of cut depends on many factors, but mainly on the properties of the material, such as Young's modulus of elasticity, yield point, the rounding of the cutting edge and the cutting speed (temperature). Values less than this minimum and the material will not be cut, just deformed. In machining with a single point tool, the depth of cut for the secondary cutting edge varies from

zero to this minimum value, and so leaves a portion of material on the surface. This elastic recovery is called *springback* [21] and also contributes to the variation of surface roughness. This can cause a groove in the tool. As the groove is formed the surface roughness increases. Surface roughness increases with the time of cutting and tends towards a constant value after a certain distance travelled by the tool because the groove depth becomes stabilised. However, the number of grooves can increase and cause chatter, deteriorating the surface.

Experiments with tools with cutting edge radii (radius of intersection between rake face and flank face) equal to the depth of the layer of material removed (considering the case of orthogonal cutting) [56], showed that there is a critical value for the cutting edge radii (or rake angle) such that at any value greater than or equal to this critical value, workpiece material is ploughed. During this action, part of the material in front of the cutting tool is compressed under the flank face and elastically recovers and part is plastically deformed to spread sideways without separating from the workpiece material. It is analogous to what happens in abrasion tests, only a proportion of the scratch volume is removed, the remainder is displaced to the edges of the groove [57]. It suggests that this recovery or the contact of the workpiece material with the tool flank face could be estimated using Hertz theory of contact, or theory of hardness test. A more detailed discussion of this subject is in Appendix A.

The tool nose radii will have effect on the escape of plastic material around the end of the cutting tool. [3] shows an example of the sensitivity of surface roughness to the blending of the nose radius with the end cutting edge of the tool.

When there is no BUE the roughness of the tool flank face affects the roughness between the feed marks on the workpiece. The marks on the tool will be impressed on the workpiece, as demonstrated by [58] in experiments to show that

there is contact between the newly formed surface and the flank face. This zone of contact with the flank results from a force normal to it, which could force the portion of the workpiece below the flank face to be squeezed to the side and cause the side flow of material to alter the feed marks. [59] showed that the direction of flow is almost perpendicular to the direction of cut and that the amount of side flow decreased with increasing cutting speed.

However this force that acts on the tool flank face represents only a small proportion of the cutting forces. It is only for small values of chip thickness that it is proportionately large. This ploughing action explains the so called 'size effect' [19]. This term refers to the increase in specific cutting energy (the energy required to remove a unit volume of metal) at low values of undeformed chip thickness, and is similar to grinding, in which to produce very thin chips greater power is required.

There exists also a hypothesis that the squeezing occurs just above the rake face in the lower part of the primary shear zone, because the chip is often wider than the undeformed material to be cut [21].

Supposing that a BUE is part of the tool and the newly machined surface and chip are formed by cracks that are formed at the ends of the BUE. Depending on the size and shape of the BUE the machined surface is formed as the BUE acts as a cutting tool with a negative rake angle that can be very large. Experiments in sliding wear, abrasion or grinding show that the removal of material depends on the shape of the particles, asperities or abrasive and for large rake angles there is no cutting. Instead there is a ploughing action and the material is just deformed and moved to form a groove, but not removed. This ploughing action could also occur with the machined surface and the part of the BUE in contact. The size and shape of BUE will affect this and therefore the side flow of material will be variable.

Surfaces machined under conditions of discontinuous chip show areas of smooth cut intermittent with rough areas with cavities where the work material seems to have been removed from below the general level of the surface. This is due to the mechanism of formation of the discontinuous chip [43]. In this case it is suggested that the primary shear plane extends into the workpiece to a depth greater than the feed. As the material is sheared and a discontinuous chip is formed, a hollow is formed in the surface as the chip is created. Figure 2.11 illustrates this process.

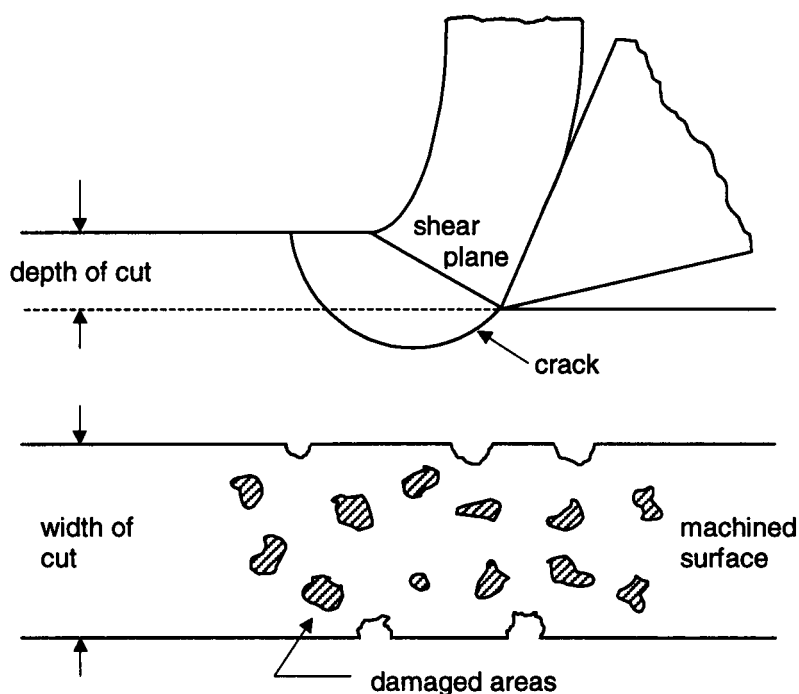


Figure 2.11 Schematic diagram showing crack formation [43].

In the case of two phase alloys containing a hard second phase, plastic deformation can lead to microvoid formation because of decohesion at the particle-matrix interface. [60] when machining resulphurised steel at low cutting speeds where there was a BUE, the presence of many craters with grooves emanating from them, ploughed into the surface were observed. They observed that the frequency of

occurrence of these craters corresponded closely to the frequency of occurrence of the manganese sulphide inclusions in the steel. They suggested that these inclusions were responsible for the formation of the craters and a built-up cap on the cutting edge of the tool, with subsequent fractured points left on the workpiece surface. The same explanation [61] was used for the microasperities found when machining several materials. It is suggested that when one of the inclusions approaches the cutting zone (cutting edge) the stress field near the cutting edge is affected because of the discontinuity of mechanical strength and this could cause the formation of a micro-BUE. This small BUE soon disappears and the surface of the material contains microasperities, traces of BUE and tool material. It was also observed that wear particles of the cutting tools are left on the workpiece surface near these microasperities.

The formation of microchips as a result of the sliding contact between the workpiece and flank face contributes to the surface roughness. [51] observed microchip formation over the entire range of cutting conditions used in his investigation on machining of AISI 4340 steel. In his tests there was a stable BUE present at a cutting speed of around 9m/min and flow zone in the range from around 20m/min. The length of the microchip grooves depends on the cutting speed and the wear land length of the tool. However the width of the microchip grooves was in the range from 5 to 10 μ m, and appeared to be insensitive to cutting speed. It was found that three forms of microchips could be identified as being fundamentally different:

- microchip remains attached to the workpiece surface but has left a groove in the region in which it was formed

- microchip has been removed completely from the workpiece surface and carried away by the tool. In many instances it was noticed that these

microchips were deposited on the workpiece surface elsewhere as metal debris -microchip has been formed and remains as part of the workpiece surface as identified in the first form but an appendage of a dissimilar material is attached to the microchip, which is a fragment of the cutting tool

The explanation for the formation of these microchips originates from studies of sliding contact between surfaces, where the contact between them is through the asperities of both surfaces, which is unlikely to happen in machining.

Residual stress is probably one of the most important factors affecting the properties of a machined part and forms part of the alterations of the surface due mainly to plastic deformation. Residual stress will affect in service properties like fatigue and corrosion resistance. The high shear stress that the material is submitted to in the cutting zone and heat generation are responsible for deformation of the material beneath the machined surface. This indicates that some of the energy expended during cutting is used to cause this subsurface deformation. If the layer of deformed material can be measured it is possible to estimate the amount of work done. In the case of the machined surface this work can be used to calculate the temperature rise of the surface, [62].

As an analogy with subsurface microstructure associated with severe sliding wear in metal [23], the material nearest the surface when machining without BUE often has a different structure from that of the original material. It has very fine grains and contains components not present in the original material, such as material transferred from the counterface and oxides. Material near the top often shows a lamellar structure, resulting from alignment of dislocation cell walls and subgrain boundaries parallel to the direction of cut. The thickness of the deformation zone decreases with cutting speed, which means that the work done is concentrated in a

thinner region, and the temperature of the workpiece increases.

During the generation of the machined surface, the outside layer of the workpiece material is plastically deformed while the inside structure is elastically deformed. Following the machining process, the elastic deformation tends to recover. However, this recovery is restrained by the plastically deformed layer that leads to the creation of residual stress in the machined component [63]. Normally the surface is under tension and an inner layer under compression, but the variation of stress is complex. Usually residual stress decreases as the cutting speed increases and increases with feed rate.

Residual stresses are not only the result of mechanical stress due to formation of the new surfaces, but can be thermal stress or phase transformation of the machined material. In machining of steel martensite can be formed near the surface depending on the temperature achieved. Thermal stress in interrupted cutting is an important parameter to be controlled to avoid premature failure of the cutting tool.

2.7 Metal Cutting Temperature

The power consumed in metal cutting is largely converted into heat. This heat is dissipated by the four systems processing the material: the cutting tool, the workpiece, the chip formed and the cutting fluid. The temperature of the tool is an important aspect and most of the time is the factor that limits the rate of material removal. As the temperature of the tool increases its strength decreases. The influence of cutting temperature on tool life has been the subject of the major part of the work done on metal cutting, but the heat generated may also affect the surface integrity of the workpiece for example [4]. These effects may be more important than the tool life.

As temperature is of fundamental importance in the metal cutting operation many attempts have been made to predict it. Some works simply use a relationship between the work done and the volume of metal involved in the process to obtain an average temperature. Other works using computer models help give the distribution of temperature on tool, chip and workpiece close to the cutting edge. The methods used to measure temperature in metal cutting have not been improved much (particularly in obtaining temperatures in very small regions) for a number of years.

2.7.1 Heat Generation in Metal Cutting

Nearly all the work expended in the process of metal cutting is converted into heat. This is because there is friction (external or internal) to overcome. In a simple manner the total work done can be divided in three quantities; (i) work done to shear the material to form the chip and the new surface; (ii) work done to move the chip over the rake surface of the tool and (iii) work done in moving the freshly cut surface over the flank face of the tool. The work expended in shearing the material to form the chip involves dissipation of heat due to internal friction. The other two are necessary to overcome the friction between the tool and chip or workpiece, which may involve internal "friction" because of seizure between the surfaces.

These works will depend on the material being cut. Ductility, hardness, work hardening and thermal properties all have definite effects on the tool forces and affect the temperature. These properties in addition to the tool material characteristics, cutting conditions and geometry of the process will define the power required and therefore the heat generation.

In early works concerning the relationship between the chip geometry, power

consumption and cutting parameters [22,64,65], the formation of chips was considered as shearing on a simple and well defined plane, and the generation of heat on the rake face was treated on the basis of classical friction theory. The work done on the flank face of the tool was taken into account only if there was flank wear. The results are a good indication of the influence of some parameters, like rake angle and cutting speeds. However the shearing action does not happen on a simple plane and the results have to be interpreted with care. Likewise, what happens on the rake surface of the tool is complex and cannot be treated as classical friction, as seen in previous sections, because of the high stress acting on the tool surface.

As has been shown [26,27,28], the heat generated at the tool-work interface is of major importance in relation to tool performance, and is particularly significant in limiting the rates of metal removal. Along the greater part of the contact between chip and tool, there is a seizure zone where these two materials are in a close contact. There is no relative movement between the chip and the tool at the surface of the tool and depending on the cutting speed a flow zone in the chip with large strains and strain rates or a BUE (for relatively low cutting speed) is established.

The contact between the work material and the flank face of the tool can occur even for tools without wear, and may contribute to an increase in the work material temperature. The movement of the freshly cut surface over the flank face of the tool may be treated in the same manner as the secondary shear zone, depending on the cutting conditions and the tool wear rate.

When a BUE is formed the heat generation due to the movement of the chip is over a short distance and above the flank face. The size and stability of the BUE are affected by this temperature [2].

A schematic of a single point cutting operation without BUE is shown in

figure 2.12 with the zones of heat generation.

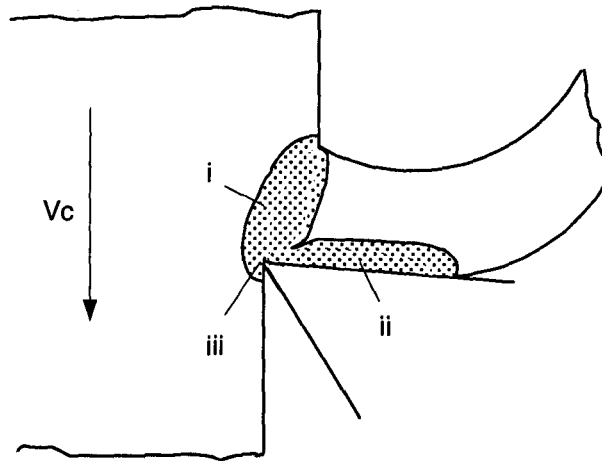


Figure 2.12 Heat generation zones in an orthogonal cutting.

Using cine-photography to observe the cutting process, [66] found that when mild steel was machined at low speeds, the primary shear zone had approximately the form shown in figure 2.12, but extended below the cutting edge into the workpiece. Therefore zone (iii) is just an extension of (i). In the works of [5], there is evidence of the zone (iii) when the tool is not sharp, but it is not a prolongation of zone (i).

The cutting tool, the chip, the cutting fluid and the workpiece dissipate the heat. Therefore, it is evident that the tool is heated as well as the workpiece and this is fundamental to the process. The greatest part of the heat produced is due to work done in chip formation, and the largest part of this heat passes into the chip and a proportion is conducted into the work material. This proportion may be higher for low rates of metal removal and small shear zone angles, but for high rates of metal removal this proportion is small. Considering the primary shear zone as a simple plane, the proportion of heat going into the workpiece depends on the inclination of

the plane. If the shear angle decreases, more heat goes into the workpiece.

[19] proposed a method for calculating the approximate mean temperature rise in the body of the chip from measurement of tool forces, knowledge of the cutting parameters and data for the thermal properties of the work material. Again, it is assumed for simplicity that the shear zone (i) is a plane and the chip temperature is independent of the work done in the other plane (ii). The power expended in the shear zone during machining, N_s , is converted into heat that is shared by chip and workpiece. Assuming that the proportion of heat that goes into the workpiece is given by β , the mean temperature there is:

$$T = \frac{(1 - \beta)N_s}{\rho c V_c t_1 d} \quad (2.6)$$

where:

T-temperature in the chip close to the primary shear plane

β -proportion of heat that goes into the workpiece

ρ -density of work material

c-specific heat of work material

V_c -cutting speed

t_1 -undeformed chip thickness

d-width of cut

Equation (2.6) can give a good indication of the magnitude of temperature to expect for the chip. The problem in applying this equation is the value of the coefficient β . [67] produced an equation to give the value of β as a function of the shear plane angle, cutting speed, density of workpiece material and its thermal properties. This shows that more heat goes into the workpiece as the cutting speed

decreases.

The same equation can be used to estimate the temperature rise of the workpiece [62]. In this case the undeformed chip thickness must be replaced by the thickness of the plastic deformation under the machined surface.

In the same manner the temperature in the flow zone could be calculated using this time the feed power, N_f , and a coefficient that predicts the percentage of heat that goes into the tool.

It is unlikely that heat is lost by the chip to the tool. This is because the temperatures in the secondary shear zone are higher than the temperatures in the body of the chip. This is why the tool-work interface has been more important in respect of the metal removal rate. The largest part of heat generated in this region goes into the tool and chip and as the tool is stationary, its temperature is higher. A cutting fluid used in the case of a continuous chip will show little or no effect on the maximum tool temperature [68].

The heat generated at the tool-work interface will also be conducted to the tool holder. This can affect the dimensional accuracy of the workpiece. Depending on the temperatures achieved and the material of the tool holder it is possible to have dilation in the order of $30\mu\text{m}$ [69], thus affecting the accuracy of the operation. In this case the cutting fluid may be effective.

The increase in the temperature of the workpiece is due to work done in zone (i) and (iii), in figure 2.12. These temperatures may affect the dimensional accuracy of the workpiece because of thermal deformation, if it causes position errors between the cutting tool and surface [70,71].

The heat generation during interrupted cutting, like milling for example, is an important parameter for tool life control. The heat is generated in the same way but

the changes in the temperature are cyclical, increasing during the active time and decreasing in the inactive time [72,73,74,75]. These fluctuations can cause thermal fatigue on the cutting tool and the impact of the tool contributes to increasing the possibility of failure [76,77].

2.7.2 Temperature Measurement in Metal Cutting

The difficulties in calculating the temperatures and temperature gradients in the cutting zone, for even simple conditions, emphasise the usefulness of practical methods to measure temperatures.

In order to evaluate the temperatures arising in the cutting zones, several techniques have been developed over the past seventy years [78]. Most of these techniques are used to measure the temperature of the cutting tool.

The most extensively used method is the tool-work thermocouple [2,79]. This method is useful in showing the effect of cutting conditions, such as cutting speed and feed rate, but the absolute values are inaccurate.

In this method the thermo-electric emf generated between the tool and workpiece during cutting is measured. The cutting zone forms the hot junction, while an electrical connection to a cold part of the tool and the workpiece forms the cold junction. The tool and workpiece need to be electrically insulated from the machine tool. One of the difficulties of this method is the necessity for an accurate calibration of the tool and workpiece materials as a thermocouple pair [80,81].

There is a temperature gradient along the contact of the tool with the chip and it is uncertain if the thermocouple is measuring the lowest temperature at this interface or a mean value.

According to [82], the quantity measured in the tool-work thermocouple method is the average thermoelectric emf at the interface between the tool and workpiece. In general this emf does not correspond to the average interfacial temperature, this is the case only if the temperature is uniform or if the thermoelectric emf of the tool-work material combination varies linearly with temperature.

Tool materials such as ceramics (used at high speed cutting), are brittle and their electric resistance is high making it difficult to implement a contact type sensor such as described above [83].

Another method used to measure temperature and gradients in the tool is inserted thermocouples [84]. Using thermocouples of small diameters it is possible to obtain good results of the temperature gradients into the tool by means of many small holes in different positions. The error here is that it is impossible to put thermocouples very near the cutting edge where there are high temperature gradients and the hole in which the thermocouple is placed may affect the heat flow.

A very interesting method was developed to measure the temperature in the flank face of the tool [85], using wire of a material different from the workpiece and tool. This wire is insulated and inserted into the workpiece in a hole of a small diameter. When the material is cut, this wire will be machined too and when this happens, a thermocouple is formed between the wire and the tool. The results indicate that the temperature of the tool flank face is little affected by cutting speed, feed rate and depth of cut. For carbon steel, for example, the temperature obtained was about 400°C, independent of the tool material. The temperatures obtained by this method are smaller than obtained when using the tool work thermocouple.

The errors in this method arise by the fact that it is uncertain what happens when the thermocouple touches the cutting zone. Moreover the duration of the contact

is very short.

[86] developed a method to measure tool temperature distribution within the tool by means of fine powders that have a constant melting point. The tool was divided into two symmetric parts parallel to the chip flow direction and fine powders were scattered on one side of the divided surfaces. The tools were put together and used to cut. The distribution is obtained using different powders and observations of the extent of the melted areas. Some results using this method show that the temperature tends to saturate gradually at a point away from the cutting edge but very rapidly at the cutting edge and the time required is about 1 to 2 min. The temperature gradient obtained was little different from other methods.

The temperature distribution in the tool may be obtained by using information about the changes in hardness and microstructure in steel tool [87]. It is necessary to calibrate the hardness of the tool against the temperature and time of heating and the samples of structural changes at corresponding temperatures. These methods permit measurement of temperatures with an accuracy of $\pm 25^{\circ}\text{C}$ within the heat affected region. These methods are arduous and difficult to use [88].

The techniques to measure temperature by measurement of radiation are sometimes very useful to obtain the surface temperature of workpiece, chip and tool [89,90,91,92,93,94]. This method gives information only about the temperature on the exposed surfaces, although some experimental techniques tried to measure the temperature distribution on the flank or rake face of the tool through small holes on the workpiece [95,96], or cutting tool [97]. These holes change the process to interrupted cutting and it is doubtful if the temperature measured is the same for a non interrupted cutting.

The radiation methods are complicated and suitable only for laboratory

studies. Extreme care was required in assembling and using the radiation pyrometer [98] and the minimum temperature detectable was a limiting factor for the use of these set-ups. Today there are simpler infrared sensors available with quick response and there is no minimum temperature for application in metal cutting [99].

Another method involving the use of thermal-sensitive paints gives results not considered to be accurate [90].

2.7.3 Analytical and Numerical Models of Temperature Distributions

There are many analytical treatments [100,101,102], finite element methods [69,83,103,104,105,106,107,108,109], boundary element methods [110] of heat conduction with moving or stationary heat sources together with kinematics, geometry and energetic aspects of the metal cutting process.

In the analytical models, it is often assumed that the chip is formed instantaneously by a shearing action in a plane (shear zone). Also, the chip-tool interface is assumed to be a uniform plane and the heat generated is due to friction between the two surfaces.

The analysis of [100] assumes that shear and frictional energy is distributed uniformly, and there is no redistribution of the thermal shear energy going into the chip during the very short time the chip is in contact with the tool. The relative importance of the several variables influencing tool rake face temperatures was discussed in this paper. The results suggested that high temperatures that are observed in machining titanium alloys could be obtained analytically.

[101] applied relaxation methods to the workpiece and shear plane temperature problem, and was able to solve the equation for heat transfer in a material

moving in a direction perpendicular to a stationary heat source numerically. The complete temperature distribution in the workpiece and chip was obtained. [97] assumed that heat transferred by conduction in the direction of motion of the workpiece or chip may be neglected.

The finite element analyses of [102] allowed for the primary and secondary zones being finite in size and obtained temperatures for the workpiece lower than [101].

Using finite element analyses [105] has investigated the influence of several process variables on temperature distributions on the tool flank face and rake face. The rate of heat generation was calculated using some experimental methods to measure strain in the primary and secondary deformation zones. An empirical expression was used to relate the flow stress of the material being cut to the strain, strain rate and temperature. Errors may arise in the results due to these measurements and estimating. The results obtained are very interesting and show the effects of the main variables. For example, the highest temperature along the tool flank, similar to the tool rake face, occurs at some distance from the cutting edge, and increases with cutting speed and feed rate, contrary to the experimental results of [85]. According to [111] the calculation of the thermal energy from frictional resistance is affected by a number of factors. Material properties are constantly changing and difficulties also arise when attempting to quantify the real area of contact.

[108] analysed the dependency of the thermal failure of a cutting tool on temperature gradient. They suggested that by cooling the lower face of the tool it is possible to increase the temperature gradient towards the cutting surface, thus decreasing the wear level of the tool. They considered the effect of the contact between tool and workpiece only if there was flank wear.

All these works are fundamental and use powerful tools. The results give an excellent idea of the influence and importance of the parameters involved in the process and the temperature gradients and distribution. It is difficult however to confirm these models by experimental methods.

2.7.4 Temperature and Cutting Conditions

The major part of the work about temperature in metal cutting has been focused on tool temperature and the analytical models. The reason for this is that the wear of tools has been the concern. Many researches are due to the fact that wear is sensitive to the temperature in the cutting zone.

The temperature in the cutting zones will be affected by the cutting conditions: cutting speed, feed rate, depth of cut, and tool geometry. It will also depend on the properties of the workpiece material, as well as the physical properties of the tool.

There are plenty of results in the literature, both analytical and experimental, about the influence of cutting conditions on the temperature of the tool, workpiece or chip. The temperature increases because more heat is being generated and/or is concentrated in a small area and/or less heat is being dissipated. This is then affected by the cutting conditions (cutting speed, feed rate and depth of cut). Less obvious effects are tool geometry, material (workpiece, tool) and cutting fluid.

Using the tool-work thermocouple method, [112] obtained the results shown in figure 2.13, for a low alloy engineering steel machined with cemented carbide tools. Temperature was measured as a function of cutting speed for three different feed rates and compared with the results for dry cutting and a cut using water as a cutting fluid.

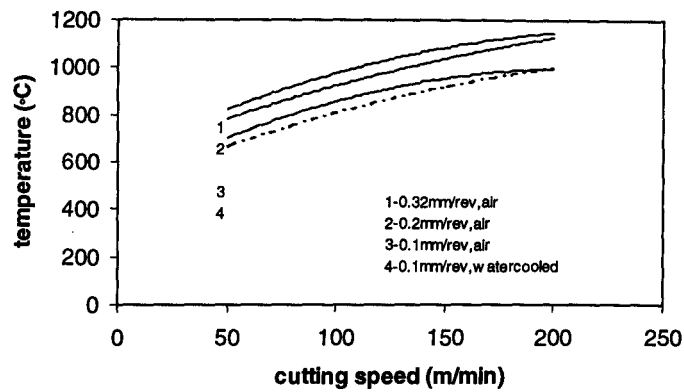


Figure 2.13 Effect of cutting speed, feed and cutting fluid on temperature [112].

The results give a good indication of the values of tool temperature, as well as the effect of some cutting conditions. The water used acted as a coolant and its effect decreased as the cutting speed increased. As the temperature affects the properties of the material it became more easily deformed at higher temperatures, when the cutting fluid is used it changes the properties of the material in the same manner. It seems that equilibrium is achieved between the effect of the cutting fluid and the heat generated for those cutting conditions.

The same trend can be obtained using a simple analytical method to determine the approximate temperature in the interface of the chip/tool [100]. The heat in this region comes from the work done to move the chip over the flank face, so there is a contribution from seizure zones and sliding zones. The errors will arise from the fact that it is impossible to distinguish between these two regions and the need to measure the strain in the seizure zone. The method used to measure these strains is the quick-stop, which consists of a device to retract the tool very quick while it is cutting. This freezes the motion in the cutting zone, but some damage may be done.

Both experimental and analytical methods are affected by the presence of a

BUE.

Some works using metallographic techniques and changes in the hardness of the tool show the distribution of temperature in the tool. According to these results the maximum temperature on the rake face of the tool is remote from the cutting edge. An example is shown in figure 2.14.

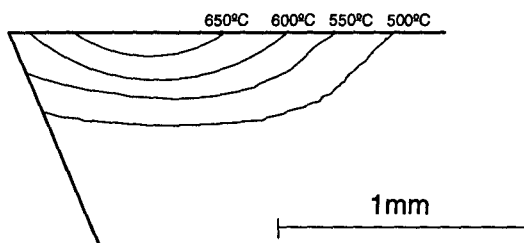


Figure 2.14 Distribution of temperature on the rake face of a tool [5].

[113] obtained the same model of temperature distribution, i.e., the highest temperature on the rake face of the tool is remote from the cutting edge.

A similar distribution is obtained when finite element models are applied. A maximum temperature is at some distance from the cutting edge and good agreement is obtained with experimental results [106]. The difference in terms of distribution patterns is in the region near to the cutting edge, where the calculation gives lower values for temperatures.

These temperatures have been explained in terms of the seizure zone at the cutting tool interface. According to [5] the formation of a crater on the rake face of the tool will start in that region of higher temperature. This happens for many materials and cutting conditions, although for some materials there is a great difference from the above model. Figure 2.15 shows the results using the same method for high conductivity copper.

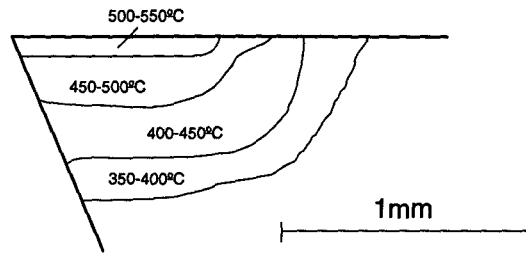


Figure 2.15 Distribution of temperature on the rake face of tool when cutting high conductivity copper [5].

These results can be explained by the fact that the ductility of the copper is high and the seizure zone, if formed, extends to the cutting edge of the tool.

Generally, the results have shown that for a fixed combination of tool and workpiece, the tool temperature will be affected by the extent of the contact length between chip and tool. The temperature will increase with the contact length. Consequently the parameters that affect this zone will affect the temperature [90]. A lubricant, for example, will affect the temperature at the interface if it decreases the seizure zone.

Figure 2.16 represents the results obtained by [114], where the effect of the contact length between chip and tool was studied for orthogonal cutting of aluminium. The cutting conditions were maintained constant (cutting speed 120m/min, depth of cut 1.59mm) and the different contact lengths were obtained by means of restriction of the rake face of the tool. There is a critical contact length above which there is no change in temperature. These results can be compared to the effect of the seizure zone size. This means that if lubrication is achieved at the tool-chip interface and the critical contact length decreases, the effect will be a drop in the heat generation and a decrease in temperature. It is important to notice that the method used to measure temperature in this case (tool-work thermocouple) may not be so accurate to affirm

that 20°C (the difference between temperatures for the three feeds) is a significant difference. The temperature may not be the maximum temperature at the interface either.

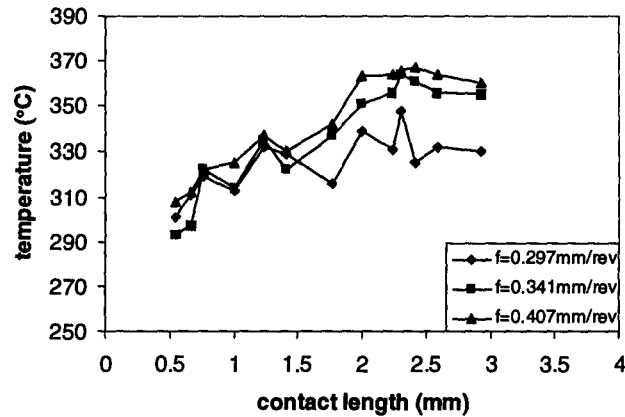


Figure 2.16 Temperature for different contact lengths and feed rates [114].

2.8 Cutting Fluids

Cutting fluids were first introduced in machining operations to increase the production rates and tool life. The reason for this improvement at the early stages of the development of metal cutting was due to cooling action as cutting tools at that time could not support even relatively low temperatures, and therefore water was used as coolant. Water started to be applied at irregular intervals in operations, as in boring of guns for example [115]. After some experiments and practical observations it was suggested that if water was applied at a continuous stream it could be more effective. Probably soda and soap are the first additives used for cutting fluids. They were added to water to improve its wet ability.

To overcome the disadvantage of corrosion caused by water to the workpiece, tool and machine tool, oil was mixed to the water to form an emulsion and improve

the lubricity of it. These emulsions are known as soluble oils, and these have been the most used cutting fluids for many years.

Then the possibility of lubrication in metal cutting directed the use of mineral oils (neat or straight oils) and natural fats (organic materials) such as lard, tallow, and suet [116]. Fatty oil is a very good lubricant resulting in a good surface finish and improving tool life, but has the disadvantage of becoming rancid. A blend of mineral and fatty oil resulted in a good lubricant, more stable than the fatty oil, and with the same qualities. Indeed a low percentage of fatty oil added to mineral oils proved to be satisfactory.

Additives like sulphur, chlorine and phosphorus improved further the quality of these oils concerning metal cutting. These are the so called E.P. (extreme pressure) additives. While the high temperature, which can occur between two surfaces sliding against each other, is responsible for the breakdown of the lubricant film between them, it is the activation energy for these E.P. additives. Thermal decomposition of the additive induces the formation of a compound with the metal surface that acts as a lubricant reducing friction or the amount of wear [117].

With the development of the cutting fluid industry, as a necessity with the development of modern machine tools and new generations of tools increasing productivity rates, researches, and also pressure by environmental agencies and health authority, new coolants and lubricants were introduced into the market. The main aim of the new cutting fluids have been to be safer to the operator, to last considerably longer and with less disposal problems than a straight mineral oil for example [118]. The synthetic fluids represent the latest development in cutting fluid. Synthetic mineral oils and esters are some examples of them [119]. They are blended with water to form a solution or emulsion. The advantages of these fluids are cleanness and

disposal. Because they do not contain oil they cause less damage to the environment, are less susceptible to bacteria growth, promote less irritation to the skin and present less odour. They are applied mainly to grinding operations [120].

Synthetic oils have no oil in their composition, but can be mixed with soluble oil to improve lubrication and corrosion properties. These mixtures are known as semi-synthetic fluid [121].

Apart from the E.P. additives applied as lubricant that can be added to practically every cutting fluid, there are other additives that must be used. Typical additives include: biocides; corrosion inhibitors; defoamers; emulsifiers; pH adjusters; deodorizers; dyes; emulsion breakers, and flocculents, among others [122].

There are different types of cutting fluids used and the choice will depend on the material of the workpiece, material of the tool and machining operation. The effect of material is the chemical activity with the cutting fluid, strength, and temperatures during the cut. Magnesium for example easily reacts with water and there is risk of fire. The tool material can affect the choice when there is a tendency to form cracks due to thermal shock, like in some ceramics. Finally depending on the machining operation a fluid is necessary to cool rather than lubricate, or the fluid is necessary just to clean the chip from the cutting zone. Some tests to evaluate cutting fluids indicate that their performance depends on the operation and on the criteria used to evaluate them (tool life or surface finish for example) [123].

Actually the name cutting fluid sometimes refers to a liquid, gaseous or solid lubricant. Soluble oil is the best example and probably the most used lubricant/coolant. Air is an example of gaseous and some alloying elements in the workpiece material can act as solid lubricants. Manganese sulphide inclusions in resulphurised free-machining steels are an example of a solid lubrication.

Almost all these types of liquid cutting fluids are applied to the metalworking processes in general. Perhaps a simple division of all cutting fluids would be: straight oils, soluble oil, semi-synthetic fluid and synthetic fluid [124]. A more general classification of lubricants can be found in standards [125], which give a rough guide to the choice according to the machining operation. Some other simple substances can be used as lubricants or coolants, in industry or in laboratory tests. Compressed air [126] and carbon tetrachloride are some examples.

2.8.1 Functions of Cutting Fluids

Amongst the functions of a cutting fluid cooling and lubrication are generally regarded as the most important since they are directly related to tool life and surface integrity of the workpiece.

Fluid is applied to lubricate at low cutting speeds because it is believed that it can penetrate the interfaces to perform its task, as hydrodynamic lubrication in some cases and as boundary lubrication in others. Furthermore, temperature is not a problem at low cutting speeds for most of the metals and cooling is not important. Surface finish improvements and increase in tool life are the main benefits when applying a lubricant. On the other hand, at high cutting speeds it is difficult for the lubricant to penetrate into the interfaces and so lubrication is not possible, therefore the fluid is applied to cool the system (tool, workpiece and chip). Cooling the tool helps to increase its life (when temperature is the limiting factor) or allows higher speeds to be used, and so increase the production rate.

There are other reasons to apply cutting fluid that in some circumstances can be more important than lubrication or cooling. Materials that form long chips can be a

problem during the cutting, for the workpiece, machine tool or the operator. Small chips also have to be flushed away from the cutting zone. For these cases a cutting fluid can be applied just to help clean the swarf from the cutting zone, or to break it to facilitate its disposal. Drilling operations on brittle materials is a good example where the chip represents a serious problem. It can prevent workpiece and parts of the machine tool from rust as well, having no effect on the process at all.

A cutting fluid also has to satisfy some requirements from the point of view of applicability. For example: stability in storage, to retard deterioration; freedom from odour; avoid foaming when circulated in the machine; in the case of soluble oil, provide stable emulsions with different water supplies; do not pollute the environment or cause harm to the operator.

Carbon tetrachloride (CCl_4) for example is one of the most effective cutting fluids to machine steel at low cutting speeds [2, 127], but its use is forbidden for safety reasons. It is toxic and can even cause death.

2.8.2 Action of Cutting Fluids

In the metal cutting process, lubrication and cooling are actions that can affect chip formation, tool wear and surface finish. The cooling action of the cutting fluid is simply to extract heat from the cutting zone (tool, workpiece and chip). The purpose of decreasing temperature is to increase tool life, or increase the rate of material removal, for the cases where temperature is the limiting factor.

Increase of tool life by cooling is possible when the wear mechanism is dependent on temperature, which normally happens at high cutting speed. At high speeds the time available to exchange heat with the moving parts is very short and so

the efficiency of the coolant decreases. There is a possibility however that cooling the toolholder and workpiece could change the temperature distribution in the tool.

The cutting speed where the BUE disappears seems to be determined by temperature, a coolant could therefore increase the BUE range and affect the process. Nevertheless there are cases where application of water as coolant increases the temperature of the workpiece, near to the cutting edge, increasing tool wear [128]. It was explained that water affected chip curl by its cooling action on the free surface of the chip without however cooling the surface of the chip in contact with tool rake face. It decreases the primary shear plane angle and increases the heat that flows back into the workpiece increasing its temperature.

Cooling the workpiece can avoid dimensional changes, if temperature is high enough to cause sufficient dilatation. This can be an important factor in finishing operations, as small dimensional variations affect the tolerances. Experiments measuring the machined surface temperature in turning [129] show that the cooling rate of the workpiece can be very high and indeed dimensional variation caused by localised heating can be discarded.

Lubrication in metal cutting, as defined by lubrication theories considering two sliding surfaces, will depend on the ability of the fluid to penetrate into the interfaces of the cutting zone. If the lubricant can penetrate into the secondary shear zone, it will reduce the contact length and decrease the forces, heat generation, temperatures and tool wear. Its ability to improve surface finish is attributed to the fact that it can lubricate the rake face and avoid formation of BUE, avoiding adherence. If the lubricant cannot penetrate into the entire contact length it could at least lubricate part of the contact where there is no adherence, the sliding zone, to reduce the shear stress distribution on the rake face therefore reducing the energy and

so the temperature [130]. It is not clear however, if a fluid can penetrate into the interface, there are some divergent theories about this subject. Before the concept of seizure at the chip tool interface was accepted normal friction between chip and tool was admitted to happen. Therefore contact was between the asperities of the two surfaces and fluid could penetrate by capillarity action by the network formed [131]. This is still being used to explain a possible penetration into the sliding zone.

Lubrication can have an effect on the depth of workhardening of the surface of the workpiece [132]. When there is flank wear, contact between machined surface and tool is likely to happen, for low cutting speed this will depend also on the size and shape of the BUE.

Chemical reaction of the oil additives to avoid tool wear by diffusion or to form a low shear strength layer of solid lubricant (as in boundary lubrication) has been used to explain longer tool life or the decrease of the coefficient of friction on the rake face when different cutting oil is applied [133,134]. That is the reason to the application of extreme pressure additives.

This chemical reaction is not always beneficial. It can decrease tool life by increasing the ease of plastic flow on the tool, by affecting the mobility of dislocations near the surface. This effect is also known as the Rebinder effect [135]. This can happen for some ceramics (alumina for example) where crack growth is sensitive to environmental influence [23]. The effect of cutting fluid on tool life depends on the effect on the wear mechanisms and its form, which can give a longer or shorter tool life.

In the case of carbon tetrachloride it has been suggested that it could penetrate microcracks formed in the machined surface in previous cuts, and then weakening the shear strength of the material by preventing these microcracks rewelding, which

normally occurs in a dry cut, or it could penetrate by diffusion and reach the chip tool interface and form a layer of low shear strength [134]. There are more microcracks at low cutting speeds, which explains the excellent lubrication ability of this substance at low cutting speeds.

Experiments with carbon tetrachloride resulted in the following suggested characteristics for a lubricant in machining: small molecular size; chemically reactive; able to form a boundary layer of lower shear strength than the chip material; should have a large number of reactive atoms to ensure sufficient lubrication [134].

Different forms and directions of application have been used to help the cutting fluid to penetrate as closely as possible to the cutting edge to lubricate. The most traditional method to apply a cutting fluid is through flooding the cutting zone (overhead) with sufficient fluid to cool or lubricate everywhere. Even though the areas to lubricate are small, a huge volume of lubricant is applied. High volumes of fluid can be justified if it is a coolant. However there is some indication that a mist application can give better results than a flood of high volume of coolant. [128] using just water as a coolant explained that at high temperature steam forms at the surface and gives rise to a poor heat transfer. When a mist is applied the steam can escape and improve the heat transfer coefficient. In mist application the fluid passes through a specially designed nozzle to form droplets that are distributed in a large volume of air at low pressure.

More directional methods apply the fluid to the clearance face (between machined workpiece and tool flank face), supposing that the fluid can penetrate into chip tool interface and cause hydrodynamic lubrication. There is evidence of a contact length between machined surface and tool flank face below the cutting edge [20], which can avoid penetration of any fluid. However it seems that there is no such

contact when machining some materials and this form of application of cutting fluid can give good results.

The direction of application of cutting fluid will depend on the temperature distribution in the tool, which depends on the material being cut. When machining iron for example temperature distribution on the tool is such that the maximum temperature is at some distance from the cutting edge. This region of maximum temperature can extend to the end clearance face and therefore application of a coolant below the end clearance face can improve tool life or avoid tool failure [68]. The coolant can affect temperature distribution, the depth of the heat affected region, but it does not change the highest temperature on the rake face. Coolant increases the heat conduction in the tool.

Application of cutting fluid to the rake face, against the movement of the chip can give some good results when the fluid is applied at high pressure. Again it is not certain if any fluid can penetrate the chip tool interface, especially that part of it where there is seizure. However, according to the normal stress distribution on the rake face, sliding can happen at the extremities of the contact and it is possible to have lubrication in this area. This method of application is known as high-jet method [136], or jet-assisted machining [137] and can give good results at high cutting speeds. Another benefit from this high-pressure system is that the flow of fluid can act as a chip breaker. Experiments using mineral soluble oil showed that the method acted as a good chip controller when machining titanium alloy and nickel alloy and is a good coolant to the tool [138]. However it did not change cutting forces or surface finish when compared with the normal overhead system, even though it reduces chip tool contact length. It is suggested that the cooling of the workpiece increases its strength and compensates for a reduction of force due to lubrication on the rake face. The fluid

can also be applied through a hole in the tool to reach close to the cutting edge from the flank face or rake face [139], or simply to cool the toolholder to increase the heat transfer and change temperature distribution [140,141]. This can be very useful in drilling operations to help to clean the chip.

As a tendency and pressure to reduce the risk to the environment from pollutants and waste from cutting fluids used on machining, a mist application seems to be the answer to reduce the volume of oil. Some experiments with very low volume of lubricant show that it is possible to have the same benefits from oil lubricants and the cooling action of air [142,143]. Some systems of application reduce the rate of oil to 10ml/h, in a continuous operation.

3 EXPERIMENTAL TECHNIQUES

This chapter describes the procedures, materials and methods used in the experimental tests. The machining operation used was external cylindrical turning using a single point tool and a CNC machine tool of 38KW power (TORSHALLA S250 lathe equipped with a General Electric-GE 2000 CNC control). The machine has a variable spindle speed from 40 to 2800 rpm and a variable feed rate from 0.001 to 2.8 mm/rev. The workpiece material, tool material, and tool geometry were held constant for all tests.

Cutting forces and temperature of the transient workpiece surface (see figure 2.2) were measured during machining. After the test surface finish was measured and chip samples were collected for thickness measurements and to observe possible changes to the chip shape.

Samples from the machined surface were examined in the scanning electron microscope. This analysis is very important to study surface finish. The sample was analysed at different positions and stereo photography was used to help in the examination of the surface.

Each test lasted for about 40 seconds, allowing time for the transient workpiece surface temperature to stabilise.

A quick stop test was carried out for every condition used. This is a test where the tool is removed from the cutting zone at high speed, using a humane killer gun. A sample that contains the chip still attached to the workpiece is then cut off to be analysed. This sudden action of stopping the cutting retains some important details of the cutting action. Samples can be used to identify the existence of BUE, and if it exists, to measure its size.

Quick stops can also be useful in measuring the primary shear plane, depth of deformation below workpiece surface, and observation of the secondary shear zone. More details of such equipment can be found in [144].

The samples obtained from the quick stop tests were analysed using electron and optical microscopy after suitable preparation. The samples are cleaned using acetone and ultrasonic vibration and then dried. This observation is aimed at detecting features on the surfaces (chip, transient surface and machined surface). To reveal the microstructure of the sample for use with the optical microscope the samples were mounted in a thermoset resin and ground using a 240-grid paper followed by 400, 600 and 1200. They were polished using 6 μm diamond followed by 3 and 1 μm . The specimens were then etched for 10s in 2% nital. The same procedure was used to obtain the microstructure of the tool (using diamond as the abrasive for grinding), but the etching in this case is Murakami's reagent: 10g $\text{K}_3\text{Fe}(\text{CN})_6$ (potassium ferricyanide), 10g NaOH (sodium hydroxide) and 100ml H_2O .

3.1 Material and Conditions

A.I.S.I. 1040 steel was used for the workpiece material, in the hot rolled condition. This material had an average hardness of 199HV and the following composition:

0.43 % C; 0.83% Mn; 0.19% Si; 0.035% S; 0.07% P; 0.19% Cu; 0.11% Ni; 0.14% Cr; 0.05% Mo; 0.027% Al 0.04% Ti

The material was in the form of bars of diameter 180mm and length 400mm. The choice for this relatively large diameter is due to the method used to measure surface

temperature, as described in section 3.3. The bars can only be used to measure temperature until they reach a diameter of 80mm, after that they were used in the quick stop tests or tests to obtain samples from the machined surface.

Table 3.1 shows some nominal mechanical and physical properties of this material.

Table3.1-Mechanical and physical properties of AISI 1040 steel [145].

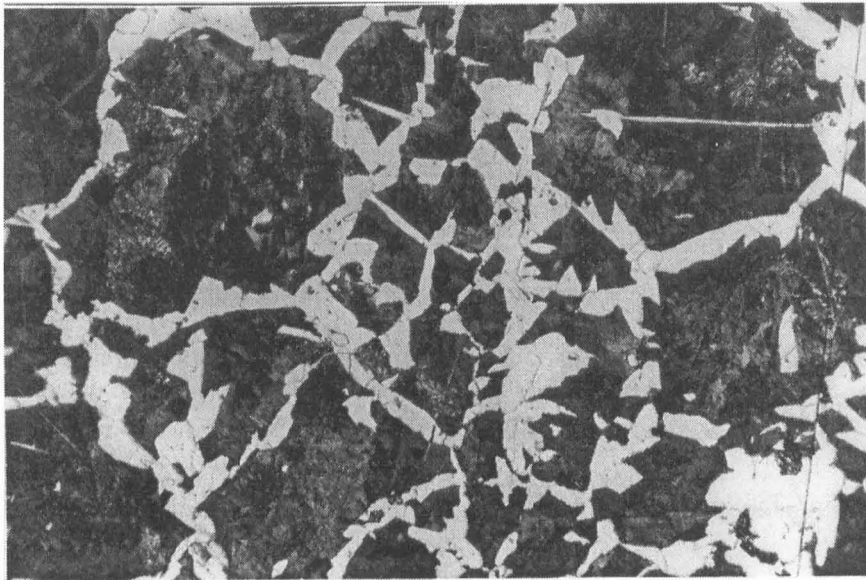
Tensile strength (MN/m ²)	Shear strength (MN/m ²)	Young's modulus (KN/m ²)	Poison's ratio ν	Density ρ (Kg/m ³)	Specific heat c (J/KgK)
627	480	21	0.3	7200	502

The microstructure of the material is presented in figure 3.1 for two different samples extracted from the bar, at diameters of 180 mm and 100 mm.

The lubricant used was a refined mineral oil, BP100 SP and the additive was Additin RC 2415 supplied by the manufacturer. This additive is a sulphurised vegetable fatty acid ester, with approximately 15% by weight of sulphur and 5% active sulphur. The oil was used with 0%, 1%, 2%, 3%, 4% and 5% by weight of the additive. These concentrations are used in this work to identify the lubricant. Therefore 0% refers to oil without the additive, 1% refers to oil with 1% of the additive and so on. Before each test the sump of the machine tool was dried and cleaned to avoid contamination of the lubricant. The lubricant was applied using the traditional way known as overhead flood cooling at an average rate of 25ml/s with an effective zero static pressure. The cooling capacity of each lubricant (different concentration of sulphur) was verified in a simple test for possible effects of the additive concentration. A stainless steel sphere of diameter 20mm with a thermocouple inserted in the centre was heated to 100°C. After that the sphere was immersed into a definite volume of lubricant at room temperature. The time

for the sphere to cool down to room temperature was the same for all concentrations used and therefore they have the same cooling capacity.

(a)



(b)

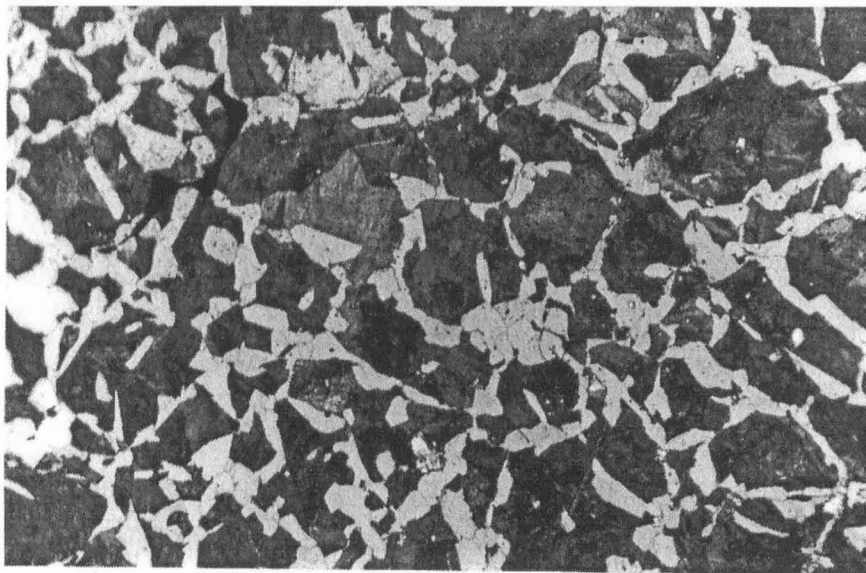


Figure 3.1 Microstructure of AISI 1040 steel used in the tests. a) diameter 100mm, b) diameter 190mm, 150x.

Three cutting speeds were used: 22, 30 and 40m/min; and three feed rates: 0.05, 0.1, 0.15mm/rev. The depth of cut was held constant at 2mm. This resulted in nine different tests for each lubricated condition. These cutting conditions were selected because they are the minimum cutting speed for the lathe and the maximum cutting speed possible without a lot of smoke from the oil lubricant. The smoke being caused by contact with the chip after it leaves the cutting zone.

The cutting tool used was a cemented carbide ISO designation SNMG120404 class M35 with chip-breaker geometry MF. It is triple coated with TiN-TiC-TiN. The toolholder has specification CSSNR/L3225 M12. When in the tool holder the rake angle is 5°, clearance angle 5°, approach angle 45° and zero inclination of the cutting edge. The insert has a nose radius of 0.4mm. Figure 3.2 shows the microstructure of this tool material.

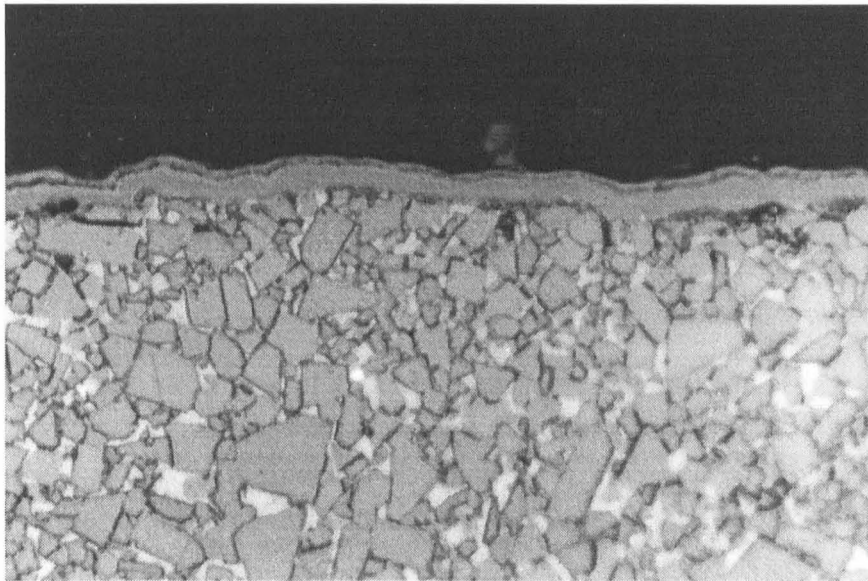


Figure 3.2 Microstructure of the tool material used in the tests, 1500x.

The same cutting edge was used for three tests only to make sure that wear does not affect the results. As the test lasts for only about 40 seconds, and considering that the cutting conditions are not severe for the material being cut, there is no detectable tool wear.

3.2 Measurements

Forces, surface finish, and chip thickness were measured using the traditional methods and equipment used in machining experiments. The procedures are described in the next sections.

There is no one conventional method of measuring cutting temperature. For every experiment it is necessary to apply one of the methods described in chapter 2. For this work the temperature was measured using an infrared sensor. Because it is a new method to access workpiece temperature it will be described in the separate section 3.3.

3.2.1 Forces

Three forces were measured during cutting: the cutting force, feed force and thrust force (F_c , F_f and F_t , respectively). Cutting force, F_c , is in the direction of the cutting speed. Feed force, F_f , is in the direction of the feed. Thrust force, F_t , is in a direction radial to the bar, perpendicular to cutting speed and feed directions. These forces were measured using a piezoelectric dynamometer Kistler Type 9263 and the signal was recorded every second and stored in a computer. The final result, which is

presented, is the average of the signals a few seconds after start of the test.

The graph of force against time is also important information. The average force can be used to compare any effect of lubrication, but the variation of force during cutting is also a parameter which may be used in the study of lubrication. The standard deviation is used in this case to measure such variation.

3.2.2 Surface Finish

For each condition used the surface finish of the workpiece was measured using the parameter Ra, average roughness. A Taylor-Hobson Surtronic 3 was used with a cut off of 15mm. Four different positions, separated by an angle of 90° around the bar were used, and the result presented is the average of these readings.

3.2.3 Chip Thickness

A point micrometer of 0.005mm resolution was used to measure the chip thickness. For each test several samples of the chip were collected and then measured. The results of chip thickness are the average from measurements of ten different samples.

As the section of a chip may vary from the centre to the edges, especially for high feed rates when the chip breaks in small pieces, the chip thickness was measured at the centre of the cross section.

3.3 Temperature Measurements

Temperature measured in this work is the temperature of the transient surface of the workpiece using an infrared sensor. The sensor used was a model LTCF1 manufactured by Raytek. This sensor measures temperatures in the range of -18 to 870°C with an accuracy of $\pm 1.0^\circ\text{C}$. Its response time is 400msec and emissivity compensation built in is from 0.10 to 1.00. The sensing head has a cylinder shape of 187mm length and 42mm diameter. The sensor measures surface temperature in an area corresponding to a spot diameter of 2.5mm when its lens is 76mm from the surface. The size of the measured surface is very dependent on the distance from the lens to the surface. The size of the surface will be bigger if the sensor is not at the exact distance of 76mm and therefore the positioning of the sensor is very important.

The temperature on the transient surface of the workpiece was measured in three different positions below the cutting edge: i.e. 3, 6 and 9mm from the cutting edge, as illustrated in figure 3.3 for an orthogonal cutting.

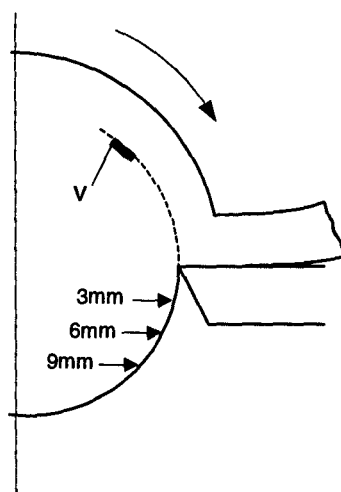


Figure 3.3 Positions where the temperatures are measured.

Figure 3.3 shows a volume (v) of material near the surface of the workpiece. As it approaches the cutting zone its temperature increases because of heat conduction in the material. This heat comes basically from the work done to shear the material on the primary shear plane. When the volume v of figure 3.3 reaches the tool cutting edge it is at the maximum temperature. After crossing the cutting zone (which includes primary shear plane and eventually contact with tool flank face) the volume of material will lose heat by conduction into the workpiece that acts like a sink. Its temperature then decreases.

The three results of temperature below the cutting edge represent then the cooling rate of the material as it leaves the cutting zone. If the cooling rate could be represented by a curve of temperature against distance in a Cartesian representation, then these three results would be on to this curve. Therefore they can be used to obtain the representative equation of the machined workpiece temperature against distance (or time), where the cutting edge represents the zero position. [62] measured temperature of the workpiece during machining using a similar method and obtained very high cooling rates for dry conditions. It was suggested that the majority of heat loss into the bar as thermal conductivity far exceeded any heat loss to air in the time taken for the bar to move between the sensor positions. Also the zone in which the heat has been created is small (about 0.1 mm in thickness). Under these conditions the rate of loss of heat will be proportional to the temperature difference between the surface and the bar material. This gives rise to:

$$\frac{dT}{dt} \propto T_s - T_b \quad (3.1)$$

Where T is temperature, t is time, T_s is the temperature of the surface and T_b is the

temperature of the bar. On integrating this gives:

$$T_s = e^{Kt} + T_b \quad (3.2)$$

Where K is an integrating constant. Thus the temperatures of the surface with time can be reasonably approximated by an exponential curve.

The curve of temperature against time represents therefore the cooling curve of the surface. The time necessary for a point on the surface of the workpiece to cover 3mm in distance for the three cutting speeds is:

22m/min: 8.2ms

30m/min: 6.0ms

40m/min: 4.5ms

During the test the temperature is recorded at intervals of 1 second and the final result for each position (3, 6 and 9mm) is the average after the temperature has stabilised. Cutting force is almost instantly stabilised after the cut starts, but temperature takes about 30 seconds.

The room temperature or the bulk temperature of the workpiece will affect the final result not because the heat generated will be affected but that the starting temperature will affect the final temperature. This temperature could not be controlled therefore it was measured using a thermocouple. The temperature measured with the infrared sensor is subtracted from room temperature. The result is then the graph of the rise of transient workpiece temperature against time, with its origin at the cutting edge where the time is zero.

3.3.1 Experimental Apparatus

The representation of figure 3.3 is for orthogonal cutting with an exaggerated clearance angle. This gives the impression that access is relatively easy to the positions where temperature is being measured. For this work the infrared sensor was fixed between the workpiece and the tool holder on the tool carriage enabling it to access the transient surface and to move with the tool. Figure 3.4 is a schematic illustration of the process.

Due to lack of space there is a minimum diameter of the workpiece that can be used. For this particular case and lathe the minimum diameter was about 80mm. Less than this value and the sensor would touch the tail-stock of the lathe.

The device that holds the sensor onto the tool carriage permits easy positioning in relation to the workpiece by allowing movements in three perpendicular directions and rotation of the sensor. The sensor needs to be at exactly 76mm from the machined surface to guarantee that the diameter of the surface where temperature is being measured is 2.5mm. This positioning is done by adjusting the device that holds the sensor to the tail-stock using a model of the sensor with a laser pen in the centre. Once the sensor is installed the correct distance from the surface is obtained by simple measurements.

The emissivity of the surface depends somewhat on the inclination of the sensor in relation to the surface. In this case the infrared sensor was not at a high angle to the machined workpiece and tests showed that compensation was not required for this effect.

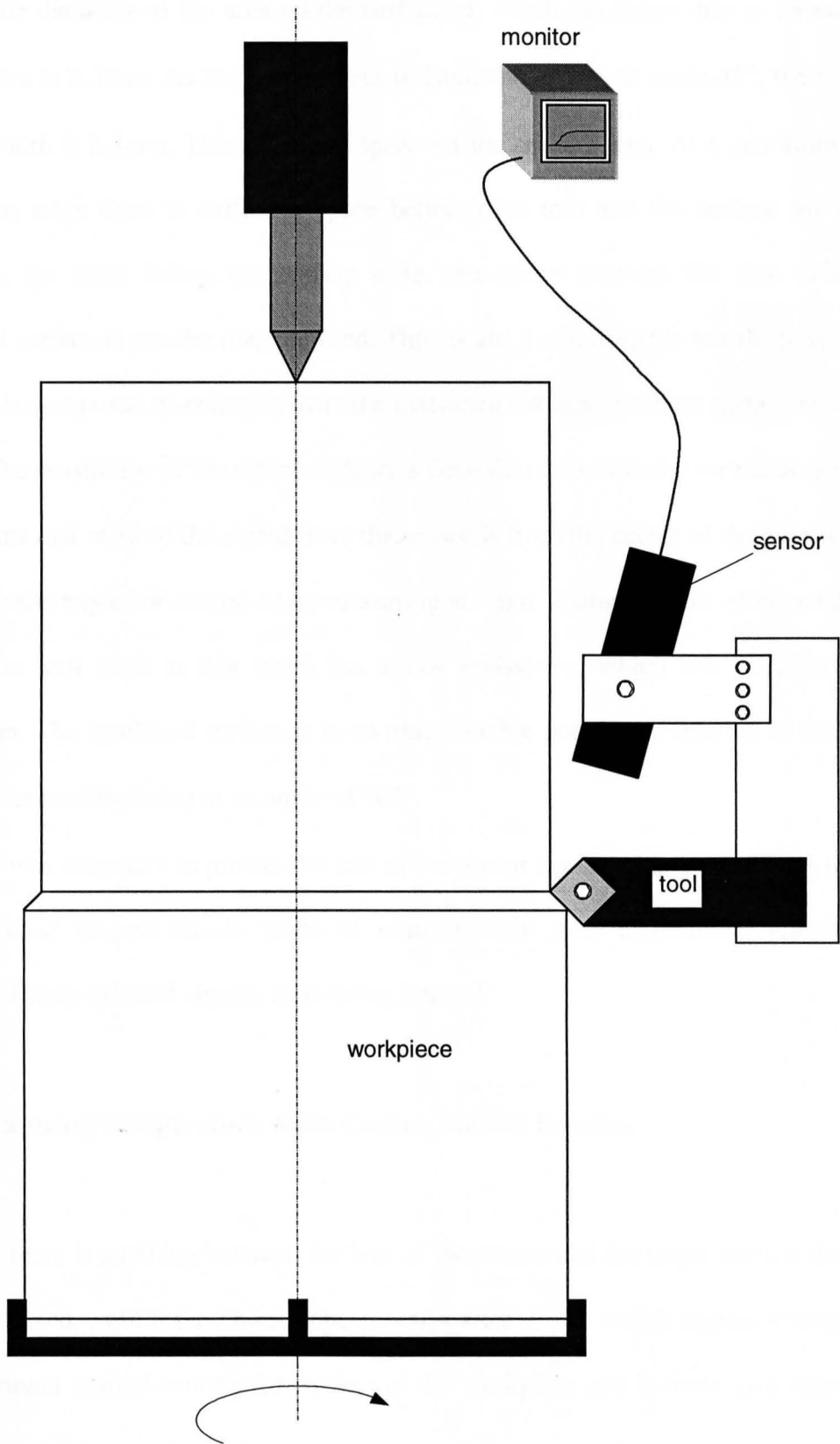


Figure 3.4 Scheme of the infrared sensor installed.

The diameter of the area on the surface on which the sensor has to measure the temperature is 2.5mm. As the depth of cut is 2mm and approach angle 45° , the transient surface width is 2.8mm. This is enough space for the sensing area. At 6 and 9mm below the cutting edge there is sufficient space between the tool and the surface for access. However, for 3mm below the cutting edge, the space between the tool insert and machined surface is smaller than required. This means that during the test the temperature recorded is composed of radiation from the machined surface, transient surface and tool.

The sensitivity of the sensor follows a Gaussian distribution over the area sensed. This means that most of the signal from the sensor is from the centre of the spot, and this will minimise any error caused when measuring at 3mm. Along with the effect mentioned above, the tool used in this work has a low emissivity, which was verified during calibration. The machined surface is in an unfavourable position in relation to the sensor to affect the reading being at an angle of 165° .

It was necessary to protect the lens of the sensor against chips, which was done by using a cone shaped nozzle made of commercially pure aluminium. Which again minimised stray infrared signals from being imaged.

3.3.2 Measuring Temperature when Cutting Fluid is Present.

If there is anything between the lens of the sensor and the target surface the signal can be affected, even if the object appears transparent in the visible region. Cutting fluid will be spread around wetting the surface of the workpiece and it could also damage the lens of the sensor.

The solution found was the use of compressed air applied in the cone, as shown in figure 3.5.

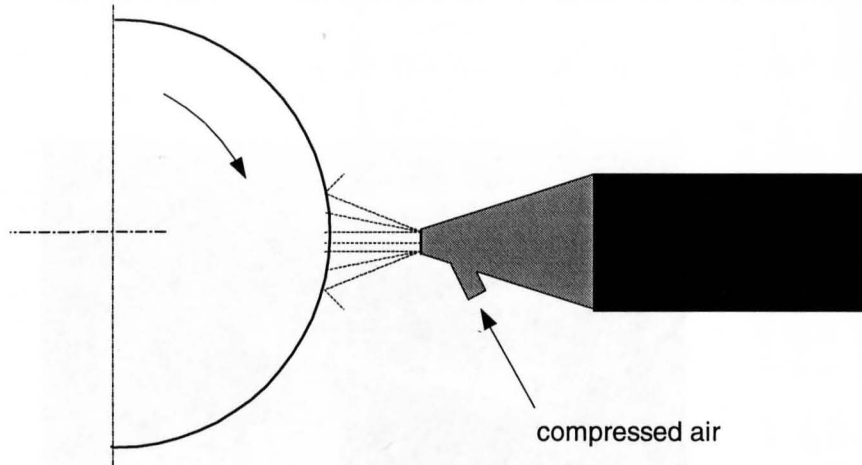


Figure 3.5 Sensor with compressed air to be used when cutting fluid is applied.

The air will protect the lens against chips and cutting fluid and at the same time air will remove the cutting fluid from the surface of the workpiece leaving a free path for the radiation.

Even with the application of air, a thin layer of fluid can remain on the surface of the workpiece. This could make the emissivity of the material larger and become dependent on the fluid used [146]. Special attention was given to the calibration in this case.

For this work the suitable air pressure was found to be 2bar. This pressure is enough to avoid the contact of the fluid with the lens and to clean the transient surface, but minimise its cooling effect. Several tests for dry conditions showed that the compressed air has no effect on the final temperature of the workpiece. Two reasons seem to contribute to this. First there is little time for the air to cool the workpiece.

Second the rotation of the workpiece is already contributing to heat transfer by convection.

Figure 3.6 shows a picture of the sensor mounted in the machine tool and ready to be used.

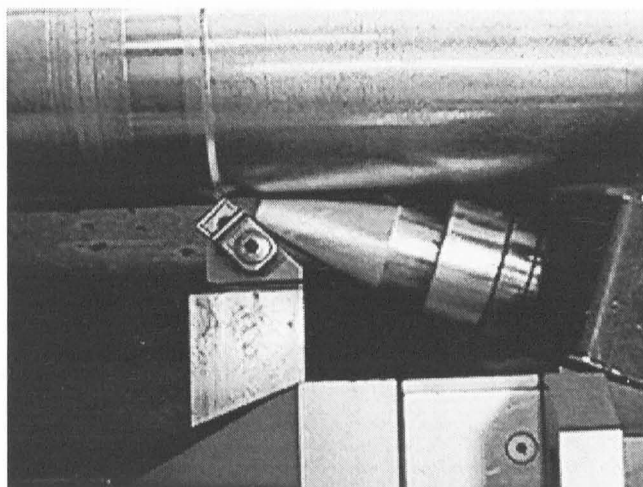


Figure 3.6 Infrared sensor in position to measure temperature on transient surface.

3.3.3 Calibration of the Infrared Sensor

The system needs to be calibrated to determine the emissivity of the material. For the calibration a sample of the material was heated using a hot plate. The sensor was positioned at the same angle as on the lathe relative to the transient surface. At the same time the temperature of the surface of the sample was measured using a thermocouple, which is positioned on the surface.

During the calibration the emissivity is adjusted to the value of 0.8 on the sensor and held constant. This value is the emissivity of the steel at 100°C. A curve was obtained relating the temperature measured by the sensor to the temperature measured

with the thermocouple indicating that emissivity changes with temperature, in the range of 0.7 to 0.8. For every temperature measured compensation was applied using this curve as the temperature measured by the thermocouple is assumed to be the reference.

During the calibration it was confirmed that the surface finish does not interfere with the results for this particular case.

The calibration curve to be used for measuring temperature when cutting fluid is applied is obtained by wetting the sample with lubricant just using the finger. In this case the emissivity is slightly higher than for the dry sample.

The two calibration curves, one for dry and the other for lubricated conditions, are presented in figure 3.7.

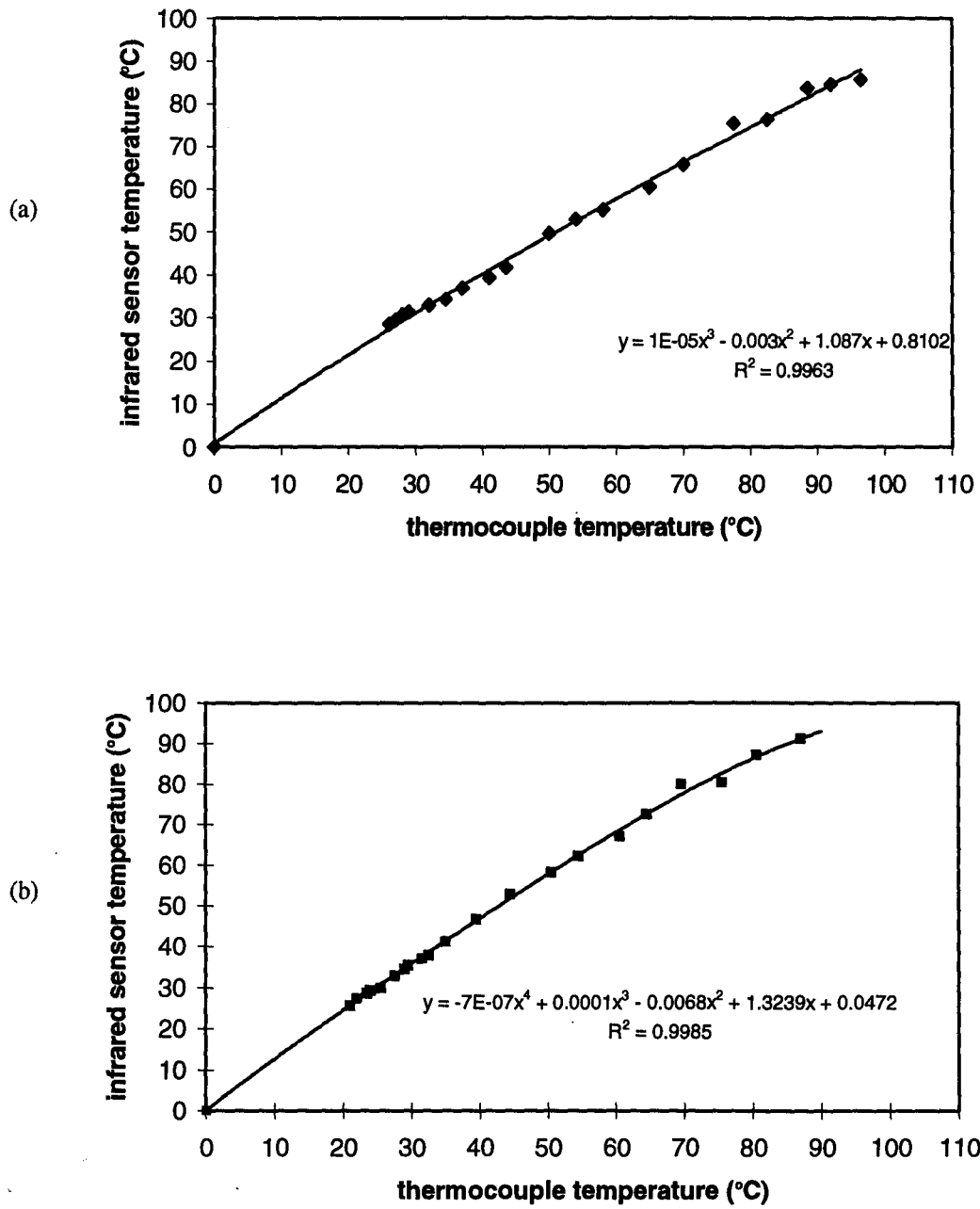


Figure 3.7 Calibration curve for the infrared sensor. a)dry, b)lubricated condition.

4 RESULTS

4.1 Cutting Forces

Figures 4.1 to 4.4 represent the typical variation of the cutting force F_c during cutting for dry and lubricated conditions at 40m/min and 0.1mm/rev. It is observable in the graphs that as soon as the cut starts the forces reach a stable value and have an oscillation around this value.

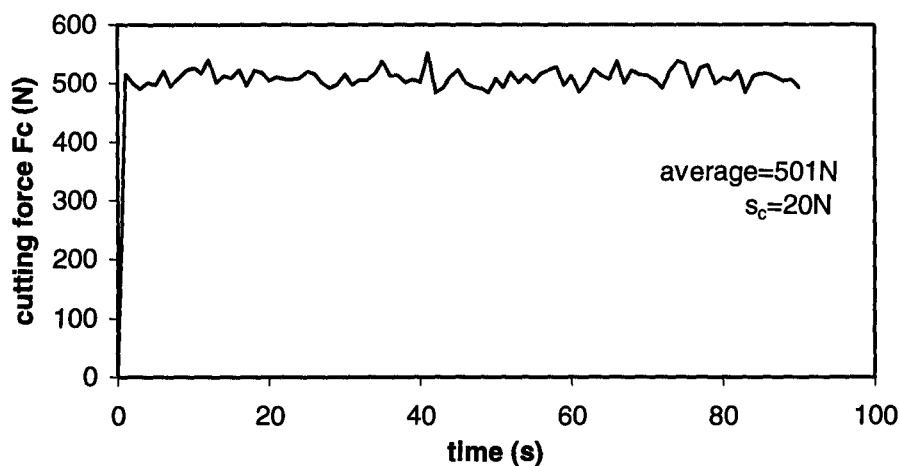


Figure 4.1 Variation of cutting force F_c during cutting, 40m/min, 0.1mm/rev, dry.

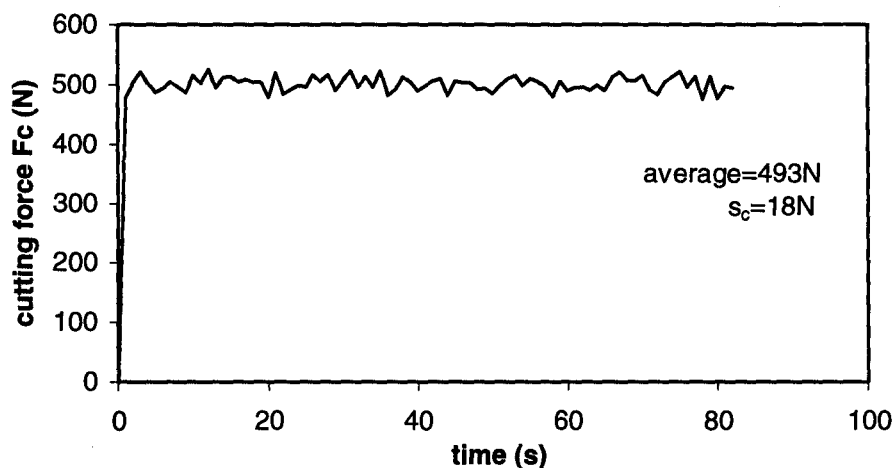


Figure 4.2 Variation of cutting force F_c during cutting, 40m/min, 0.1mm/rev, 0%.

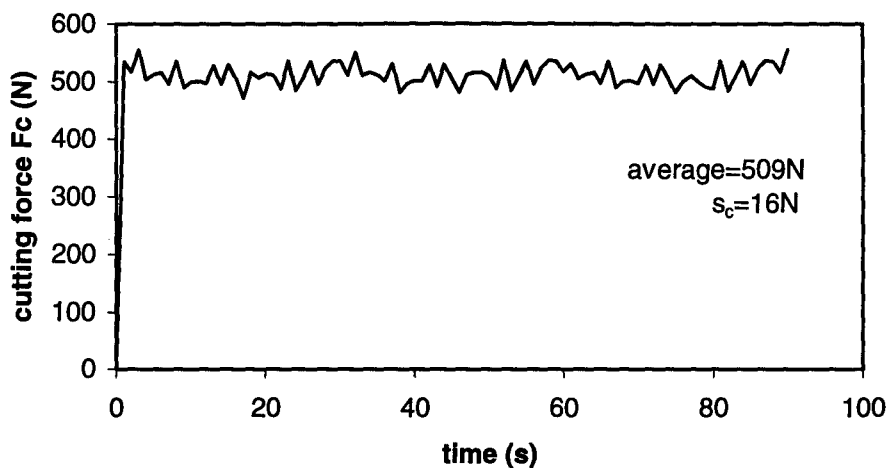


Figure 4.3 Variation of cutting force F_c during cutting, 40m/min, 0.1mm/rev, 1%.

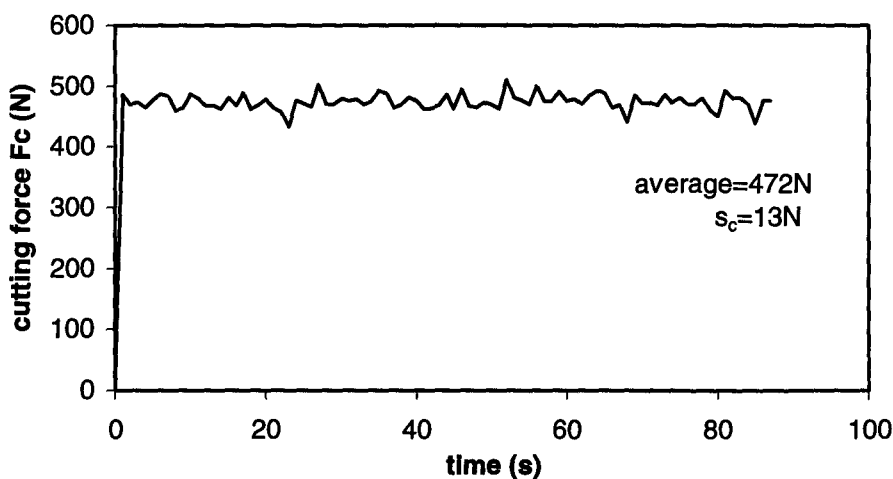


Figure 4.4 Variation of cutting force F_c during cutting, 40m/min, 0.1mm/rev, 5%.

The average for each test is shown in the figures, which was obtained a few seconds after the start of the test. The sample standard deviation (s_c) for the cutting force F_c is also shown in the figures for each test, as it can be used to detect possible effects of the lubrication.

Table 4.1 presents the results of these averages of two forces measured, cutting force (F_c) and feed force (F_f), and the respective standard deviation (s_c) for cutting force F_c for all cutting conditions used in this work.

Table 4.1-Cutting forces and standard deviation.

Vc (m/min)	f (mm/rev)	Lubricant	Fc (N)	Ff (N)	s _c (N)
22	0.05	Dry	299	131	14
		0%	282	125	6
		1%	287	114	9
		2%	293	105	10
		3%	292	111	8
		4%	293	120	8
	5%	260	92	9	
	0.10	dry	535	237	25
		0%	526	242	14
		1%	531	233	17
		2%	540	251	16
		3%	520	227	15
		4%	498	220	12
	5%	488	215	13	
	0.15	dry	790	437	61
		0%	770	324	44
		1%	812	398	39
		2%	794	405	41
3%		791	490	37	
4%		787	390	35	
5%	972	676	36		
30	0.05	dry	283	118	15
		0%	269	121	7
		1%	270	95	9
		2%	271	109	10
		3%	282	105	11
		4%	287	105	10
	5%	264	97	9	
	0.10	dry	519	242	20
		0%	507	239	18
		1%	517	239	15
		2%	512	240	13
		3%	516	228	12
		4%	516	212	14
	5%	478	211	11	
	0.15	dry	976	566	66
		0%	765	429	64
		1%	846	478	40
		2%	960	617	30
3%		945	584	42	
4%		938	594	49	
5%	908	572	28		
40	0.05	dry	276	115	19
		0%	263	117	15
		1%	267	108	11
		2%	279	118	14
		3%	276	102	12
		4%	269	104	9
	5%	267	102	10	
	0.10	dry	501	236	20
		0%	493	232	18
		1%	509	245	16
		2%	505	245	16
		3%	501	237	15
		4%	487	214	12
	5%	472	214	13	
	0.15	dry	931	597	46
		0%	902	624	40
		1%	916	589	39
		2%	889	565	34
3%		894	583	38	
4%		860	519	22	
5%	853	533	29		

BUE has great effect on forces for the range of cutting conditions used in these tests. Figure 4.5 shows the variation of force with cutting speed for dry conditions and 0.15mm/rev.

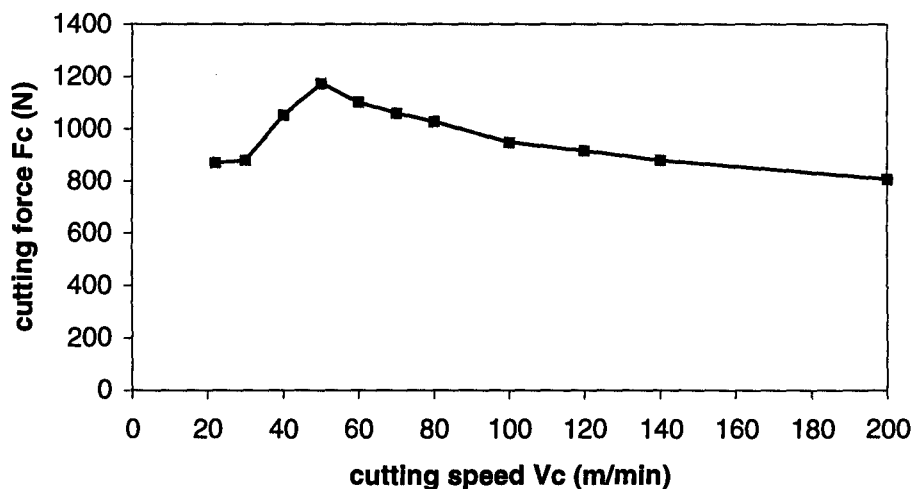


Figure 4.5 Variation of cutting force F_c with cutting speed, 0.15mm/rev, dry condition.

According to the graph the cutting speeds used in this work are in the range of BUE formation for this feed rate. When BUE starts to form the forces decrease and then increase again as BUE disappears. For the other feed rates the behaviour is similar, however there is little variation with cutting speed. It seems either BUE is present during all the speeds or there is no BUE. Quick stop tests can help to identify if there is a BUE.

The feed has an effect on the cutting force. The combined effect of speed and feed on cutting force F_c is shown graphically in figures 4.6 to 4.12 for all the lubricants used.

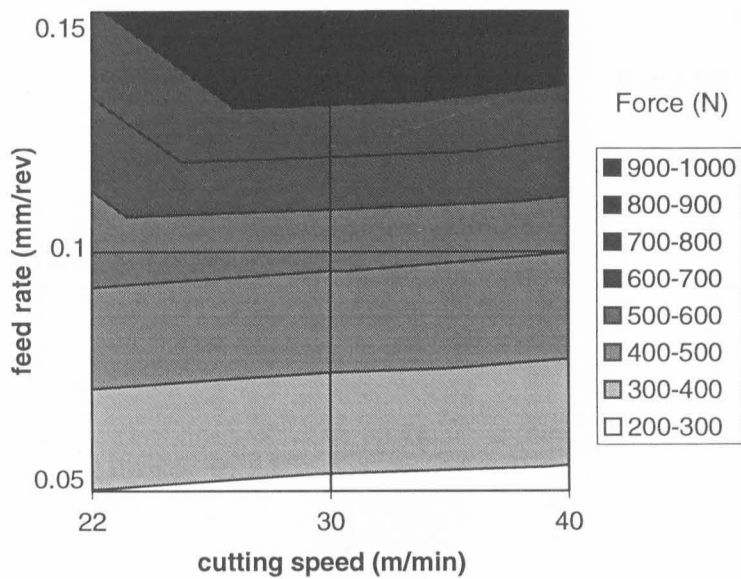


Figure 4.6 Effect of cutting speed and feed rate on cutting force, dry.

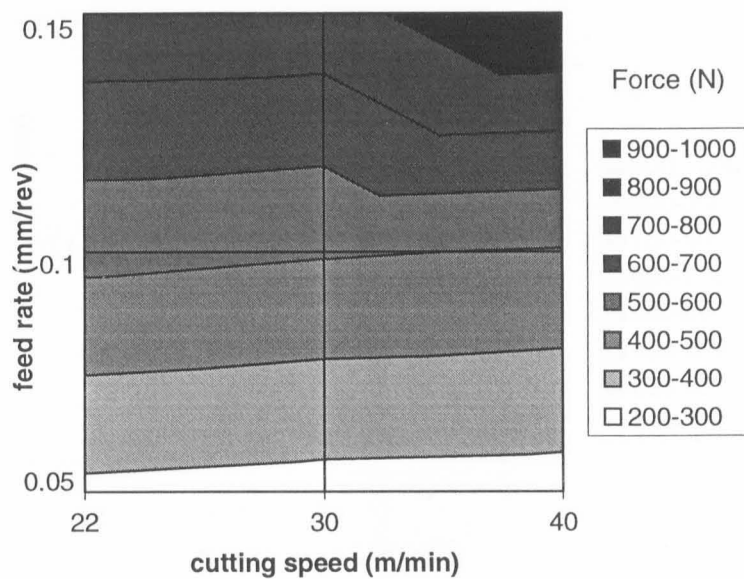


Figure 4.7 Effect of cutting speed and feed rate on cutting force, 0%.

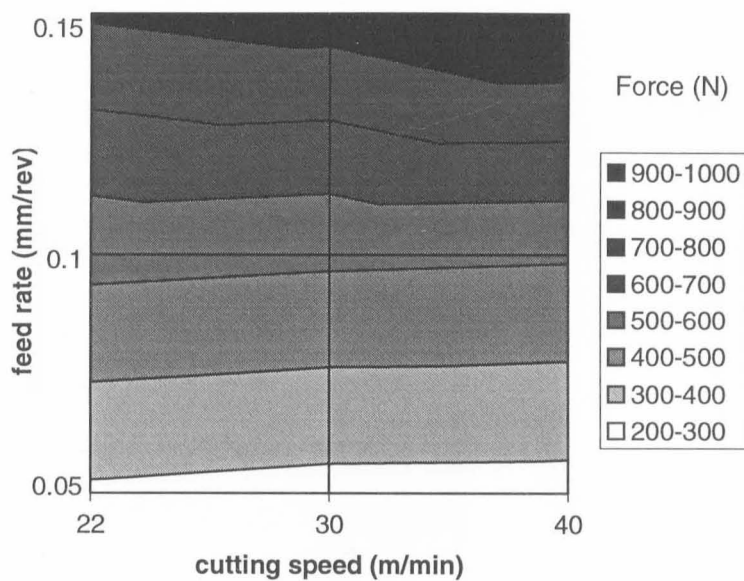


Figure 4.8 Effect of cutting speed and feed rate on cutting force, 1%.

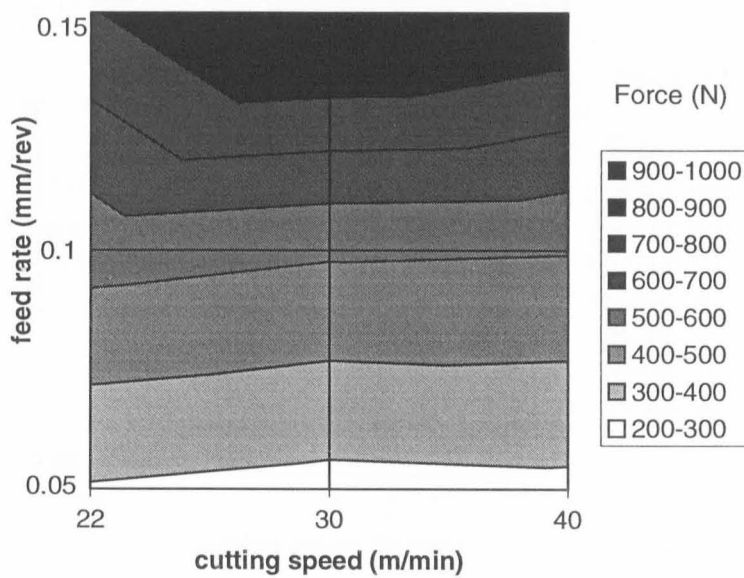


Figure 4.9 Effect of cutting speed and feed rate on cutting force, 2%.

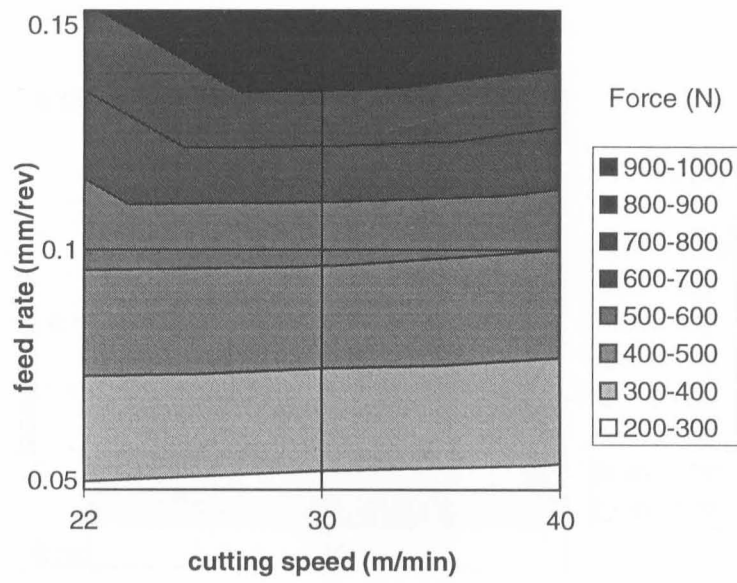


Figure 4.10 Effect of cutting speed and feed rate on cutting force, 3%.

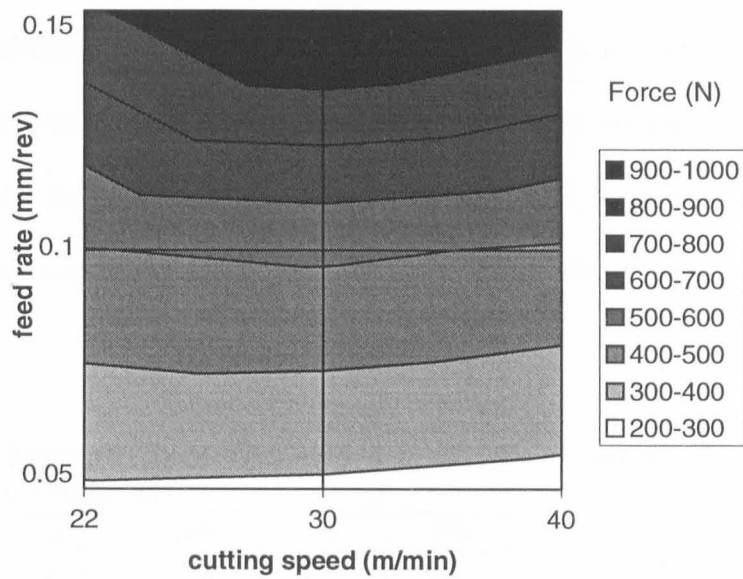


Figure 4.11 Effect of cutting speed and feed rate on cutting force, 4%.

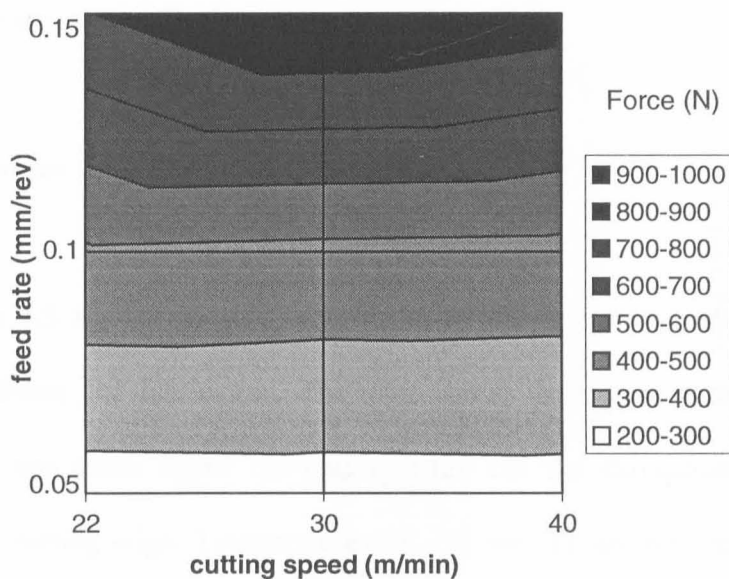


Figure 4.12 Effect of cutting speed and feed rate on cutting force, 5%.

The results showed that the lubricant did not have a significant effect on the values of force. An analysis of variance using three results for each condition showed that statistically the results are the same. An example of force results used for such analysis is shown in table 4.2 for 30m/min and 0.15mm/rev.

Table 4.2-Measured forces (F_c) used in an analysis of variance, 30m/min, 0.15mm/rev.

	dry	0%	1%	2%	3%	4%	5%
Cutting forces (N)	976	765	846	960	945	938	908
	970	899	809	947	935	913	869
	843	795	834	801	867	869	868

The effect of cutting speed and feed rate on cutting force is similar for all lubricated conditions. There is little variation with speed for feeds below 0.1mm/rev.

Between 0.1mm/rev and 0.15mm/rev there is a range of cutting speeds where the forces have a sharp change.

4.2 Temperature

Table 4.3 shows the temperature rise of the transient surface according to cutting conditions and lubrication. The table shows the temperature rise obtained at 3mm, 6mm, and 9mm below the cutting edge and the extrapolated result, which means at the cutting edge. Temperatures T9, T6 and T3 are not the absolute values obtained during the test. These values are the absolute values measured by the infrared sensor after compensation using the calibration curve according to the lubrication used and subtracted from the room temperature. The temperature T for each test is the temperature rise after extrapolation.

For all tests the variation of temperature after the cut starts is similar and it takes about 30 seconds to be stable. Figures 4.13 to 4.15 show the graphs of temperature against time during the cut for dry condition, lubricated with oil and oil +1% additive, respectively, using 30m/min and 0.1mm/rev.

The results for 6mm and 9mm below the cutting edge showed similar variations.

Figures 4.16 to 4.18 show the extrapolation curves for the same lubrication conditions of figures 4.13 to 4.15 respectively and for the three feed rates used.

Table 4.3-Temperature rise on transient surface.

Vc (m/min)	f (mm/rev)	Lubricant	T9 (°C)	T6 (°C)	T3 (°C)	T (°C)
22	0.05	Dry	7	13	20	35
		0%	7	11	20	33
		1%	6	11	21	39
		2%	7	12	19	40
		3%	5	14	19	42
		4%	6	11	19	34
	0.10	dry	9	16	30	55
		0%	10	19	33	61
		1%	11	19	28	46
		2%	11	21	29	50
		3%	10	19	32	58
		4%	9	15	29	51
	0.15	5%	7	17	25	52
		dry	14	21	52	93
		0%	12	20	42	76
		1%	14	22	44	75
		2%	16	24	47	77
		3%	15	24	52	92
30	0.05	4%	13	19	47	82
		5%	15	25	48	84
		dry	7	16	26	53
		0%	7	10	29	52
		1%	7	15	20	37
		2%	8	15	29	55
	0.10	3%	9	15	24	39
		4%	5	10	19	37
		5%	6	10	25	48
		dry	9	22	31	63
		0%	11	20	35	63
		1%	12	20	33	55
	0.15	2%	12	20	33	55
		3%	12	21	35	60
		4%	9	16	28	50
		5%	9	16	27	47
		dry	17	30	54	96
		0%	13	29	44	86
40	0.05	1%	15	24	45	76
		2%	18	30	53	90
		3%	14	28	50	96
		4%	14	23	44	76
		5%	15	23	50	86
		dry	7	18	28	61
	0.10	0%	7	15	28	57
		1%	6	17	25	57
		2%	8	17	29	57
		3%	6	15	25	55
		4%	6	13	25	52
		5%	8	15	28	52
	0.15	dry	12	24	37	68
		0%	9	21	29	57
		1%	14	22	36	57
		2%	14	25	36	60
		3%	15	22	37	57
		4%	11	20	35	63
0.15	5%	12	18	35	57	
	dry	25	49	64	110	
	0%	17	33	56	104	
	1%	19	30	58	98	
	2%	19	30	61	105	
	3%	16	35	58	116	
	4%	17	29	55	97	
	5%	16	30	54	100	

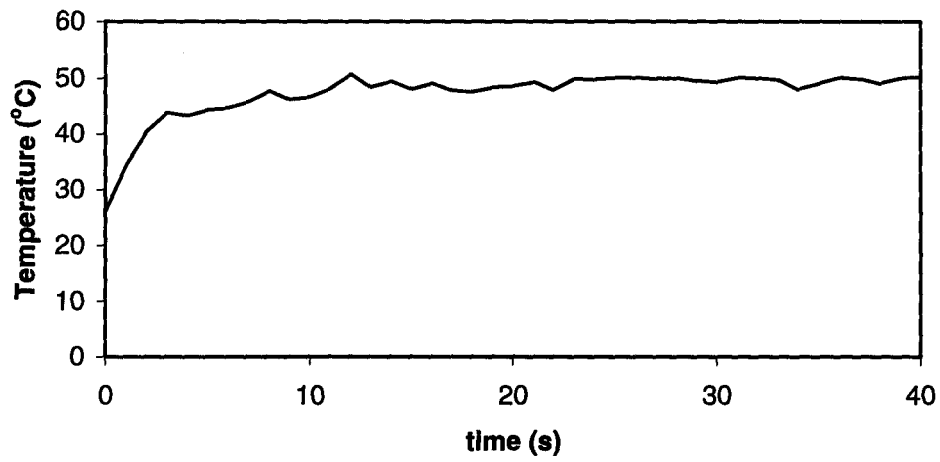


Figure 4.13 Variation of temperature at 3mm below cutting edge after start of cutting.
30m/min, 0.1mm/rev, dry.

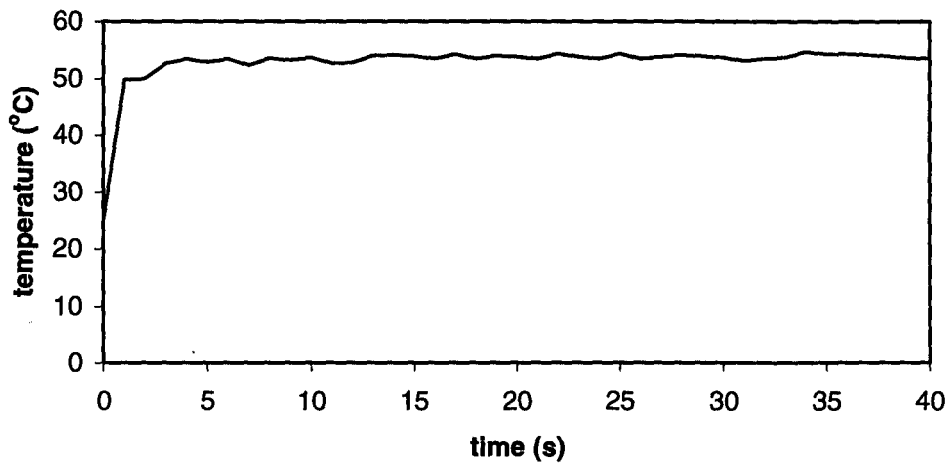


Figure 4.14 Variation of temperature at 3mm below cutting edge after start of cutting.
30m/min, 0.1mm/rev, 0%.

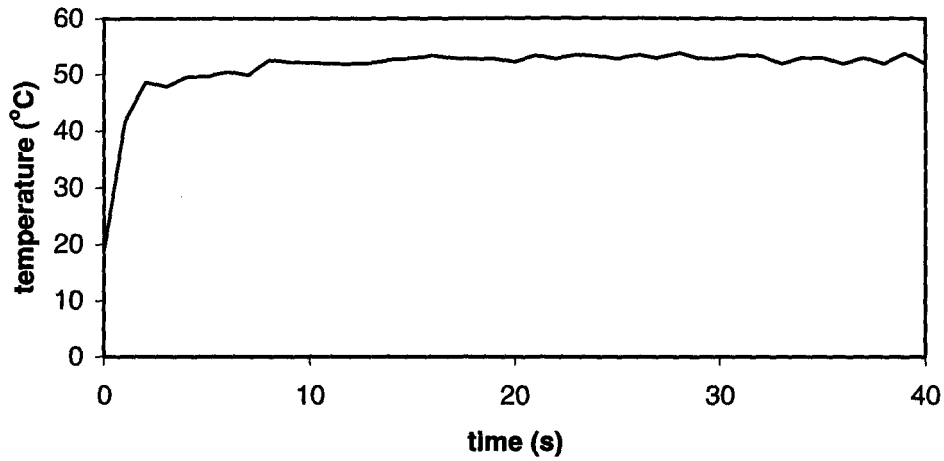


Figure 4.15 Variation of temperature at 3mm below cutting edge after start of cutting. 30m/min, 0.1mm/rev, 1%.

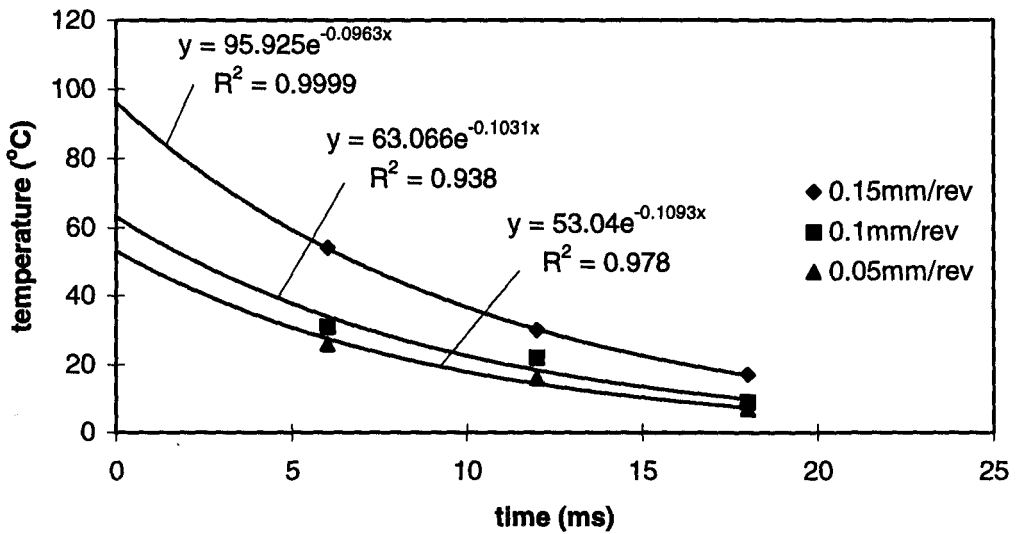


Figure 4.16 Extrapolation of temperature in the transient surface, 30m/min, dry.

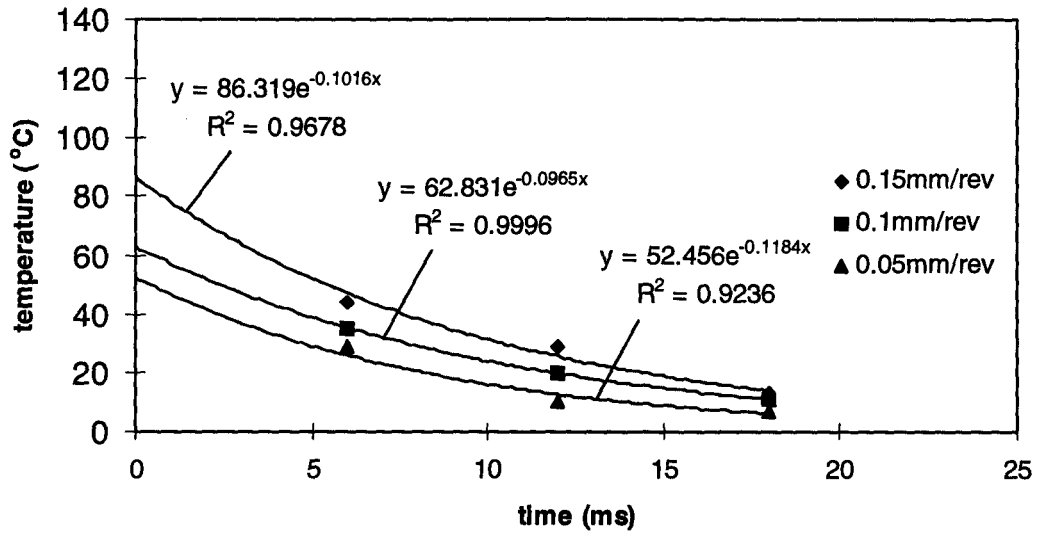


Figure 4.17 Extrapolation of temperature in the transient surface, 30m/min, 0%.

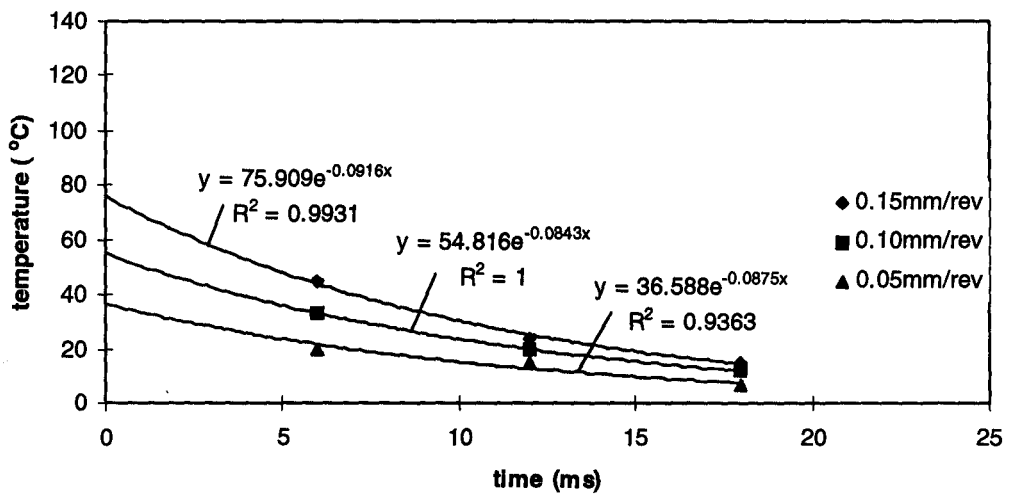


Figure 4.18 Extrapolation of temperature in the transient surface, 30m/min, 1%.

The results fit very well into the exponential equation, as can be seen by the high coefficient of correlation shown with the respective equations.

Using the results of temperature measurements for 3, 6 and 9mm the cooling rate of the workpiece can be estimated, which is very high. As the cooling curve is not straight the cooling rate is not constant and depends on time. For example, the cooling rate for the first 3mm below the cutting edge is about 8,000°C/s for dry conditions, 40m/min and 0.15mm/rev.

The same type of graph that was done for force to show the combined effect of cutting speed and feed rate can be done for temperature. Figures 4.19 to 4.25 show these graphs for all lubricated conditions used.

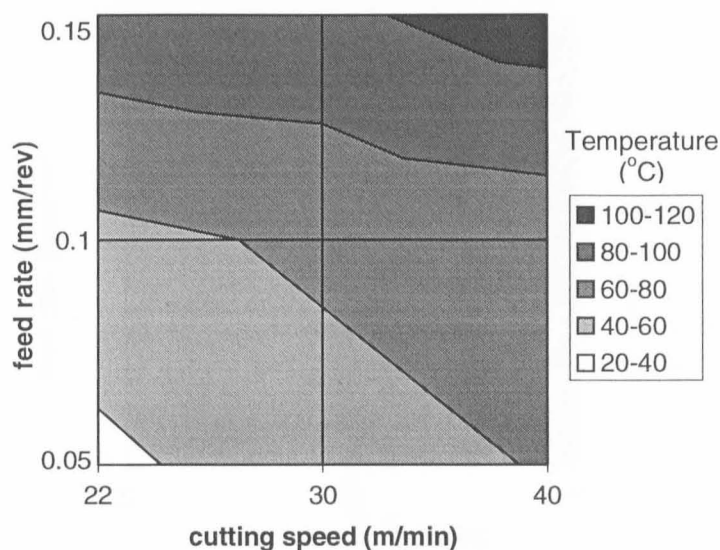


Figure 4.19 Effect of cutting speed and feed rate on variation of temperature, dry.

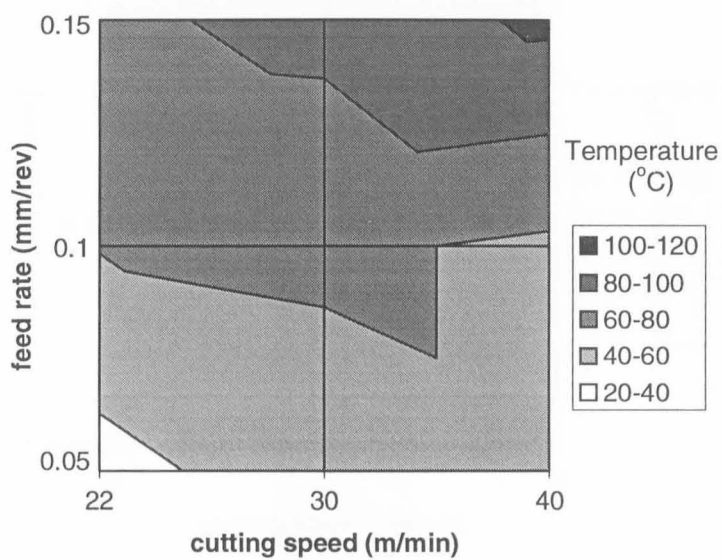


Figure 4.20 Effect of cutting speed and feed rate on variation of temperature, 0%.

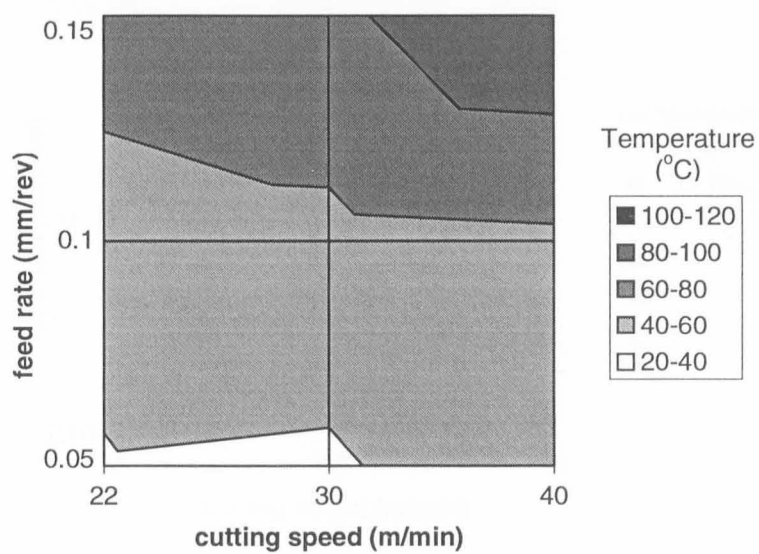


Figure 4.21 Effect of cutting speed and feed rate on variation of temperature, 1%.

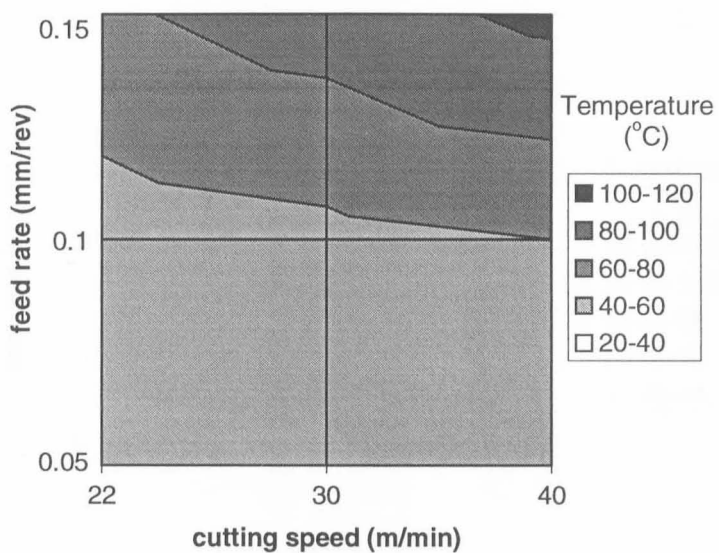


Figure 4.22 Effect of cutting speed and feed rate on variation of temperature, 2%.

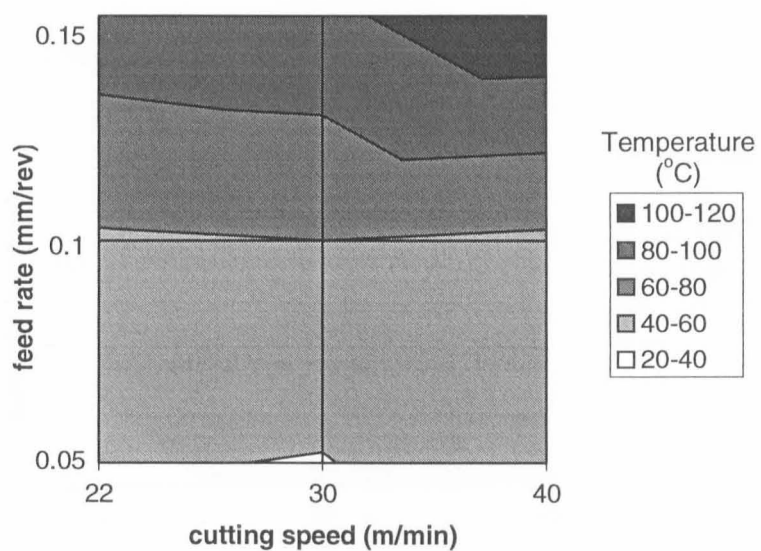


Figure 4.23 Effect of cutting speed and feed rate on variation of temperature, 3%.

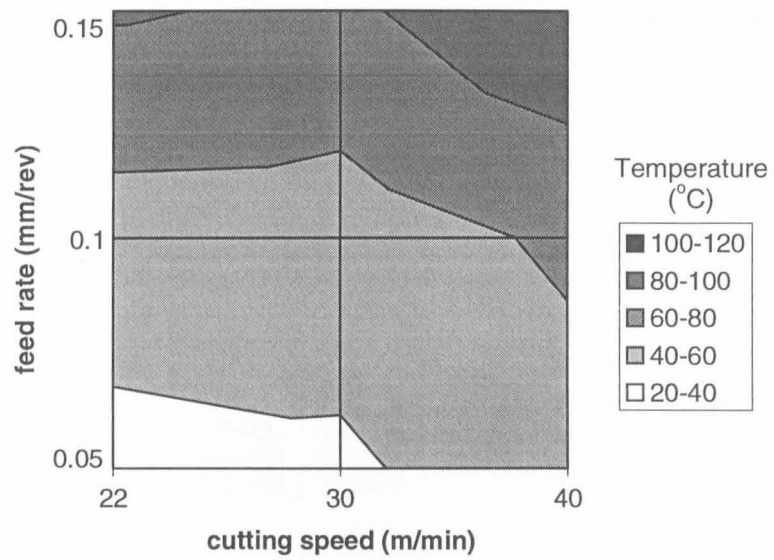


Figure 4.24 Effect of cutting speed and feed rate on variation of temperature, 4%.

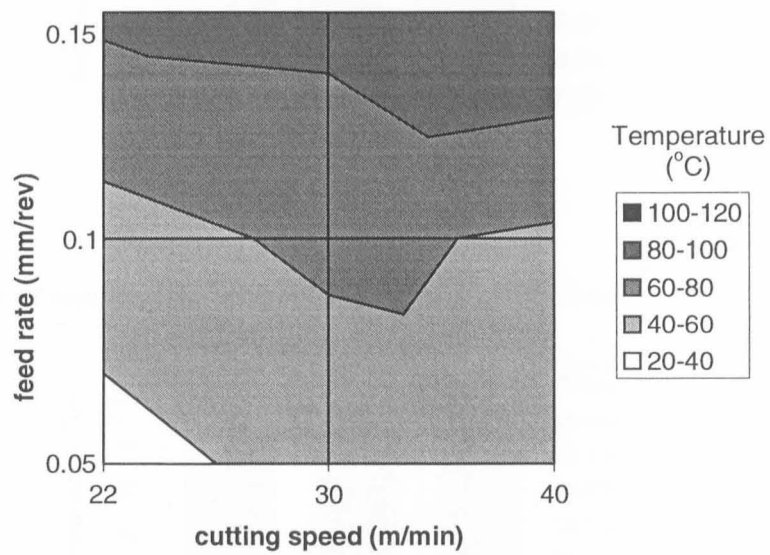


Fig.4.25-Effect of cutting speed and feed rate on variation of temperature, 5%.

The effect of cutting conditions and lubrication on workpiece temperature seems unclear according to the graphs. Figures 4.26 to 4.28 show the variation of temperature against cutting speed for the feed rates used.

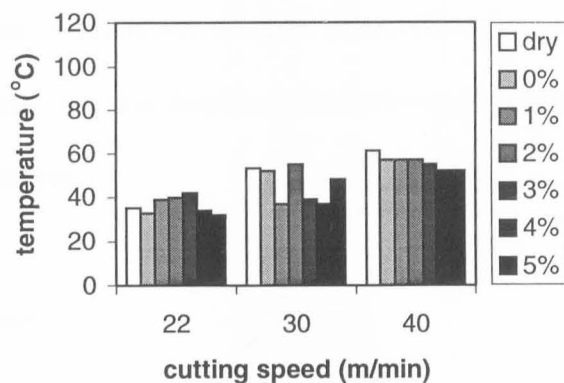


Figure 4.26 Rise of temperature with cutting speed, 0.05mm/rev.

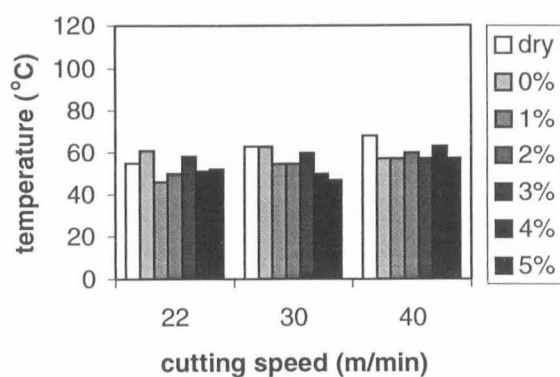


Figure 4.27 Rise of temperature with cutting speed, 0.10mm/rev.

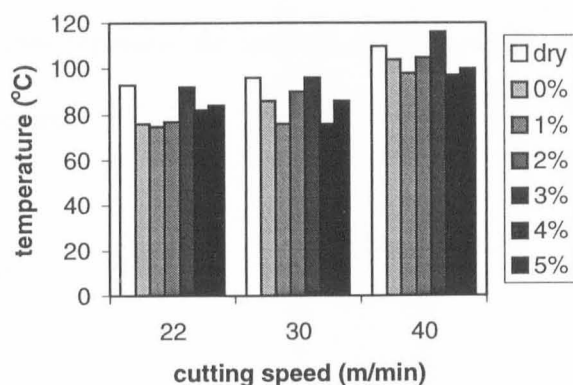


Figure 4.28 Rise of temperature with cutting speed, 0.15mm/rev.

According to the graphs there is little effect on temperature due to lubrication. Moreover the effect is sometimes to increase the temperature and sometimes to decrease it. It seems that the additive also did not have any effect on temperature.

An attempt to correlate the increase of temperature on transient surface with cutting speed and feed rate was done and the following results were obtained for dry and lubricated conditions:

$$\text{Dry: } T=50.Vc^{0.52}.f^{0.62}$$

$$\text{Oil: } T=54.Vc^{0.44}.f^{0.57}$$

$$1\%: T=42.Vc^{0.48}.f^{0.55}$$

$$2\%: T=41.Vc^{0.47}.f^{0.49}$$

$$3\%: T=139.Vc^{0.27}.f^{0.70}$$

$$4\%: T=60.Vc^{0.44}.f^{0.65}$$

$$5\%: T=63.Vc^{0.42}.f^{0.63}$$

T in °C, Vc in m/min, f in mm/rev.

These equations represent the increase of temperature on the transient surface, close to the cutting edge.

4.3 Chip Thickness

Table 4.4 presents the chip thickness for all cutting conditions used in the tests and the chip ratios.

Table 4.4-Chip thickness for all the cutting conditions.

Vc (m/min)	f (mm/rev)	Lubricant	Chip thickness (mm)	Chip ratio
22	0.05	Dry	0.086	2.4
		0%	0.107	3.0
		1%	0.089	2.5
		2%	0.104	2.9
		3%	0.097	2.7
		4%	0.090	2.5
	0.10	dry	0.188	2.7
		0%	0.215	3.0
		1%	0.210	3.0
		2%	0.210	3.0
		3%	0.207	2.9
		4%	0.202	2.9
	0.15	dry	0.445	4.2
		0%	0.338	3.2
		1%	0.416	3.9
		2%	0.479	4.5
		3%	0.408	3.8
		4%	0.384	3.6
30	0.05	dry	0.083	2.3
		0%	0.082	2.3
		1%	0.083	2.3
		2%	0.089	2.5
		3%	0.086	2.4
		4%	0.080	2.3
	0.10	dry	0.203	2.9
		0%	0.208	2.9
		1%	0.191	2.7
		2%	0.192	2.7
		3%	0.187	2.6
		4%	0.179	2.5
	0.15	dry	0.400	3.8
		0%	0.316	3.0
		1%	0.355	3.3
		2%	0.437	4.1
		3%	0.387	3.6
		4%	0.418	3.9
40	0.05	dry	0.088	2.5
		0%	0.088	2.5
		1%	0.084	2.4
		2%	0.096	2.7
		3%	0.089	2.5
		4%	0.088	2.5
	0.10	dry	0.176	2.5
		0%	0.183	2.6
		1%	0.170	2.4
		2%	0.172	2.4
		3%	0.149	2.1
		4%	0.160	2.3
	0.15	dry	0.363	3.4
		0%	0.428	4.0
		1%	0.355	3.3
		2%	0.298	2.8
		3%	0.312	2.9
		4%	0.364	3.4
	5%	0.343	3.2	

Figures 4.29 to 4.31 presents the chip ratio against cutting speed for all lubricated conditions and feed rates.

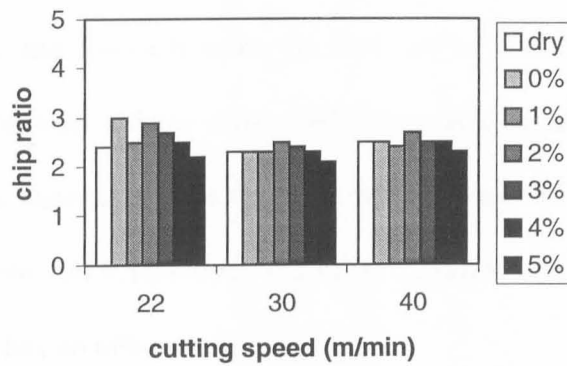


Figure 4.29 Variation of chip ratio with cutting speed, 0.05mm/rev.

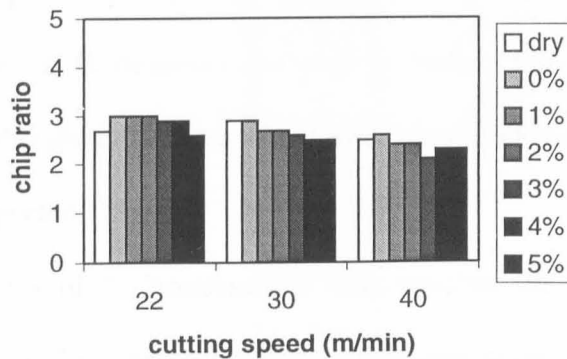


Figure 4.30 Variation of chip ratio with cutting speed, 0.10mm/rev.

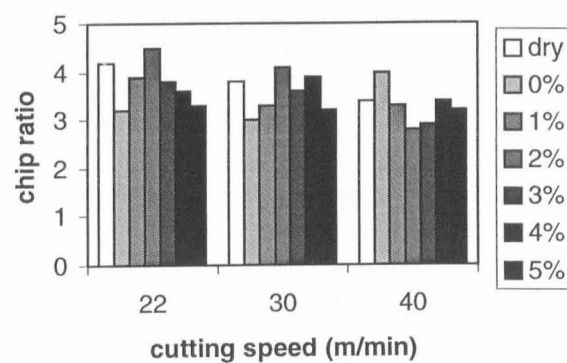


Figure 4.31 Variation of chip ratio with cutting speed, 0.15mm/rev.

The chip ratio increases with feed and varies very little with cutting speed. This is similar for all lubrication conditions. The results seem to be scattered and no

single effect of the lubricant could be detected. The effect seems to be dependent on cutting speed, but it is not uniform. For instance, oil without sulphur gives smaller values for 22m/min and 30m/min when the feed rate is 0.15mm/rev, but the effect is the opposite for 40m/min and the same feed. There is a trend on the results of chip ratio indicating that there is a little decrease with the speed, exceptions are for dry condition at 40m/min and 0.1mm/rev, and oil at 40m/min and 0.15mm/rev. It seems that the lubrication has no effect on it.

The shape of the chip changes with cutting conditions. For 0.05mm/rev and 0.1mm/rev at any speed the chip is continuous and helical, its length increases with the speed. However at 0.15mm/rev the chip is broken into small pieces. For the highest feed it is therefore difficult to measure chip thickness, and more scattered results are to be expected.

For feed rates of 0.15mm/rev the chip touches the workpiece surface, as shown in figure 4.32. This figure shows a quick stop sample for 40m/min and dry condition. A higher magnification, using the optical microscope, of the contact between chip and workpiece after polishing is also shown in the figure. For this particular case the chip started to cut the workpiece, acting like a tool. This action lasts for some seconds as the chip breaks.

The results of chip thickness can be used to calculate the theoretical primary shear plane angle, ϕ , for each condition using the single relationship between chip thickness, thickness of the undeformed cut and rake angle, according to figure 2.3 and equation (2.1). In that case the undeformed chip thickness, t_1 , is given by feed multiplied by $\sin(45^\circ)$, which is the approach angle. Table 4.5 shows the results of these calculations for all cutting conditions.

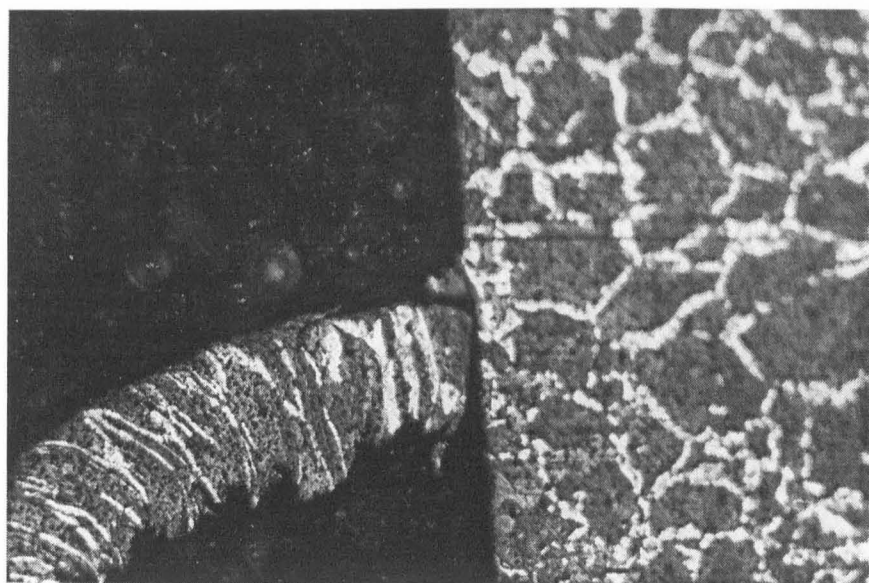
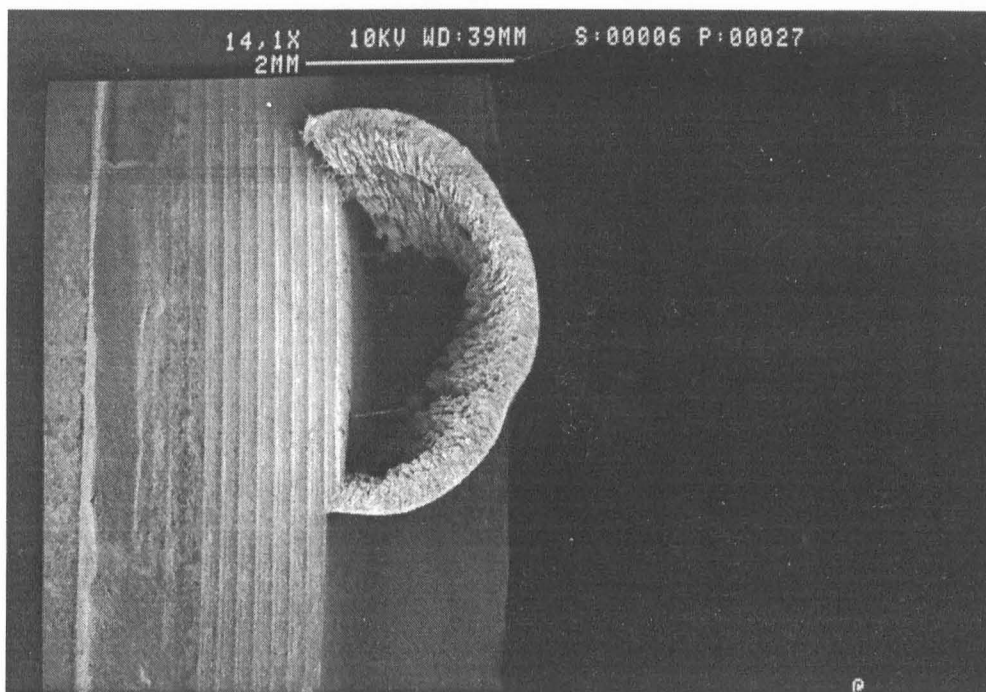


Figure 4.32 Quick stop sample for 40m/min and 0.15mm/rev, dry condition, (a)14.1x, (b)150x.

Table 4.5-Primary shear plane angle for all cutting conditions.

Vc (m/min)	f (mm/rev)	Lubricant	Primary shear plane angle (degree)
22	0.05	dry	23
		0%	19
		1%	22
		2%	19
		3%	21
		4%	22
	5%	25	
	0.10	dry	21
		0%	19
		1%	19
		2%	19
		3%	19
		4%	20
	5%	22	
	0.15	dry	14
		0%	18
		1%	15
		2%	13
3%		15	
4%		16	
5%	17		
30	0.05	dry	25
		0%	24
		1%	24
		2%	22
		3%	23
		4%	25
	5%	26	
	0.10	dry	20
		0%	19
		1%	21
		2%	21
		3%	21
		4%	21
	5%	22	
	0.15	dry	15
		0%	19
		1%	17
		2%	14
3%		16	
4%		14	
5%	18		
40	0.05	dry	23
		0%	23
		1%	24
		2%	21
		3%	22
		4%	23
	5%	23	
	0.10	dry	23
		0%	22
		1%	23
		2%	23
		3%	26
		4%	25
	5%	24	
	0.15	dry	17
		0%	14
		1%	17
		2%	20
3%		19	
4%		17	
5%	18		

Shear plane angle decreases with feed rate for all lubrication conditions, but again the effect of the lubrication is uncertain. Figures 4.33 to 4.35 show the variation of the primary shear plane angle with cutting speed for all lubricated conditions and feed rates.

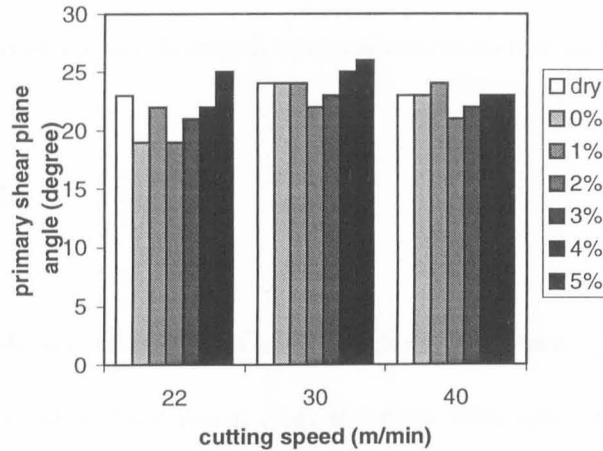


Figure 4.33 Variation of primary shear plane angle with cutting speed, 0.05mm/rev.

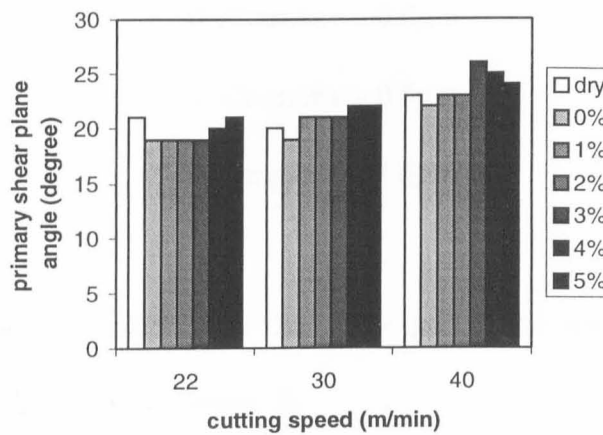


Figure 4.34 Variation of primary shear plane angle with cutting speed, 0.10mm/rev.

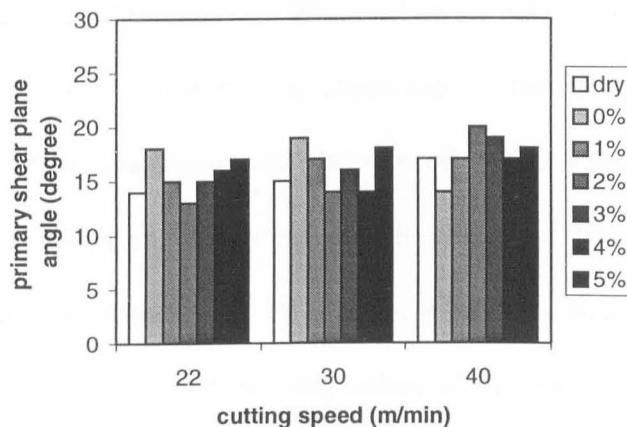


Figure 4.35 Variation of primary shear plane angle with cutting speed, 0.15mm/rev.

According to the accuracy of the micrometer used to measure chip thickness (0.005 mm), an error of 5° is to be expected for the calculation of the theoretical shear plane angle.

The shear plane angle for 0.15mm/rev seems lower than the normal values expected. These however are theoretical values which do not include BUE effects.

4.4 Surface Finish

Table 4.6 shows the results of surface finish, measured by the parameter Ra.

The theoretical surface finish (Ra) for each feed rate calculated according to equation (2.5) is:

$$0.05\text{mm/rev} - 0.2\mu\text{m}$$

$$0.10\text{mm/rev} - 0.8\mu\text{m}$$

$$0.15\text{mm/rev} - 1.8\mu\text{m}$$

These values are rather lower than the experimental results, as was expected due to the reasons discussed in chapter 2.

Surface roughness seems to be constant with the increase of feed rate or cutting speed at least until 0.1mm/rev. When oil or oil with sulphur is used, finish is improved and the effect of the cutting conditions is the same. There is a slight increase in the surface roughness with the rate of material removal for lubricated conditions. There is less effect of lubrication at 40m/min and 0.15mm/rev.

Surface finish as measured by Ra is lower when oil with sulphur is applied, for any cutting condition. Moreover it is independent of the percentage of additive used

for feed rates of 0.05mm/rev and 0.1mm/rev. In this case the application of the mineral oil without sulphur improves surface finish.

When feed of 0.15mm/rev is used, oil without sulphur does not change the surface finish and the results are similar to dry condition. It can be even higher as in the case of 22m/min. Application of sulphur keeps the values of surface finish lower.

Figures 4.36 to 4.42 show the combined effect of cutting speed and feed rate on the surface finish.

Table 4.6-Surface finish for all cutting conditions.

Vc (m/min)	f (mm/rev)	lubricant	Ra (μm)
22	0.05	dry	5.72
		0%	1.64
		1%	2.42
		2%	0.96
		3%	1.91
		4%	1.07
	0.10	5%	1.35
		dry	4.59
		0%	2.70
		1%	2.81
		2%	1.71
		3%	2.30
	0.15	4%	2.66
		5%	2.33
		dry	12.33
		0%	12.9
		1%	4.67
		2%	3.07
30	0.05	3%	4.22
		4%	4.43
		5%	3.77
		dry	5.62
		0%	2.10
		1%	2.11
	0.10	2%	1.48
		3%	1.00
		4%	0.89
		5%	1.66
		dry	4.63
		0%	2.82
	0.15	1%	2.83
		2%	2.25
		3%	2.44
		4%	2.36
		5%	2.58
		dry	7.36
40	0.05	0%	7.18
		1%	3.73
		2%	4.33
		3%	4.73
		4%	3.37
		5%	3.49
	0.10	dry	5.50
		0%	1.89
		1%	1.39
		2%	2.29
		3%	1.61
		4%	1.33
	0.15	5%	1.81
		dry	5.42
		0%	3.38
		1%	3.41
		2%	3.13
		3%	2.80
0.15	4%	3.09	
	5%	2.60	
	Dry	5.20	
	0%	5.42	
	1%	4.36	
	2%	4.51	
0.15	3%	3.51	
	4%	3.41	
	5%	3.70	

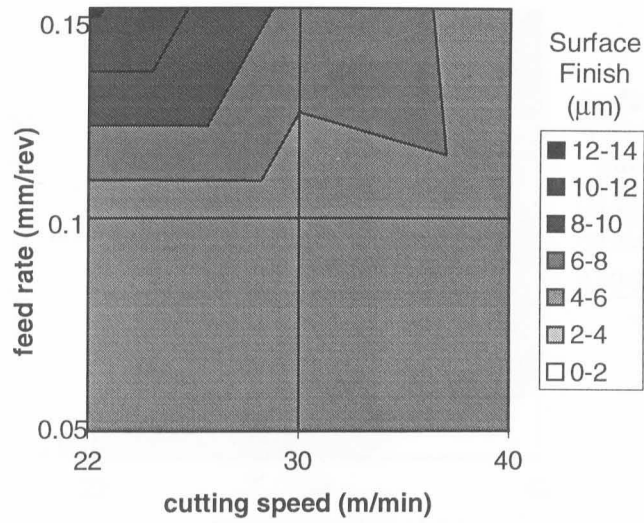


Figure 4.36 Effect of cutting speed and feed rate on surface finish, dry.

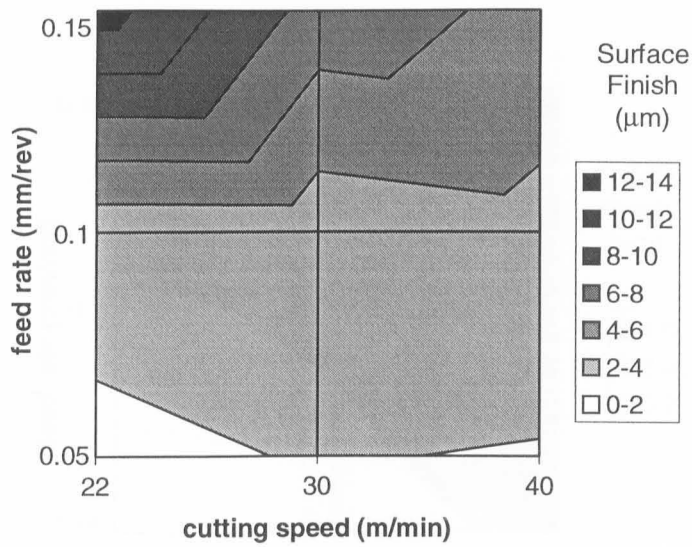


Figure 4.37 Effect of cutting speed and feed rate on surface finish, 0%.

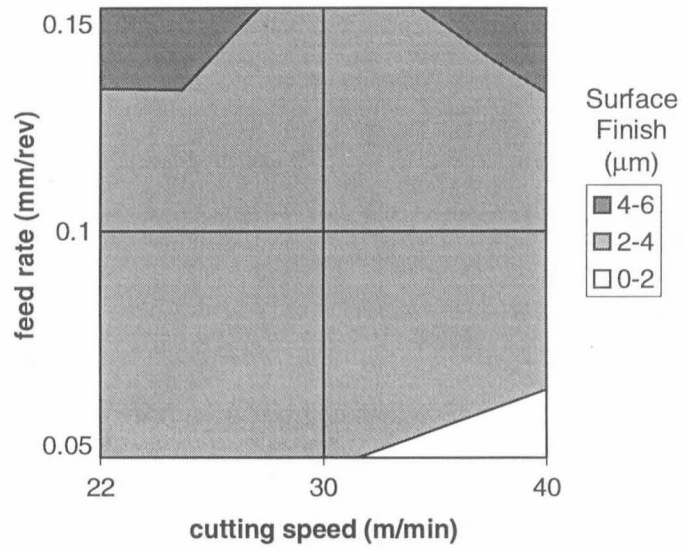


Figure 4.38 Effect of cutting speed and feed rate on surface finish, 1%.

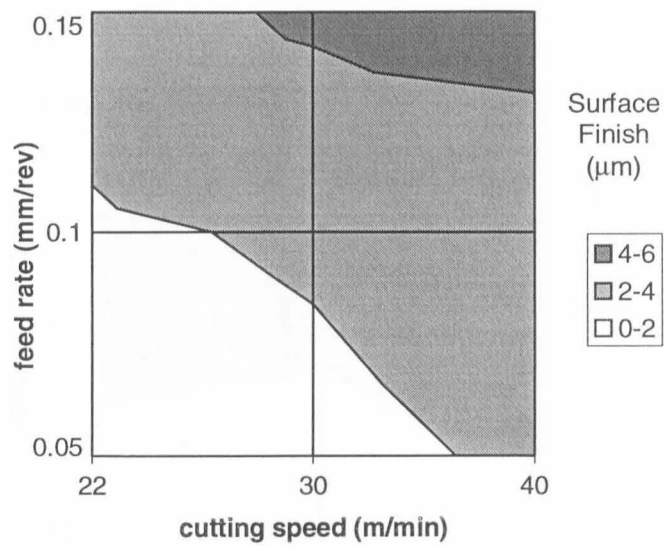


Figure 4.39 Effect of cutting speed and feed rate on surface finish, 2%.

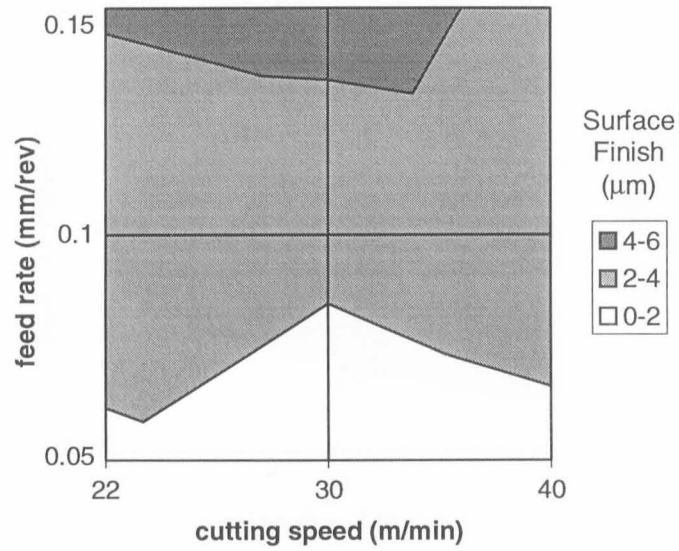


Figure 4.40 Effect of cutting speed and feed rate on surface finish, 3%.

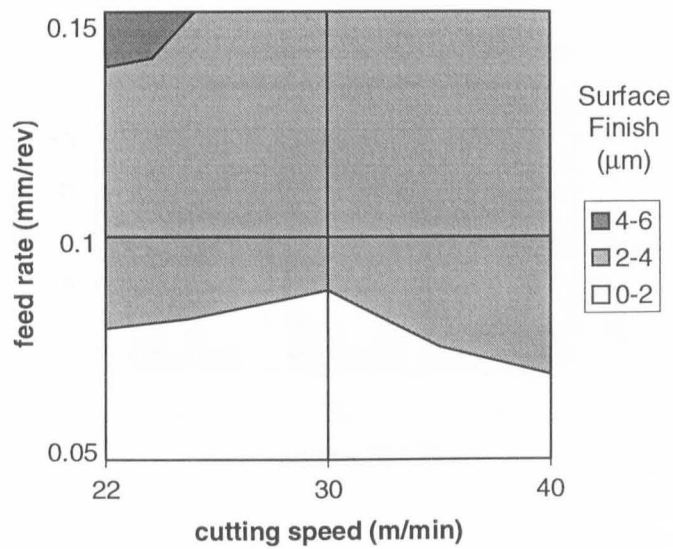


Figure 4.41 Effect of cutting speed and feed rate on surface finish, 4%.

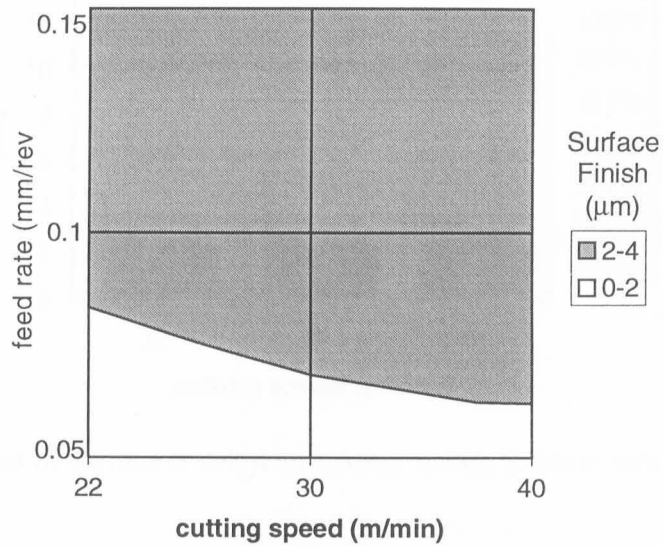


Figure 4.42 Effect of cutting speed and feed rate on surface finish, 5%.

Figures 4.43 to 4.45 show the variation of surface finish with cutting speed and feed rate for all cutting conditions.

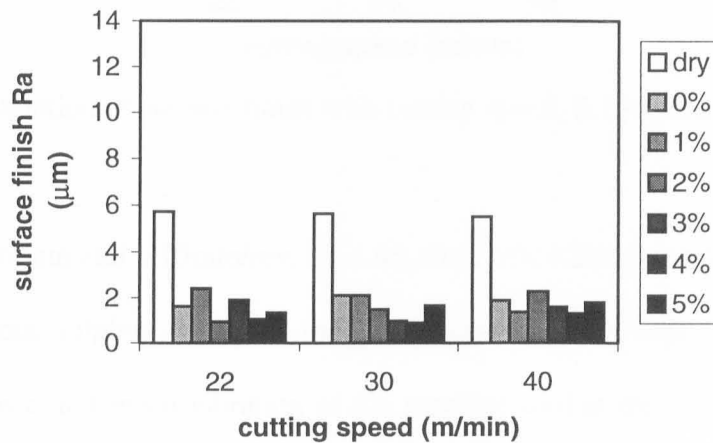


Figure 4.43 Variation of surface finish with cutting speed, 0.05mm/rev.

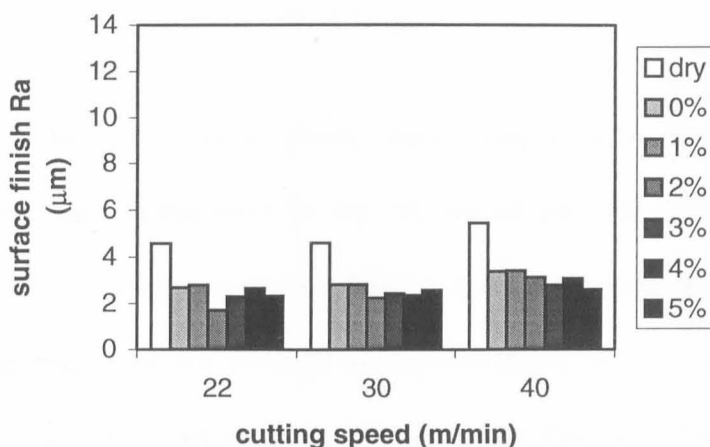


Figure 4.44 Variation of surface finish with cutting speed, 0.10mm/rev.

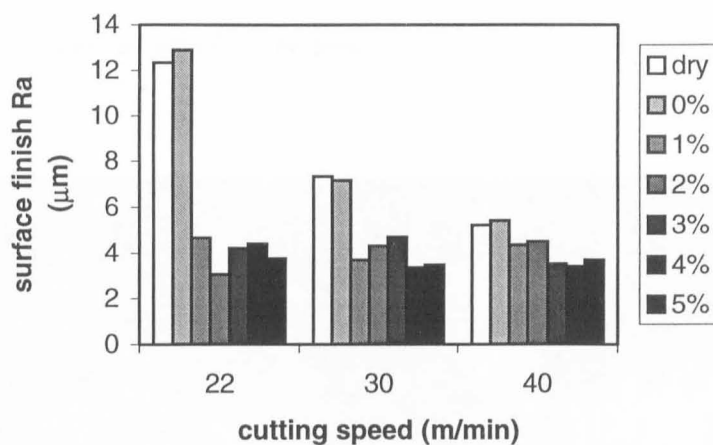


Figure 4.45 Variation of surface finish with cutting speed, 0.15mm/rev.

At 22m/min and 0.15mm/rev, fig 4.45, the surface finish for dry and lubricated with oil without sulphur is higher than the normal values expected in a turning operation. This could mean vibration of the machine tool at this particular condition affecting the surface roughness. However such an effect was not observed for oil with sulphur.

It is clear that the percentage of sulphur does not have any effect on the performance of the lubricant as far as surface finish is concerned, at least for 1% and more of the additive.

4.5 Quick Stop Samples

Figures 4.46 to 4.72 show optical micrography of quick stop samples for all cutting conditions used in this work for dry, oil, and oil with 1% of additive. They can be used to identify in which case there is BUE and to compare the shape and size of it. For all tests the chip remained attached to the workpiece. In some cases, mainly for 0.05mm/rev, as the chip is thin it can easily bend in the direction of the tool when it is moving away. It gives the impression of a high rake angle. In other cases it seems that there was a BUE, but it was not left with the sample after the test, either it was broken and lost or it remained attached to the tool.



Figure 4.46 Optical microscope view of section through quick stop sample for 22m/min and 0.05mm/rev, dry, 300x.

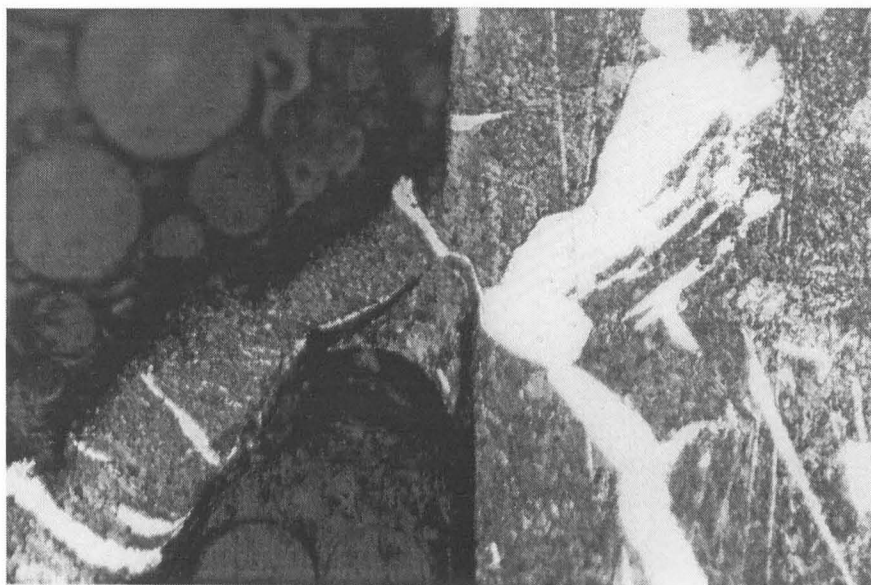


Figure 4.47 Optical microscope view of section through quick stop sample for 22m/min and 0.05mm/rev, 0%, 300x.

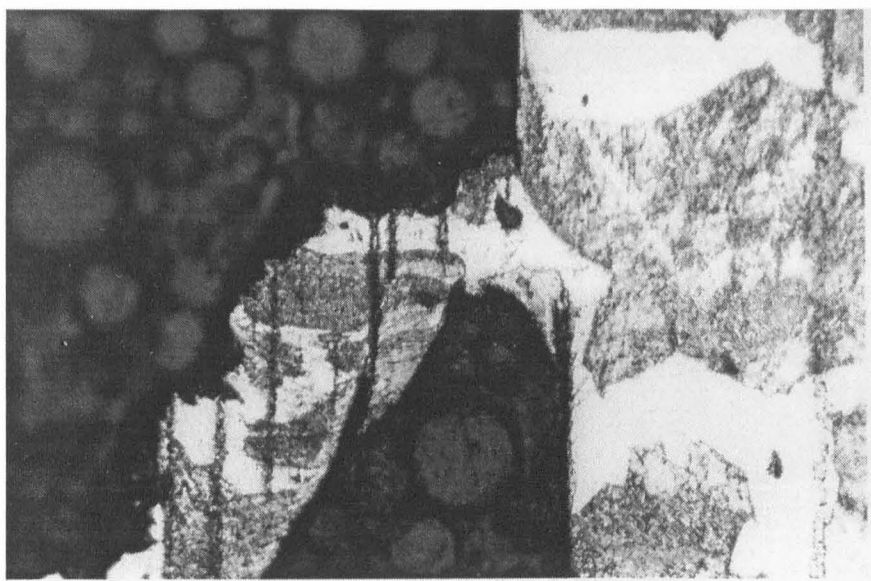


Figure 4.48 Optical microscope view of section through quick stop sample for 22m/min and 0.05mm/rev, 1%, 300x.

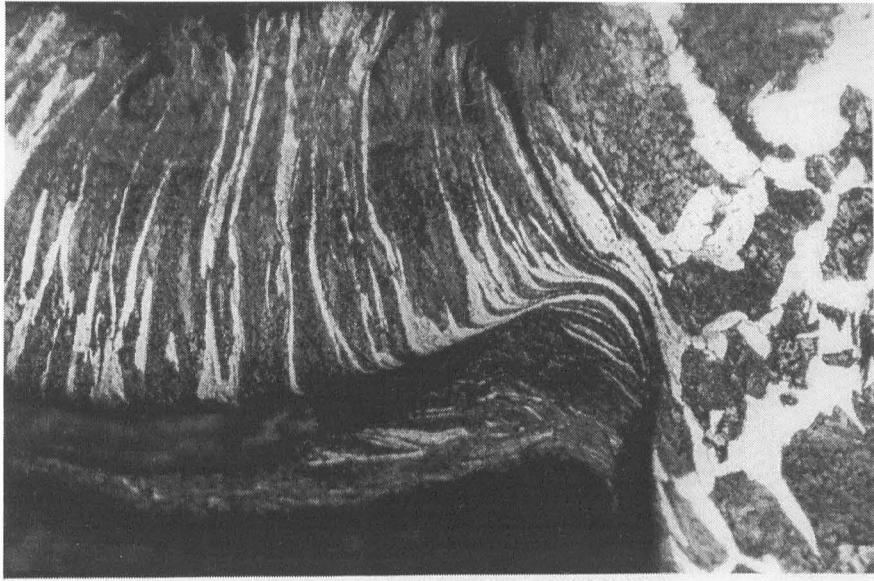


Figure 4.49 Optical microscope view of section through quick stop sample for 22m/min and 0.10mm/rev, dry, 300x.

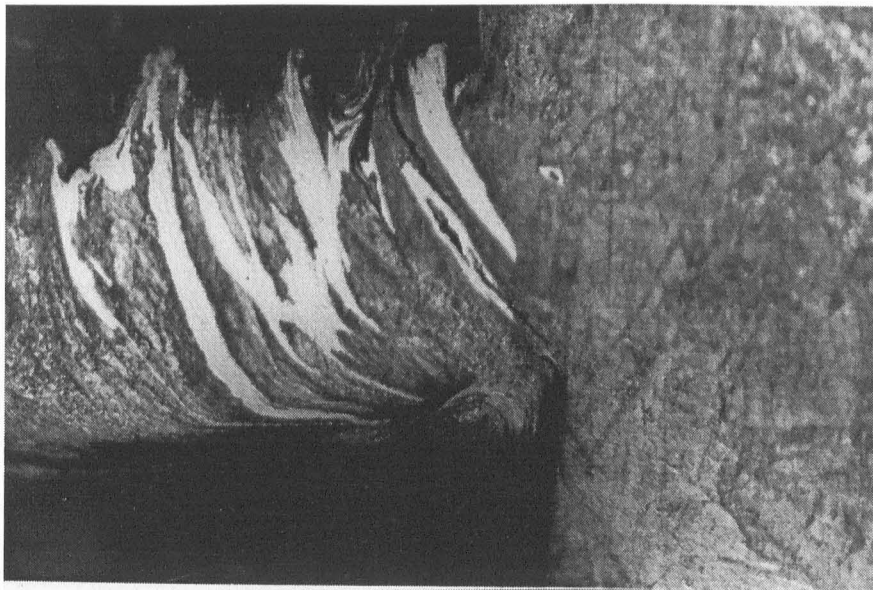


Figure 4.50 Optical microscope view of section through quick stop sample for 22m/min and 0.10mm/rev, 0%, 300x.

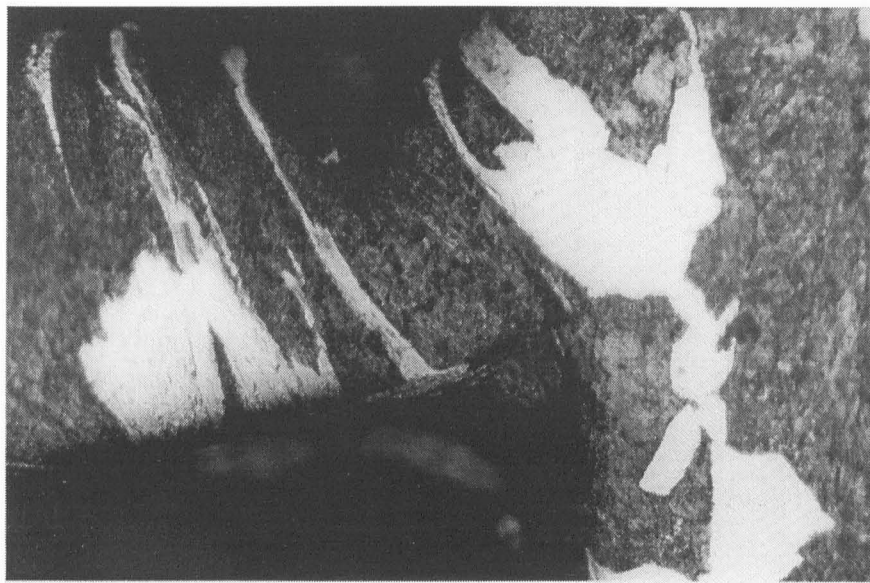


Figure 4.51 Optical microscope view of section through quick stop sample for 22m/min and 0.10mm/rev, 1%, 300x.

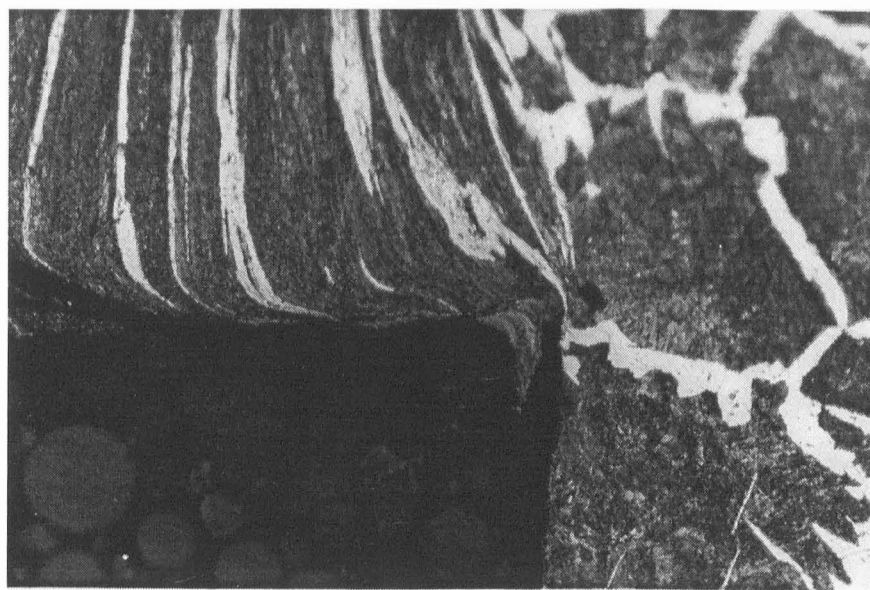


Figure 4.52 Optical microscope view of section through quick stop sample for 22m/min and 0.15mm/rev, dry, 150x.



Figure 4.53 Optical microscope view of section through quick stop sample for 22m/min and 0.15mm/rev, 0%, 150x.

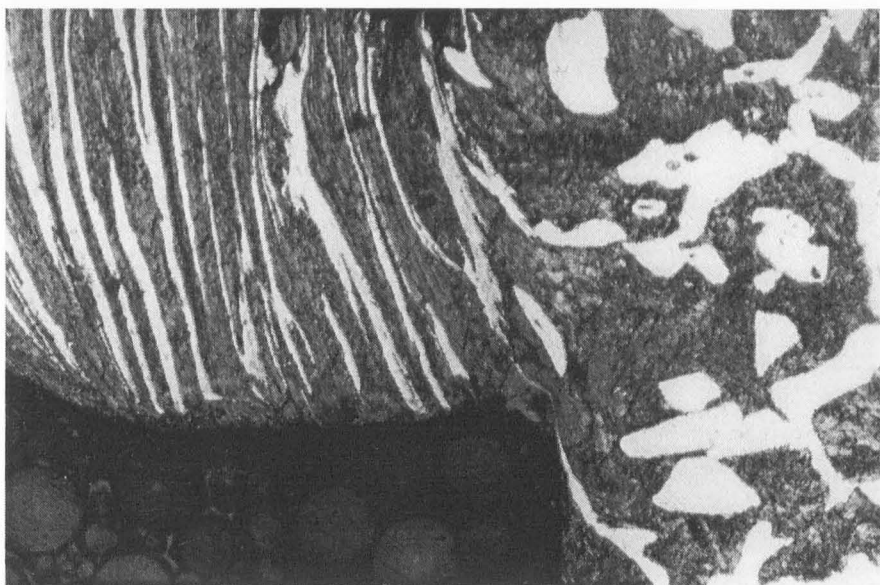


Figure 4.54 Optical microscope view of section through quick stop sample for 22m/min and 0.15mm/rev, 1%, 150x.



Figure 4.55 Optical microscope view of section through quick stop sample for 30m/min and 0.05mm/rev, dry, 300x.

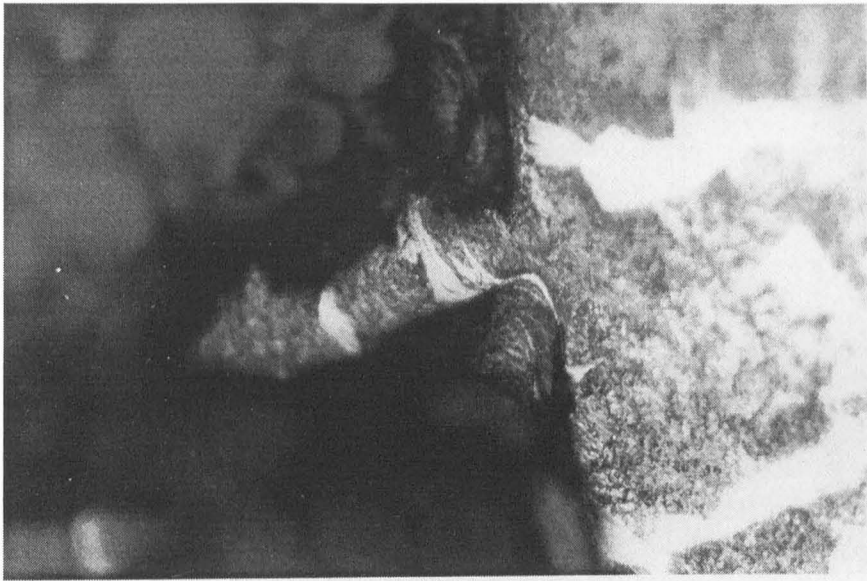


Figure 4.56 Optical microscope view of section through quick stop sample for 30m/min and 0.05mm/rev, 0%, 300x.

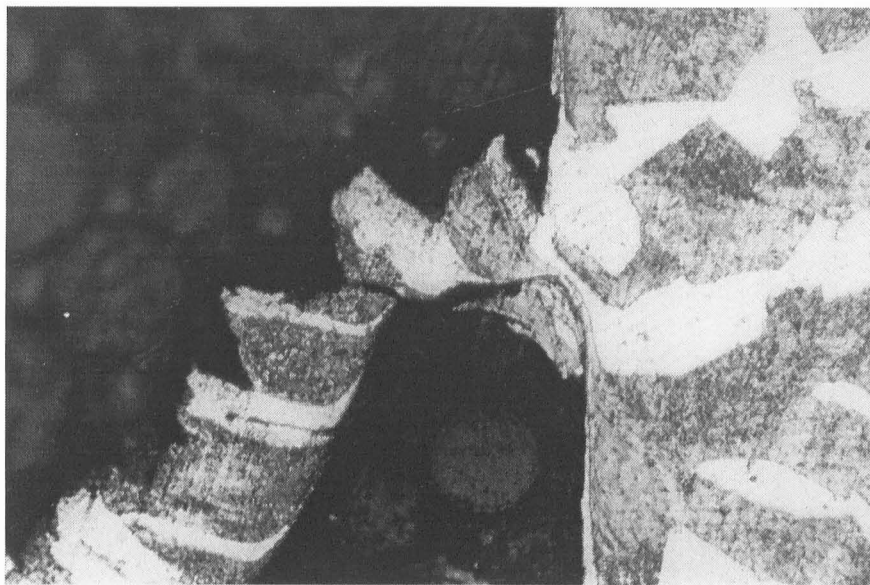


Figure 4.57 Optical microscope view of section through quick stop sample for 30m/min and 0.05mm/rev, 1%, 300x.

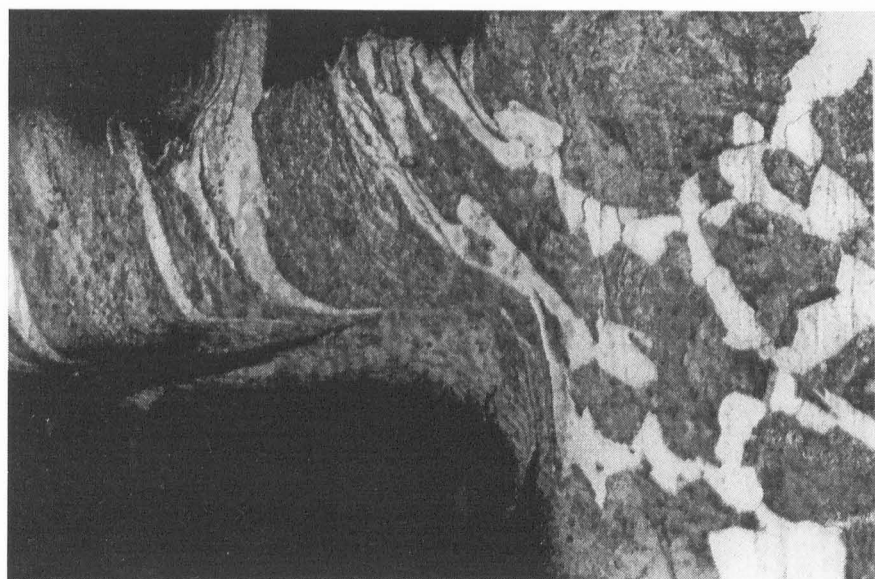


Figure 4.58 Optical microscope view of section through quick stop sample for 30m/min and 0.10mm/rev, dry, 300x.

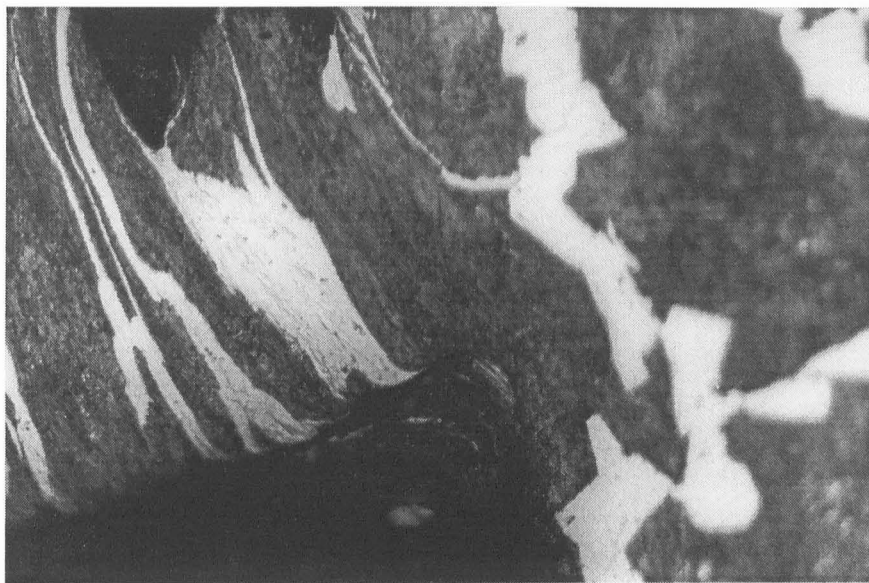


Figure 4.59 Optical microscope view of section through quick stop sample for 30m/min and 0.10mm/rev, 0%, 300x.

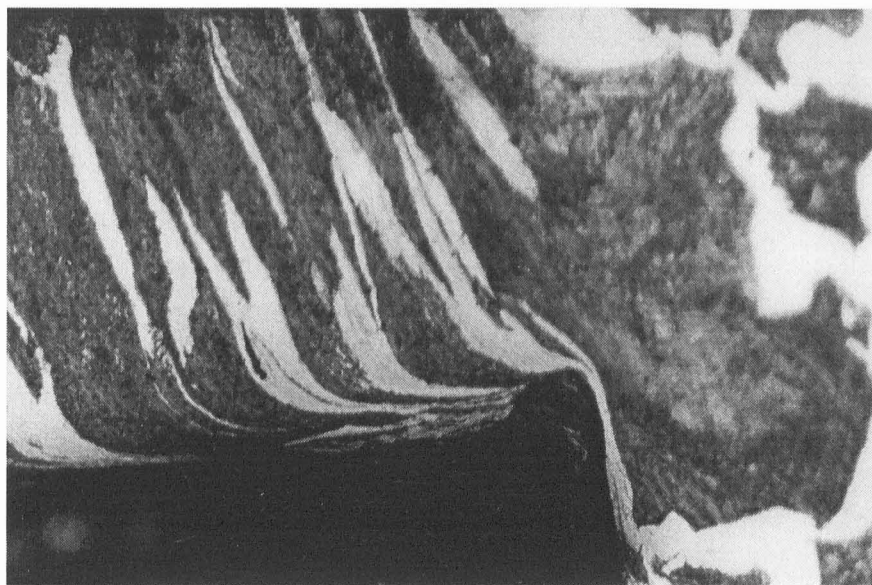


Figure 4.60 Optical microscope view of section through quick stop sample for 30m/min and 0.10mm/rev, 1%, 300x.



Figure 4.61 Optical microscope view of section through quick stop sample for 30m/min and 0.15mm/rev, dry, 300x.

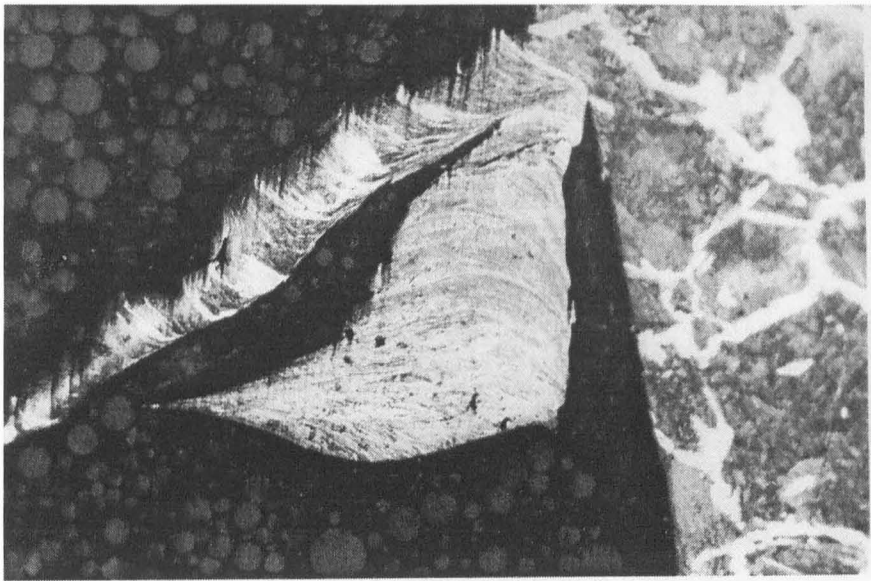


Figure 4.62 Optical microscope view of section through quick stop sample for 30m/min and 0.15mm/rev, 0%, 100x.

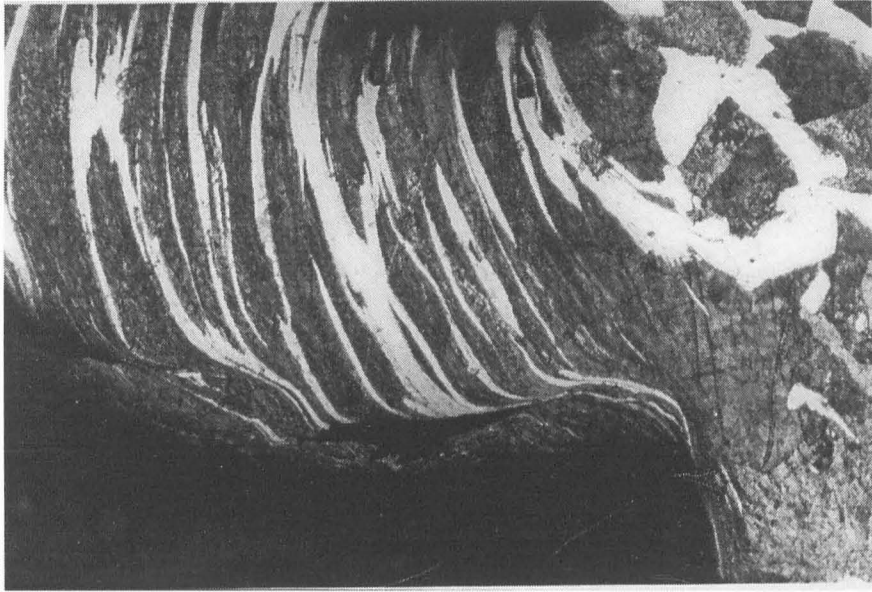


Figure 4.63 Optical microscope view of section through quick stop sample for 30m/min and 0.15mm/rev, 1%, 300x.



Figure 4.64 Optical microscope view of section through quick stop sample for 40m/min and 0.05mm/rev, dry, 300x.



Figure 4.65 Optical microscope view of section through quick stop sample for 40m/min and 0.05mm/rev, 0%, 300x.

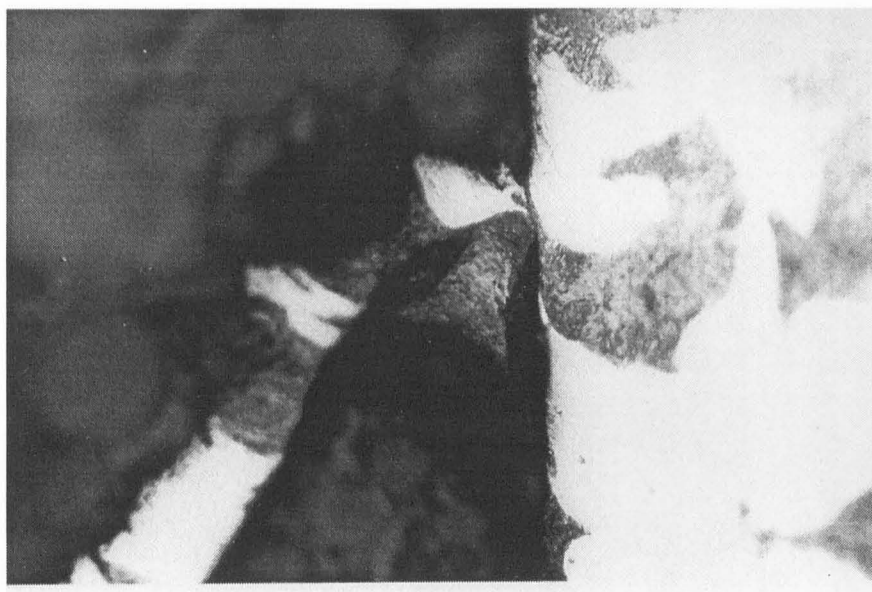


Figure 4.66 Optical microscope view of section through quick stop sample for 40m/min and 0.05mm/rev, 1%, 300x.

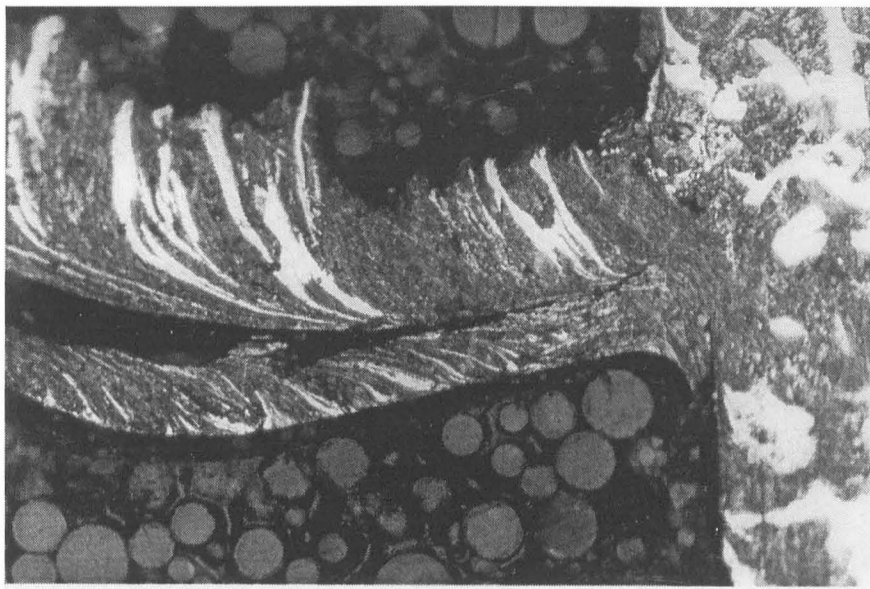


Figure 4.67 Optical microscope view of section through quick stop sample for 40m/min and 0.10mm/rev, dry, 150x.

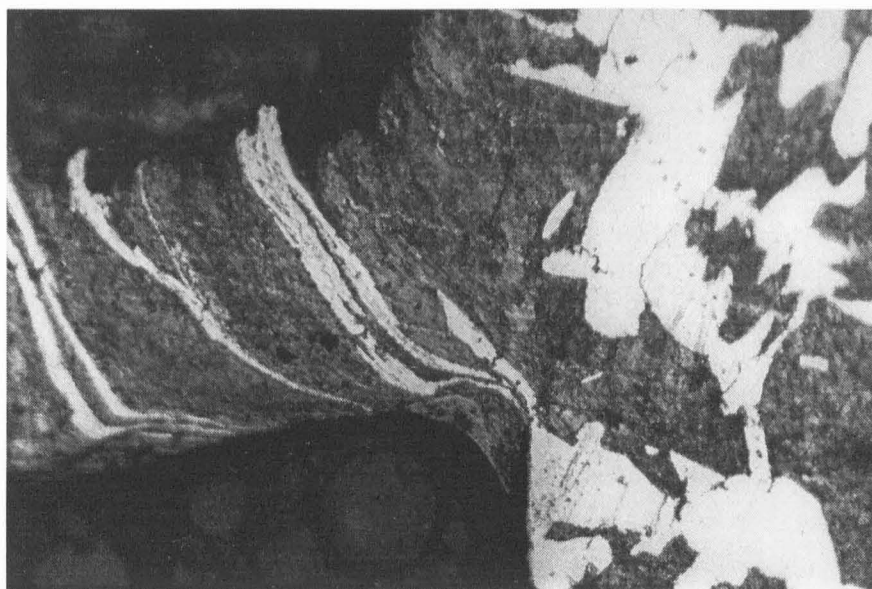


Figure 4.68 Optical microscope view of section through quick stop sample for 40m/min and 0.10mm/rev, 0%, 300x.

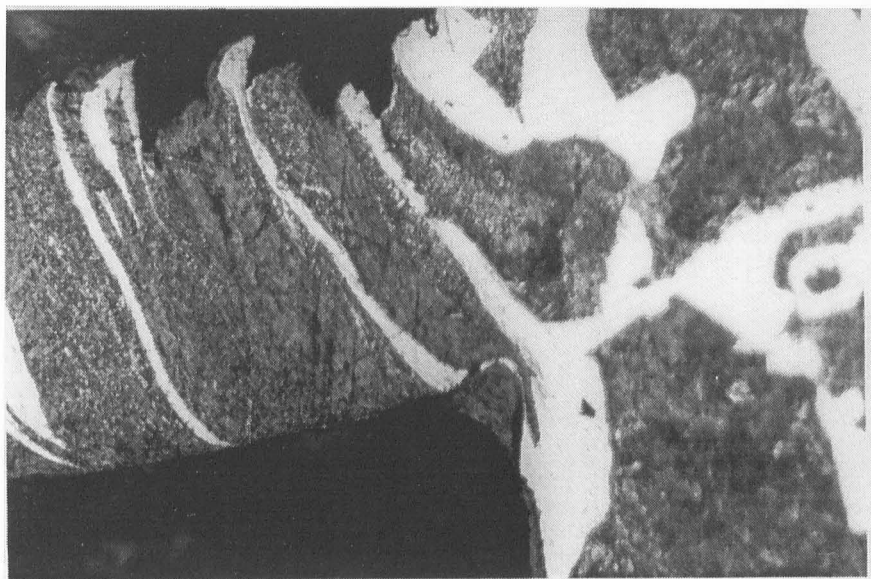


Figure 4.69 Optical microscope view of section through quick stop sample for 40m/min and 0.10mm/rev, 1%, 300x.

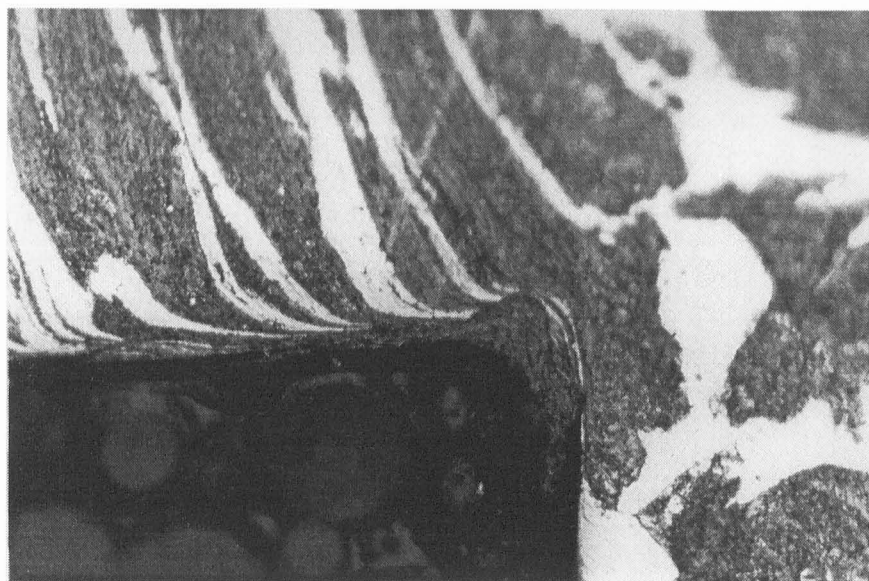


Figure 4.70 Optical microscope view of section through quick stop sample for 40m/min and 0.15mm/rev, dry, 300x.

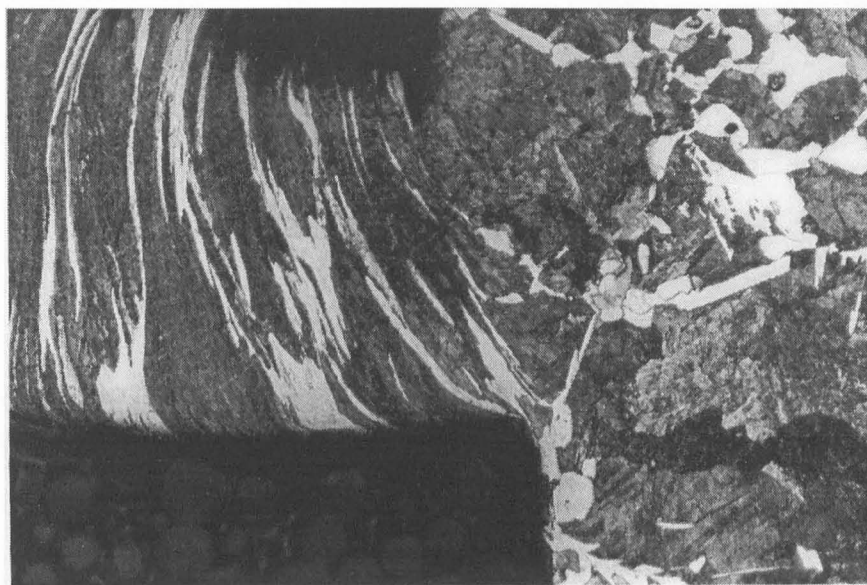


Figure 4.71 Optical microscope view of section through quick stop sample for 40m/min and 0.15mm/rev, 0%, 150x.

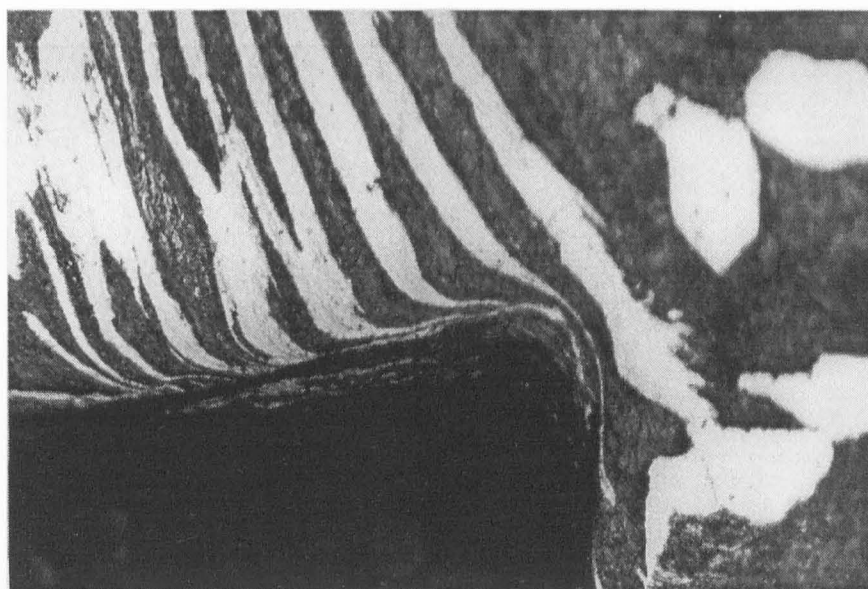


Figure 4.72 Optical microscope view of section through quick stop sample for 40m/min and 0.15mm/rev, 1%, 300x.

A big BUE appears for 30m/min and 0.15mm/rev when oil is applied. This BUE seems to be avoiding any contact of the chip with the tool rake face and the transient surface with the tool flank face. The result is a thinner chip and a high shear plane angle if compared with dry condition. However the cutting force for this condition is comparable with all the other lubrication conditions, especially oil with 1% of sulphur.

For some samples the BUE is very small and looks rather like dead material deposited on the cutting edge of the tool. Moreover, observations of these samples under the electron microscope before polishing to reveal the microstructure showed that the BUE might not be uniform along the cutting edge. Therefore the size of it may be misleading when using the optical microscope. Figures 4.73 to 4.80 show some views of quick stop samples taken within the electron microscope.

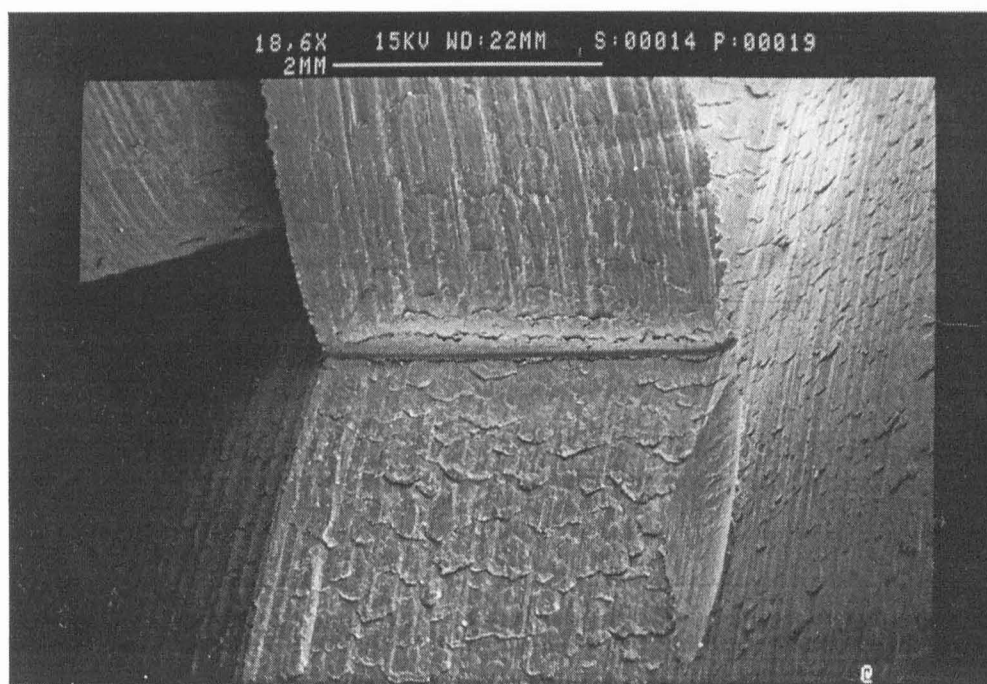


Figure 4.73 Quick stop sample for dry condition at 30m/min and 0.1mm/rev, 18.6x.

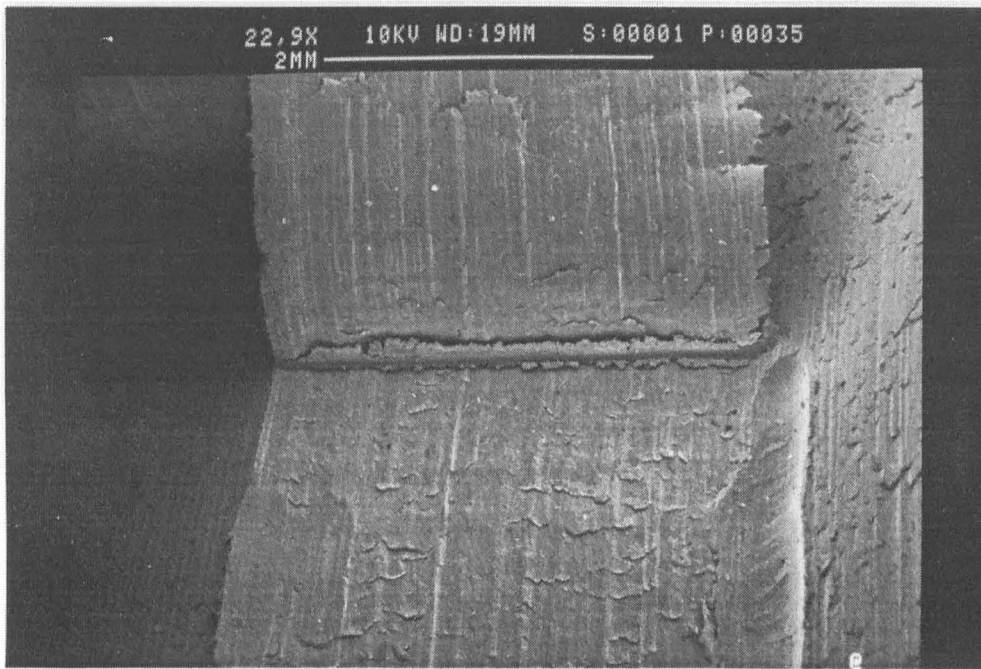


Figure 4.74 Quick stop sample for dry condition at 40m/min and 0.05mm/rev, 22.9x.

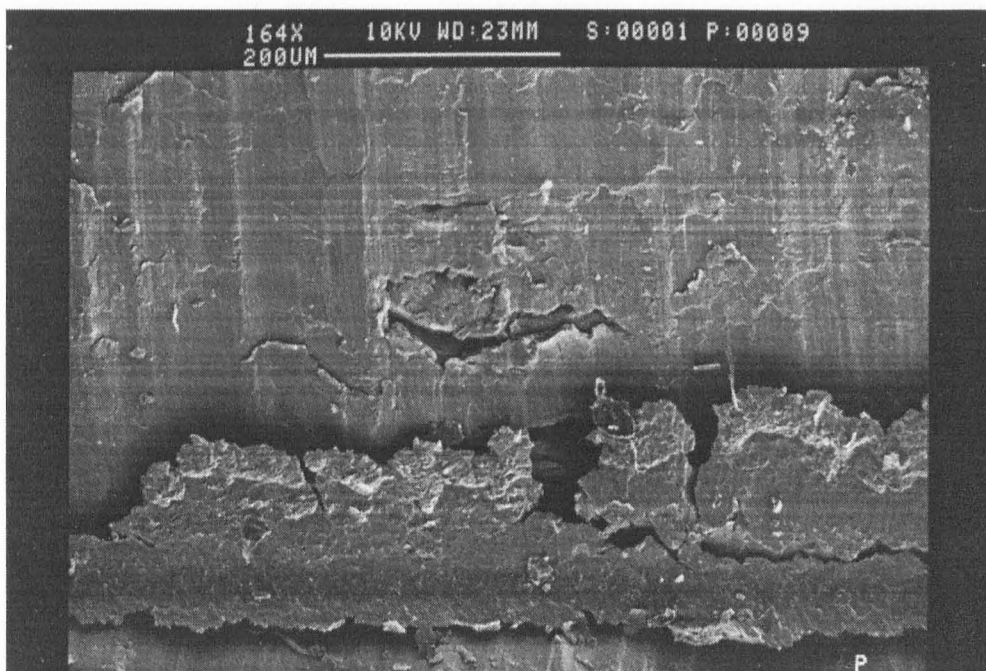


Figure 4.75 Detail of the BUE of the sample of figure 4.74, 164x.

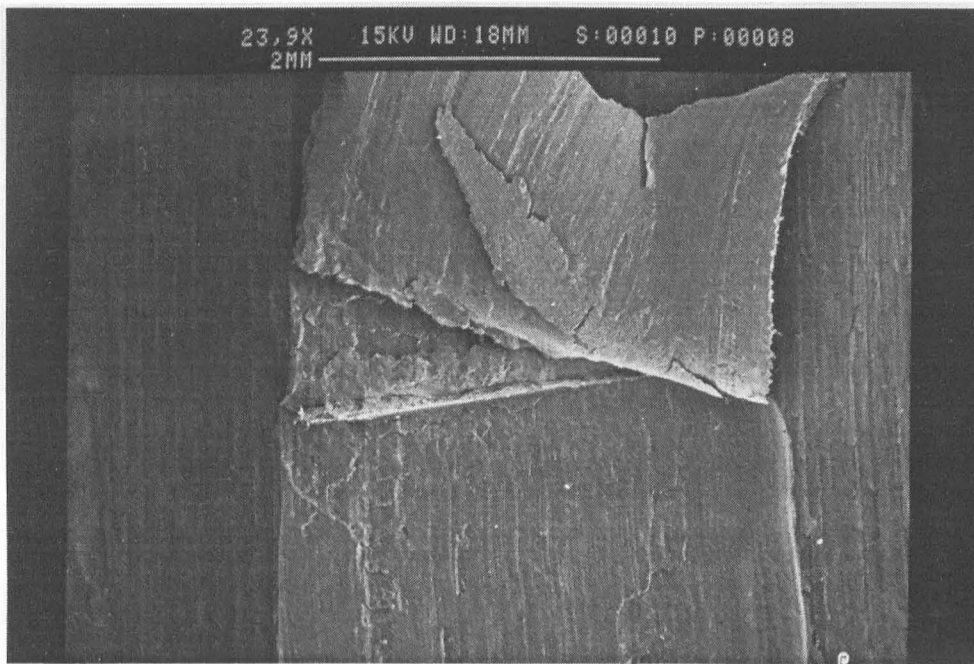


Figure 4.76 Quick stop sample for lubricated (0%) condition at 22m/min and 0.15mm/rev, 23.9x.

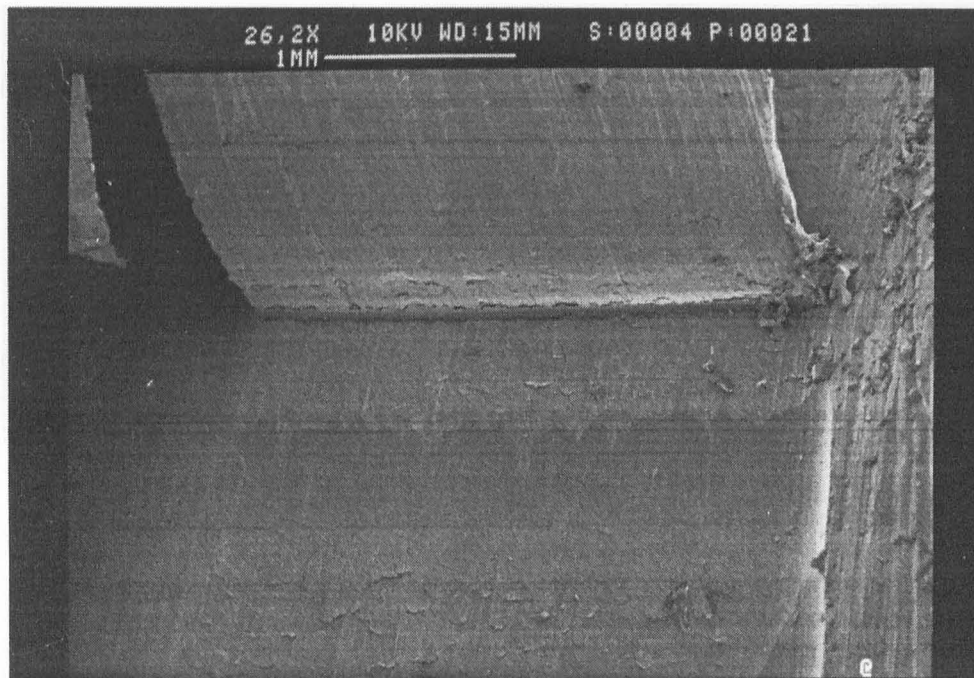


Figure 4.77 Quick stop sample for lubricated (0%) condition at 40m/min and 0.05mm/rev, 26.2x.

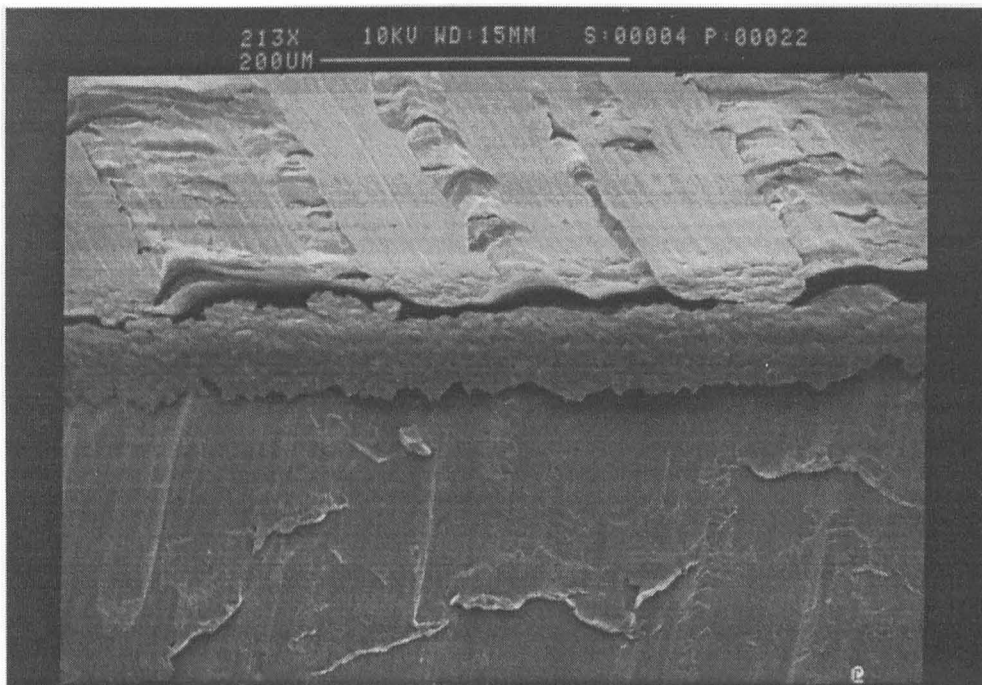


Figure 4.78 Detail of the BUE of the sample of figure 4.77, 213x.

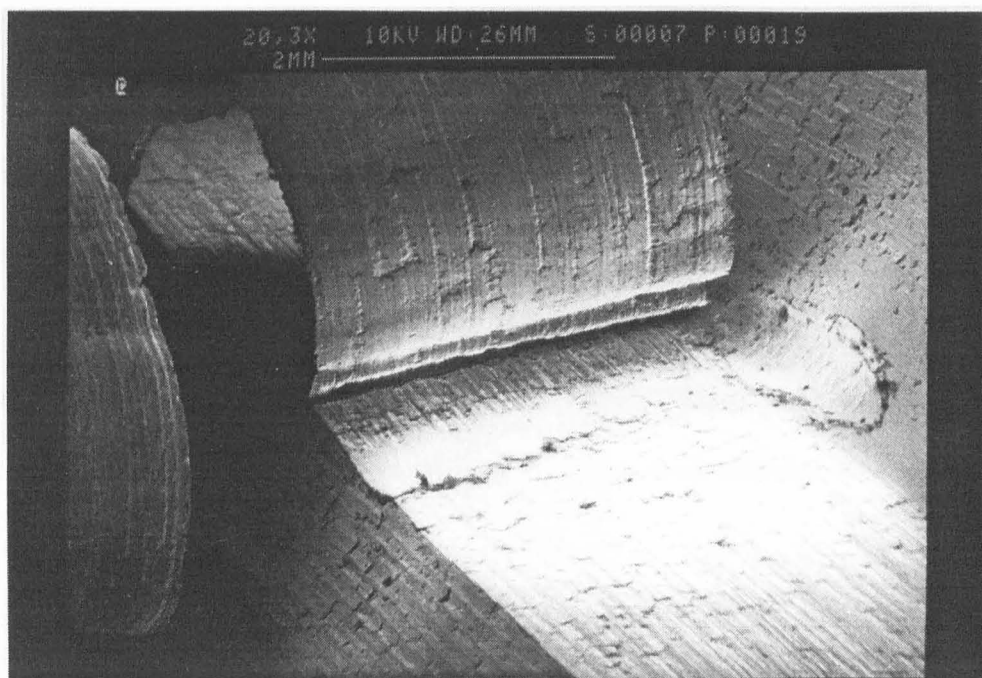


Figure 4.79 Quick stop sample for lubricated (5%) condition at 40m/min and 0.05mm/rev, 20.3x.

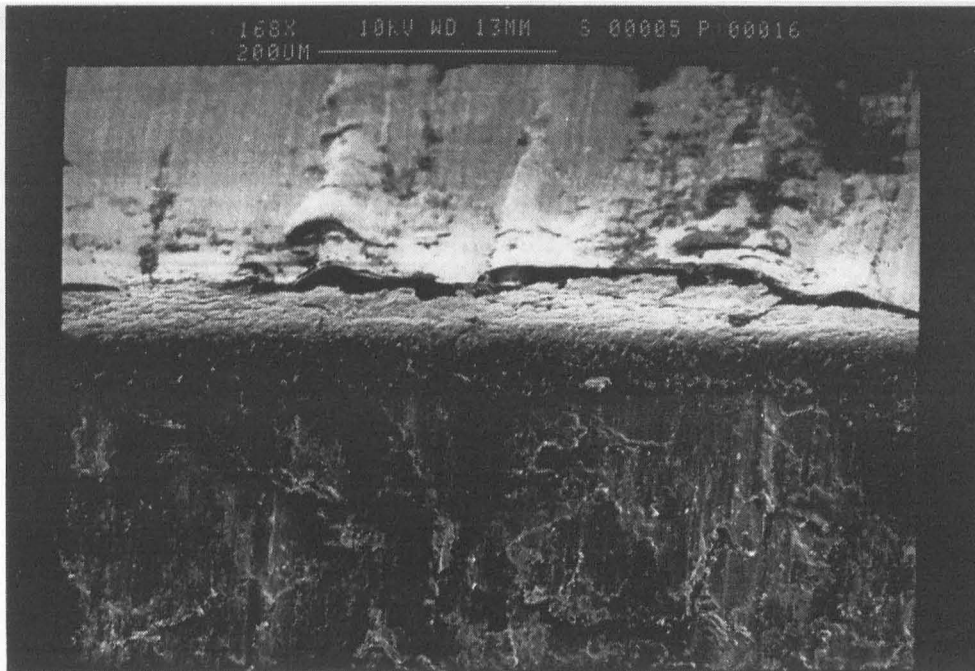


Figure 4.80 Detail of the BUE for lubricated (5%) condition at 22m/min and 0.1mm/rev, 168x.

For some samples at 0.05mm/rev is not always possible to see the region of separation between chip and transient surface. However, it is possible to see the transient surface and the scales caused by BUE or dead material deposited on the cutting edge.

There are some grooves on the surfaces (transient surface and chip) as a result of the non-uniformity of BUE formation or dead material. The transient surface seems very similar for the three conditions (dry, oil, oil+additive) at each cutting condition.

Quick stop samples under the electron microscope show the damage caused by the cutting tool when it moves away during the test. There is a smooth surface on the machined surface that is caused by rubbing of the tool insert, which for some samples extends to the transient surface. For the particular case of the test using oil as lubricant and at 22m/min and 0.15mm/rev shown in figure 4.76, the chip has broken during the test. However the part of it close to the tool nose remained attached to the workpiece. The result is that it gives an impression that the chip is rubbing against the machined surface, but this did not happen. Under the same condition but for dry cut the chip was left completely attached to the workpiece and was driven way from the bar during the cut.

4.6 Machined Surface Samples

The surfaces of the workpiece were examined under the electron microscope in an attempt to identify the differences between them, as there is much improvement on surface finish when lubricant is applied, particularly lubricant with sulphur. It seems at this point that the amount of sulphur did not make any difference on the parameter Ra. Therefore it is worth comparing the surfaces for dry cut and when oil with additive (any percentage) is applied.

Figures 4.81 to 4.98 show samples of the workpiece surface machined under dry, and oil with 5% of additive for all cutting conditions.

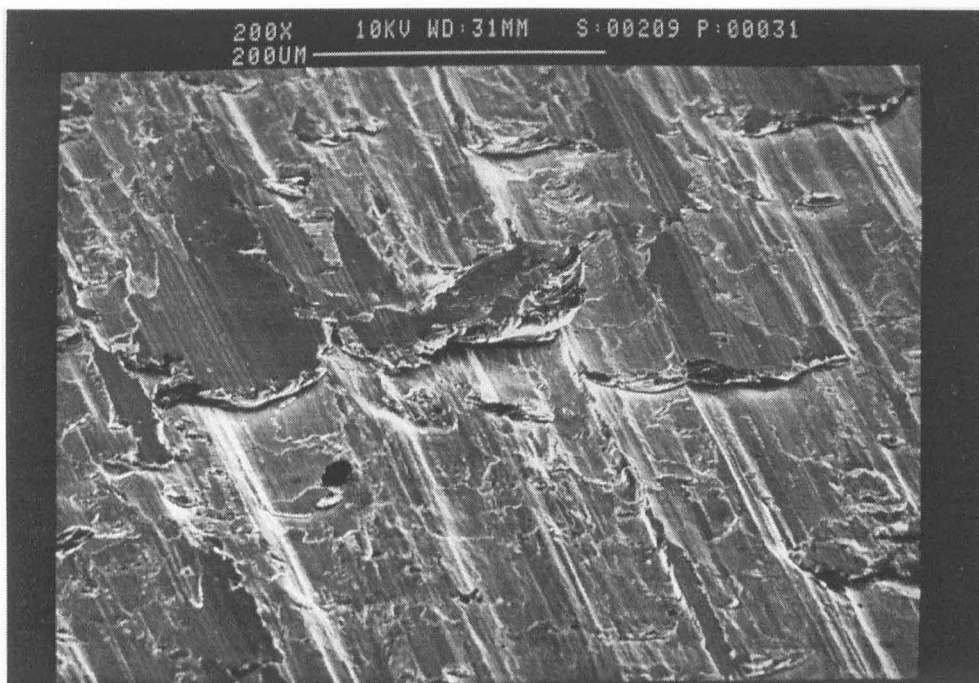


Figure 4.81 View of machined surface on the electron microscope, 22m/min, 0.05mm/rev, dry, 200x.

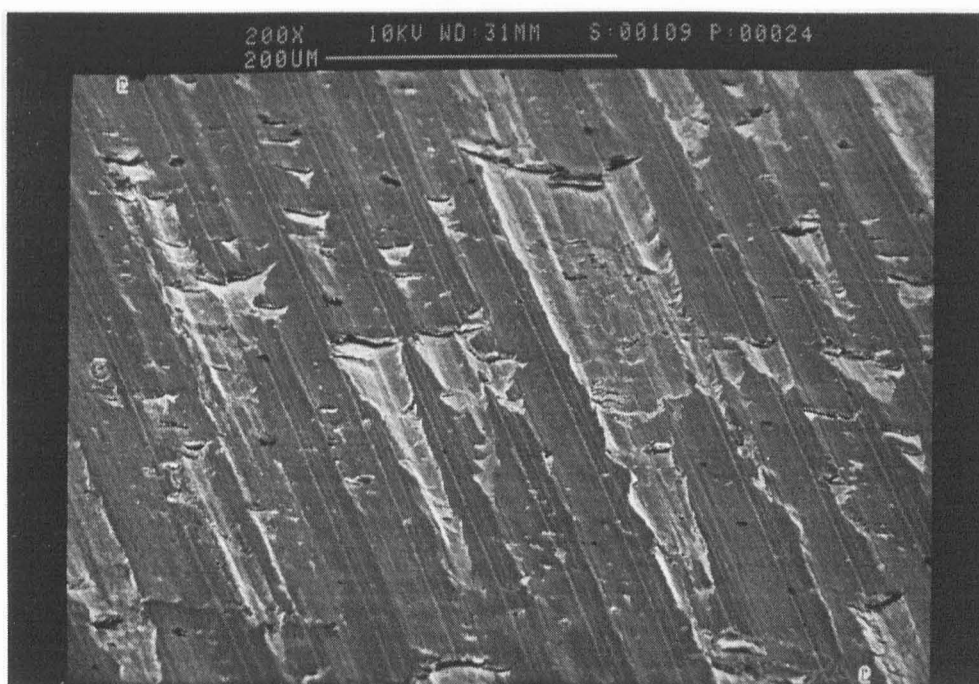


Figure 4.82 View of machined surface on the electron microscope, 22m/min, 0.05mm/rev, 5%, 200x.



Figure 4.83 View of machined surface on the electron microscope, 22m/min, 0.10mm/rev, dry, 197x.

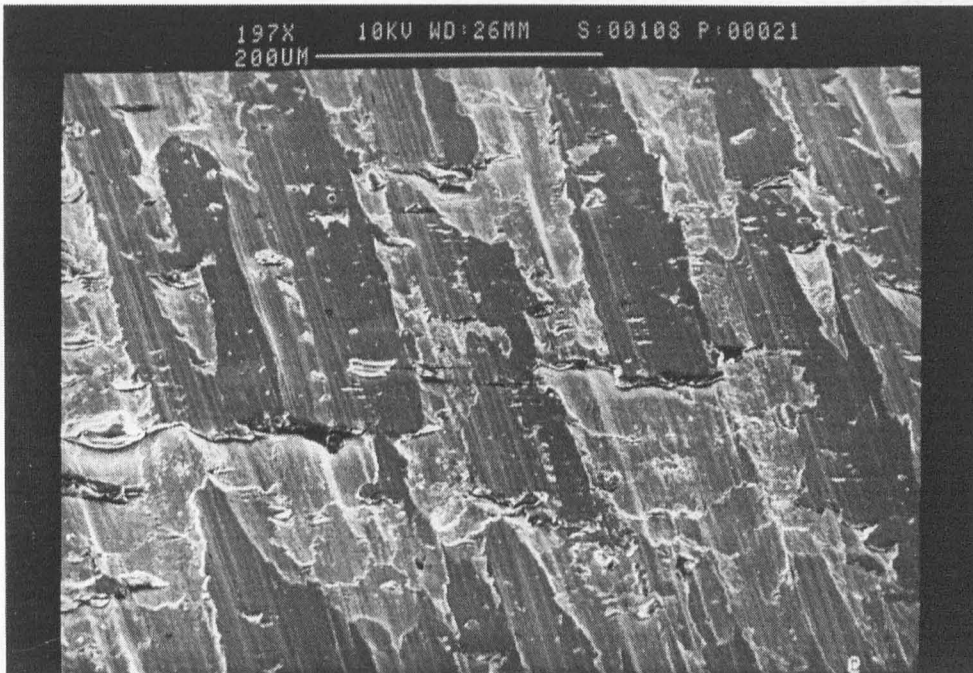


Figure 4.84 View of machined surface on the electron microscope, 22m/min, 0.10mm/rev, 5%, 197x.

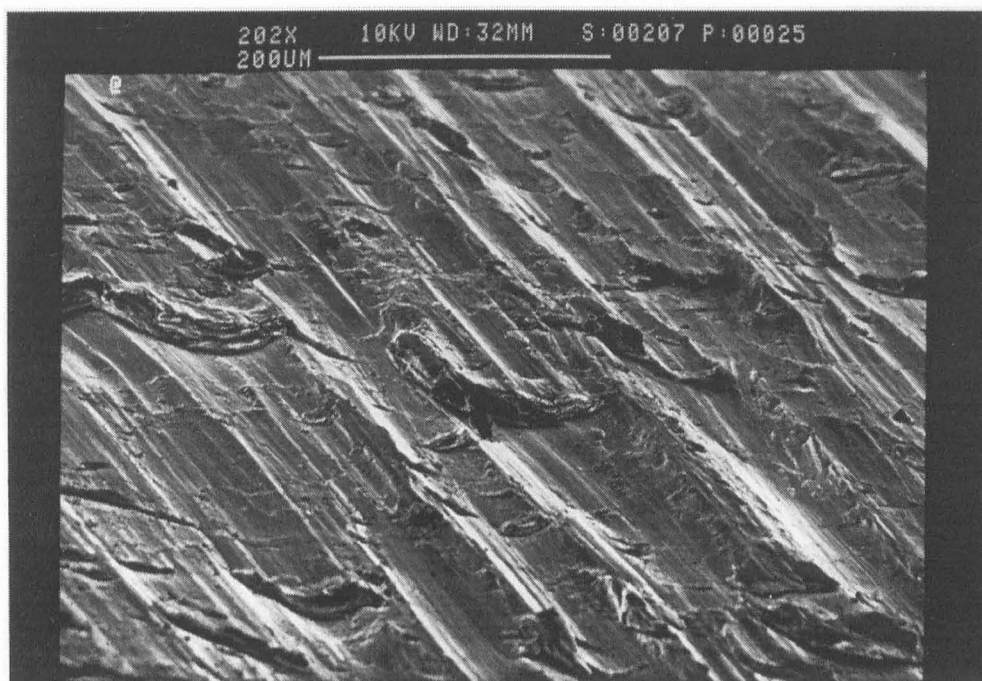


Figure 4.85 View of machined surface on the electron microscope, 22m/min, 0.15mm/rev, dry, 202x.

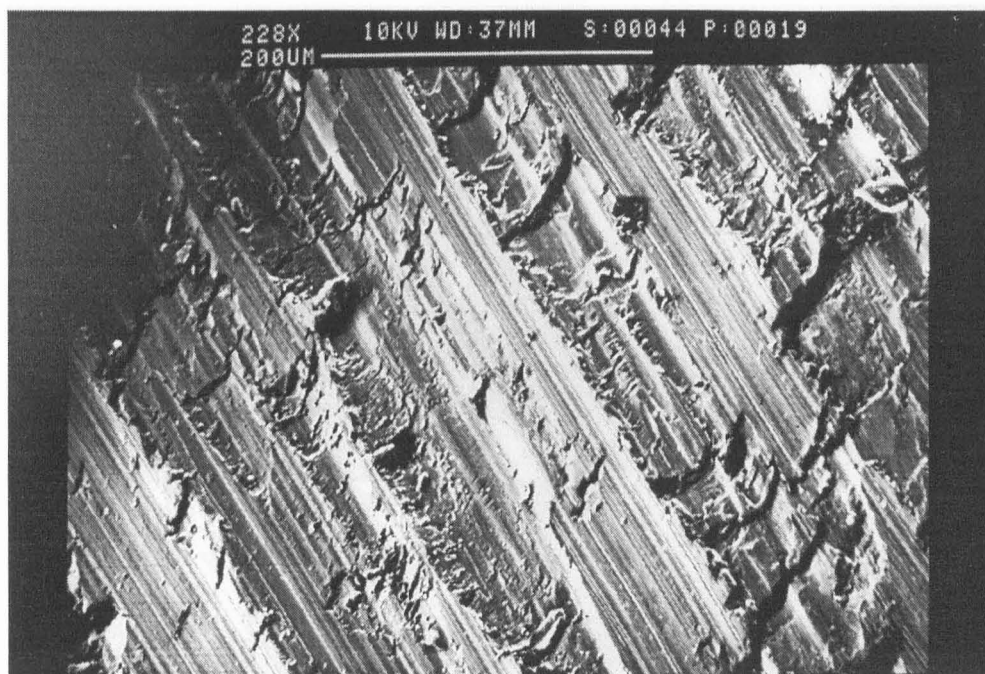


Figure 4.86 View of machined surface on the electron microscope, 22m/min, 0.15mm/rev, 5%, 228x.

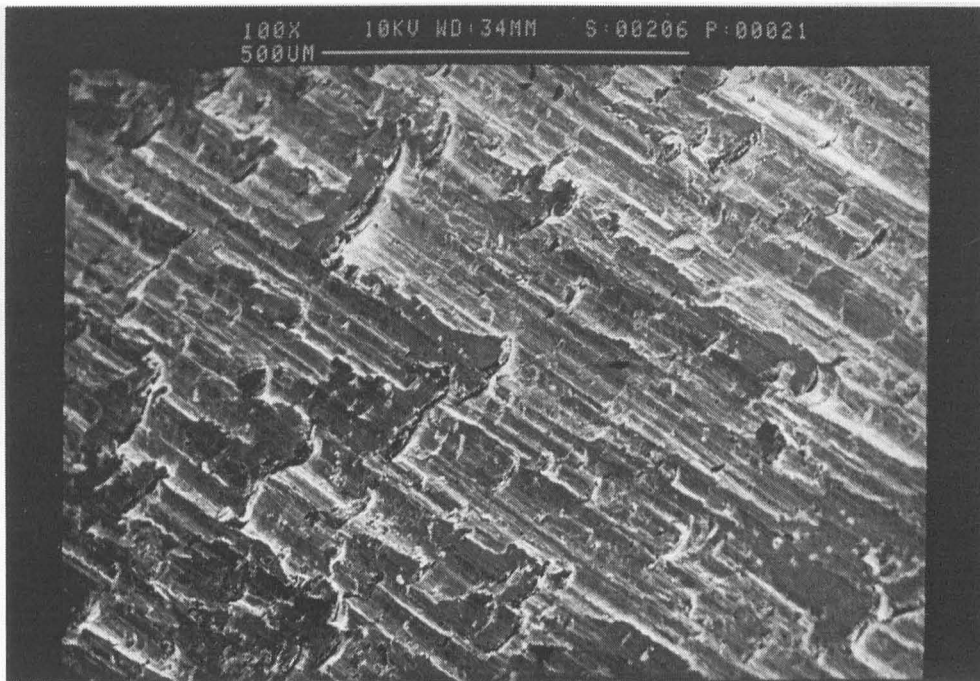


Figure 4.87 View of machined surface on the electron microscope, 30m/min, 0.05mm/rev, dry, 100x.

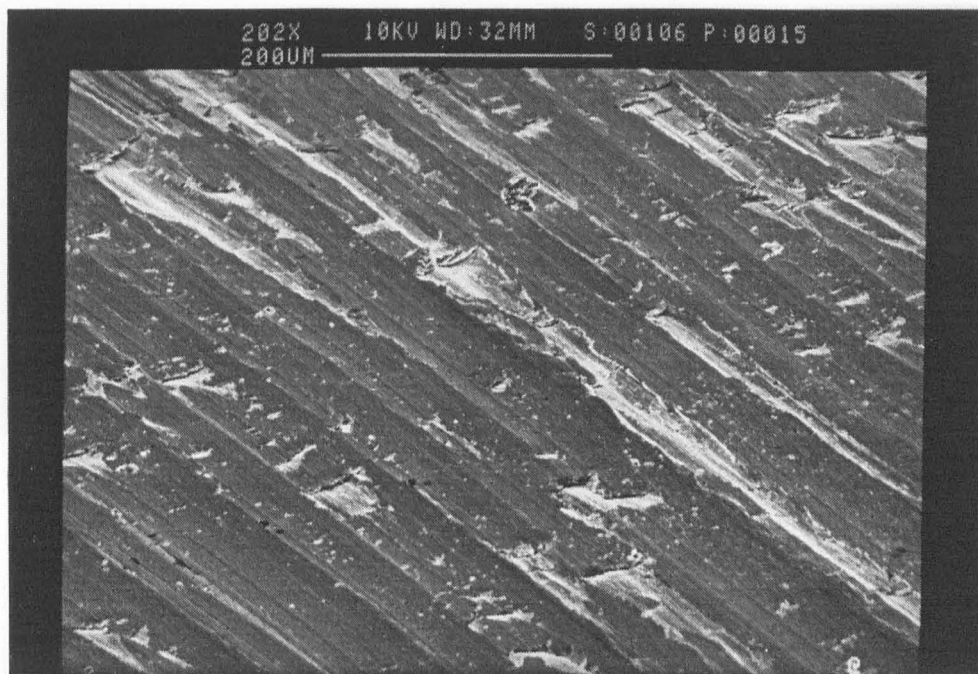


Figure 4.88 View of machined surface on the electron microscope, 30m/min, 0.05mm/rev, 5%, 202x.

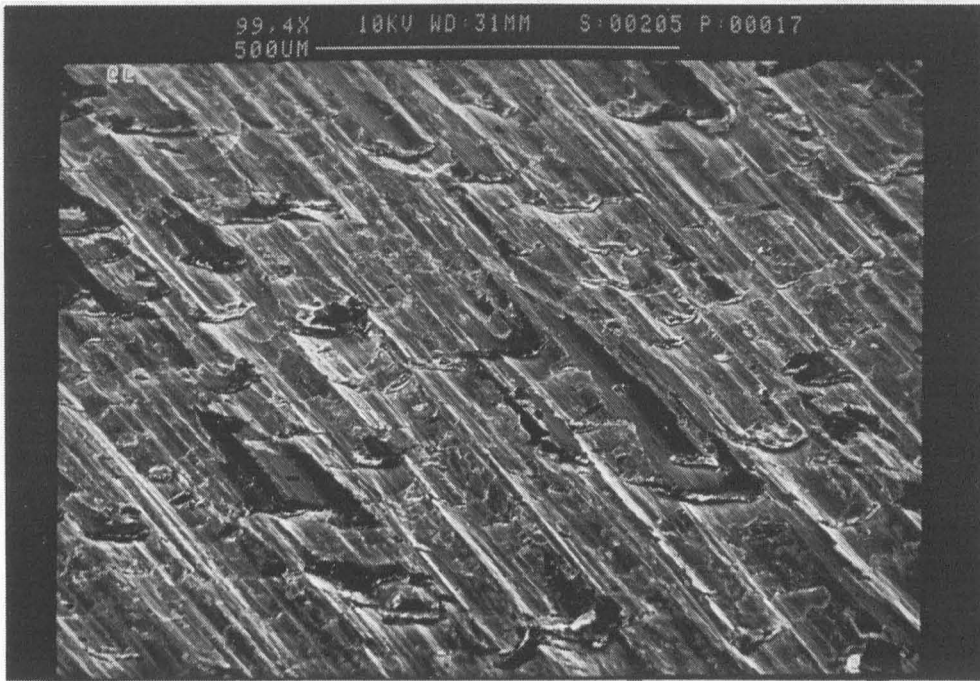


Figure 4.89 View of machined surface on the electron microscope, 30m/min, 0.10mm/rev, dry, 99.4x.

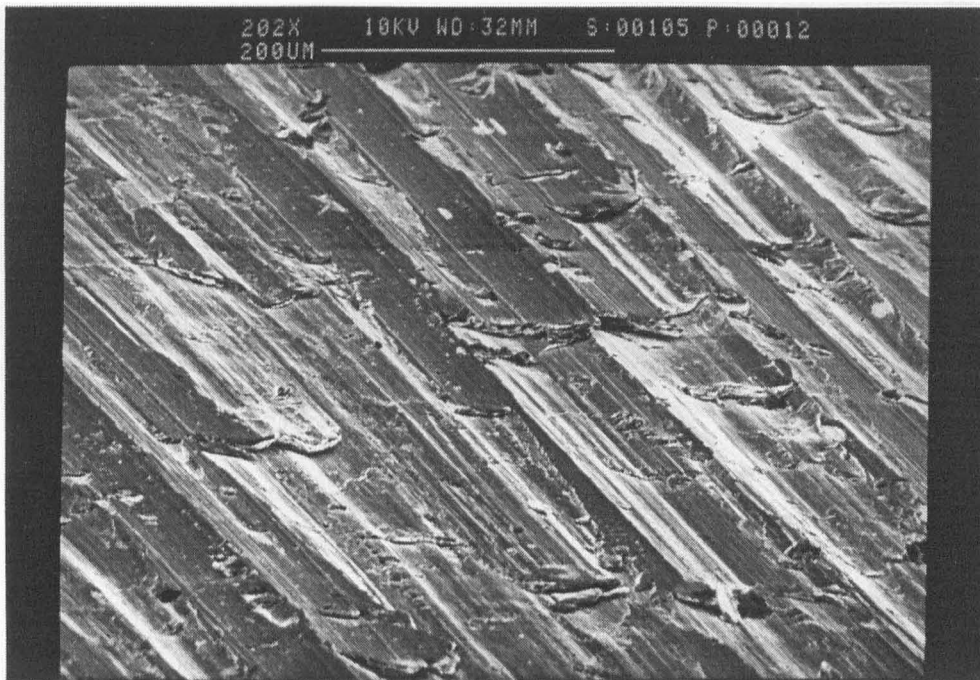


Figure 4.90 View of machined surface on the electron microscope, 30m/min, 0.10mm/rev, 5%, 202x.



Figure 4.91 View of machined surface on the electron microscope, 30m/min, 0.15mm/rev, dry, 202x.

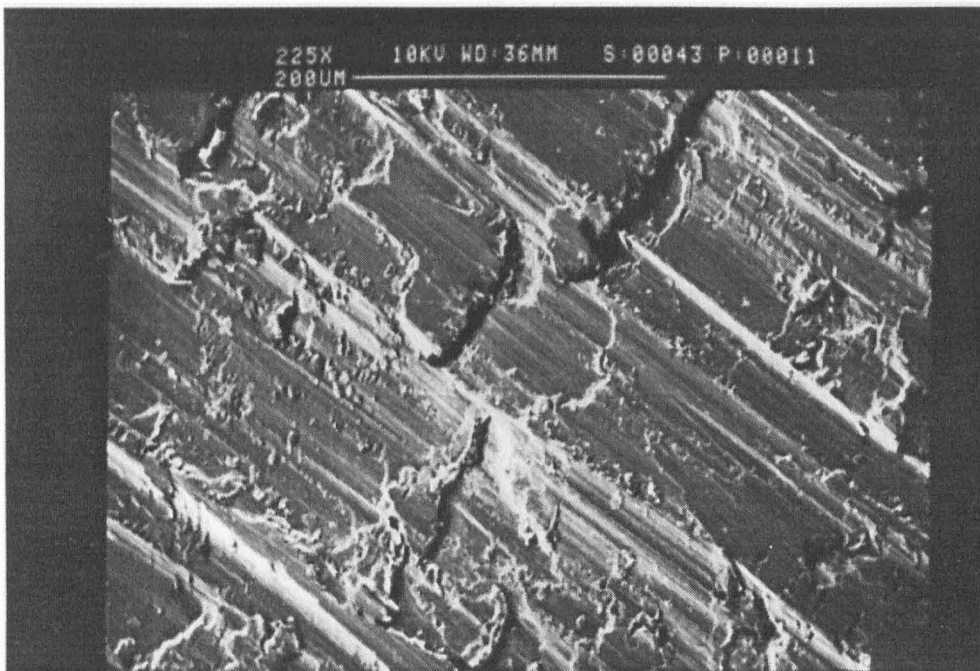


Figure 4.92 View of machined surface on the electron microscope, 30m/min, 0.15mm/rev, 5%, 225x.

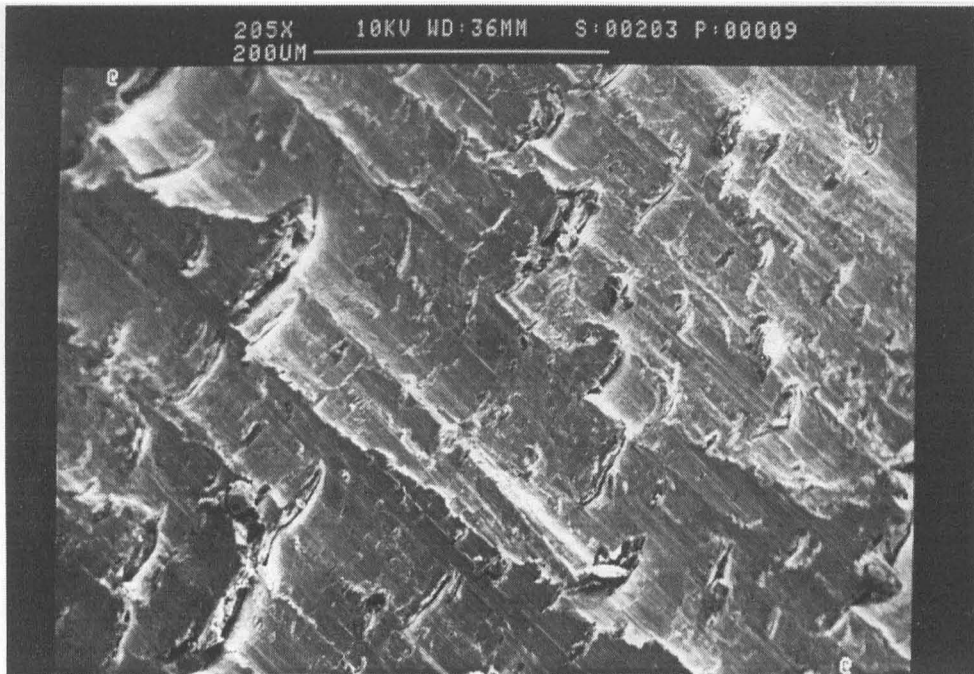


Figure 4.93 View of machined surface on the electron microscope, 40m/min, 0.05mm/rev, dry, 205x.

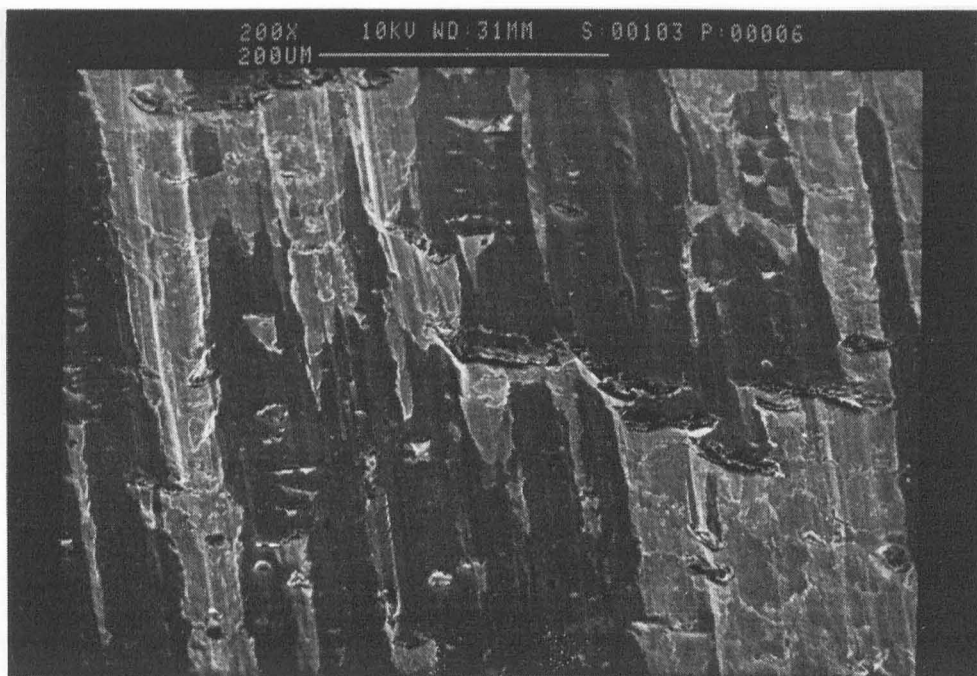


Figure 4.94 View of workpiece surface on the electron microscope, 40m/min, 0.05mm/rev, 5%, 200x.

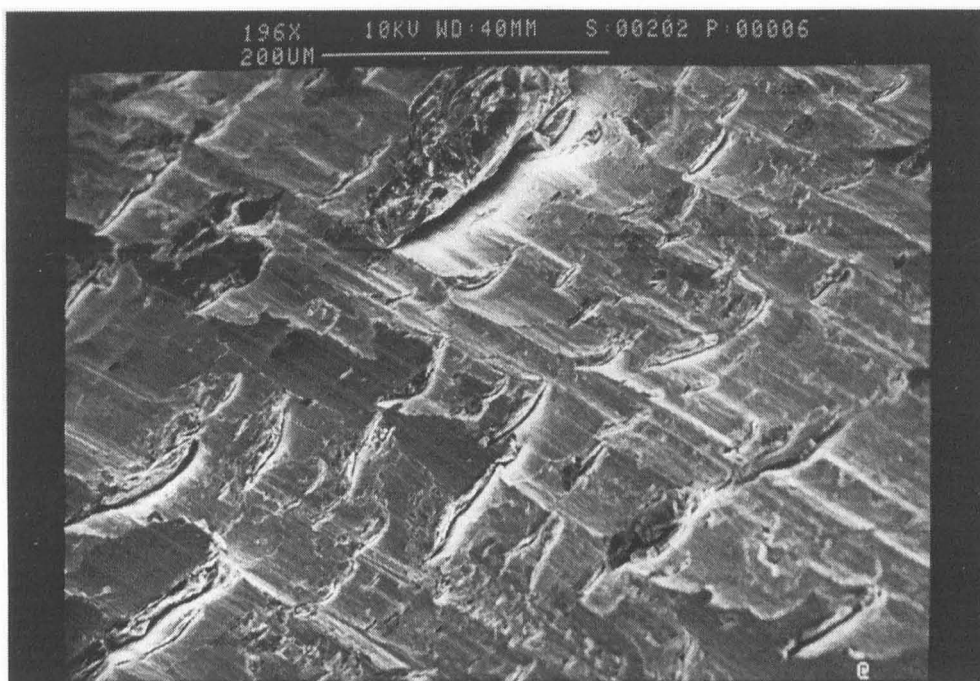


Figure 4.95 View of machined surface on the electron microscope, 40m/min, 0.10mm/rev, dry, 196x.

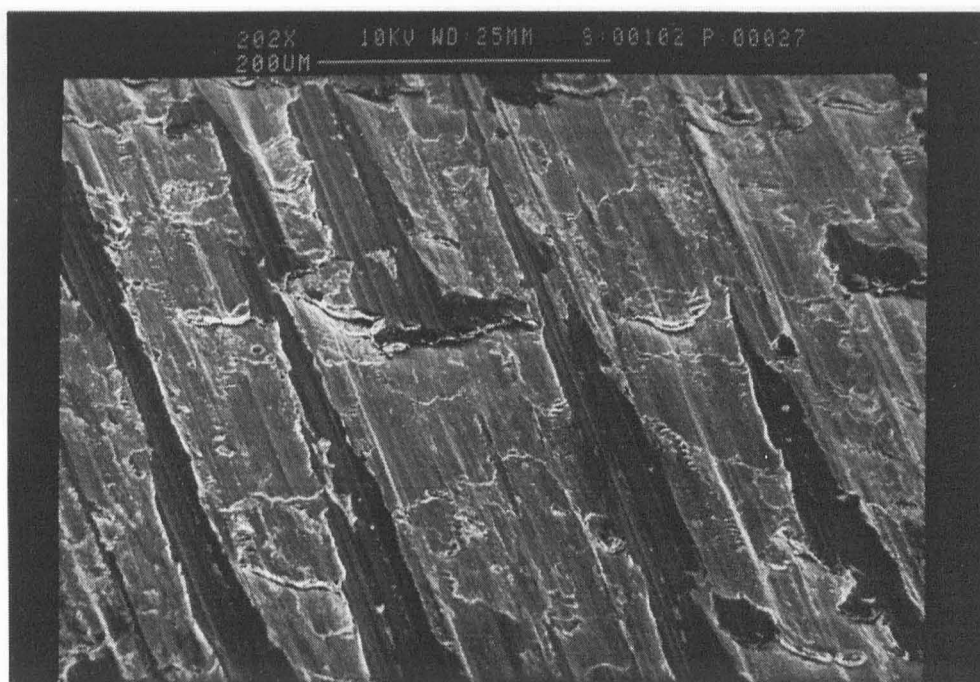


Figure 4.96 View of machined surface on the electron microscope, 40m/min, 0.10mm/rev, 5%, 202x.

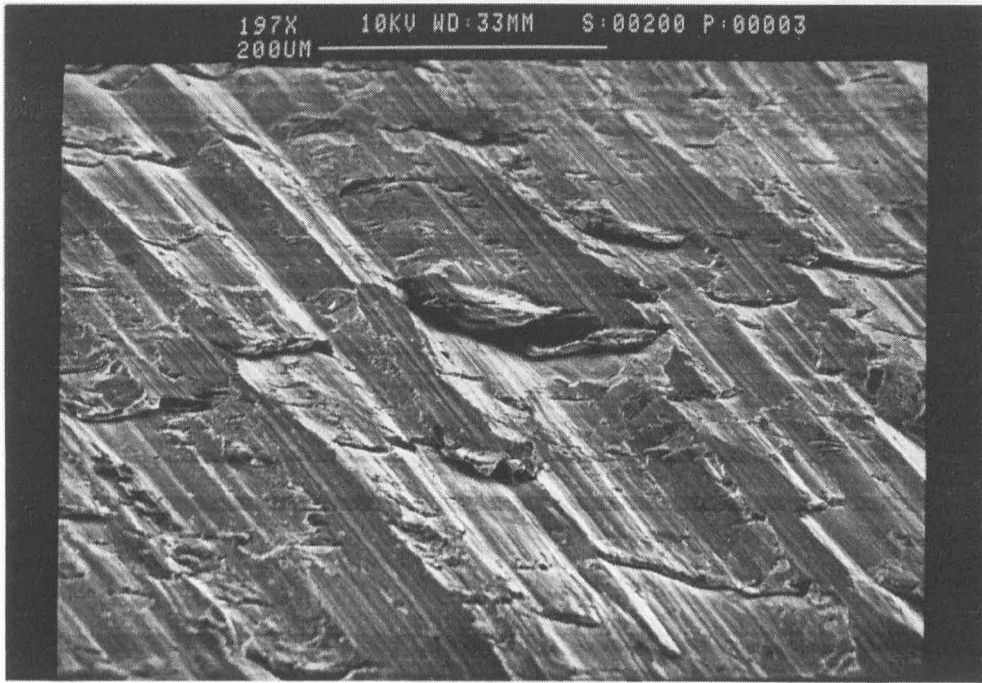


Figure 4.97 View of machined surface on the electron microscope, 40m/min, 0.15mm/rev, dry, 197x.

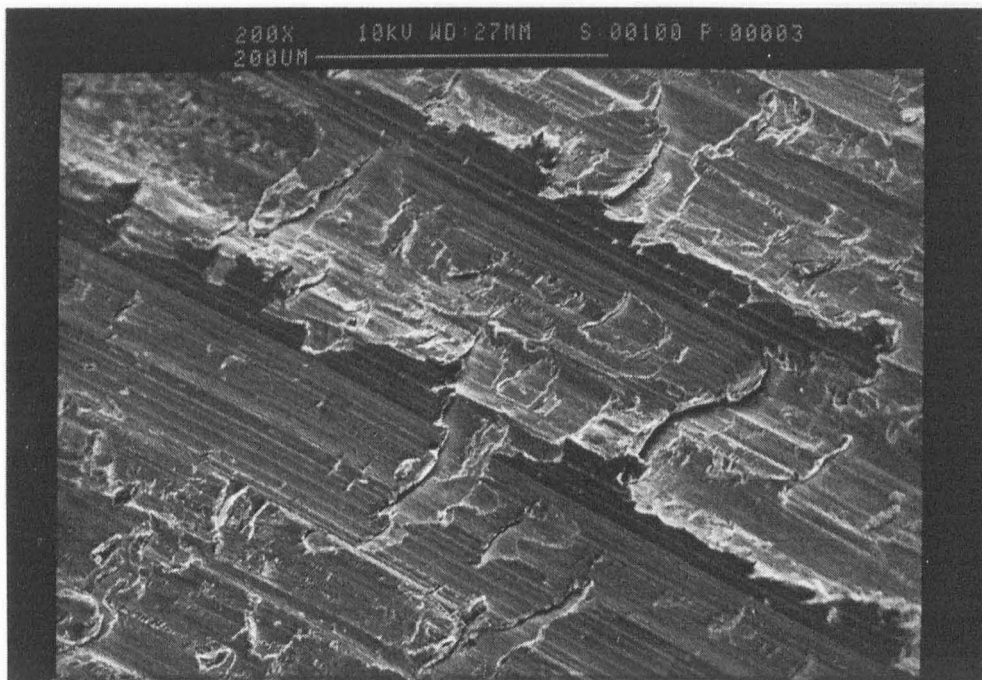


Figure 4.98 View of machined surface on the electron microscope, 40m/min, 0.15mm/rev, 5%, 200x.

In some samples the feed marks can be clearly identified. They can be uniform, with a relative uniform width, or they can be very irregular, with the width varying and at some points becoming difficult to distinguish the feed marks. The feed marks can match with the feed rate or they can appear to be wider by more than two times.

The feed marks are distinguished by a ridge in some samples, while for others there is a rather smooth surface, as if it was ironed and it is not possible to distinguish the feed marks.

Many features of a machined surface described in section 2.6 Surface Conditions in Machining, are observed on these surfaces, like grooves, tearing, and ploughing.

Inside those grooves that are formed apparently by the tool nose, there are other secondary grooves that are interrupted at certain intervals.

5 DISCUSSION

The main function of a cutting fluid is to lubricate and to cool. Lubrication is concerned at the chip tool interface, which should result in lower cutting forces and less heat generation. The cooling action of cutting fluids could affect the temperature of the workpiece, cutting tool and chip and also could affect cutting forces. As cutting conditions used in this work are in the range of BUE formation lubrication could alter BUE size or even avoid its formation. Any effect on BUE size should change surface finish of the workpiece and therefore lubrication of the interface may imply better surface finish of the workpiece.

5.1 Temperature Measurement Technique

It is not easy to measure temperature in machining and several experimental methods have been developed previously. Infrared methods have been used to measure temperatures from exposed surfaces such as the top surface of the chip or the exposed tool rake face. The method described here enables the results from experimental measurements to be used to calculate the temperature of the workpiece close to the primary shear plane, where the workpiece temperature is probably the maximum and where the sensor cannot measure directly. The method used to measure temperature in this work is a new technique and therefore some comments about the technique will be worthwhile.

5.1.1 Errors

In a conventional measuring instrument it is important to know some operational characteristics and the accuracy of the system. The characteristics of the instrument are determined by calibration. This means the use of another instrument (of which the characteristics are known) to measure a reference value.

It was not possible to calibrate the technique used in this work directly. The surfaces where the temperatures were measured are difficult to access by any other technique. However the variation of the measured temperature for identical conditions can be obtained (i.e. repeatability). This was done for the infrared technique to estimate the possible range of temperatures for the same cutting conditions. The same test to measure temperature was carried out ten times for each position. The sensor was removed from the position before each test and the procedure for the installation was done again. The intent of this procedure was to include the errors due to positioning, which also affect the repeatability. The results show repeatability in the range of $\pm 5^{\circ}\text{C}$ at 3mm below the cutting edge. At 6 and 9mm this variation is less than 5°C . This is very good in a metal cutting application considering that there are so many variables that affect the temperature which are not controllable (like the homogeneity of the workpiece material for example).

The final temperature (i.e. the temperature of the machined workpiece at the cutting edge) is not measured directly by the infrared sensor. Instead it is obtained by extrapolation of the three measurements at different distances below the cutting edge (3, 6 and 9mm), which means that the accuracy of the final temperature is not $\pm 5^{\circ}\text{C}$, but depends on the equation of the trendline used to extrapolate the results.

For a dry cut at 40m/min and 0.15mm/rev the three mean temperatures measured with the sensor at each position, after subtracting the respective room temperature are:

3mm: 64°C

6mm: 49°C

9mm: 25°C

The equation to extrapolate the results back to 0mm is then:

$$T = 110e^{-0.1t} \quad (5.1)$$

with a coefficient of correlation R^2 equal to 0.9415. Where T is the difference between the temperature of the surface and room temperature (temperature rise of the workpiece) and t is time in milliseconds. The time along with the cutting speed gives the position where the temperature is being measured.

Figure 5.1 shows these three points in a graph with the extrapolation curve.

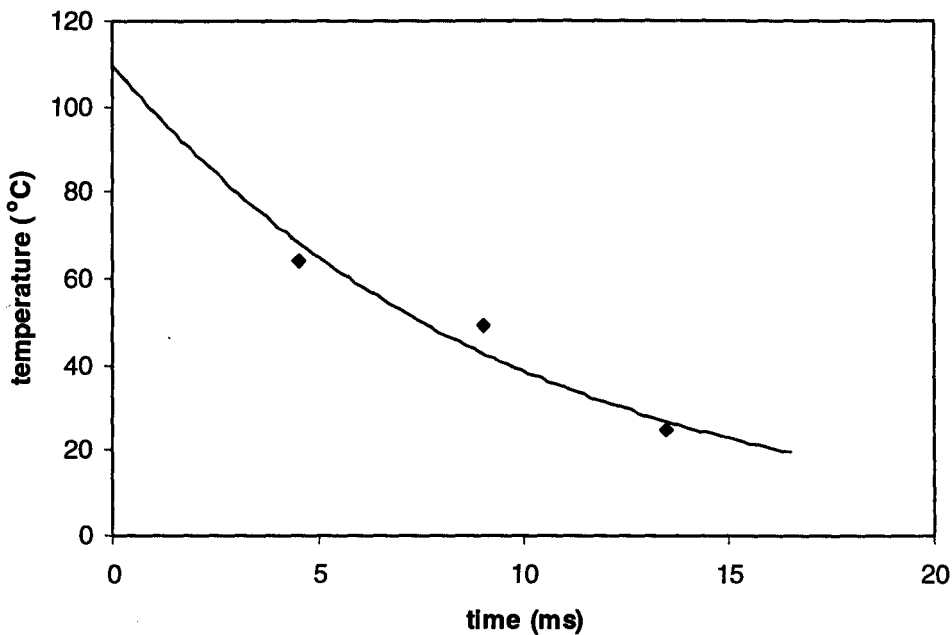


Figure 5.1 Extrapolation of the results of temperature measured for dry cut at 40m/min and 0.15mm/rev.

This equation gives a temperature rise at the cutting edge of 110°C (when $t=0$). For this particular case the confidence interval for the mean value of temperature [147], when $t=0$, was calculated to be $\pm 13^{\circ}\text{C}$ with a probability of 95%. This range is made up of several factors and includes errors of positioning the sensor. Also the difference can originate from errors of the infrared equipment itself ($\pm 1^{\circ}\text{C}$), errors in the method and simple differences due to the process of machining itself. The error due to the method can be due to emissivity changes (changes in the workpiece material) and reflected radiation. During the calibration of the equipment it was verified that the emissivity of the workpiece material is constant for a determined temperature. The change in emissivity with temperature was compensated for by calibration. The cone nozzle attached on the sensor eliminated the effect of possible reflected radiation. Errors also are due to the alignment of the sensor in relation to the transient surface, errors of the distance from the target surface and also errors in the distance from the point where the temperature is measured below the cutting edge. The alignment of the sensor was fixed for every test nevertheless small errors of alignment may occur.

The correct distance of the sensor from the surface where it is measuring the temperature is 76mm. At this distance the target spot diameter is 2.5mm. This distance can be adjusted with an error of 0.5mm, which has little effect on the spot diameter. If the distance were 76.5mm, for instance, the spot diameter would be 2.6mm instead of 2.5mm [148], which would have no effect on the signal as the transient surface (the target) is 2.8mm wide and thus the temperature sensed would be the same.

The distance below the cutting edge, where the temperature is measured can be adjusted with an accuracy of 0.25mm. Assuming that the curve shown in figure 5.1

represents the actual cooling curve of the surface, the temperature at 3mm below the cutting edge is 69°C, according to equation (5.1). The temperature at 2.75 (an error of -0.25mm) is 71°C and at 3.25mm (an error of +0.25mm) is 66°C. The error of 0.25mm on the position in this case can therefore result in error of 3°C in the measured temperature at 3mm below the cutting edge. This is the largest error and accounts possibly for 60% of the overall repeatability. Also as the temperature curve has a smaller gradient at 6mm and 9mm it accounts for the better repeatability at these distances compared to that at 3mm.

5.1.2 Effect of the Air

Air is a good lubricant in machining as it forms oxides that can minimise the seizure zone compared to machining in vacuum. The newly formed chip provides a reaction surface for oxygen from the air and this should result in rapid oxide formation that could decrease the area of adhesion. Tests were carried out to examine the effect of the compressed air that is used in the technique when a lubricant is present. Measurements of temperature and forces without air, for dry and lubricated conditions showed that the results are statistically the same as when air is applied.

A second test was carried out in which the cut was started without air (for dry and lubricated conditions), after 30 seconds the air was applied. The results for temperature showed that there was no effect on the extrapolated temperature, and the cooling rate was the same. There was no effect on forces, in either the dry or lubricated conditions.

Although air has been shown to be a good lubricant (experiments in vacuum show that air is more effective in reducing force than the conventional boundary

lubricants [149]), in a real machining operation air is already present and affecting the cut. Oxide formation does not always decrease adhesion in metal cutting, as it depends on the combination of the tool/workpiece, and the properties of sliding between the oxide formed by the material of the chip and the oxide formed on the surface of the tool [150].

Compressed air at the pressure (2bar) and temperatures (room temperature) used in this work has been shown to not affect the cutting operation in terms of lubrication (i.e. a lowering of forces) probably because there is plenty of oxygen present from the air in the atmosphere. Also the air does not reduce the temperatures or for that matter increase the cooling rate at the surface. With the surface cooling by conduction into an infinite heat sink at a rate of over 2,000°C/s perhaps this is not surprising.

5.2 Effect of Lubrication on BUE Size

The quick stop samples were observed in the optical microscope. From figures 4.46 to 4.72 it is difficult to distinguish the conditions where there was BUE formation and the size and shape of it. For all samples there is some kind of material deposited on the cutting edge, from some conditions the size and shape of this material is more like a conventional BUE, for others it is more like a dead material that envelopes the tool cutting edge.

The presence, size and shape of the BUE depend on many factors and amongst them tool material and tool geometry. As a first approximation of the conditions where BUE may be expected the chart of figure 5.2 can be used.

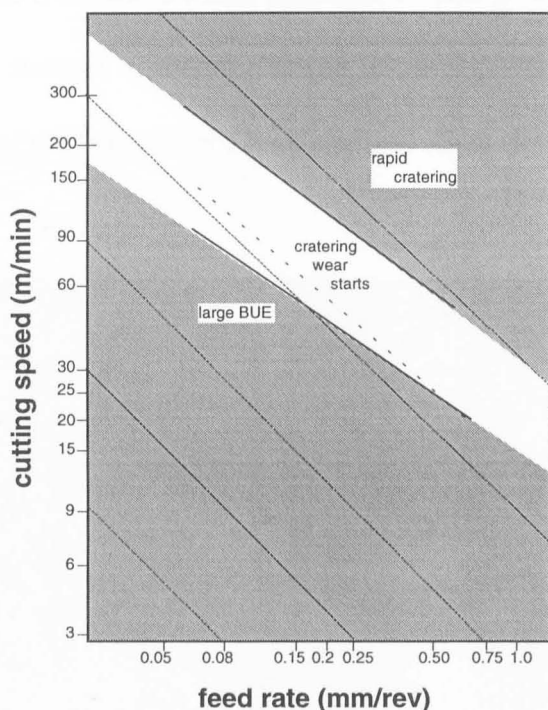


Figure 5.2 Machining chart for WC+6%Co tool cutting 0.4% steel with hardness 200HV [5].

For dry conditions at 22m/min and 0.15mm/rev, the micrograph shows that there is some material that adheres and envelops the cutting edge. However the under surface of the chip seems to have material from a BUE at some distance from the cutting edge. This material could have been sheared from the top of a BUE, but it could also be disturbance from the quick stop test as well. It can also be an example of sporadic BUE formation (i.e. the BUE is unstable [31]).

It is difficult to compare the size of the BUE for the different conditions. The size can be measured by the height or the length of the base of the BUE. However as BUE is a dynamic structure it is possible to get different sizes and shapes under the same cutting conditions. Its apparent geometry depends on the instant at which the test is interrupted.

Even if the BUE was a stable structure, its size is not uniform along the cutting edge. Figure 5.3 shows a scanning electron microscope view of a quick stop sample. This indicates that the length of the base changes along the cutting edge.

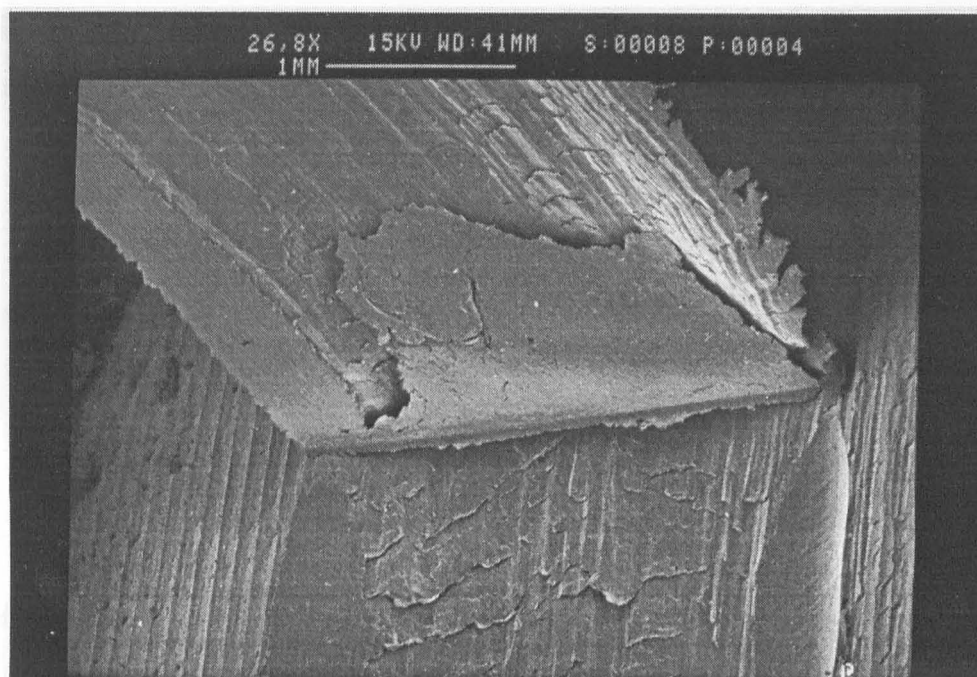


Figure 5.3 Electron microscope view of a quick stop sample for lubricated (0%) condition, 30m/min, 0.15mm/rev, 26.8x.

It is normal then to measure the length of the base at the middle of the BUE, where (for this case) it is probable the maximum. However that is not always what happens. Figure 5.4 shows another electron microscope view of a quick stop sample when oil without sulphur is applied. In this case the length of the base of the BUE changes along the cutting edge, and it seems that there are a number of BUEs, instead of just one structure. This is suggested by the under surface of the chip, with smooth paths alternated by grooves. It seems that the smooth part is because the chip contacts the tool without formation of BUE.

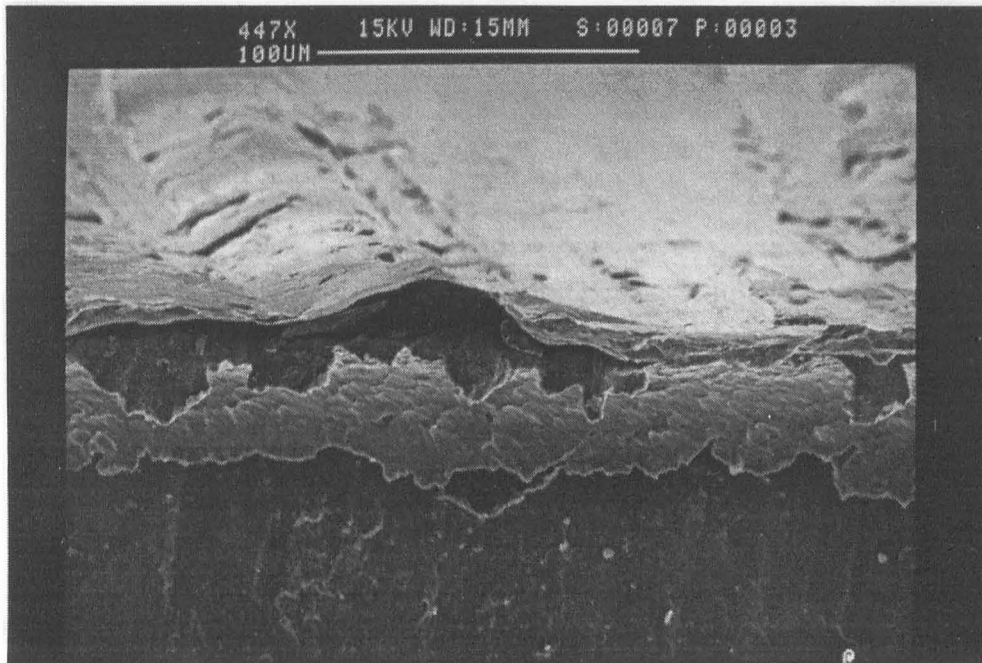


Figure 5.4 Electron microscope view of a quick stop sample when oil without sulphur is applied, 30m/min, 0.05mm/rev, 447x.

Another example illustrates the difficulties of measuring the BUE size. Figure 5.5 shows a scanning electron microscope view of a quick stop sample (the polished cross section is shown in figure 4.67). While the last figure suggests that a huge BUE has been formed, the former figure shows that it does not form for the whole depth of cut. It is formed for just half the length of the cutting edge. If the size is measured by the height the difficulties will be the same. In this case it is difficult to distinguish the top of the BUE from the chip or workpiece. As it is difficult to determine the BUE size it is difficult to directly evaluate the effect of lubrication by analysis of quick stop samples.

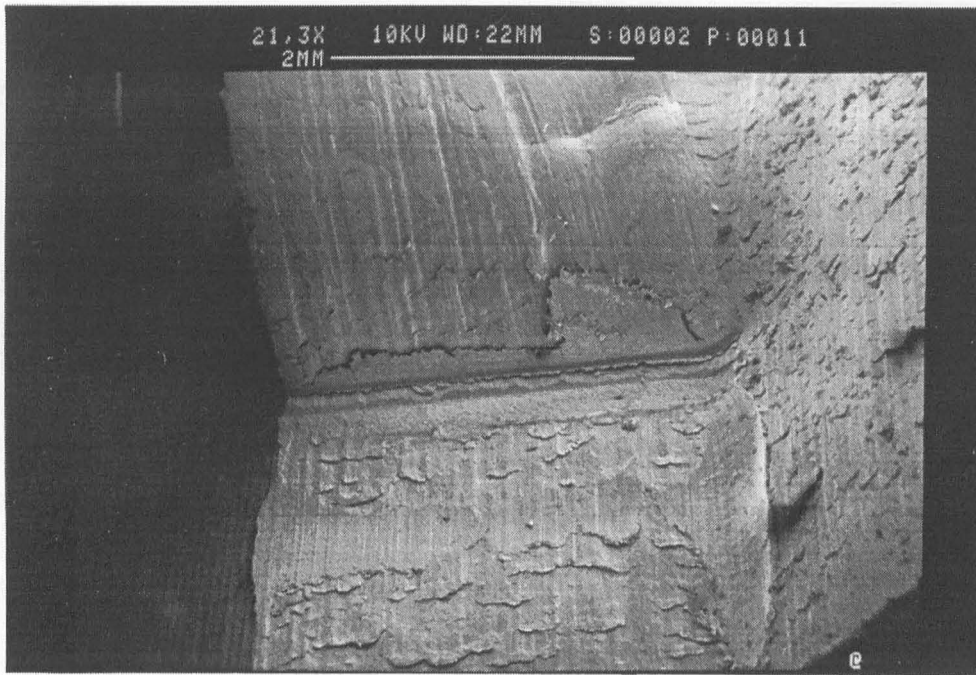


Figure 5.5 Electron microscope view of a quick stop sample for dry condition, 40m/min, 0.1mm/rev, 21.3x.

If penetration of the cutting fluid to the chip/tool interface was possible it may be thought possible to prevent the formation of the BUE by lubrication of the contact. On the other hand, [144,145] supports the idea that air is a good lubricant for metal cutting, and is probably better than the mineral oil. The oxides that can form due to contamination of air can decrease the adherence between surfaces in the case of steel. Application of mineral oil could protect the cutting zone from penetration of air, creating conditions for good adherence and conditions for formation of a BUE. It is therefore not clear what action may be expected from application of a lubricant.

If BUE size is affected by lubrication a change in shear plane angle should occur and affect cutting forces and temperatures. Therefore the cutting fluid effect on BUE size can be inferred indirectly by observing the changes in the forces and temperatures.

5.3 Cutting Forces

5.3.1 Effect of Lubrication on Absolute Value of Cutting Forces

The contact forces between chip and tool greatly affect the force to shear the material and form the chip on the primary shear plane. The resistance to movement on the rake face generates a compressive force on the primary shear plane (F_{nz} in figure 2.4), which affects geometry of the chip. High forces at the tool chip contact means that high shear force is necessary and that the chip is thick and the primary shear plane angle is low. For steel under normal cutting conditions this normal force on the primary shear plane prevents fracture of the chip. The result is that the chip is long (although it may break into smaller parts due to mechanical obstacles like chip breakers, tool holders or the workpiece).

Cutting force should decrease with the increase in BUE size because the effective rake angle increases. The BUE acts like an extension of the rake face of the tool. Therefore an increase on BUE size means an increase in primary shear plane angle and a decrease in chip thickness.

If lubrication of the contact was possible, as in hydrodynamic lubrication, the feed force should decrease as a result of the decrease in friction between the surfaces and consequently cutting force would also decrease. As there will be no force to avoid fracture of the material during shear, the chip would be truly discontinuous. However as has been demonstrated [151], friction in metal cutting does not follow this reasoning. This is mainly due to the large pressures involved in the process between chip and tool which makes it difficult for cutting fluid to penetrate the interface.

It is difficult to calculate accurately the mean pressure on the rake face because it is difficult to measure the chip tool contact length. Assuming that this

contact is about 1.5 times [6] the undeformed chip thickness it is possible to have an estimate of the mean normal stress. For 0.05mm/rev and 2mm depth of cut, the contact area will be 0.15mm² approximately. For 0.15mm/rev it is about 0.45mm². The normal force is about 200N and 1000N, for feed of 0.05mm/rev and 0.15mm/rev respectively. Therefore the average normal stress is about 2GPa. Even if the stress distribution shown on figure 2.9 is taken as a reference, the mean normal stress is a high value concerning lubrication. Other workers have shown peak pressures of up to 3.5GPa for some steels [19], and this would prevent the penetration of lubricant into the chip tool interface. Under these high-pressures sliding may occur in the early stages of the cut until oxide layers have been removed from the tool but then adhesion between the tool and work materials is inevitable. The cleanliness of the fresh surface of the chip that is formed, (free from any contaminants and with high surface energy) is also favourable to adhesion. As the surface of the tool is being swept constantly by the chip these good conditions for adhesion are constantly renewed.

According to the theory of hydrodynamic lubrication, for fluid film lubrication to occur it is necessary that the lubricant must flow into a converging channel formed between both surfaces, as in the lubrication of a journal bearing [111]. The movement of the chip is in such a direction as to minimise any penetration of cutting fluid for fluid film lubrication. In fact the movement of the chip tends to remove fluid from the contact region rather than feed it in. Boundary lubrication is another possibility for lubrication in metal cutting. In this type of lubrication the surfaces are separated by thin films, if not over the entire contact area, at least in parts of it. Chemical and physical properties of the surfaces and lubricants are important because reaction between them has to occur to form a film separating both surfaces. However, penetration of the boundary lubricant into the interface under high pressure is still a

problem and several mechanisms for cutting fluid access to the rake face have been proposed. Amongst them: i) access through a capillary network between chip and tool; ii) access through voids connected with BUE formation; iii) access into the gap created by tool vibration; iv) propagation, from chip back surface, through a distorted lattice structure [152]. All of these mechanisms of lubrication should result in some changes in cutting forces.

The distribution of stress on the rake face as seen in chapter 2, shows that there is the possibility of dividing the contact into two distinct regions, the sticking zone (BUE or flow zone) and the sliding zone. Therefore there is a possibility that a cutting fluid could at least penetrate the sliding region of the contact. In that case a small effect on forces could be expected. Within the accuracy of the technique shown here, this has not been seen. Previous work on the use of high-pressure lubrication to better penetrate the sliding region has shown that this is feasible [6]. When machining Titanium and Nickel based alloys a reduction in contact length was achieved. However under these conditions no change in forces was observed.

As there was no effect on forces when lubricant is applied, the chip thickness and shear angle did not change if compared to dry conditions. The size of the BUE thus must be the same for dry and lubricated conditions. The size will change with cutting conditions but not when lubricant is applied.

5.3.2 Cooling Aspects on Forces

The effect of cutting fluid on forces is not only due to lubrication of the rake face. As the strength of a material depends on the temperature, there is a possibility of alteration of the strength if the cutting fluid can cool the material.

The measured forces originate from the force necessary to shear the material and the force to move the chip over the rake and flank face.

The force to shear the material on the primary shear plane depends on the strength of the material and the primary shear plane angle. The strength on the primary shear plane will depend on the amount of heat that is developed by the shearing action and the rate of removal of this heat. Together these determine the temperature. One of the reasons why cutting force decreases as cutting speed increases under cutting conditions in which a continuous chip without BUE occurs, is the increase in temperature on the primary shear plane. The strength of materials in general decreases with temperature, but the behaviour of a material under such strain rate is largely unknown.

The fact that the BUE decreases in size as the cutting speed increases may be related with the increase in temperature and the behaviour of the material. Cooling of the cutting zone could therefore change the size of the BUE.

As the temperature is a balance between the heat generated and that removed the coolant capacity of a cutting fluid may have an effect on forces even if the fluid does not lubricate. If the cutting fluid has enough time it may extract heat from the cutting zone decreasing the mean temperature and potentially increasing the strength of the material.

Such an effect was used to explain the results obtained by [153] when comparing the performance of synthetic and mineral soluble oil when turning AISI8640 steel. The measured cutting force for dry cutting and when soluble oil was used as coolant was similar. However the measured forces increased when a synthetic fluid was used.

Straight mineral oils have poor cooling ability and the EP additive has little or no effect on its thermal properties, as shown by simple experiments described in chapter 3 (Experimental Procedure).

The time available for the cutting fluid to extract heat from the cutting zone is very short. Consider the case of the test using a cutting speed of 22m/min and a feed rate of 0.05mm/rev, when applying oil without sulphur. The mean chip thickness for this condition is 0.107mm, which means that the chip is moving at speed of approximately 121mm/s. Assuming a contact length of 0.2mm (a large over estimate as this is four times the undeformed chip thickness), the chip stays in contact with the tool for only 0.002s. This means that the cutting fluid must extract heat from the secondary zone very quickly. To decrease the temperature of the chip 1°C in this time would require a cooling rate of 500°C/s. To extract heat from the primary shear zone the time is even shorter requiring cooling rates by the coolant to exceed those seen in cooling into the bar itself!

Considering that the extrapolated temperatures should represent the temperatures expected for the primary shear plane, they do not appear to be sufficiently high to affect the strength of the workpiece material. Therefore even if the cutting fluid could cool the cutting zone it would not change the strength of the material and this is in line with the experimental results.

5.3.3 Effect of Lubrication on Force Oscillation

One of the tool wear mechanisms at lower cutting speeds is attrition. This wear mechanism is encouraged by force oscillation during the cut. Lubrication could also be effective in reducing force oscillation and therefore improving the cutting

operation. The effect of lubrication therefore should also be measured by the force oscillation, not only the mean value of forces.

Force oscillation can be caused by several factors. The graphs for the cutting force show that the amplitude of oscillation of cutting force against time (during the cut) at 0.15mm/rev is higher than 0.1 or 0.05mm/rev. However the coefficient of variation (standard deviation divided by the absolute value of force) are not greatly affected by feed rate or cutting speed for most of the tests (when comparing tests under the same lubrication condition). The shape of the chip for 0.05 and 0.1mm/rev are similar. They have a long and continuous helical shape. In the case of 0.1mm/rev the length of the chip is rather uniform, as the chip breaks every time it touches the tool holder, or other parts of the machine tool. For 0.05mm/rev, the chip being thinner is more flexible than the 0.1mm/rev and therefore is more difficult to break. The chip shape for 0.15mm/rev is small and curled. For this case the chip curls and touches the machined surface above the cutting zone, which causes the chip to break into small pieces. Moreover these small chips are very irregular, and have a non-uniform cross section. This may in part explain the high amplitude of oscillation of the forces for the 0.15mm/rev feed rate compared to the other conditions.

The variable force could also be due to the BUE. BUE is a periodical phenomenon, forming and disappearing during the cut, which would cause variation in the forces. The BUE increases in height by layers of work hardened materials depositing on it. This periodicity can cause a periodic variation of the force as observed on the graphs.

One of the theories about the action of cutting fluids at low cutting speeds and feed rates is that the fluid can penetrate into the spaces provided by BUE. Depending on the sizes and shapes of BUE it is possible that the chip touches the rake face after

being formed over the BUE leaving a gap between the second contact and the point where the under surface of the chip is formed. The friction of the new contact can be due to sliding or it could be a stick slip contact. This intermittent contact can add to the periodicity of BUE formation and the unstable forces.

Considering that the contact between the chip and the tool is composed of the sticking zone and the sliding zone as proposed by [5], the proportion of the length of these zones should depend on the stress distribution as suggested by [25]. The length of the whole contact will depend on the undeformed chip thickness, or the feed rate, as does the stress distribution. In general some oscillation is observable when measuring force even when a BUE is not present. This could mean that the sliding zone, where the normal force is low and the shear stress is decreasing, might experience intermittent contact.

If the lubricant can penetrate the gap between the tool, BUE and the chip it should bring some benefits. It may lubricate and avoid metal-metal adhesive contact, but it is likely that it can lubricate just part of the contact where there is sliding or intermittent adhesion. Therefore the lubricant should decrease the amplitude of force oscillation. Figure 5.6 illustrates an orthogonal cutting operation where a BUE is formed and there is a further contact, of length ℓ , between chip and rake face after it has been formed.

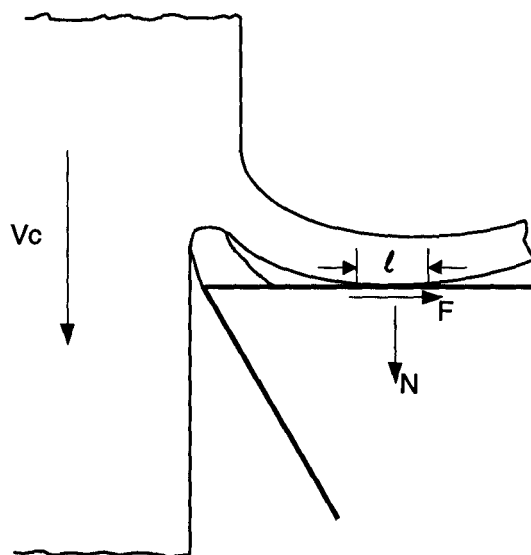


Figure 5.6 Orthogonal cutting operation with BUE.

To analyse the possible effect of the lubricant, the size and the magnitude of the forces acting on the contact l must be known. However it is difficult to measure such parameters directly. Assuming that the oscillation of the force is due to this sliding contact only, the magnitude of the oscillation should be of the same order as the magnitude of a force necessary to change the direction of the chip movement. The reasoning here is that when the chip moves freely then the force (F of figure 5.6) must be at its lowest value whereas when the full frictional restraint occurs then the total force must be a maximum.

An example using the results of force measurements will illustrate the situation. For dry cut, 30m/min and 0.1mm/rev the oscillation of cutting force was 20N and the oscillation for feed force was 17N. The approach angle used was 45° and the tool rake angle was 5° , therefore it is necessary to resolve the forces to obtain forces F and N represented on figure 5.6.

$$N = s_c \cos 5 - \frac{s_f \sin 5}{\cos 45} \quad (5.1)$$

$$F = \frac{s_f}{\sin 45 \cos 5} - s_c \cos 85 \quad (5.2)$$

Where s_c is the oscillation of cutting force, s_f is the oscillation of feed force.

This equation gives $N=18\text{N}$ and $F=22\text{N}$.

If a friction coefficient (μ) could be applied to this contact then it will be the force F divided by the force N . This results in a friction coefficient of approximately 1.2 which is a high value for friction involving steel. Therefore the intermittent chip tool contact cannot be the only cause of oscillation of the measured forces.

When the lubricant (oil+5%additive) is applied the oscillation of cutting force and feed force is respectively 11 and 9N. The difference between the oscillations for dry and lubricated conditions is 9N for cutting force and 8N for feed force. If the reduction on force oscillation when the lubricant is applied is due to reduction of force F this reduction must represent the force acting on that region for dry condition. Applying equations (5.1) and (5.2) for the difference between the forces results:

$$F=10\text{N}$$

$$N=8\text{N}$$

The friction coefficient for this case is very close to the previous calculation for dry condition, approximately 1.25. As it is a high value of friction coefficient if lubrication is causing this effect the lubricant must also be acting on other sources of force oscillation. Therefore resolving the forces F and N acting on the contact ℓ of figure 5.6 may not represent the real effects happening.

In section 5.6 the effect of lubrication on other sources of force oscillation (which are related to the surface finish) will be discussed.

5.4 Workpiece Temperature

A cutting fluid can affect the temperature in metal cutting in two ways. It can lubricate and decrease heat generation and therefore temperature or it can cool the cutting zone increasing heat exchange and carrying part of this heat away.

The increase of temperature of the workpiece is due to the work done on the primary shear plane. Part of this heat is conducted to the chip and the rest is conducted back into the workpiece. The proportion depends on many factors, but mainly on the inclination of the shear plane, which is measured by the shear plane angle ϕ . For given cutting conditions the presence and size of the BUE changes this angle. The heat generated on the rake face, which could be affected by lubrication, does not have a direct effect on the temperature of the workpiece. However less resistance to the movement of the chip over the rake face causes an increase of the shear angle, which decreases the amount of heat that is conducted back into the workpiece. Therefore lubrication of chip tool interface could result in variation of the temperature of the workpiece, which relates to a variation of the size of the BUE.

The smoke that is produced in some tests when the lubricant wets the chip means that it has an effect on the temperature of the chip. However smoke is observed for the highest feeds used on the tests, and for these feeds the chip is broken into small pieces and losses contact with the cutting zone. The action of the lubricant on the chip will therefore not have any effect on temperature of the workpiece.

Regarding the main function of the cutting fluid used in this work, i.e. lubrication, as there was no difference in force measurements for lubricated conditions compared to dry conditions there should be no effect on temperatures generated by applying lubrication.

Lubrication at the chip tool interface should mean that less work is done and so less heat is generated. However the chip and the tool will dissipate the work done at this interface and no heat from this interface will go into the workpiece. The effect of lubrication on workpiece temperature would therefore be indirect. As there is no evidence of lubrication on the rake face (there are no changes in cutting forces) and calculations of the shear plane angle show no changes when lubricant is applied, there is no evidence of lubrication at the chip tool interface.

As there is BUE formation (or dead metal) on the cutting edge for all cutting conditions used in this work the contact between the machined surface and the tool flank face therefore does not occur. The workpiece temperature is then due to the work done only in the primary shear plane.

The size of the BUE can affect the primary shear plane angle and therefore affect the portion of heat that goes into the workpiece. If lubrication on the rake face is possible and the BUE was affected the heat partition could change. Lubrication on the rake face does not mean that temperature on the workpiece will decrease. If there is a smaller BUE the shear plane angle decreases and therefore the primary shear plane length increases and is closer to the workpiece than when BUE is present. This could be expected to give a temperature rise.

Apart from the temperature of the workpiece the method used to measure temperature gives information on the heating and cooling rate of the workpiece. One important observation from temperature measurements is the variation of the

workpiece temperature at the start of cutting. Examples are shown in figures 4.13 to 4.15. The behaviour of the heating curve of the workpiece when lubricant is applied is similar to that for the dry conditions. In both cases the time for the temperature to stabilise is about the same, i.e. 30 seconds. The temperature of the workpiece will not be the same for the whole bar, as the diameter is relatively high. Therefore the equilibrium in this case is between the heat generation and the dissipation of heat into the workpiece. Cooling action for example from the tool holder remote from the cutting zone could have an effect on the temperature of the workpiece or tool because more heat will be conducted away from the cutting zone if the temperature of the tool holder decreases. It is unlikely however that the lubricant is cooling part of the system far from the cutting zone itself as the cutting lasts for just 40 seconds and cutting speed is low the temperature in these regions is low. Therefore a poor coolant like mineral oil would have little effect. Therefore heat loss by conduction into the metal parts of the system will be the only cooling effects and this will be the same for all conditions, dry or lubricated. Addition of sulphur to the oil will not change this characteristic.

The highest increase in temperature in the workpiece for these tests is about 110°C when machining at 40m/min and 0.15mm/rev for dry conditions. The cooling rate at this cutting condition then is about 10,000°C/s for the first 3mm below the cutting edge, where the temperature drops to about 40°C above room temperature. The time to travel this 3mm is about 0.0045s. This means that if the lubricant has any coolant effect on the workpiece it must extract heat at a higher rate than this.

If compared with the velocity of cooling normally used for heat treatment this rate is very high. For example the rate of cooling for the centre of a long cylinder of an austenitic Fe-Ni alloy of diameter 25.4mm is 38°C/s when the centre is at 550°C

using water in agitation as coolant [154]. If oil is used instead of water the cooling rate drops to about 40%. An approximation for cooling rate of the surface by water is about 100°C/s when the temperature is around 100°C , as seen in figure 5.7.

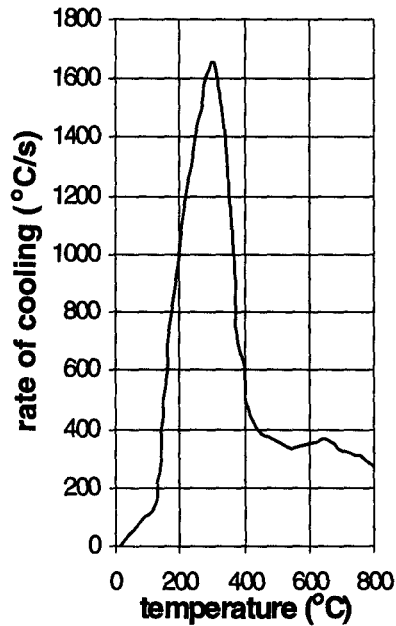


Figure 5.7 The cooling capacity of pure water [155].

If this rate is applied to machining, the surface of the workpiece will be cooled by only 1°C during the first 3mm below the cutting edge. The additive cannot change the cooling ability of the mineral oil as observed in the tests described on chapter 3, and even if they did the difference will be negligible

As the work, and so the heat, is concentrated in a very thin layer on the surface of the workpiece it may be possible for a fluid to cool this small volume at high cooling rates, after the material leaves the cutting zone. In this region the air used with the temperature sensor blows the cutting fluid away and avoids contact with the machined surface. Therefore it can be concluded that the cutting fluid will not cool the machined surface after the cutting zone.

As the cutting fluid does not cool the workpiece the extrapolated temperatures represent the temperature of the workpiece due to the heat from the primary shear zone. As there is no difference in the temperatures for dry and lubricated conditions this heat and the primary shear plane angle must be similar for dry and lubricated conditions. This means that the lubricant does not affect the conditions at the chip-tool interface and therefore does not affect BUE size or shape.

In early work on lubrication in machining, or even some work today [156], the friction between the parts of the system is treated as a classical Coulomb friction. This simplification is used in some theoretical analysis to calculate the amount of energy expended during the process. The temperature rise in the system can then be estimated because almost all the energy expended in the process is converted into heat. This is presented on Appendix B.

5.5 Surface Finish

5.5.1 Effect of Lubricant on Ra

When a good surface finish is aimed at in machining the operation is normally carried out at high cutting speeds. This is because the formation of a BUE is one of the main causes of poor surface quality. The well known improvement in surface finish by cutting fluids is often attributed to the effect of lubrication on the tool rake face to prevent BUE formation and therefore give a better surface finish.

As discussed in previous sections, lubrication did not have an effect on the BUE size and shape. However it did have an effect on surface finish as seen in figures 4.36 to 4.42. Also for some cutting conditions the effect of oil on surface finish does

not depend on addition of sulphur to the oil. The results also suggest that the effect of the mineral oil without sulphur on the surface finish depends on the feed rate. The sulphur addition was necessary only at the highest feed rate of 0.15mm/rev, where the oil alone failed to improve the surface finish. There thus appears to be a critical value for the feed rate above which (independent of the cutting speed) oil without the additive has no effect. The addition of sulphur therefore is critical above this feed rate but has no effect below it. According to the graphs of figures 4.43 to 4.45, the surface finish assumes values between 2 and 6 μ m as the cutting speed increases, for dry and lubricated conditions. This range of values is higher than the theoretical roughness calculated according to equation 2.5.

The effect of sulphur on lubrication seems therefore to be related to the temperature of the surfaces. Most mineral oils fail to lubricate satisfactorily at temperatures in excess of 200°C [116], and therefore this could indicate that the temperatures (at the interface where the oil is lubricating) for feed rates of 0.1mm/rev and 0.05mm/rev were below this value. The sulphur containing compound is intended to decompose at higher temperatures to permit the formation of a protective film of metallic sulphide, which can withstand temperatures up to about 750°C on steels [116].

As seen in the results presented in table 4.6, and figures 4.36 to 4.42 and 4.43 to 4.45 the percentage of sulphur does not have an effect on the performance of the oil, (at least above 1% of the additive). Therefore the effect of lubricant with sulphur can be discussed with reference to just one concentration. The percentage of 5% level was chosen to ensure that the results were clearly from ones with an excess of sulphur required for lubrication.

Analyses of the polished section of a quick stop sample produced when oil without sulphur was used (30m/min and 0.15mm/rev) reveals that a large BUE forms. However the surface finish (R_a) is very similar under these conditions to machining dry (7.36 μm for dry and 7.18 μm when oil is applied). Apparently the big difference in the size of the BUE for these two conditions (when comparing the polished sections presented in figures 4.61 and 4.62) did not have an effect on surface finish. This fact could imply one of two things.

First it could imply that the big BUE for the lubricated condition is stable and therefore has little effect on the surface. If the standard deviation of cutting force is an indication of the variation on BUE size during the process, the results being similar for both conditions (66N for dry and 64N for lubricated condition), indicates that the behaviour and size of the BUE must also be very similar. The difference in size of the BUE seen in the two figures must therefore be due to the normal size variation with time that occurs with a dynamic structure of this type.

A second implication could be that the surface finish of workpiece is not influenced by BUE size. This is contrary to current thinking and will be discussed in the next section.

5.5.2 Machined Surface Geometry

Machined surfaces produced in turning operations are the results of the feed marks (theoretical surface finish) and the addition of disturbances inherent to the process. The most important of these disturbances are imperfections of the cutting edge, vibration, chatter, inaccuracy of machine tool movement and BUE. As both the BUE and flow zones formed on the rake face of the tool occur due to the adherence

between chip and tool, it could be argued that lubrication should have some effect on them both. According to the previous discussion of the effect of lubrication on BUE size it was concluded that the application of the lubricant did not change BUE size compared to dry conditions. Therefore the improvement of surface finish when a lubricant is applied must be due to the action of another source of roughness.

It is difficult to separate the effects of the various factors on surface roughness by examining the workpiece surface (figures 4.81 to 4.98) but important information can be obtained.

The difference between dry and lubricated conditions depends on cutting speed and feed rate. For example at 0.05mm/rev the feed marks are more visible for the dry condition and at 22m/min they are very irregular. Otherwise for the lubricated conditions the feed marks are not so definite, but their width seems to be more constant and the surfaces appear more uniform and smooth than the dry conditions.

These characteristics change for 0.15mm/rev. At this feed rate it is more difficult to distinguish the feed marks for dry conditions than it is for the lubricated conditions. However they are still more irregular for dry conditions.

An interesting characteristic of these surfaces is that there is evidence that some material is deposited on the surface after the feed mark is formed. It is even a common feature that this deposited material covers more than one feed mark. Other usual characteristics from the machined surfaces can also be observed like burs and fractures.

Figure 5.8 shows the machined surface for dry cutting at 40m/min and 0.15mm/rev. At the centre of the photo a particle can be seen that seems to be deposited on the surface after the surface has formed. A closer view at this debris reveals flow marks on the material in the direction of the feed, figure 5.9.

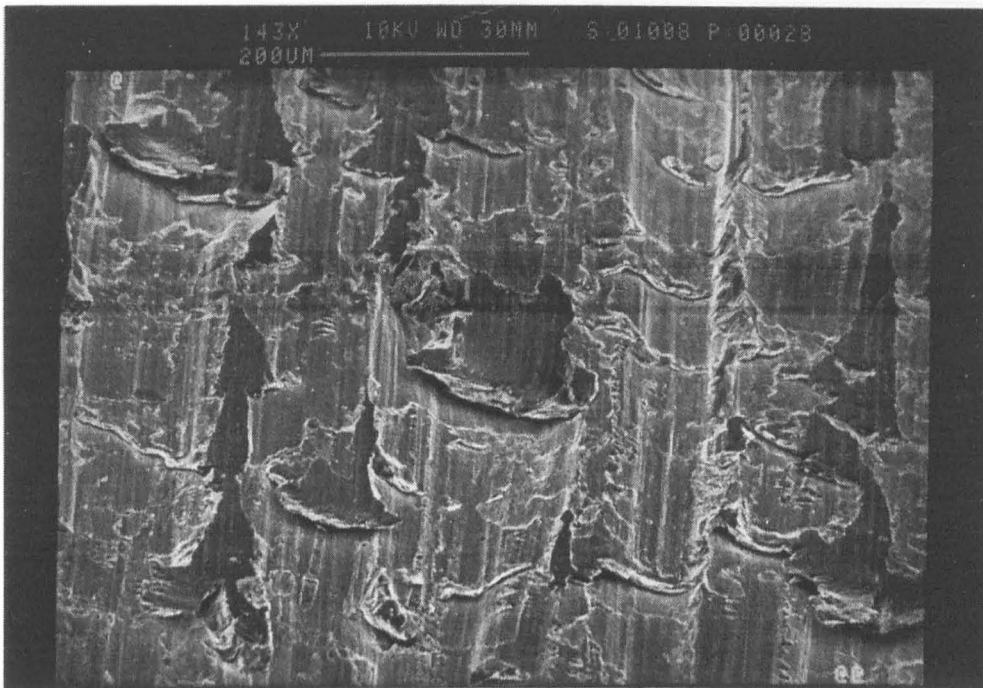


Figure 5.8 Machined surface for dry cutting, 40m/min, 0.15mm/rev, 143x.

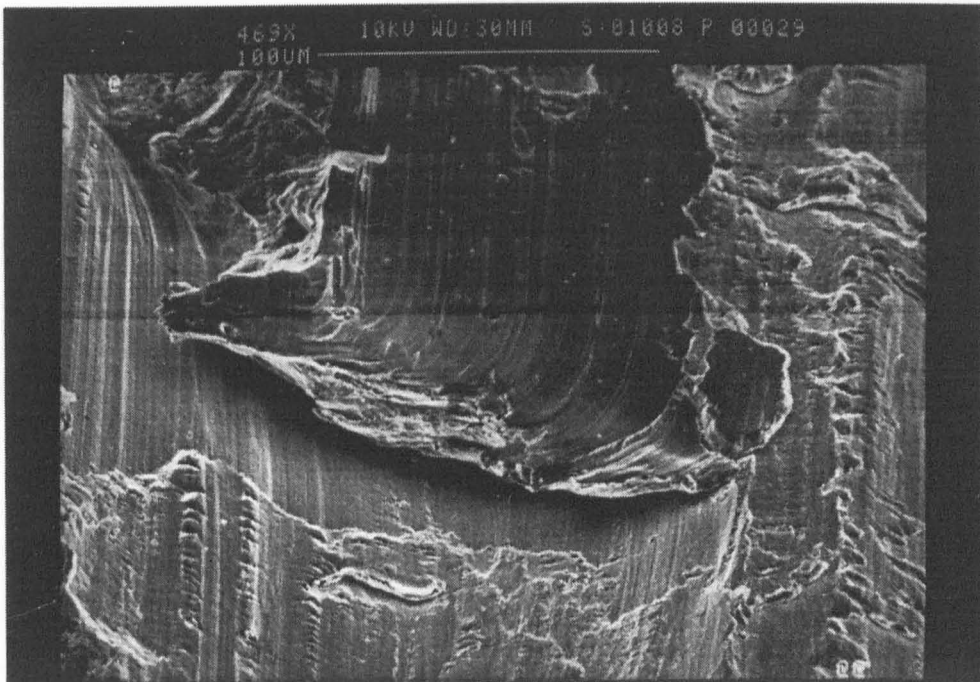


Figure 5.9 Same as figure 5.8, 469x.

A dimpled fracture area on the debris deposited on the machined surface is observable on the upper left of figure 5.8, suggesting that there was a fracture by tension. This area is shown at higher magnification in figure 5.10.

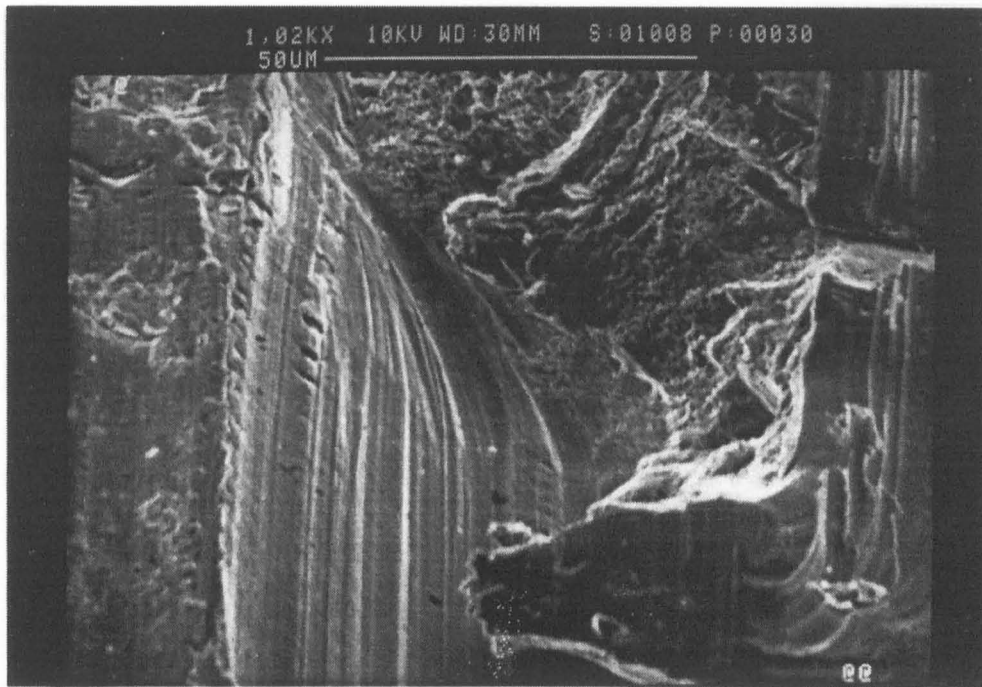


Figure 5.10-Same as figure 5.8, 1020x.

The fracture area on this particle means that the force of the bond that created the fracture was very high. From the flow of material and the dimple fracture this debris could have originated from a tearing action at the edge of the chip, close to the tool nose. This is supported by the fact that this edge of the chip is also very irregular and a number of fractures are encountered.

However if there is such fracture action during the formation of the chip it should appear on the ridge of the feed marks, as occurred in many tests. This is

because the ridges separating the feed marks represent the region where the mechanism of surface formation is uncertain for a three-dimensional cutting operation. Material flow and fracture in this localised area is complex with the surface and the chip travelling almost at right angles to one another.

The bonded particle in figure 5.8 could have been formed remote to the place where it was bonded, for example on the other side of the chip. This would then require it to be transported to the surface and a bonding mechanism that would consistently orientate the particle correctly would also be required. As these particles were a frequent characteristic (under these cutting conditions) and the fact that the flow marks are always at the same direction this seems improbable.

Depending on its size and form, a BUE will prevent contact of the machined surface with flank face of the tool. However a BUE may not form uniformly along the whole contact of the rake face and contact on the end clearance face may thus still exist. In a cylindrical turning operation particularly using a single point tool with an approach angle it is possible that the material, which accumulates as a BUE, is squeezed in a direction parallel to the primary cutting edge of the tool.

Figure 5.11 shows a scanning electron microscope view of a quick stop sample for a dry cutting. This figure shows the end cutting edge of the tool at a point where it loses contact with the material and the new surface is formed. The BUE seems to be rolling or squeezing towards the fresh surface of the workpiece. Periodically small pieces of that BUE are broken off, as suggested by the micrograph, and the surface of the material has smooth paths on the grooves between the feed marks separated by some material, which looks like burrs. These burrs are higher than the grooves formed by the feed marks and will contribute for the high surface roughness measurements.

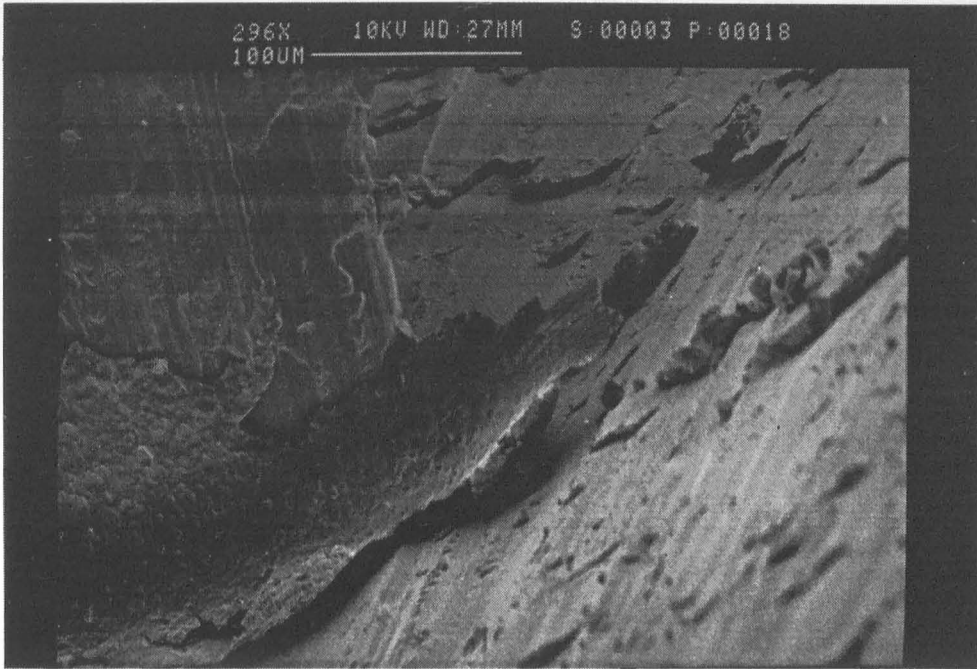


Figure 5.11 View of the point where the cutting edge loses contact with the workpiece, 40m/min, 0.15mm/rev, dry, 296X.

The same kind of configuration of BUE is observed when cutting with oil and oil with 5% of sulphur. Figure 5.12 is the sample for oil with sulphur machined under the same cutting conditions as figure 5.11. In this case the feed marks are clearer and there are no burrs formed inside the grooves (see figures 4.97 and 4.98). It is suggested that the material squeezed to the sides of the BUE may act as a wiping edge. For dry cutting this wiping edge adheres to the workpiece surface forming the burrs. When lubricant is applied it prevents this adherence. This results in an improved Ra value and the change in the appearance of the surface.

Figure 5.13 shows the surface of the workpiece relating to figure 5.12. For these cutting conditions (used in the tests of figures 5.11 and 5.12) the surface finish (Ra) is: 5.2 μm for dry; 5.42 μm for oil and 3.7 μm for oil with 5% of sulphur additive.

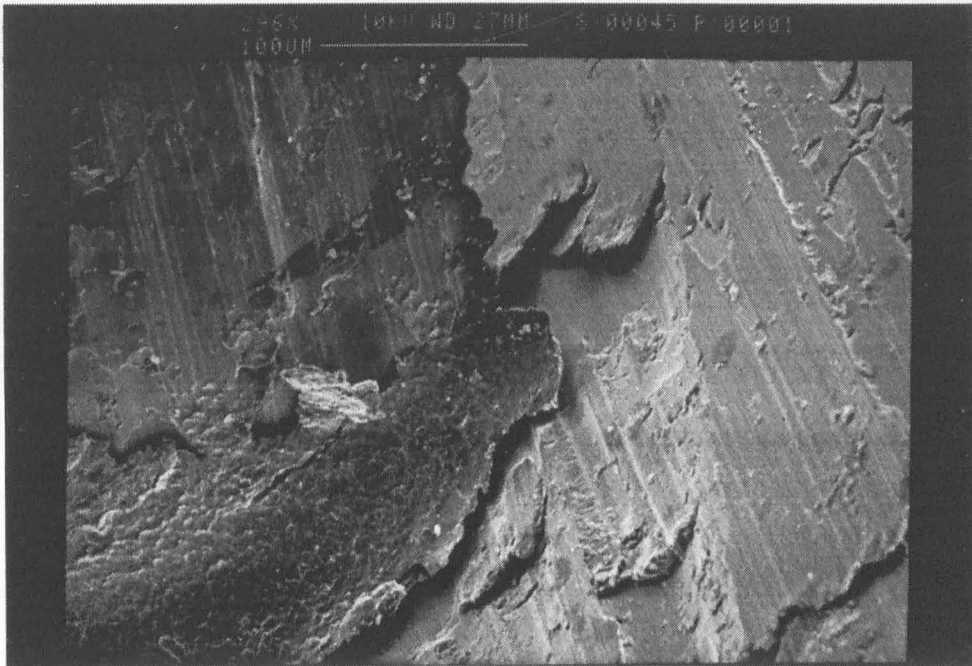


Figure 5.12 View of the point where the cutting edge loses contact with workpiece, 40m/min, 0.15mm/rev, 5%, 296.

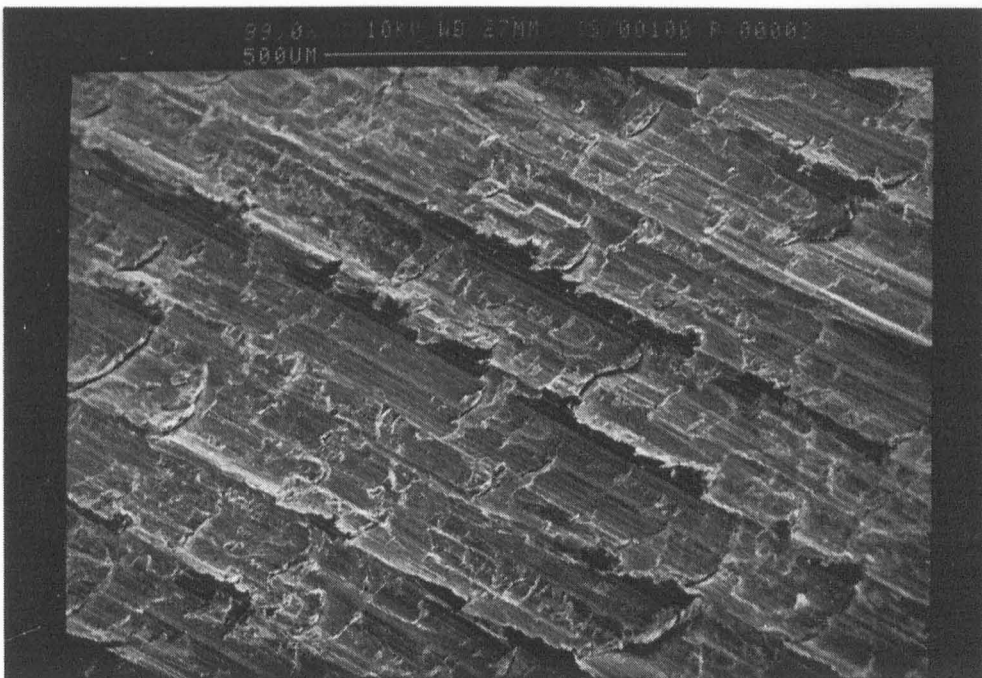


Figure 5.13 Machined surface of the workpiece of figure 5.12, 99x.

This squeezing can be a very important aspect of surface finish and where the lubricant is most effective.

In figure 5.14, it is possible to distinguish the feed marks on the surface, but they are very irregular and difficult to measure (the width). Apart from other surface defects that include bonded debris there is some periodic deposition of material that seems to be pointing in a direction opposite to the feed. Material has been deposited across the feed marks and then it spreads in the direction of the cutting speed, decreasing in width until it disappears, then another piece is deposited and so on. Figure 5.15 is a higher magnification of the same surface of figure 5.14.

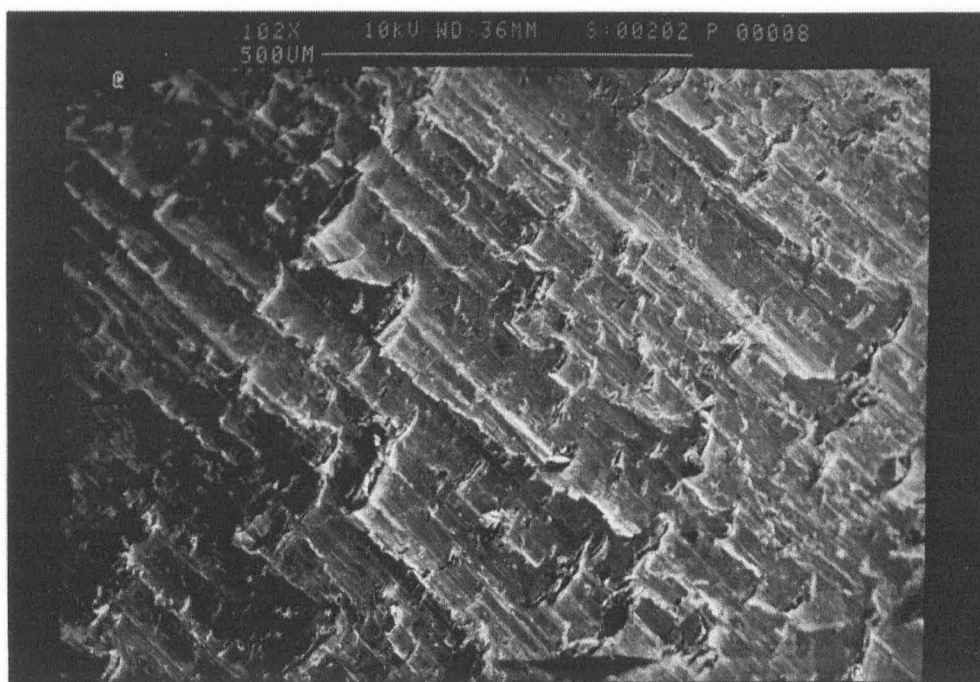


Figure 5.14 Electron microscope view of a machined surface, 40m/min, 0.05mm/rev, dry condition, 102x.

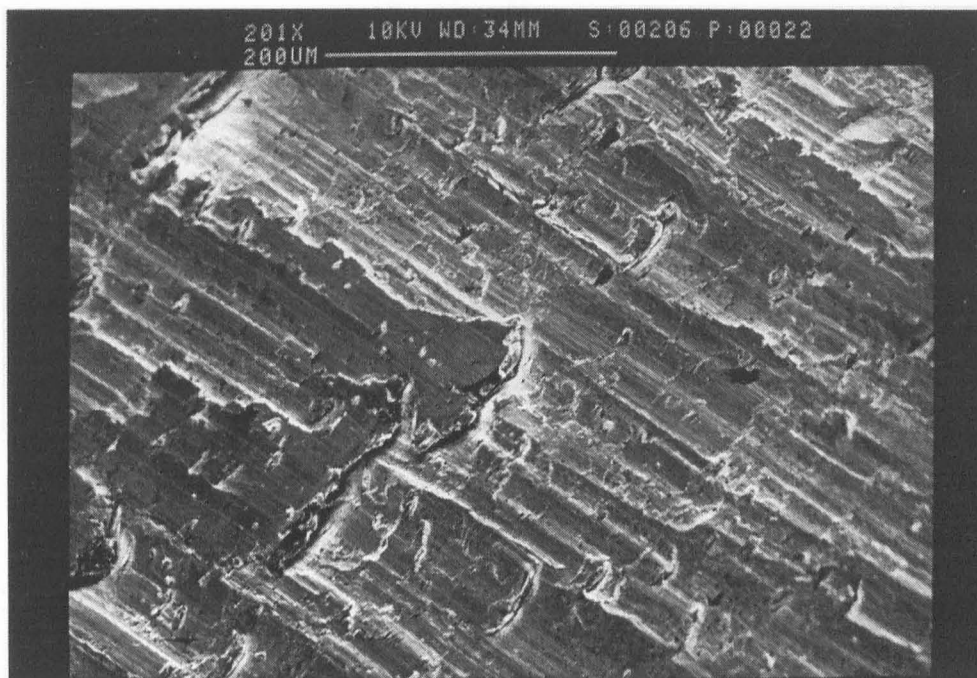


Figure 5.15 Same as figure 5.14, 201x.

Again it looks like this material was deposited after the machined surface was formed. A new test was designed in an attempt to verify this kind of deposition of material. The aim of the test was to have a gap or a groove in the surface of the material to be machined. After the operation the analyses of the surface in the region that contains this gap could indicate if material is deposited over this gap. From observations of the previous machined surface, (figure 5.14 for example) it was concluded that the width of the gap should be in the range between 5 to 10 μm . This gap was obtained by splitting part of the workpiece bar and then attaching both parts again very tight using bolts. The gap was formed due to the roughness and geometrical defects of faces. Figure 5.16 shows a schematic view of this workpiece.

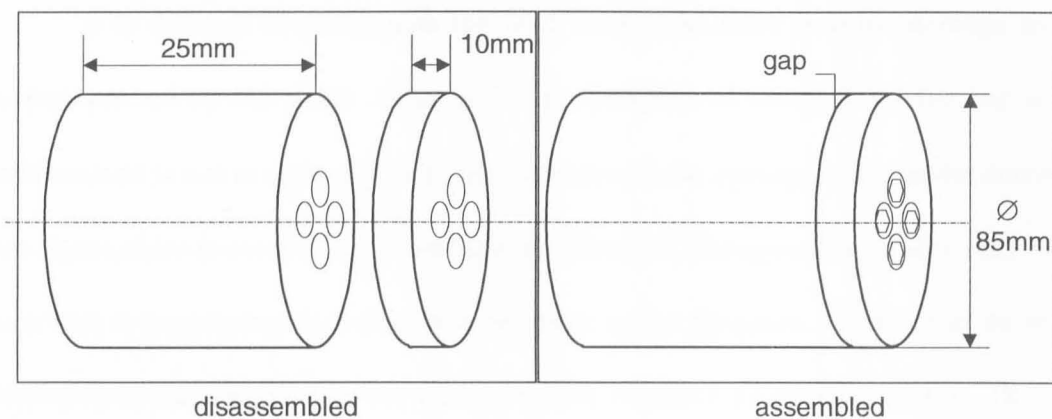


Figure 5.16-Split workpiece.

Before the operation this workpiece was machined to obtain a uniform surface. This workpiece was then machined at $V_c=35\text{m/min}$ and $f=0.14\text{mm/rev}$ with no lubricant. Samples of the surface containing the gap were then removed and observed at the electron microscope. During sample production it was necessary to avoid the split and any relative movement that could damage the sample during the sawing operation, this was done by bonding the parts together using two welding spots. An electron microscope view of such sample is shown in figure 5.17.

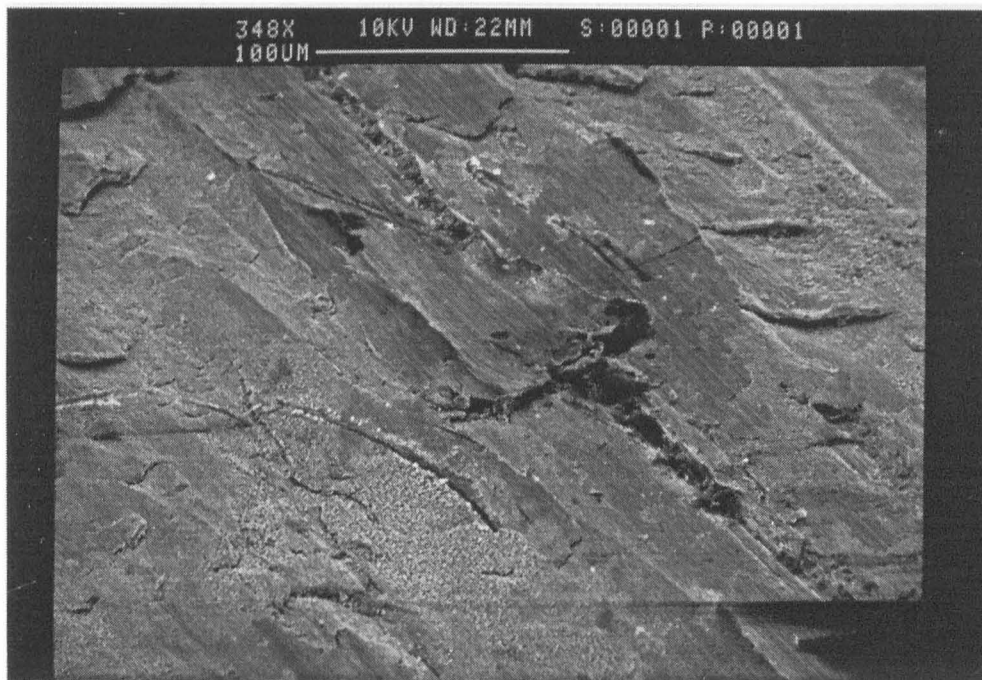


Figure 5.17 Electron microscope view of a sample of machined surface of the workpiece of figure 5.16, 35m/min, 0.14mm/rev, dry condition, 348x.

It is difficult to distinguish the feed marks and there is some damage to the surface caused by the weld. As expected the junction of the parts of the bar is not uniform and is not at right angles to the direction of the cutting speed. In the centre of this figure there is material that overlaps the junction. The geometry of this material is such that it is pointing in a direction opposite to the direction of feed and its width decreases in the direction of the cutting speed. Figure 5.17 clearly suggests that this material in the centre of the photo was deposited after the machined surface of the bar was created otherwise a discontinuity at the junction would be seen. This configuration is similar to the one of figure 5.14.

Figure 5.18 shows a diagrammatic model of the proposed mechanism by which the BUE alters the surface and the action of cutting fluid.

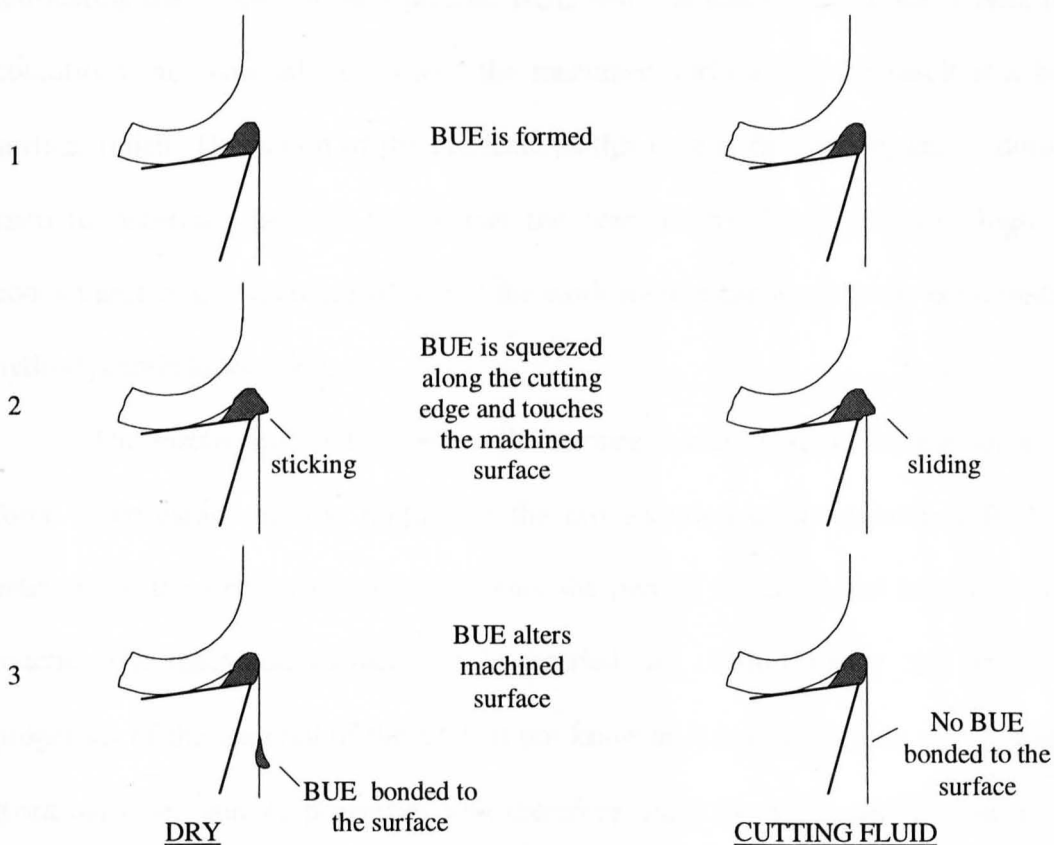


Figure 5.18 Alteration of the machined surface by squeezed BUE and the action of cutting fluid.

The BUE is squeezed along the cutting edge during the cut and touches the machined surface. The BUE rubs against the surface and periodically bonds to it. This action increases the surface roughness. This area is where the cutting fluid acts lubricating the contact between squeezed BUE and machined surface avoiding the bond. This is the mechanism by which the cutting fluid improves surface finish. There are even conditions for hydrodynamic lubrication in this small area close to the tool nose.

This section shows evidence of some alterations in the machined surface during the operation. Debris particles, squeezing the BUE and tearing of the chip all contribute to the surface roughness of the workpiece. The lubricant applied can therefore improve surface finish by avoiding the bonding of these debris particles and lubricating the contact of the squeezed BUE with the machined surface. Under these conditions this material can "wipe" the machined surface and the result is a better surface finish. The action of the lubricant in this case is favourable, and it does not need to penetrate the rake face where the compressive forces are very high. The contact area of the squeezed BUE and the work surface can even create conditions for hydrodynamic lubrication.

The instant the BUE bonds to the surface it may increase cutting force, as a force is necessary for the rupture of the cross-section of the squeezed BUE. An estimate of the force necessary to rupture the part of the BUE that is squeezed and touches the machined surface can be carried out. Unfortunately the mechanical properties of the material of the BUE is not known as it is material that was extremely work-hardened and its properties will therefore differ from the parent material. An approximation for the cross section of this part of the BUE will be $100 \times 10^{-3} \text{ mm} \times 50 \times 10^{-3} \text{ mm}$ which gives an area of the cross section of $5 \times 10^{-3} \text{ mm}^2$. The approximate

tensile strength for the material of the workpiece is estimated as 600N/mm^2 . Therefore the force necessary (assuming the squeezed BUE will be under axial tension) to rupture is the area multiplied by the strength, which gives approximately 3N. The value of 3N is of the same order as the difference in force oscillation between dry and lubricated conditions calculated in section 5.3.3. However if the lubricant just reduced the number (or frequency) of bonded particles, no effect on the **range**, i.e. maximum to minimum, of force oscillation should be detected. The distance between each bonded BUE is about $300\mu\text{m}$ (for $V_c=40\text{m/min}$). Forces are measured each second during the cut and according to the cutting speed the tool travels a distance of 0.7m between each reading. If the bonded particles are separated by $300\mu\text{m}$ this means that there are approximately 2,500 bonded particles being formed between each reading. If the lubricant reduces the number of particles bonding to less than 2,500 per second there will be no effect on the range of force oscillation (but it will be shown by the standard deviation of the signal). Every time one particle bonds to the surface the force necessary to break this contact will contribute to the measured cutting force. For the standard deviation be affected it is necessary a great reduction in the number of bonded particles to decrease the probability of effect on the measured cutting force and therefore decreasing the standard deviation.

For this mechanism to have an effect on force oscillation without affecting the force average first it is necessary that the range of force be the same. Also the period of the graph of force against time should be higher for lubricated conditions than dry conditions. To satisfy both conditions it means that the bonding is still happening for lubricated conditions, but it is less frequent, and more gradual. This means that the squeezed BUE rubs against the machined surface for a longer period of time than it does for dry conditions before adhering to the machined surface. The equipment used

to measure force together with the effects of environment and material composition do not allow confirmation that there were no small effects on force average. The result of less force oscillation can therefore be either due to less bonding or no bonding. In both cases the squeezed BUE rubs against the machined surface for the case of lubricated conditions and improves the surface finish.

When there is BUE the cutting force F_c is acting on the top of it, resulting in very high compressive stress. Using the measured values of cutting forces and the micrographs shown in figures 4.46 to 4.72, the compressive stress can be estimated. This results in the range of 2 to 8GPa, with an average of 4GPa. Under this high stress the material of the BUE could easily deform along the cutting edge.

The strain rate of the deformation of the BUE along the cutting edge can also be estimated by observations of the machined surfaces that contain bonded parts of the BUE. The length of the bonded BUE part and the distance between them (in the direction of cutting speed) suggest a strain rate around $4 \times 10^2 \text{s}^{-1}$ in the direction parallel to the cutting edge.

While it is uncertain what the properties and behaviour of the material of the BUE are, the strain rate and stress are very high for the mechanism of deformation under standard tension test conditions to be applied.

5.6 Optimised Cutting Fluid System

Previous sections discussed the effect of lubrication on cutting forces, workpiece temperature and surface finish. It has been shown that there was no effect on measured forces and this was explained by the fact that the lubricant cannot penetrate the chip-tool interface. As there was no reduction on cutting forces and

therefore no reduction on heat generation no effect on workpiece temperature was detected. High cooling rates for the workpiece were obtained for dry cutting, suggesting that it will be almost impossible for a cutting fluid to cool the workpiece significantly above this rate. The only significant effect of lubrication was the improvement in surface finish. This improvement was attributed to the action of the lubricant in a region close to the tool nose. As the lubricant does not cool the workpiece and lubrication occurs for a very small region (compared to the cutting zone) it seems that the volume of cutting fluid used (25ml/s) is much more than is needed to affect the operation.

Even if lubrication of the rake face was possible the volume of cutting fluid applied in practical operations are much higher than the amount necessary to lubricate such small area. At 40m/min, 0.15mm/rev and dry cutting the chip thickness is 0.363mm. This means that the speed of the chip is 15m/min. At this speed and considering 2mm depth of cut and an approach angle of 45° then the area of the lower surface of the chip that is produced each minute is about $42,000\text{mm}^2$. Considering that the lubricant will contaminate this area by attaching one chain of the molecule to each atom of the surface (consider the case where the surface is smooth and perfect and plan area of one atom of 10^{-18}mm^2) then it will require 7×10^{20} molecules. Assuming a molecular weight of 300 for the lubricant (which is a long chain [112]) it would be required approximately $300 \times 7 \times 10^{20} / 6.03 \times 10^{23}$ ml/s. This rate is equivalent to about 0.3ml/s, which is about one hundred times less than the volume normally applied.

For lubrication of the region close to the tool nose less fluid will be needed, as the area is smaller than the chip tool interface. A length of $100\mu\text{m}$ is a good approximation for the length of the squeezed BUE that extends beyond the cutting edge. For a cutting speed of 40m/min it means that a contact area of $4,000\text{mm}^2$ is

produced each minute. This is ten times less than the area required to contaminate the interface therefore following the same procedure as in the last paragraph a volume of approximately 0.03ml/s would be required. Assuming an efficiency of 10% the volume required would be 0.3ml/s, which is nearly one hundred times less than the volume used.

To verify the effect of low volume of cutting fluid the flow rate of lubricant was reduced by restraining the nozzle of the cutting fluid line. The flow rate was reduced to 4ml/s. For this case the lubricant is applied in the same way, overhead, but directed over the tool nose. Tests were carried out using the same cutting conditions used in this work and the surface roughness of the machined surface was measured.

The surface roughness results were similar to the results obtained using the normal flow rate of lubricant. Even when the lubricant, (applied at the rate of 4ml/s), is applied 10mm back from the cutting edge the results are similar. In this case the amount of lubricant reaching the rotating workpiece (due to spreading) is very low and it still seems effective.

The flow rate was further reduced to 0.03ml/s using a hypodermic needle to replace the nozzle. In this case the flow of lubricant was not continuous instead the lubricant was applied in a rate of 1.3 drops/s directly onto the region where the chip loses contact with the workpiece (the same as the flow of 4ml/s was applied). The surface roughness improved if compared to dry condition and the results were again similar to the normal lubricated tests.

These low volumes of lubricants are enough to improve the surface roughness because the area that requires lubrication is extremely small. Because the area affected is so small, there is no measurable effect on forces (even when flow rate of 25ml/s is used).

With these low volumes of lubricant and the way they are applied, i.e. indirectly, it is probable that the oil does not reach the chip tool interface. This fact ratifies what is proposed in this work that lubricant does not need to avoid the formation of the BUE, or lubricate the rake face of the tool (even if this were possible), but only needs to lubricate the region near to the tool nose.

The fact that a very low volume of lubricant is enough to affect the surface finish of the workpiece can explain the effect of the percentage of sulphur. It was observed that a percentage above 1% (of the additive) does not affect the performance of the oil. The oil being applied at 25ml/s means that enough amount of sulphur is delivered to the small areas to be lubricated.

It should be noted that others functions of the cutting fluid will not be performed when very low lubricant volumes are applied in this manner (e.g. cleaning the swarf from the cutting area and protection to the machine tool). Also there will be no cooling of the tool and tool holder which may be necessary. However these other functions of a cutting fluid can be performed by any other fluid and does not need to be a lubricant and therefore oils or potentially harmful additives may be avoidable.

A cutting fluid is also applied to prevent the workpiece from rusting when machining iron based materials. However when machining material and alloys like titanium, copper and aluminium there is no need for such protection. In these cases there is no need to use large volumes of oil containing cutting fluids.

With the growing volume of mandatory government legislation in Europe to reduce lubricant application mainly to reduce the impact on the environment [157], the application of low volume of lubricant could be the best option. It will reduce drastically the pollution of the environment and related problems of health and safety. Reducing the volume of lubricant will reduce the costs related to recycling and

disposal of the cutting fluid. In addition, there is a possibility of using more expensive cutting fluids.

6 FUTURE WORK

BUE is one of the factors responsible for the poor surface finish. This work suggests that the lubricant will not avoid BUE formation but still improves the surface finish. It would be interesting then to investigate the effect of the same lubricants used in this work when machining a pure metal or a metal that does not form a built-up edge.

It was observed that the BUE can be squeezed along the cutting edge and touches the workpiece surface altering its finish. The tool geometry can have a significant effect on this mechanism, mainly the approach angle, tool nose radius and chip breaker geometry. Therefore an investigation of different tool geometry would be recommended. It would be very interesting if the tool geometry shown in figure 6.1 was possible. The figure shows optimised geometry of the tool nose. The tool is composed of the normal cutting edge with the normal nose radius and a new cutting edge that wipes the workpiece surface after it is formed. Such tool geometry should be possible but depends on the dimensions (not given on figure 6.1).

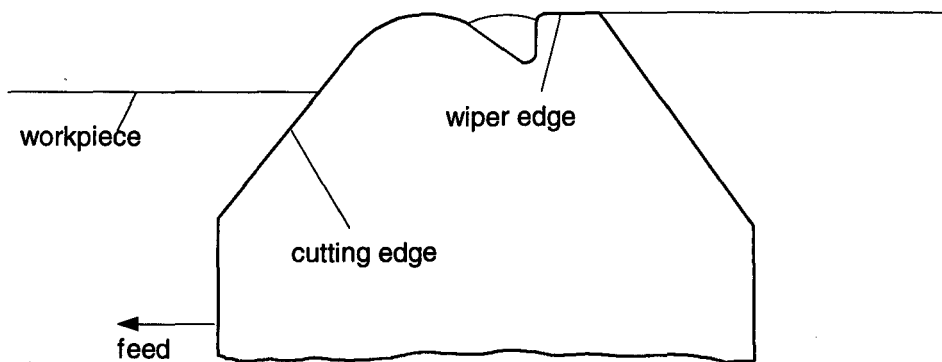


Figure 6.1 Optimised tool geometry to improve surface finish.

The effect of the lubricant was measured through cutting forces and workpiece temperature. However another important function of cutting fluids is to increase tool life. Investigations on the performance of the lubricant using the same approach of this work incorporating tool life test will complete the investigation. However the material and cutting conditions used in this work result in long tool lives, and the tests could not be feasible. It is necessary therefore to use a different workpiece material, or another tool material.

The method to measure temperature described in this work proved to be reliable and depending on the conditions more accurate than other methods used in metal cutting. Cutting temperatures were used to investigate the performance of a cutting fluid that was predominantly a lubricant and has poor cooling ability. An investigation of the effect on the workpiece temperature using cutting fluids with high cooling abilities would be interesting.

This work measured the workpiece temperature and the results could be related to the work expended in the cutting zone using theoretical relationships. These theoretical relationships assume that almost all the work done during machining is converted into heat. The workpiece, chip and tool dissipate this heat. To complete the relationship between temperatures and work it would be interesting if temperatures of the chip and tool could be included. Particularly the temperature of chip/tool interface could be measured by the more traditional methods (metallographic method or tool-work thermocouple described in chapter 2, section 2.6.2).

It was suggested by this work that the volume of lubricant necessary in machining is very low if compared to the traditional over head flow system. While rates of 25ml/s are currently used on machining operations good results were obtained with volumes of only 0.03ml/s. This encourages the development of new systems of

fluid application and more tests on the effect on forces, temperature, surface finish and tool life.

7 CONCLUSIONS

The results of the experimental tests carried out in the present work for the specific cutting conditions, workpiece material, geometry and material of the tool and lubricant allow the following conclusions to be drawn:

1. The method to measure temperature using an infrared sensor is a reliable method for metal cutting applications. Its accuracy, if compared with other methods used to measure cutting temperature, is very good.
2. Using this method it was possible to obtain information about the cooling rate of the workpiece as the new surface is produced, which is very high (1,600 to 13,000°C/s).
3. The lubricant (with or without the EP additive) did not change the absolute values of the measured cutting forces compared to dry conditions.
4. The lubricant did not change BUE size.
5. The fact that the cooling rate of the workpiece by conduction into the bar is very high and the cutting fluid has poor cooling abilities resulted in the cutting fluid having no effect on the measured workpiece temperature.
6. The cutting fluid improved the surface finish compared to dry conditions for feed rates of 0.05 and 0.1mm/rev. However the cutting fluid without the additive failed to improve the surface for a feed rate of 0.15mm/rev at any cutting speed.
7. The EP additive to the oil improved the surface finish for all cutting speeds and feed rates used in the tests. More than 1% of additive did not make any difference to the performance (measured by cutting forces, workpiece temperature and surface finish) of the lubricant.

8. A model of lubrication is proposed, figure 5.18, based on electron microscope photos of quick stop samples and machined surface samples. In this model the cutting fluid does not penetrate into the contact area between chip and tool to avoid BUE formation. Instead, the lubricating action happens after the machined surface has been formed and prevents sticking of the squeezed BUE to the machined surface.
9. As a result of conclusion 8 a very small volume of cutting fluid (0.3ml/s) should be enough to improve the cutting operation. This work gives evidence of the improvements given by a very small volume of cutting fluid (0.03ml/s) if compared to the traditional method of applying cutting fluid. This suggests the reason why very low proportion (1%) of additive is sufficient for lubrication.

REFERENCES

- 1-Bever, M.B.; Marshall, E.R. and Ticknor, L.B. - "*The Energy Stored in Metal Chips During Orthogonal Cutting*" - Journal of Applied Physics, vol. 24, pp 1176-1179, 1953.
- 2-Shaw, M.C. - "*Metal Cutting Principles*" - Oxford University Press, USA, 1984, ISBN 0-19-859002-4.
- 3-Nakayama, K.; Shaw, M.C. and Brewer, R.C. - "*Relationship Between Cutting Forces, Temperatures, Built-up Edge and Surface Finish*" - Annals of the CIRP, vol. XIV, pp 211-223, 1966.
- 4-Shouckry, A.S. - "*The Effect of Cutting Conditions on Dimensional Accuracy*" - Wear, vol. 80, pp 197-205, 1982.
- 5-Trent, E.M. - "*Metal Cutting*" - Butterworths-Heinemann Ltd, 3rd edition, 1991, ISBN 0-7506-1068-9.
- 6-Machado, A.R. - "*Machining of Ti6Al4V and Inconel 901 with a High Pressure Coolant System*" - PhD Thesis, University of Warwick, England, UK, 1990.
- 7-Wise, M.L.H. and Milovic, R. - "*Ranges of Application of Free-Cutting Steels and Recommended Tool Materials*" - Materials Science and Technology, October, vol. 4, pp 933-943, 1988.

- 8-Kalpakjian, S. - *"Manufacturing Process for Engineering Materials"* - Addison-Wesley Publishing Company, 1985, ISBN 0-201-11690-1.
- 9-Degarmo, E.P.; Black, J.T. and Kosher, R. - *"Materials and Process in Manufacturing"* - Macmillan Pub. Co., New York, 7th edition, 1988, ISBN 0-02-946140-5.
- 10-Lindberg, R.A. - *"Processes and Materials of Manufacture"* - Allyn and Bacon, USA, 4th edition, 1990, ISBN 0-205-12031-8.
- 11-Schey, J.A. - *"Introduction to Manufacturing Processes"* - McGraw-Hill International Editions, 2nd edition, 1987, ISBN 0-07-100311-8.
- 12-British Standard - *"Specification for Single Point Cutting Tools"* – Part 2, Nomenclature, BS 1296/2, 1972.
- 13-ASM Metals Handbook, vol. 16, Machining, 9th edition, USA, 1989.
- 14-Ernest, H. and Merchant, M.E. - *"Chip Formation, Friction and High Quality Surfaces"* - Proc. Symp. Surface Treatment of Metals, Cleveland, USA, 21-25 Oct, pp 299-378, 1940.
- 15-Lee, E.H. and Shaffer, B.W. - *"The Theory of Plasticity Applied to a Problem of Machining"* - Journal of Applied Mechanics, vol. 18, n 4, pp 405-413, 1951.

- 16-Shaw, M.C.; Cook, N.H. and Finnie, I. - "*The Shear Angle Relationship in Metal Cutting*" - Trans. of ASME, USA, vol. 75, pp 273-288, 1953.
- 17-Komanduri, R. and Shroeder, T.A. - "*On Shear Instability in Machining a Nickel-Iron Base Superalloy*" - Trans. of ASME, Journal of Engineering for Industry, vol. 108, May, pp 93-100, 1986.
- 18-ISO Standard - "*Tool Life Testing with Single-Point Turning Tools*" - ISO 3685, 1977.
- 19-Boothroyd, G. and Knight, W.A. - "*Fundamentals of Machining and Machine Tools*" – Marcel Dekker, Inc, 2nd edition, 1989, ISBN 0-8247-7852-9.
- 20-Wallbank, J. - "*Flow at the Cutting Edge and the Generation of New Surfaces During Metal Cutting*" - PhD Thesis, University of Birmingham, 1978.
- 21-Pekelharing, A.J. and Gieszen, C.A. - "*Material Side Flow in Finish Turning*" - Annals of the CIRP, vol. 20/1, pp 21-22, 1971.
- 22-Merchant, M.E. - "*Mechanics of the Metal Cutting Process. I: Orthogonal Cutting and a Type 2 Chip*" - Journal of Applied Physics, vol. 16, n 5, May, pp 267-275, 1954.
- 23-Hutchings, I.M. - "*Tribology - Friction and Wear of Engineering Materials*" - Edward Arnold, London, 1992, ISBN 0-340-56184-X.

24-Trent, E.M. - "*Cutting Steel and Iron with Cemented Carbide Tools - Part II: Conditions of Seizure at the Tool/Work Interface*" - Journal of the Iron and Steel Institute, Nov, pp 923-932, 1963.

25-Zorev, N.M. - "*Interrelationship Between Shear Processes Occurring Along Tool Face and on Shear Plane in Metal Cutting*" - Proc. Int. Prod. Eng. Res. Conf., Pittsburgh, Pennsylvania, USA, Sep, pp 42-49, 1963.

26-Trent, E.M. - "*Metal Cutting and the Tribology of Seizure: I-Seizure in Metal Cutting*" - Wear, vol. 128, pp 29-45, 1988.

27-Trent, E.M. - "*Metal Cutting and the Tribology of Seizure: II-Movement of Work Material Over the Tool in Metal Cutting*" - Wear, vol. 128, pp 47-64, 1988.

28-Trent, E.M. - "*Metal Cutting and the Tribology of Seizure: III-Temperature in Metal Cutting*" - Wear, vol. 128, pp 65-81, 1988.

29-Heginbotham, W.B. - "*Metal Cutting and the Built-up Nose*" - Proc. Instn. Mech. Engrs., vol. 175, n 18, pp 892-905, 1961.

30-Iwata, K.; Aihara, J. and Okushima, K. "*On the Mechanism of Built-up Edge Formation in Cutting*" - Annals of the CIRP, vol. XVIV, pp 323-330, 1971.

31-Williams, J.E.; Smart, E.F. and Milner, D.R. - "*The Metallurgy of Machining Part2: The Cutting of Single-Phase, Two Phase and Some Free Machining Alloys*" -

Metallurgia, February, pp 51-59, 1970.

32-Yaguchi, H. - "*Effect of Soft Additives (Pb, Bi) on formation of Built-up Edge*" - Materials Science and Technology, October, vol. 4, pp 926-931, 1988.

33-Milovic, R. and Wallbank, J. - "*The Machining of Low Carbon Free Cutting Steels with High Speed Tools*" - Journal of Applied Metal Working, vol. 2, n 4, January, pp 249-257, 1983.

34-Philip, P. K. - "*Built-Up Edge Phenomenon in Machining Steel with Carbide*" - International Journal of Machine Tool Design and Research, vol. 11, pp 121-132, 1971.

35-Ramaswani, R. - "*The Effect of the Built-up Edge (BUE) on the Wear of Cutting Tools*" - Wear, vol. 18, pp 1-10, 1971.

36-Gordon, M.B. - "*The Applicability of the Binomial Law to the Process of Friction in the Cutting of Metals*" - Wear, vol. 10, pp 264-290, 1967.

37-Ramalingam, S. A - "*Photoelastic Study of Stress Distribution During Orthogonal Cutting - Part 2: Photoplasticity Observations*" - Trans. of ASME, Journal of Engineering for Industry, May, pp 538-544, 1971.

38- Ramalingam, S. and Lehn, L.L. - "*A Photoelastic Study of Stress Distribution During Orthogonal Cutting - Part 1: Workpiece Stress Distribution*" - Trans. of

ASME, Journal of Engineering for Industry, May, pp 527-537, 1971.

39-Kato, S.; Yamaguchi, K. and Yamada, M. - "*Stress Distribution at the Interface Between Tool and Chip in Machining*" - Trans. of ASME, Journal of Engineering for Industry, May, 683-689, 1972.

40-Barrow, G.; Graham, W.; Kurimoto, T. and Leong, Y.F. - "*Determination of Rake Face Stress Distribution in Orthogonal Machining*" - International Journal of Machine Tool Design and Research, vol. 22, n 1, pp 75-85, 1982.

41-Childs, T.H.C. and Mahdi, M.I. - "*On the Stress Distribution Between the Chip and Tool During Metal Turning*" - Annals of the CIRP, vol. 38, n 1, pp 55-58, 1989.

42-Field, M. and Kahles, J.F. - "*Review of Surface Integrity of Machined Components*" - Annals of the CIRP, vol. 20/2, pp 153-163, 1971.

43-Bailey, J.A. and Azargoon, G.A. - "*Some Recent Observations Concerning the Impact of Machining on Surface Condition*" - SME Tech. Pap. n IQ75-126, 1975.

44-Fan, K.C. and Chao, Y.H. - "*In-Process Dimensional Control of the Workpiece During Turning*" - Precision Engineering, January, vol. 13, n 1, pp 27-32, 1991.

45-Schaffer, G.H. - "*The Many Faces of Surface Texture*" - American Machinist & Automated Manufacturing, June, pp 61-68, 1988.

- 46-Whitehouse, D.J. - "*Review Article: Surface Metrology*" - Meas. Sci. Technol., n 8, pp 955-972, 1997.
- 47-Garbini, J.L.; Koh, S.P.; Jorgensen, J.E. and Ranulu, M. - "*Surface Profile Measurement During Turning Using Fringe-Field Capacitive Profilometry*" - Journal of Dynamic Systems Measurement and Control, June, vol. 114, pp 234-243, 1992.
- 48-Black, J.T. and Ramalingam, S. - "*Fine Structure of Machined Surfaces*" - Int. J. Mach. Tool Des. Res., vol. 10, pp 439-463, 1970.
- 49-Jang, D.Y. - "*A Unified Optimization Model of a Machining Process for Especificed Conditions of Machined Surface and Process Performance*" - Int. J. Prod. Res., vol. 30, n 3, pp 647-663, 1992.
- 50-Selvam, M.S. and Radhakrishnan, V. - "*Groove Wear, Built-up Edge and Surface Roughness in Turning*" - Wear, vol. 30, pp 179-188, 1974.
- 51-Bailey, J.A. - "*On Surface Damage During Machining of AISI 4340 Steel*" - Wear, vol. 27, pp 161-173, 1974.
- 52-Backer, W.R.; Marshall, E.R. and Shaw, M.C. - "*The Size Effect in Metal Cutting*" - Trans. of ASME, vol. 74, pp 61-71, 1952.
- 53-Sata, T. - "*Surface Finish in Metal Cutting*" - Annals of the CIRP, vol. 12, n 4, pp 190-197, 1963.

54-Ansell, C.T. and Taylor, J. - "*The Surface Finishing Properties of a Carbide and Ceramic Cutting Tool*" - Proceedings of the 3rd International MTDR Conference, Advances in Machine Tool Design and Research, University of Birmingham, Sep, pp 225-243, 1962.

55-Lambert, H.J. - "*Two Years of Finish-Turning Research at the Technological University, Delft*" - Annals of the CIRP, vol. 10, pp 246-255, 1961.

56-Sarwar, M. and Thompson, P.J. - "*Cutting Action of Blunt Tools*" - Proc. of the 22nd Int. Mach. Tool Design and Research Conference Held in Manchester, 16-18 September, pp 295-304, 1981.

57-Buttery, T.C. and Archard, J.F. - "*Grinding and Abrasive Wear*" - Proc. Instn. Mech. Engrs., vol. 185, n 43, pp 537-551, 1970-71.

58-Wallbank, J. - "*Surfaces Generated in Single-Point Turning*" - Wear, vol. 56, pp 391-407, 1979.

59-Selvam, M.S. and Radhakrishanan, V. - "*Influence of Side-Flow and Built-up Edge on the Roughness and Hardness of the Surface Machined with a Single Point Tool*" - Wear, vol. 26, pp 393-403, 1973.

60-Wilber, W.J.; Chisholm, A.W.J. and Pattinson, E.J. - "*Use of the Scanning Electron Microscope to Study the Function of Manganese Sulphide Inclusions in Resulphurised Free-Machining Steels*" - Proc. of the 12th Int. Mach. Tool Design and

Research Conference, held in Birmingham, 15-17 September, pp 499-506, 1971.

61-Nishima, K. - "*On the Micro-Asperities of Machined Surface in High Speed Metal Cutting*" - Bull Japan Soc. of Prec. Engg., vol. 8, n 4, December, pp 159-160, 1974.

62-Chu, T.H. - "*An Experimental Study of the Workpiece Temperature on the Machined Surface During Metal Cutting*" - PhD thesis, University of Warwick, 1998.

63-Bayoumi, A.E.; Xie, Q. and Hamdan, M.N. - "*Effect of Cutting Conditions on Dynamic Properties and Surface Integrity of Work Material*" - Wear, vol. 146, pp 301-312, 1991.

64-Pispanem, V. - "*Theory of Formation of Metal Chips*" - Journal of Applied Physics, vol. 19, pp 876-881, 1948.

65-Merchant, M.E.; Field, M. - "*Mechanics of Formation of the Discontinuous Chip in Metal Cutting*" - Trans. of ASME, vol. 71, pp 421-428, 1949.

66-Palmer, W.B. and Oxley, P.L.B. - "*Mechanics of Orthogonal Machining*" - Proc. Instn. Mech. Eng., vol. 173, n 24, pp 623-651, 1959.

67-Weiner, J.H. - "*Shear-Plane Temperature Distribution in Orthogonal Cutting*" - Trans. of ASME, vol. 77, pp 1331-1341, 1955.

68-Smart, E.F. and Trent, E.M. - "*Coolants and Cutting Tool Temperatures*" -

Proceedings of the 15th Int. Mach. Tool Design and Research Conference, Birmingham, 18-20 September, pp 187-195, 1974.

69-Childs, T.H.C.; Maekawa, K. and Maulik, P. - "*Effects of Coolant on Temperature Distribution in Metal Machining*" - Materials Science and Technology, November, vol. 4, pp 1006-1019, 1988.

70-Chandiramani, K.L. and Cook, N.H. - "*Investigation on the Nature of Surface Finish and its Variation with Cutting Speed*" - Trans. of ASME, Journal of Engineering for Industry, May, pp 134-140, 1964.

71-Peklenik, J. and Gartner, J.R. - "*Workpiece Accuracy Criterion for the Dynamic Machine Tool Acceptance Test*" - Int. J. Mach. Tool Des. Res., vol. 7, pp 303-324, 1967.

72-Bathia, S.M.; Pandey, P.C. and Shaw, H.S. - "*The Thermal Condition of the Tool Cutting Edge in Intermittent Cutting*" - Wear, vol. 61, pp 21-30, 1986.

73-Chakraverti, G.; Pandey, P.C. and Mehta, N.K. - "*Analysis of Tool Temperature Fluctuation in Interrupted Cutting*" - Precision Engineering, vol. 6, n 2, pp 99-105, 1984.

74-Wang, K.K.; Tsao, K.C. and Wu, S.M. - "*Investigation of Face-Milling Tool Temperatures by Simulation Techniques*" - Trans. of ASME, Journal of Engineering for Industry, pp 772-780, 1969.

75-Palmai, Z. - "*Cutting Temperature in Intermittent Cutting*" - International Journal of Machine Tools Manufacture, vol. 27, n 2, pp 261-274, 1987.

76-Zorev, N.N. and Sawlaskin, K. A. - "*Carbide Tool Life at interrupted Cut with Continuous Cycles*" - Russ. Eng. J., vol. 43, n 2, pp 43-47, 1963.

77-Pekelharing, A.J. - "*The Exit Failure in Interrupted Cutting*" - Annals CIRP, vol. 27, pp 5-10, 1978.

78-Byrne, G. - "*Thermoelectric Signal Characteristics and Average Interfacial Temperatures in the Machining of Metals Under Geometrically Defined Conditions*" - Int J Mach Tools Manufact, vol. 27, n 2, pp 215-224, 1987.

79-Herbert, E.G. - "*The Measurement of Cutting Temperatures*" - Proc Inst Mech Eng, vol. 1, pp 289-329, 1926.

80-Braiden, P.M. - "*The Calibration of Tool/Work Thermocouples*" - Proc. 8th Int. Mach. Tool Design and Research Conf., Manchester, Sept, pp 653-666, 1967.

81-Alvelid, B. - "*Cutting Temperature Thermo-electrical Measurements*" - Annals of the CIRP, vol. XVIII, pp 547-554, 1970.

82-Stephenson, D.A. - "*Tool-Work Thermocouple Temperature Measurements - Theory and Implementation Issues*" - Trans. of ASME, Journal of Engineering for Industry, Nov, vol. 115, pp 432-437, 1993.

83-Lin, J.; Lee, S.L. and Weng, C.I. - "*Estimation of Cutting Temperature in High Speed Machining*" - Trans. of ASME, Journal of Engineering for Industry, July, vol. 114, pp 289-296, 1992.

84-Qureshi, A.H. and Koenigsberger, F. - "*An Investigation into the Problem of Measuring the Temperature Distribution on the Rake Face of a Cutting Tool*" - Annals of the CIRP, vol. XIV, pp 189-199, 1966.

85-Hirao, M. - "*Determining Temperature Distribution on Flank Face of Cutting Tool*" - J Mater Shapin Technol, vol. 6, n 3, pp 143-148, 1989.

86-Kato, S.; Yamaguchi, K.; Watanabe, Y. and Hiraiwa, Y. - "*Measurement of Temperature Distribution within Tool Using Powders of Constant Melting Point*" - Trans. of ASME, Journal of Engineering for Industry, May, pp 607-613, 1976.

87-Smart, E.F.; Trent, E.M. - "*Temperature Distribution in Tools Used for Cutting Iron, Titanium and Nickel*" - Int J Prod Res, vol. 13, n 3, pp 265-290, 1975.

88-Wright, P.K. - "*Correlation of Tempering Effects with Temperature Distribution in Steel Cutting Tools*" - Trans. of ASME, Journal of Engineering for Industry, May, vol. 100, pp 131-136, 1978.

89-Boothroyd, G. - "*Photographic Technique for the Determination of Metal Cutting Temperatures*" - British Journal of Applied Physics, May, vol. 12, pp 238-242, 1961.

90-Chao, B.T.; Li, H.L. and Trigger, K.J. - "*An Experimental Investigation of Temperature Distribution at Tool-Flank Surface*" - Trans. of ASME, Journal of Engineering for Industry, Nov, pp 496-503, 1961.

91-Lin, J.; Chen, T.C. and Weng, C. I. - "*Development of the Infrared Pyrometer with Fibber Optic for Measuring Cutting Temperature at High Speed Cutting*" - Symposium on Monitoring and Control for Manufacturing Process, ASME, Winter Annual Meeting, Dallas, PED, vol. 44, pp 17-32, 1990.

92-Barrow, G. - "*A Review of Experimental and Theoretical Techniques for Assessing Cutting Temperatures*" - Annals of the CIRP, vol. 22, n 2, pp 203-211, 1973.

93-Reichenbach, G.S. - "*Experimental Measurement of Metal Cutting Temperature Distributions*" - Trans. of ASME, vol. 80, pp 525-546, 1958.

94-Kuoliang, W. - "*The Application of Infrared Thermometry in Metal Cutting*" - Proc. of the First International Metal Cutting Conference, March, 14-17, Guangzhou, China, pp 213-223, 1983.

95-Trigger, K.J. - "*Temperatures in Machining and Their Importance*" - International Prod. Eng. Res. Conference, ASME, Pittsburgh, Pennsylvania, USA, 9-12, Sept, 1963.

96-Bickel, E. - "*The Temperature on a Turning Tool*" - International Prod. Eng. Res. Conference, ASME, Pittsburgh, Pennsylvania, USA, 9-12, Sept, 1963.

97-Muller-Hummel, P. and Lahres, M. - *"Infrared Temperature Measurements on Diamond-Coated Tools During Machining"* - Diamond and Related Materials, n 3, pp 765-769, 1994.

98-Lenz, E. - *"Temperatures in Metal Cutting"* - Proc. Int. Conf. Manuf. Tech., Ann Arbor, Michigan, USA, Sept, 25-28, ASTME, pp 553-567, 1967.

99-Da Silva, M.B. and Wallbank, J. - *"Temperature Measurements in Machining Using Infrared Sensor"* - XIV COBEM, Brazilian Congress of Mechanical Engineering, Bauru SP, Brazil, Dec, 1997.

100-Loewen, E.G. and Shaw, M.C. - *"On the Analysis of Cutting Tool Temperatures"* - Trans. of ASME, vol. 76, pp 217-221, 1954.

101-Stephenson, D.A. - *"Assessment of Steady-State Metal Cutting Temperature Models Based on Simultaneous Infrared and Thermocouple Data"* - Trans. of ASME, Journal of Engineering for Industry, vol. 113, pp 121-128, 1991.

102-Lo Casto, S.; Lo Valvo, E.; Piacentini, M. and Ruisi, V.F. - *"Metodo per la Determinazione di Taglio All'interno di Utensili in Materiale Ceramico"* - La Metallurgia Italiana, vol. 85, n°12, pp 751-755, pp 1993.

103-Chow, J.G. and Wright, P.K. - *"On-Line Estimation of Tool/Chip Interface Temperature for a Turning Operation"* - Trans. of ASME, Journal of Engineering for Industry, vol. 110, pp 56-64, 1988.

104-Tay, A.O.; Stevenson, M.G. and Vahl Davis, G. - "*Using the Finite Element Method to Determine Temperature Distribution in Orthogonal Machining*" - Proc of Inst of Mech Eng, vol. 188, pp 627-638, 1974.

105-Muraka, P.D.; Barrow, G. and Hinduja, S. - "*Influence of the Process Variables on the Temperature Distribution in Orthogonal Machining Using the Finite Element Method*" - Int J Mech Sci, vol. 21, pp 445-456, 1979.

106-Stevenson, M.G.; Wright, P.K. and Chow, J.G. - "*Further Developments in Applying the Finite Element Method to the Calculation of Temperature Distribution in Machining and Comparisons with Experiment*" - Trans. of ASME, Journal of Engineering for Industry, vol. 105, pp 149-154, 1983.

107-Dawson, P.R. and Malkin, S. - "*Inclined Moving Heat Source Model for Calculating Metal Cutting Temperatures*" - Trans. of ASME, Journal of Engineering for Industry, vol. 106, pp 179-186, 1984.

108-Ber, A. and Goldblatt, M. - "*The Influence of Temperature Gradient on Cutting Tool's Life*" - Annals of the CIRP, vol. 38, pp 69-73, 1989.

109-Obikawa, T. and Usui, E. - "*Computational Machining of Titanium Alloy - Finite Element Modelling and a Few Results*" - Trans. of ASME, Journal of Manufacturing Science and Engineering, vol. 118, May, pp 208-215, 1996.

110-Chan, C.L. and Chandra, A. - "*A Boundary Element Method Analysis of the*

Thermal Aspects of Metal Cutting Processes" - Trans. of ASME, Journal of Engineering for Industry, Aug, vol. 113, pp 311-319, 1991.

111-Cowan, R.S. and Winer, W.O. - "*Frictional Heating Calculating*" - ASM Handbook, vol. 18, pp 39-44, 1983.

112-Kurimoto, T. and Barrow, G. - "*The Influence of Aqueous Fluids on the Wear Characteristics and Life of Carbide Cutting Tools*" - Annals of the CIRP, vol. 31/1, pp 19-23, 1982.

113-Usui, E.; Shirakashi, T. and Kitagawa, T. - "*Analytical Prediction of Three Dimensional Cutting Process - Part 3: Cutting Temperature and Crater Wear of Carbide Tool*" - Trans. of ASME, Journal of Engineering for Industry, May, vol. 100, pp 236-243, 1978.

114-Machado, A.R. et al - "*Temperatura de Corte e o Comprimento de Contato Cavaco-Ferramenta*" - IV North-Northeast Congress of Mechanical Engineering, vol. 1, 16-20, Jun, Recife PE, Brazil, pp 413-418, 1996.

115-*Cutting and Metalworking Oils*, C.C. Wakefield & Company Limited, Wakefield-Dick Industrial Lubricants Division, London.

116-Braithwaite, E.R. - "*Lubrication and Lubricants*" - Elsevier Publishing Company, Amsterdam, 1967.

117-Bowden, F.P.; Tabor, D. - *"The Friction and Lubrication of Solids"* - Oxford University Press, London, 1958.

118-Nelson, D. and Schaible, J. - *"Update: Cutting Fluids and Related Products"* - Cutting Tool Engineering, October, pp 31-35, 1988.

119-Schey, J.A. - *"Tribology in Metalworking - Friction, Lubrication and Wear"* - Metal Park, 1984, ISBN 0-87170-155-3.

120-Rauth, R.K. - *"Synthetics Can Replace Oil in Superabrasives Applications"* - AES American Engineering Society Magazine, June-July, pp 20-21, 1988.

121-Mariani, G. - *"A Systematic Approach to Selecting a Semi-Synthetic"* - Cutting Tool Engineering, October, pp 50-54, 1988.

122-Brown, J.E. - *"Fill'er Up - Tankside Additives Enhance Coolant Performance"* - Manufacturing Engineering, January, pp 55-57, 1990.

123-De Chiffre, L. - *"Testing the Overall Performance of Cutting Fluids"* - Journal of the American Society of Lubrication Engineers, May, pp 244-251, 1978.

124-Dick, R.M. and Foltz, G. - *"How to Maintain Your Coolant System"* - Machine and Tool Blue Book, January, pp 30-34, 1988.

125-International Standard ISO 6743/7 - *"Lubricants, Industrial Oils and Related"*

Products (class L) - Classification - Part 7: Family M (Metalworking) - First Edition, 01/November, 1986.

126-Simon, A.T. - "*Refrigerante para Usinagem: o Liquido e Substituido pelo Ar*" - Maquinas e Metais, Fevereiro, pp 16-18, 1992.

127-Shaw, M. - "*On the Action of Metal Cutting Fluids at Low Speeds*" - Wear, vol. 2, pp 217-227, 1958/59.

128-Shaw, M.C.; Cook, N.H. and Smith, P.A. - "*The Cooling Characteristics of Cutting Fluids*" - ASTE Research Fund, American Society of Tool Engineers, Research Report n 19, pp 1-27 plus 11 plates, 1958.

129-Chu, T. and Wallbank, J. - "*Determination of the Temperature of a Machined Surface*" - Trans. of ASME, Journal of Manufacturing Science and Engineering, May, vol. 120, pp 259-263, 1998.

130-Williams, J.A. - "*The Action of Lubricants in Metal Cutting*" - Journal of Mechanical Engineering Science, vol. 19, n 5, pp 202-212, 1977.

131-Postinikov, S.N. - "*Penetrating Ability of Cutting Fluids*" - Wear, vol. 10, pp 142-150, 1967.

132-Lau, W.S. and Rubenstein, C. - "*The Influence of Flank Wear, Cutting Speed and Cutting Fluid on the Surface and Sub-Surface Workhardening Produced in an*

Orthogonal Planing Operation” - International Journal of Machine Tool Design and Research, vol. 12, pp 311-323, 1972.

133-Dorinson, A. - “*A Theory of Cutting-Tool Wear and Cutting-Oil Action*” - Lubrication Science and Technology, ASLE Transactions, vol. 1, n 2, pp 131-138, 1958.

134-Cassin, C. and Boothroyd, G. - “*Lubricating Action of Cutting Fluids*” - Journal of Mechanical Engineering Science, vol. 7, n 1, pp 67-81, 1965.

135-Kurimoto, T. and Barrow, G. - “*The Wear of High Speed Steel Cutting Tools Under the Action of Several Different Cutting Fluids*” - Proceedings of the 22nd Int. Mach. Tool Design and Research Conference, Manchester, UK, 16-18 September, 1981.

136-Piggot, R.J. and Colwell, A.T. - “*High-Jet System for Increasing Tool Life*” - SAE Transactions, vol. 6, n 3, July, pp 547-566, 1952.

137-Lindeke, R.; Schoenig, F. and Khan, A. - “*Cool Your Jets*” - Cutting Tool Engineering, October, pp 35-37, 1991.

138-Machado, A.R. and Wallbank, J. - “*The Effects of a High-Pressure Coolant Jet on Machining*” - Proceedings of Institution of Mechanical Engineers, vol. 208, pp 29-38, 1994.

139-Sharma, C.S.; Rice, W.B. and Salmon, R. - *“Some Effects of Injecting Cutting Fluids Directly into the Chip-Tool Interface”* - Trans. of ASME, Journal of Engineering for Industry, May, pp 441-444, 1971.

140-Reznikov, A.N. and Zhivoglyadov, N.I. - *“How Internal Cooling Affects the Temperature and Life of Cutting Tools”* - Soviet Engineering Research, vol. 9, n 4, pp 99-101, 1989.

141-Maekawa, K.; Ohshima, I. and Murata, R. - *“Finite Element Analysis of Temperature and Stresses within an Internally Cooled Cutting Tool”* - Bull. Japan Soc. of Prec. Engg., vol. 23, n 3, September, pp 243-246, 1989.

142-Hug, J.L. - *“Minimum Dosing: A Draft on The Spirit of the Time”* - Machines Production, n 633, pp 41-44, 1995.

143-Machado, A.R. and Wallbank, J. - *“The Effect of Extremely Low Lubricant Volumes in Machining”* - Wear, 210, pp 76-82, November, 1997.

144-Hasting, W.F. - *“A New Quick-Stop Device and Grid Technique for Metal Cutting Research”* - Annals of the CIRP, vol. XV, pp 109-116, 1967.

145-Woolman, J. and Mottran, R.A. - *“The Mechanical and Physical Properties of the British Standard EN Steels”* - BASRA, vol. 1, 1966.

146-Wimer, D.G. and Macpherson, P.B. - *“An Infra-red Technique for the*

Measurements of Gear Tooth Surface Temperature” - ASLE Transactions, vol. 18, n 4, pp 229-238, 1975.

147-Chatfield, C. - “*Statistics for Technology – A Course in Applied Statistics*” – 3rd Edition, Chapman & Hall, 1994, ISBN 0412 25340 2.

148-Raytek, Thermalert 6 series, Operator’s Manual.

149-Rowe, G.W. and Smart, E.F. - “*Experiments on Lubrication Breakdown in Friction and in the Cutting of Metal on a Lathe*” - Proc. Inst. Mech. Engrs, Lubrication and Wear, Third Convention, 179(3J), 229-241, 1965.

150-Wright, P.K.; Horne, J.G. and Tabor, D. - “*Boundary Conditions at the Chip-Tool Interface in Machining: Comparisons Between Seizure and Sliding Friction*” - Wear, vol. 54, pp 371-390, 1979.

151-Trent, E.M. - “*Condition of Seizure at the Tool Work Interface*” - ISI, Special Report 94, Iron and Steel Institute, London, pp 11-18, 1967.

152-De Chiffre, L. - “*Mechanics of Metal Cutting and Cutting Fluid Action*” - In. J. Mach. Tool Des. Res., vol. 17, pp 225-234, 1977.

153-Machado, A.R.; Motta, M.F. and da Silva, M.B. - “*Performance of Synthetic and Mineral Soluble Oil when Turning AISI8640 Steel*” - Trans. of ASME, Journal of Manufacturing Science and Engineering, November, vol. 119, pp 580-586, 1997.

154-Chiaverini, V. - "*Aços e Ferros Fundidos*" - 5th edition, Associação Brasileira de Metais, 1984.

155-Thehning, K.E. - "*Steel and its Heat Treatment*" - Bofors Handbook, Butterworths, 1975, ISBN 0 408 70934 0.

156-Pantale, O.; Rakotomala, R.; Touratier, M. and Haken, N. - "*A Three-Dimensional Numerical Model of Orthogonal and Oblique Metal Cutting Process*" - PD-vol. 75, Engineering System Design and Analysis, ASME, vol. 3, pp 199-206, 1996.

157-Heine, H.J. - "*Dry Machining – A Promising Option*" - American Machinist, August, pp 92, 94, 1997.

Appendix A: Contact on Tool Flank Face

1.Introduction

The majority of work in metal cutting admits contact between the workpiece and the tool flank face only if there is flank wear and the tool is not sharp. The focus of attention is the region of contact on the rake face. Therefore in a turning operation with a single point tool three forces are considered: the cutting force in the direction of cutting speed; feed force in the direction of feed and thrust force in the direction perpendicular to the feed. These forces are a consequence of the force necessary to shear the material on the primary shear plane to form the chip and the new machined surface and the force necessary to overcome the resistance to chip movement on the rake face of the tool, the secondary shear zone. The contact on the flank face is not taken into account concerning the distribution of force.

Considering that the material machined is not a perfect plastic material, there could be some elastic deformation involved in the process. In fact the temperature achieved by the cutting zone and the high strain rate can affect the behaviour of the material during cutting. Because the strain rates during machining are so high, and there are no means to test a material under such conditions, the fundamental behaviour of the material is unknown. However for most ductile materials some elastic deformation during cut could be considered. Thus this elastic behaviour of the material suggests a contact of the machined surface with the tool flank face. It means that the tool needs to penetrate a specific depth into the material before starting to cut it. In other words, there is a

minimum depth of cut that will depend on many factors, but mainly on the properties of the material. For values less than this minimum the material will not be cut, just be deformed.

Some authors named the forces due to the contact between workpiece surface and tool flank face residual cutting forces or ploughing force [1], and believe that they are independent of feed rate. Therefore considering that there is no BUE the residual forces can be calculated by means of extrapolation of a curve of cutting forces back to zero feed rate. This is done assuming that the residual forces, and so the contact length on the flank face, will not change with feed. Thus the forces during cutting are composed of the force necessary to shear the material and form chip and new surface on the shear zone, the force to overcome friction (and shear the chip) on the rake face and the residual forces on the flank face.

When there is a BUE, depending on its size and shape the situation can change. The BUE formed avoids contact with the flank face, but there is still elastic recovery after the material passes the BUE. However if extrapolation of the forces as above is used to calculate the residual cutting forces, the results will be misleading, because the conditions in the cutting zone will change with the feed rate when a BUE is present.

2.Contact Length on the Flank Face

The usual representation of orthogonal cutting considers that the machined surface is being formed exactly at the cutting edge and will not have contact with the tool flank face. It is reasonable to consider chip formation by shearing action along a plane inclined with the direction of cut.

In the orthogonal cutting when the tool touches the workpiece, before it starts to cut some elastic deformation takes place. As the tool advances towards the workpiece the elastic limit of the material is reached and it starts to flow plastically. At this point there is no plastic deformation of the material but elastic deflection and no cutting. Eventually point is reached where the plastic deformation above the cutting edge compels the material to shear along the primary shear plane, and starts the chip formation. This contact with the tool rake face has a great effect on machining and the secondary shear zone. Figure A.1 illustrates these situations.

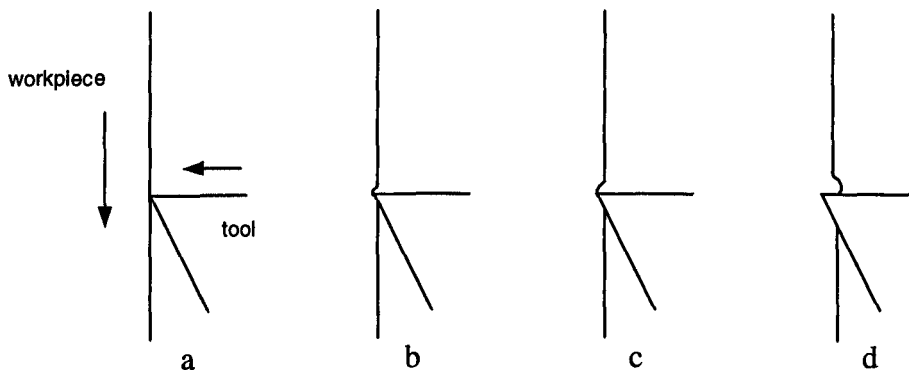


Figure A.1 Initiation of cut: a-tool touches the workpiece; b-elastic deformation; c-plastic deformation; d-about to start to cut.

After the cut has started the situation can change and either there is no more contact on the flank face or the contact can continue independent of what happens above the cutting edge. [2] found evidence of this contact below the cutting edge when cutting different materials, suggesting that the contact can still exist during the cut.

Considering a tool with a rounded cutting edge instead of sharp wedge, when it

touches the workpiece, and before it starts to cut, the movement is similar to the ploughing action of a hard particle sliding against a rigid plastic body. In this case the ridge of deformed material is pushed along ahead of the slider, no material is removed from the surface, instead the material flows beneath the particle. Three modes of sliding can be distinguished: cutting, wedge formation, and ploughing. The attack angle (inclination of the rake face) of the slider (particle in abrasion) and the conditions of the interface determine the transition between them. In experiments using a single particle as abrasive, the inclination of the cutting face determines whether material is removed or not [3].

When the sliding action results in removal of material the attack angle is the angle between the rake face and the direction of cutting speed. However, considering a rounded cutting edge at the moment when the tool touches the surface of the workpiece (without cutting) this angle is zero. As the tool penetrates into the surface this angle varies from zero to the attack angle of the tool. Therefore if the tool edge geometry is a cylinder then the depth of penetration will control the attack angle. Consequently the mode of sliding will depend on the penetration.

Figure A.2 illustrates the effect of the attack angle or depth of penetration in the sliding mode for three materials. A sphere sliding against a plane surface. The interfacial shear strength, f , is the ratio between the shear stress at the interface (tangential force necessary to continue the movement) and the shear yield stress of the material of the plane surface.

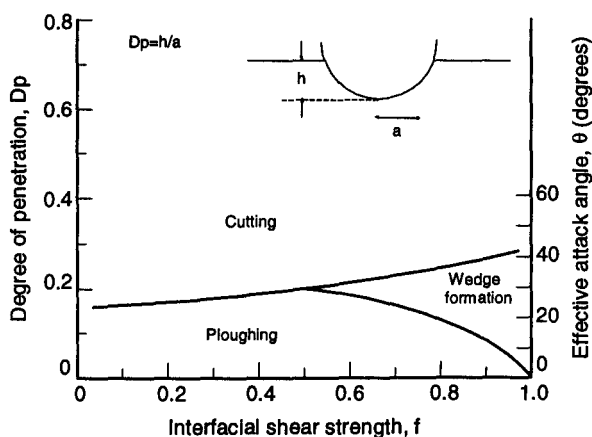


Figure A.2 Modes of deformation observed in the sliding of a hard spherical indenter on α -brass, plain carbon steel (0.45% C) and an austenitic stainless steel (AISI 304) [4](after [5]).

The mode of sliding depends on the force (normal load), radius of the indenter, and shear strength of the contact. According to the experimental results at low speeds, the transition from one mode of sliding to another depends on the lubrication. For experiment in [4] the load was about 0.7N and the radius of the indenter $27\mu\text{m}$ (and $62\mu\text{m}$).

This above graph (figure A.2) shows the condition at the rake face at the start of cutting. For example if there is complete adherence the cut starts when the attack angle is higher than 40 degrees, or degree of penetration is 0.3. When there is perfect lubrication however, the degree of penetration necessary to start cutting is less than 0.2.

In this experiment an interesting result was obtained that over a certain value of D_p the coefficient of friction is the same for both conditions, lubricated or dry.

The contact length could be estimated if the value of the forces acting on the contact is known. Assuming that the cut starts when the elastic limit of the material is reached and that there is no deformation of the tool, the contact length could be estimated

using Hertz's theory (depending on the contact length and radius of the cutting edge). Consider the idealised case where a cylinder of a rigid material is pressed against a plane of a soft material, as shown in figure A.3.

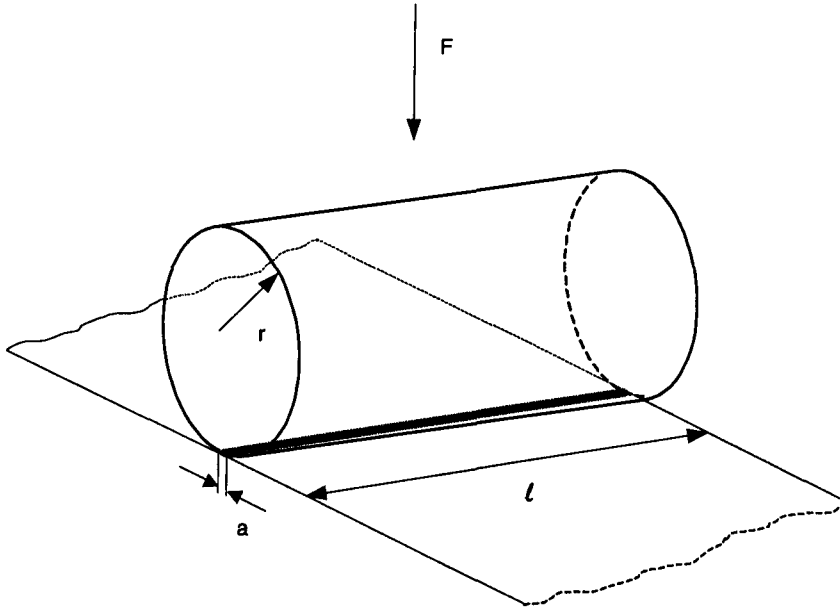


Figure A.3 The contact of a cylinder and a plane.

According to Hertz's classical equation [6], the contact length for this case can be calculated by:

$$a = \sqrt{\frac{4Fr}{\ell\pi E^*}} \quad (\text{A.1})$$

where:

$$E^* = \left(\frac{1-\nu_1^2}{E_1} + \frac{1-\nu_2^2}{E_2} \right)^{-1}$$

ℓ - width of the contact

F - load

r - radius of the cylinder

E_1 - Young's modulus for the workpiece material

E_2 - Young's modulus for the tool material

ν_1 - Poisson ratio of the workpiece material

ν_2 - Poisson ratio of the tool material

Direct measuring of the load F in cutting is not possible because it will be

necessary to adjust the depth of cut to the minimum value, which is unknown. However there are other methods to estimate this force. Supposing the contact does not depend on feed rate it is possible to measure this force for various feeds and then extrapolate back to zero feed rate as in [7]. [8] used a split cutting tool device to measure and separate the forces acting on the rake face and flank face, but some extrapolation is still needed for values close to the cutting edge.

3.Experimental Work

The machining process used was external turning of an AISI1040 rolled steel with an average hardness of 199Hv. The composition of the material was:

0.43%C 0.83%Mn 0.19%Si 0.035%S 0.007%P 0.19%Cu 0.11%Ni 0.14%Cr 0.05%Mo
0.027%Al 0.04%Ti

The tool was cemented carbide designated ISO M35 with a TiN-TiC-TiN coating. It has geometry given by SNMG 120404. When mounted in the tool holder the approach angle was 45 degrees, the rake angle was 5 degrees, the clearance angle 5 degrees and zero inclination of the cutting edge. This tool has rounded cutting edges with a radius of 0.0425mm measured in the optical microscope.

Three cutting speeds were used: 22, 30, and 40m/min. Cutting forces are measured for several feed rates (0.005, 0.01, 0.02, 0.03, 0.04, 0.05, 0.10, 0.15mm/rev) and then extrapolated to zero feed. These cutting speeds are in the region of BUE formation (for the highest feed rates), which could affect the extrapolation, however at low feed rates there is no BUE.

4.Results and Discussion

The results of the force measurements (cutting force and feed force) and the curve used to fit them are shown in figure A.4, as well as the correlation factor, which is very good, for each curve.

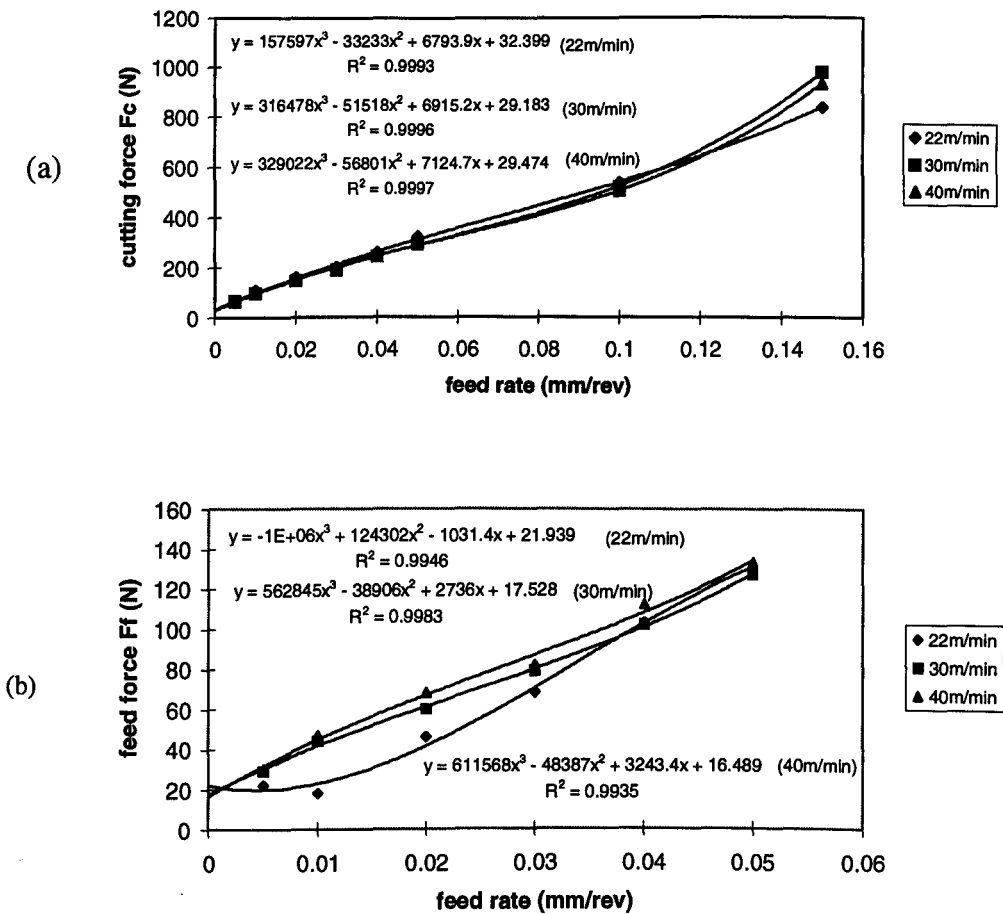


Figure A.4 Residual cutting forces. a)cutting force F_c b)feed force F_f .

According to these graphs the following residual forces are obtained:

	cutting force (N)	feed force (N)
22m/min	32	23
30m/min	29	25
40m/min	29	31

Feed force is the result of the measurement but resolved in the direction of the chip flow, which means the extrapolated value divided by $\sin(45^\circ)$.

In the case of zero feed rate, the movement of the tool against the workpiece can be considered as a mechanism of metallic friction. The force required to move the slider (tool) is considered to be the force to shear the junctions that form between the surfaces and the force necessary to displace the material of the workpiece from the front of the tool [9].

According to the theory, the ploughing force depends on the width of the track. In the case of machining the width of the cut is the depth of cut, or the length of the cutting edge that is in action.

Using the results of feed force and equation (A.1) the contact length can be estimated. The following values are obtained, in μm :

22m/min	3.3
30m/min	3.4
40m/min	3.8

These are estimated values because equation (A.1) was derived from the static situation, a hardness test, and the values for Young's modulus for the material of the tool is approximated ($E=60 \times 10^4 \text{N/mm}^2$, $\nu=0.2$). According to the results the contact length increases with cutting speed for dry conditions.

According to these results the area of contact for the case of 40m/min is about $11 \times 10^{-3} \text{mm}^2$. The normal stress due to the contact force of 31N is then about $3 \times 10^3 \text{N/mm}^2$. The engineering strain for such stress in a normal compression test should be in the order of 0.01 (if it is in the elastic region).

[2] measured a contact length of approximately 0.180mm for mild steel and dry conditions using a special quick stop device where the tool moves horizontally. The minimum depth of cut for a contact length of 0.180mm is approximately $10 \mu\text{m}$. This value is obtained by the geometry of the tool. The area of contact is then approximately 0.6mm^2 , which gives a normal stress of 42N/mm^2 ($25/0.6$). Considering Young's modulus of $20 \times 10^4 \text{N/mm}^2$ for steel, the engineering strain causing such deformation should be in the order of 10^{-3} . The same calculation for all conditions indicates an engineering strain between 10^{-4} to 10^{-3} (the strain at the limit of proportionality in a normal tension test is of the order 3×10^{-3} for steels), depending on the cutting speed. This suggests that a minimum depth of cut of $10 \mu\text{m}$ (generating a contact on the flank face of 0.180mm) could well be elastic deformation of the workpiece.

For the static situation, the theory predicts that plastic deformation begins when the mean pressure is $1.1Y$, where Y is the uniaxial yield stress of the material. This value is about 350N/mm^2 for the AISI1040. If we consider that cutting will start at the onset of plastic deformation the results of the tests gives very high values for the mean pressure to start chip formation.

On the other hand, assuming a contact length of 0.18mm the mean pressure is smaller than that necessary to start plastic deformation for the static situation. However it is an interesting observation because plastic deformation in a Hertzian contact (for the

static situation) does not begin at the surface, instead it starts at some distance below the indenter. If the same could happen in cutting so the formation of the chip and machined surface takes place at some point away from the cutting edge and some material will always be attached to the cutting edge. This means that there is always a BUE, independent of cutting conditions. [10] considers that there will be a contact length below the cutting edge on the flank face, but this contact is formed by a dead material that adheres and envelopes the cutting edge. This dead material is similar to a BUE extended to the flank face. He suggests that the new surfaces (machined surface and chip) are formed by cracks that initiate at the extremity of this dead zone which have to exist independent of the cutting conditions, otherwise separation of material is not possible. In the experiments of [2] using a horizontal quick stop, there is no sign of fracture on the contact band, which would be expected if the contact is formed by dead zone of material adhered to the tool. However this can be a mechanism of formation of the surfaces when there is BUE. Depending on the shape of the BUE formed it can extend into the workpiece, changing the tool edge geometry (edge rounding) and avoiding contact between machined surface and tool.

To calculate the contact length using expressions for the static situation it is assumed that when pressing the tool against the material the contact will persist when the tool starts to move. At this point it is interesting to recall that the hardness indentation will leave a mark in the material that depends on the ductility. For example, if we use a pyramidal indenter the shapes shown on figure A.5 are possible, and the last one are typical of ductile materials.



Figure A.5 Exaggerated shapes left on the material by a pyramidal indenter [11].

If this could persist when the indenter moves, the contact length on flank face will certainly be higher than the ones obtained by the theoretical calculations.

In the experiments of [3] to simulate the abrasive process, a pyramidal indenter was used as the tool. It was observed that the normal force is supported just by the friction of the chip with the rake face and therefore no contact with the flank face. The contact existed just for the static situation.

Assuming that it is true that the tool has to penetrate a certain depth to start to cut material and that the residual forces represents the forces acting on the cutting edge just before the cut starts it is possible to give experimental evidence of this critical penetration. In the graph of cutting force against time, the time necessary for the force to reach the mean value (and oscillate around it), represents the time since the tool first touches the surface until it is removing material at a constant undeformed chip thickness. As an example, the graph of figure A.6 presents the behaviour of cutting force against time for $V_c=22\text{m/min}$ and $f=0.001\text{mm/rev}$, for the same material and depth of cut used in this work.

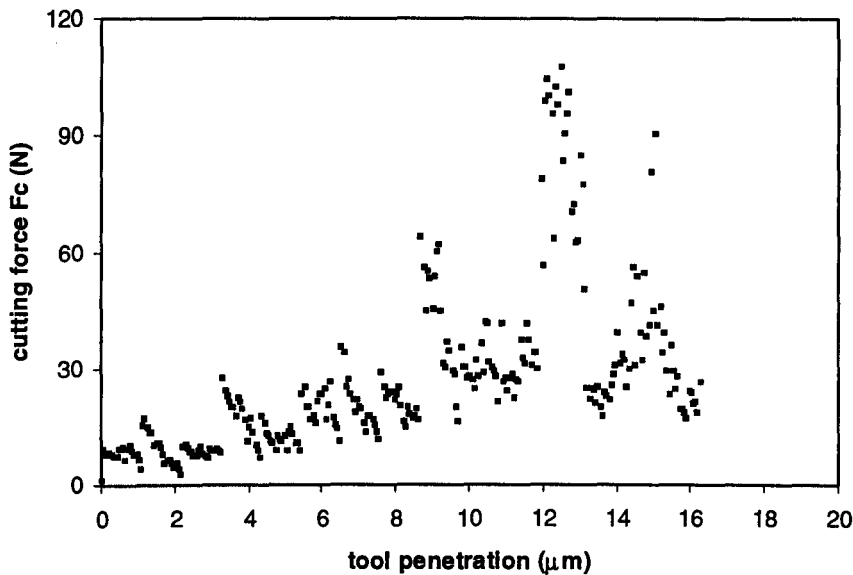


Figure A.6 Cutting force against time, 22m/min, 0.001 mm/rev.

The diameter of the workpiece was 180mm, which means that the angular speed was 39rpm. The feed speed is therefore 0.04mm/min, or 0.0007mm/s. It takes about 13s for the force to reach the mean value. The force in this graph was measured at a frequency of 12 s^{-1} . At this frequency and for the feed speed it means that the force was measured every time the tool travelled $0.05\mu\text{m}$ in the direction of the feed. According to the graph the value of 32N, which is the residual cutting force for 22m/min, is reached when the tool had penetrated more than $9\mu\text{m}$. This value is very close to the one that would give a contact length on the flank face of 0.18mm.

If this contact persists unchanged during the cut, it will generate heat to increase the temperature of the workpiece and tool. Part of the heat generated on the primary shear plane to form the chip is dissipated into the workpiece increasing its temperature. After

forming the chip, there is the contact with the tool flank face and heat generation, and a further increase in the workpiece temperature will be seen. Therefore, when using the relationship to calculate the temperature of the workpiece due to heat coming from the primary shear plane, like the one proposed for [12], another term due to the contact with the flank face has to be added.

5. Conclusions

This work shows some evidence for contact between machined surface and tool flank face. Direct measurement of this contact is very difficult, if not impossible, but it seems reasonable to expect that it will happen in machining. The theoretical calculation of this contact using the equation derived for the static situation does not give consistent results, both for the length of the contact and the stress involved in the process. However there is some experimental evidence that indicates the proportion of the contact, which could be due to elastic recovery of the material.

6. References

1-Albrecht, P. - "*New Developments in the Theory of the Metal-Cutting Process – Part 1. The Ploughing Process in Metal Cutting*" - Trans. of ASME, Journal of Engineering for Industry, November, pp 348-358, 1960.

2-Wallbank, J. - "*Flow at the Cutting Edge and the Generation of New Surfaces During*

Metal Cutting” - PhD Thesis, University of Birmingham, 1978.

3-Sedricks, A.J. and Mulhearn, T.O. - “*Mechanics of Cutting and Rubbing in Simulated Abrasive Processes*” - *Wear*, vol. 6, pp 457-466, 1963.

4-Hokkirigawa, K. and Kato, K. - “*An Experimental and Theoretical Investigation of Ploughing, Cutting and Wedge Formation During Abrasive Wear*” - *Tribology International*, February, vol. 21, n 1, pp 51-57, 1988.

5-Hutchings, I.M. - “*Tribology - Friction and Wear of Engineering Materials*” - Edward Arnold, London, 1992.

6-Johnson, K.L - “*Contact Mechanics*” - Cambridge University Press, 1996, ISBN 0521 34796 3.

7-Chu, T.H. - “*An Experimental Study of the Workpiece Temperature on the Machined Surface During Metal Cutting*” - PhD thesis, University of Warwick, 1998.

8-Gordon, M.B. - “*The Applicability of the Binomial Law to the Process of Friction in the Cutting of Metals*” - *Wear*, vol. 10, pp 274-290, 1967.

9-Bowden, F.P. and Tabor, D. - “*The Friction and Lubrication of Solids*” - Oxford University Press, London, 1958.

10-Form, G.W. and Beglinger, H. - "*Fundamental Considerations in Mechanical Chip Formation*" - Annals of the CIRP, vol. XVIII, pp 153-167, 1970.

11-Dieter, G.E. - "*Mechanical Metallurgy*" - McGraw-Hill, Inc., New York, USA, 1976.

12-Boothroyd, G. and Knight, W.A. - "*Fundamentals of Machining and Machine Tools*" - Marcel Dekker, Inc, 2nd edition, 1989, ISBN 0-8247-7852-9.

Appendix B: Heat Generation and Workpiece Temperature

Using the measured values of forces from table 4.1 it is possible to estimate the temperature of the workpiece using equation 2.6, which correlates the work done on the primary shear zone and temperature. It is an estimated result for many reasons, amongst them the fact that the equation was developed for an orthogonal cut and assuming primary (and secondary) shear zone as a distinct planes.

Assuming that all the work done in metal cutting is converted into heat. The work done can be calculated from the product of the force necessary to shear the material and the shear speed, both directed along the primary shear plane. The force to shear the material is the force F_z shown in figure 2.5 and is given by:

$$F_z = F_c \cos \phi - F_f \sin \phi \quad (\text{B.1})$$

The shear speed V_s is shown in figure 2.3 and can be geometrically obtained by equation (2.3).

The rake angle is assumed to be 5° which is the given by the geometry of the insert and the tool holder. As there is a BUE the actual rake angle will be affected and so will the calculations of the work done on the primary shear plane. Therefore the calculations performed here present error due to the presence of BUE. This error depends on the size and shape of the BUE.

Table B.1 shows the calculated values for the work expended on the primary shear plane for all conditions and also the total work expended during the process which is given by the product of cutting force F_c and cutting speed V_c .

Table B.1-Work expended on the process.

Vc (m/min)	f (mm/rev)	lubricant	Ns (W)	Nc (W)
22	0.05	dry	86	110
		0%	85	103
		1%	85	105
		2%	91	107
		3%	88	107
		4%	87	107
		5%	76	95
	0.10	dry	150	196
		0%	156	193
		1%	160	195
		2%	161	198
		3%	157	191
		4%	149	183
		5%	142	179
	0.15	dry	244	307
		0%	237	282
		1%	253	298
		2%	252	291
		3%	236	325
		4%	242	289
		5%	233	292
30	0.05	dry	110	142
		0%	104	135
		1%	110	135
		2%	110	136
		3%	114	141
		4%	114	144
		5%	104	132
	0.10	dry	198	260
		0%	206	254
		1%	206	259
		2%	203	256
		3%	207	258
		4%	210	258
		5%	190	239
	0.15	dry	403	488
		0%	300	383
		1%	341	423
		2%	394	480
		3%	379	473
		4%	387	469
		5%	351	454
40	0.05	dry	146	184
		0%	137	175
		1%	140	178
		2%	151	186
		3%	151	184
		4%	145	179
		5%	144	178
	0.10	dry	258	334
		0%	257	329
		1%	260	339
		2%	258	337
		3%	246	334
		4%	248	325
		5%	241	315
	0.15	dry	486	621
		0%	487	601
		1%	478	611
		2%	442	593
		3%	449	596
		4%	455	573
		5%	441	569

Ns-work on primary shear plane

Nc-total work done during the process

The results for N_s and N_c are very similar for all conditions. This should be expected, as there is no effect of lubrication on forces. The work N_s increases with cutting speed and feed rate. It increases with feed rate because the forces increase, as seen on the graphs of figures 4.6 to 4.12.

Figure B.1 represents the graph of the measured temperature against power on the primary shear plane. All the conditions tested are used in this graph including the dry conditions.

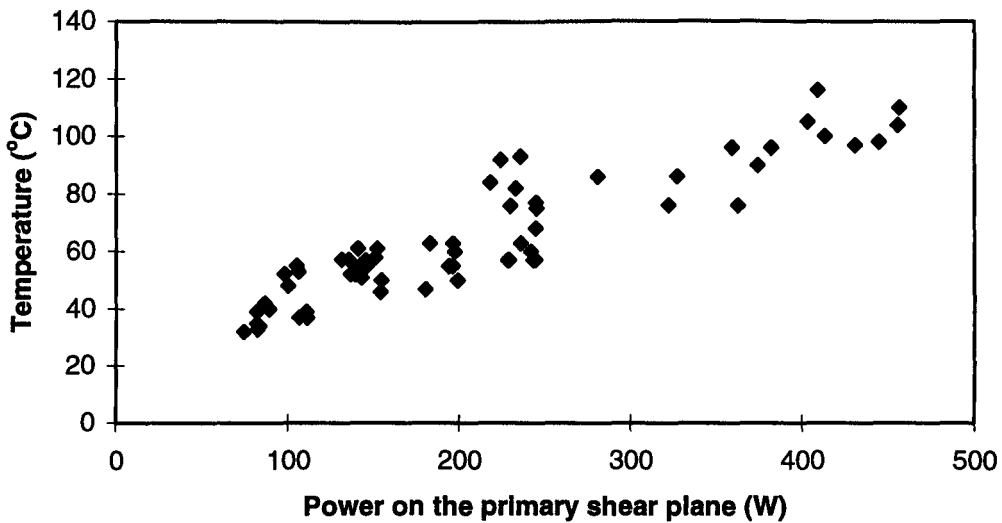


Figure B.1 Variation of workpiece temperature against power on shear plane.

There seems to be a positive correlation between work done on the primary shear plane and workpiece temperature, which means large values of both variables tend to occur together.

The work done to shear the material on the primary shear plane is converted into heat and is dissipated by the chip and by the workpiece. Most of the heat goes with the chip, and part goes back into the workpiece. These proportions depend on the position of the shear zone, or the inclination of the shear zone in relation to cutting speed direction. If this region is assumed to be a plane the proportion of heat from the

primary shear zone that goes back by conduction into the workpiece depends on the shear angle ϕ . This is represented by equation 2.4.

The rest of the work ($N_c - N_s$) is dissipated basically by the chip and tool and there is no direct effect on the temperature of the workpiece.

As the shear plane angle decreases more work is done to shear the material, which means more heat is produced. At the same time the heat source is closer to the workpiece and therefore the proportion of heat that goes back into the workpiece increases. The result is an increase of workpiece temperature.

Problems arise in estimating the percentage of heat that goes back into the workpiece. The solution proposed by [1] gives very high values at the low cutting speeds used in this work. It predicts that about 60% of the total heat generated on the primary shear plane is conducted into the workpiece. The temperatures obtained by these calculations (according to equation 2.4) are higher than the experimental values.

It is reasonable to expect that this percentage of heat conducted into the workpiece depends on the cutting speed and that it is higher for lower speeds. This is because it is related to the time available for the heat conduction. As the material passes faster through the primary shear zone it does not allow much time for the heat to go into the workpiece.

Unless the feed changes the shear angle it cannot alter the partition coefficient.

Cutting speed and feed rate can affect the partition coefficient by affecting the conditions for formation of a BUE. A BUE acts like a different tool with a different rake angle. A larger rake angle implies a larger primary shear plane angle.

Apart from speed and feed the thermal and physical properties of the material can have an effect on this percentage. Although heat generation increases as the hardness and strength of the material increases and therefore higher temperatures

should be expected, these higher temperatures themselves will have no effect on the partition. Thermal conductivity however will have a significant effect. Materials that have low thermal conductivity for example form segmented chips easily, and this is the result of the adiabatic shear zone where the heat generated is concentrated on a very narrow shear zone [2]. This effect is an extreme example where the amount of heat diffusing into the workpiece would be very low.

Despite the fact that it is difficult to obtain the fraction β to calculate the temperature of the workpiece, there seems to be a good relationship between the experimental temperature and the work done on the primary shear plane. Using the experimental results of temperature given in table 4.3, the value of β was calculated using equation 2.4. After measurements of the depth of plastic deformation under transient surface the value of 0.1mm is a good approximation for all conditions. This value changes very little with the cutting speed and feed rates used in this work. Figure B.2 shows these results plotted against temperature, again all the tested conditions (dry and lubricated) are on the graph. The values of β for this particular experiment are in the range of 0.05 to 0.15, and they increase with temperature.

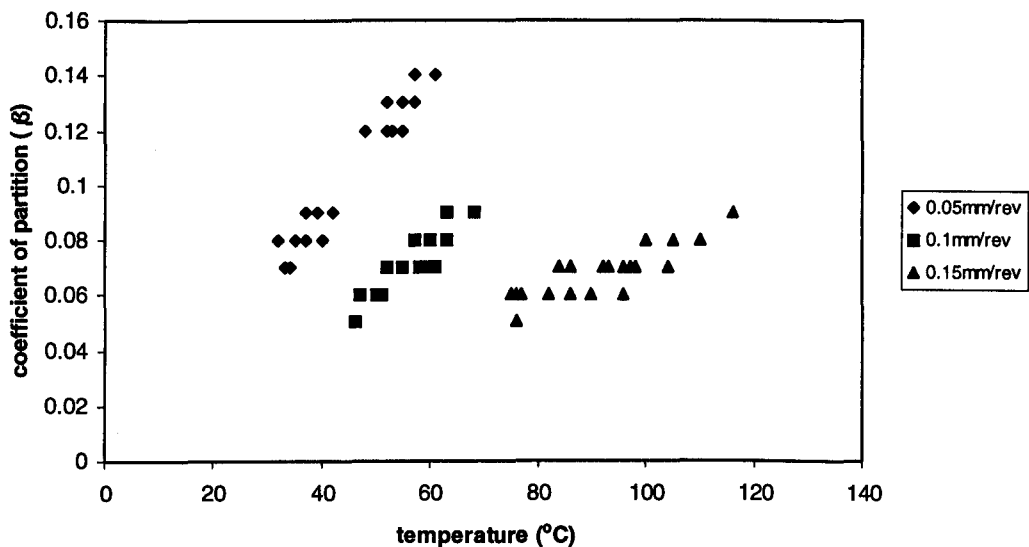


Figure B.2 Relationship between the coefficient of partition and temperature of the workpiece.

The increase of β with temperature means that it increases with cutting speed. As seen in figure 4.26 to 4.28 the temperature increases with cutting speed. This is in disagreement with the theoretical calculation proposed by [1], which predicts that the proportion of heat that is conducted to the workpiece increases as cutting speed decreases. This can be due to the size and shape of the BUE, which depends on the cutting conditions. If the size of it decreases as the cutting speed increases it means that the primary shear plane angle will decrease and the chip thickness increase. These effects can be confirmed by figures 4.29 to 4.31 and 4.33 to 4.35, which show the variation of the thickness and the angle with cutting speed and feed rate respectively.

Calculations of the partition coefficient β for cutting conditions where there is no BUE formation also give smaller values than the ones predicted by [1]. Figure B.3 shows the variation of β with cutting speed for three feed rates (0.05, 0.1 and 0.15mm/rev) according to [3].

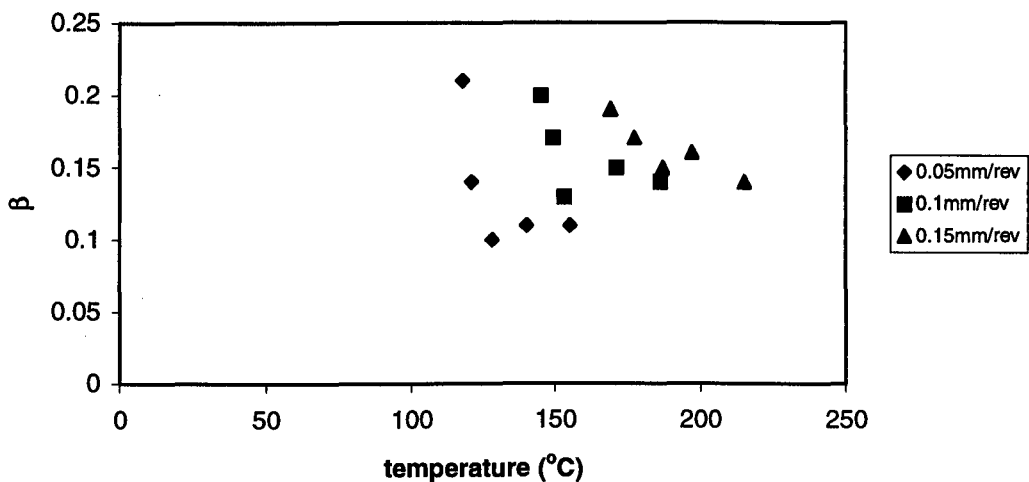


Figure B.3 Variation of β with cutting speed when there is no BUE (after [3]).

The calculated values of β are in the range between 0.1 and 0.25 while the predicted ones would be between 0.16 and 0.36. For these cutting conditions there is no BUE and therefore, as shown on figure B.3, β decreases as cutting speed increases. This variation is related to the primary shear plane angle. As there is no BUE the angle increases with cutting speed, decreasing the portion of heat that is conducted into the workpiece, as predicted by the theory.

References:

1-Weiner, J.H. - "*Shear Plane Temperature Distribution in Orthogonal Cutting*" - Trans. of ASME, vol. 77, pp 1331-1341, 1955.

2-Komanduri, R. and Brown, R.H. - "*On the Mechanics of Chip Segmentation in Machining*" - Trans. of ASME, Journal of Engineering for Industry, vol. 103, pp 33-51, 1981.

3-Chu, T.H. - "*An Experimental Study of the Workpiece Temperature on the Machined Surface During Metal Cutting*" - PhD thesis, University of Warwick, 1998.